THE UNIVERSITY *of* EDINBURGH

Dissecting roles and regulation of the fission yeast kinetochore protein Spc7

Alicja Maria Sochaj

Thesis presented for the Degree of Doctor of Philosophy

Institute of Cell Biology
The University of Edinburgh

2012

To my Mother

and to my Fiancé, Bartek

Declaration

I declare that this thesis was composed by myself and the research presented is my own except otherwise stated.

Alicja M. Sochaj, 2012

Table of Contents

Abbreviations

ATP	Adenosine Triphosphate
bp	base pair
BSA	Bovine Serum Albumin
ChIP	Chromatin Immunoprecipitation
DAPI	4',6-diamidino-2-phenylindole
DNA	Deoxyribonucleic Acid
dNTP	deoxyribonucleotide
DSP	Dithiobis[succinimidyl propionate]
ECL	Enhanced Chemiluminescence
EDTA	Ethylenediamine Tetra Acetic Acid
EGTA	Ethylene Glycol-bis-(2-aminoethyl)-N,N,N', N'-Tetraacetic Acid
FRAP	Fluorescence Recovery after Photobleaching
FRET	Fluorescence Resonance Energy Transfer
GFP	Green Fluorescent Protein
IgG	Immunoglobulin G
GST	Glutathione S-transferase
IMAC	Immobilized Metal Affinity Chromatography
IP	Immunoprecipitation
Kb	kilo base pairs
kDa/Mda	kilo Dalton/mega Dalton
LC	Liquid Chromatography
MBP	Maltose-Binding Protein
MS	Mass Spectrometry
MT	Microtubules
OD	Optical Density
PAGE	Polyacrylamide Gel Electrophoresis
PBS	Phosphate Buffered Saline
PCR	Polymerase Chain Reaction
PEG	Polyethylene Glycol
PIPES	Piperazine-1,4-bis (2-ethanesulfonic acid)
PMG	Pombe Minimal Glutamate

RNA	Ribonucleic Acid
RT	Room Temperature
rpm	revolutions per minute
SDS	Sodium Dodecyl Sulphate
SPA	Synthetic Sporulation Agar
TAP	Tandem Affinity Purification
TE	Tris-EDTA
TFA	Trifluoroacetic Acid
YES	Yeast Extract Supplemented

List of Figures

Chapter 1

Chapter 3

Chapter 6

Supplementary Figures

List of Tables

Chapter 2

Chapter 3

Abstract

Accurate chromosome segregation is critical as unequal distribution of the genomic DNA results in impaired cell function or cell death. Kinetochores, the multi-protein structures assembled on centromeric DNA, drive chromosome segregation. Chromosome segregation is under supervision of mitotic spindle checkpoint. The mitotic spindle checkpoint is a surveillance mechanism ensuring that cells enter anaphase with all kinetochores properly attached to spindle microtubules and thereby preventing missegregation. Some checkpoint proteins are localised at kinetochore where they generate and enhance the checkpoint signal. Mps1 (Mph1 in *S. pombe*) and Aurora B (Ark1 in *S. pombe*) kinases are required for precise chromosome segregation and mitotic spindle checkpoint in fission yeast.

In this study we investigate the roles of Mph1 and Ark1 in regulating the *S. pombe* kinetochore protein Spc7, which is the homologue of human Blinkin/KNL1. We demonstrated that both kinases target the N-terminus of Spc7. Loss of phosphorylation on the candidate phosphosites results in sensitivity to microtubule depolymerizing drugs indicating mitotic defects. As Blinkin has been proposed to be a docking platform for checkpoint proteins, we tested the possibility that Mph1 kinase is involved in kinetochore targeting of checkpoint proteins, Bub1 and Bub3.

Our results demonstrate that Mph1-dependent phosphorylation of Spc7 at conserved MELT motifs is required for Bub1 and Bub3 kinetochore localisation. We were able to reconstitute the interaction between Spc7 and the Bub proteins *in vitro* demonstrating that the Spc7 phosphorylation is sufficient for Bub1 and Bub3 association with Spc7, most likely with Bub3 making the Spc7 contact. Mimicking phosphorylation at the MELT motifs leads to constitutive Bub1 localisation at kinetochores.

We also showed that the N-terminus of Spc7 has microtubule binding activity regulated by Ark1 kinase. Mimicking phosphorylation at Ark1 sites results in reduced amount of recombinant Spc7 co-precipitating with microtubules in microtubule binding assays. Moreover, two stretches of basic residues, that contribute to Spc7 microtubule binding activity, have been mapped in the extreme N-terminus of Spc7. Spc7 also interacts with PP1 phosphatase, Dis2 in *S. pombe*, which

is required for checkpoint silencing, but the mechanism of this interactions remains to be determined.

These findings allow us to speculate on Spc7 role(s) in coupling microtubule binding with spindle checkpoint activation and silencing.

Chapter 1

Introduction

Chapter 1
Introduction

1.1. The Cell Cycle

The cell cycle is an orchestrated and highly regulated series of events leading to eukaryotic cell reproduction (Hartwell and Weinert 1989, Morgan 2007). Intense investigation at the cell cycle was initiated in 1858 by Rudolph Virchow's observation that every cell originates from a pre-existing cell ('*omnis cellula e cellula*'), which is known today as a Virchow's cell theory. Since that time great progress towards understanding of the cell cycle has been achieved. Detailed description of the cell cycle cytology was followed by studies revealing molecular mechanisms controlling cell cycle progression [for review see (Nurse et al., 1998)].

In single-celled organisms the cell cycle results in the generation of entire organisms whereas in multicellular organisms cell division enables tissues and organs to develop and renew. The precision of cell division, especially genetic material distribution to daughter cells, is essential for cell viability and its normal functioning. Basic mechanisms driving and controlling the cell cycle progression are universal in all eukaryotes (Morgan 2007).

The cell cycle typically consists of four phases: G1 phase, S phase, G2 phase and M phase. The two major phases of the cell cycle are S phase and M phase. During S phase genomic DNA is replicated from replication origins by DNA polymerase leading to chromosome duplication (Bell and Dutta, 2002; Kelly and Brown, 2000). Also in S phase centrosomes (spindle pole bodies, SPBs, in yeast) are duplicated. M phase consists of two events: mitosis in which the duplicated chromosomes (called sister chromatids) are equally distributed into two daughter nuclei and cytokinesis in which the cell divides itself. These two processes give rise to two daughter cells. The time window between the end of one M phase and beginning of the next one is called interphase (G1, S and G2 phases). The interphase enables preparation for cell division. The gap phases, G1 and G2, (G1 phase occurs before S

phase whereas G2 phase before M phase) give time for cell growth. They are also important transition points controlling entry to the next cell cycle stage (Morgan 2007).

1.1.1. Regulation of the cell cycle progression

1.1.1.1. Cyclins and cyclin-dependent kinases

The discovery of maturation promoting factor (MPF) in frog oocyte extracts (Duesbery and Vande Woude, 1971; Wasserman and Masui, 1976) was followed by the discovery of cyclin in sea urchin embryos (Evans et al., 1983). Identification of yeast cell division cycle (*cdc*) genes encoding proteins required for successful completion of the particular cell cycle events (Hartwell et al. 1974; Nurse 1975; Nurse et al. 1976) was a milestone in understanding the regulation of cell cycle progression. These findings all together showed that MPF is composed of the protein kinase Cdk1 (*CDC28* in budding yeast, *cdc2* in fission yeast) and mitotic cyclin (cyclin B) and that MPF is essential for entry into mitosis and early mitotic events (Labbé et al., 1989).

The order and timing of cell cycle events is tightly controlled by the cell-cycle control system. Cyclin-dependent kinases (Cdks), conserved serine/threonine protein kinases, are central to this regulatory network (Figure 1.1). Concentrations of these kinases are constant throughout the cell cycle but their activities partly depend on their interactions with the regulatory subunits called cyclins. Cyclins levels are highly regulated by gene expression and proteolysis hence different cyclins are produced at different stages of the cell cycle (G1/S, S and M phase cyclins). Oscillations in cyclin levels result in oscillations in the cyclin-Cdk complexes correlating with rises and falls of kinase activity of the particular cyclin-Cdk complexes. The waves of different cyclin-Cdk kinase activities regulate cell cycle progression (entry into S and M phase and chromosome segregation) by targeting different sets of substrates (Morgan, 1997).

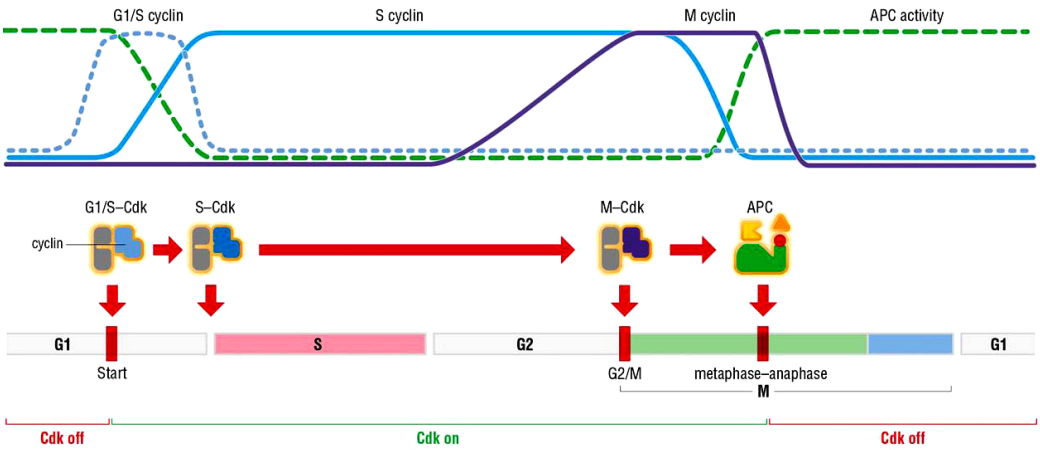

Figure 1.1. Model of the cell-cycle control system. Picture taken from D. Morgan, The Cell Cycle (Morgan, 2007). Oscillations in the levels of the three major cyclins (top) drive the cell-cycle progression. Concentrations of Cdk proteins are constant throughout the cell cycle. Formation of particular cyclin-Cdk complexes activates Cdk and reflects the waves of different cyclins. Active cyclin G1/S-Cdk1 complexes initiate a new division cycle at the Start (Restriction) point in G1. At the beginning of S phase active S-Cdk complexes drive DNA replication. Once DNA replication is completed high levels of M-Cdk lead to the G2/M transition and mitotic spindle assembly. Activation of the APC (Anaphase-Promoting Complex) results in sister chromatid separation and the metaphase to anaphase transition. The APC targets S and M cyclins for destruction which promotes mitotic exit and cytokinesis.

Cdks are master regulators of the cell cycle progression however knowledge about Cdks substrates is limited [for review see (Nigg, 2001)]. Cdk2 was shown to regulate DNA replication and centrosome duplication by phosphorylating the retinoblastoma protein, a well-known tumor suppressor (Meraldi et al., 1999; Matsumoto et al., 1999). In mitosis the cyclin-B-Cdk1 complex targets the lamina triggering mitotic lamina depolymerisation which contributes to nuclear envelope breakdown. Other mitotic substrates of Cdk1 are Eg5 (microtubule motor involved in centrosome separation) and stathmin (a microtubule depolymerising protein which activity is inhibited by phosphorylation) [for review see (Nigg, 2001). Cdk1 is also implicated in cohesin complex phosphorylation, which promotes removal of this complex from chromosome arms during prophase. However, Cdk1 activity is neither necessary nor sufficient for this process [for review see (Nasmyth, 2002)]. Other key substrates of

Cdk1 are the APC (Anaphase-Promoting Complex) activators Cdc20 and Cdh1 (Kramer et al., 2000; Zachariae, 1998; Labit et al., 2012) and the APC itself (Kraft et al., 2003). Cyclin-B-Cdk1-dependent phosphorylation of the APC activates it thereby triggering Cyclin-B-Cdk1 degradation at the end of mitosis (Kraft et al., 2003). The relevance of the APC activators phosphorylation by Cdk1 in APC activity regulation is described below.

Recently, a combination of quantitative proteomics and chemical-genetic inhibition of Cdk1 (wild type Cdk1 was replaced with a mutant protein which can be specifically and rapidly inhibited by the pyrimidine-based inhibitor 1-NMPP1) allowed identification of 308 *in vivo* Cdk1 substrates in budding yeast (Holt et al., 2009). The identified substrates consist of cell cycle-related proteins but also proteins involved in other processes including translation, chromatin remodeling, protein secretion and nuclear transport (Holt et al., 2009).

1.1.1.2. Phosphorylation in cell cycle control

Phosphorylation is omnipresent in the cell cycle. A great number of cell cycle events are modulated via phosphorylation. In addition to Cdks, other kinases such as Aurora A, B and C and Polo kinases are relevant to cell cycle progression.

1.1.1.2.1. Regulation of the Cdk activity

The activity of Cdks is also regulated by phosphorylation which contributes either to Cdk activation or Cdk inactivation depending on phosphorylated residues.
Complete activation of Cdks requires not only cyclin binding but also phosphorylation of a conserved threonine adjacent to the active site by Cdk-activating kinases (CAKs) (Solomon et al., 1992). Phosphorylation can also have an inhibitory effect on Cdk activity. In vertebrate cells phosphorylation at two conserved residues, Thr 14 and Tyr 15, located in the ATP binding site blocks Cdk activity. Wee1 kinase phosphorylates Tyr 15 whereas Thr 14 is phosphorylated by Myt1 kinase which also can phosphorylate Tyr 15 (McGowan and Russell, 1993; Liu

et al., 1997; Mueller et al., 1995b). Phosphorylation at Thr 14 and Tyr 15 is opposed by Cdc25 phosphatase, which activates Cdk (Mueller et al., 1995a).

1.1.1.2.2. Non-Cdk kinases involved in cell cycle

Apart from Cdks other kinases are involved in cell cycle progression. The most important are Polo-like kinase (Plks), Aurora kinase family proteins and Greatwall kinase.

Polo-like kinases (Plks) are conserved from yeast to humans [for review see (Archambault and Glover, 2009)]. Yeast have a single Polo-like kinase, named Cdc5 (cell division cycle 5) in *S. cerevisiae* and Plo1 in *S. pombe*, whereas metazoans have at least two Plks. Vertebrate and yeast homologues of Plk1 are required for mitotic entry by promoting Cdk1 activation (Kumagai and Dunphy, 1996; Mulvihill et al., 1999; Watanabe et al., 2004; Lee et al., 2005; Hagan, 2008). Plk1 regulates the mitotic spindle assembly and functions of spindle pole bodies in yeast and centrosomes in vertebrates [for review see (Archambault and Glover, 2009)]. Moreover, Polo kinases are required for mitotic exit and cytokinesis. Plk1 was reported to activate the APC (Anaphase-Promoting Complex), by phosphorylating Emi1-the APC inhibitor [(Hansen et al., 2004), for review see (Eckerdt and Strebhardt, 2006)].

In addition to Polo-like kinases, Aurora kinases are well known cell cycle regulators [for review see (Fu et al., 2007)]. Mammalian cells express three Aurora kinases: Aurora A, Aurora B and Aurora C, whereas both fission and budding yeast have a single Aurora kinase, Ark1 and Ipl1 respectively. Among mammalian Aurora kinases mitotic functions are exerted by Aurora A and Aurora B. Aurora A is required for centrosome maturation, mitotic entry and mitotic spindle assembly, whereas Aurora B contributes to chromatin modification, regulates kinetochore-microtubule attachments and cytokinesis [for review see (Fu et al., 2007)]. Aurora B in collaboration with Plk1 phosphorylate the cohesin complex subunit Scc3 promoting removal of the cohesin complex from chromosome arms during prophase [for review

see (Nasmyth, 2002, 2011)]. The roles of Aurora B and the yeast Aurora kinase homologues are described later in this chapter. Functions of Aurora C, which is predominantly expressed in the testis and in meiotically dividing gametes (Tseng et al., 1998; Yang et al., 2010), are not clear.

PP2A (Protein Phosphatase 2A) targets Cdk1-Cyclin B-dependent phosphosites, including Cdc25 phosphatase (which is activated once phosphorylated by Cdk1 and Plk1) and Wee1 kinase (which undergoes destruction upon Cdk1 and Plk1-dependent phosphorylation). Consistently, activity of PP2A promotes interphase (accumulation of the dephosphorylated, active form of Wee1) or leads to mitotic exit in cells undergoing mitosis (dephosphorylation of the Cdk1-Cyclin B substrates). In recent years Greatwall kinase has been shown to facilitate Cdk1-Cyclin B activity and phosphorylation of Cdk1-Cyclin B substrates. Therefore Greatwall kinase promotes mitotic entry and maintenance by inhibiting PP2A [(Castilho et al., 2009; Zhao et al., 2008; Mochida et al., 2010) for review see (Glover, 2012)].

1.1.1.3. Proteolysis in cell cycle control

Controlled proteolysis of cyclins, Cdk inhibitors and other cell-cycle regulators ensures irreversibility of transition from one stage of the cell cycle to the next (Morgan 2007).

In eukaryotic cells proteins are destroyed by a large well-characterized protease complex named the 26S proteasome. The 20S proteasome (proteolytic core complex of the 26S proteasome) was originally described as a cylinder-shaped structure (called ‘cylindrin’) of unknown function (Harris, 1968). Further studies revealed that the 26S proteasome consists of the cylinder-shaped 20S proteolytic complex and two 19S regulatory complexes containing about 18 subunits each (Da Fonseca and Morris, 2008; Walz et al., 1998; Wilk and Orlowski, 1983, 1980). The regulatory 19S complexes are usually located at one or both ends of the 20S complex. The 19S regulatory complex contains six different ATPases of the ATPases associated with a variety of cellular activities (AAA) family [for review see (Voges et al., 1999)]. The

AAA ATPases are involved in recognition of proteolytic signals (polyubiquitin chain), substrate unfolding and assembly of the proteasome (Lam et al., 2002).
Proteins selectively targeted for degradation are marked with a polymer of ubiquitins known as a polyubiquitin chain. Ubiquitin is an essential, 76-amino acid polypeptide which can be covalently conjugated to other proteins. Protein ubiquitination requires three different enzymes: E1, an ubiquitin-activating enzyme, E2, an ubiquitin-conjugating enzyme and E3, an ubiquitin-protein ligase [for review see (Pickart, 2001)]. Protein degradation in cell cycle progression is carried out by two E3 RING-type ubiquitin ligases, the SCF (Skp1, Cul1, Rbx1) complex and the Anaphase-Promoting Complex, the APC.

1.1.1.3.1. The SCF complex

The SCF complex is a key ubiquitin ligase for the G1/S transition. The SCF complex is composed of 3 main subunits: Skp1, cullin (Cul1) and the RING protein Rbx1 (RING finger-a domain which binds zinc ions). These proteins form a catalytic core complex that recruits a cognate E2 (Zheng et al., 2002; Nakayama and Nakayama, 2005; Lyapina et al., 1998). Another subunit, called the F-box protein, binds the target protein and the enzyme core via the Skp1 subunit. The F-box protein ensures substrate specificity of the E3 ligase.

The major target of the SCF complex is the Clb5,6-Cdk1 inhibitor-Sic1 (Clb5,6 are the *S. cerevisiae* S-phase cyclins; Clb5,6-Cdk1 complex drives S phase initiation). Sic1 degradation enables the G1/S transition. Initially, the SCF complex was thought to regulate only the G1/S transition (Bai et al., 1996; Feldman et al., 1997; Skowyra et al., 1997) but subsequent studies have showed that the SCF complex is involved in protein degradation through the cell cycle (Watanabe et al., 2004; Guardavaccaro et al., 2003). Recently, a global screen for SCF substrates identified more than 350 potential SCF targets including proteins involved in cell cycle, apoptosis, and signaling pathways (Yen and Elledge, 2008).
In contrast to the APC complex described below, the SCF is constitutively active. The SCF activity is partly regulated by the APC^{Cdh1} dependent proteolysis of its

F-box subunits in G1 phase (Wei et al., 2004; Bashir et al., 2004; Galan and Peter, 1999).

Phosphorylation status of the SCF substrates is also known to regulate SCF activity towards these substrates. For example, the Cdk inhibitor, Sic1, is degraded by the SCF only once it has been phosphorylated (Skowyra et al., 1997). The requirement of being phosphorylated prior to ubiquitination applies to other SCF substrates. Thus the SCF substrates contain so-called phosphodegrons, short sequence elements that are targeted by certain kinases, which lead to substrate recognition and degradation by the SCF complex [for review see (Vodermaier, 2004)].

1.1.1.3.2. The Anaphase-Promoting Complex

Overview

The Anaphase-Promoting Complex (APC) is an E3 ubiquitin ligase which triggers the metaphase to anaphase transition. The APC consists of 14 subunits in humans and at least 15 subunits in budding and fission yeast [(Ohi et al., 2007; Dube et al., 2005), for review see (Barford, 2011)] which is surprising as the SCF complex contains only four subunits. However, similarly to the SCF complex, the APC core has a cullin subunit (Apc2) associated with the RING-finger domain (Apc11), which interacts with E2 enzymes (Figure 1.2) [for review see (Peters, 2006)]. The mass of animal APC is estimated for about 1.5 MDa. It has been suggested that *in vivo* the APC complex might function as a dimer (Passmore et al., 2005). The basic structure of the APC is well conserved between species [for review see (Barford, 2011)].

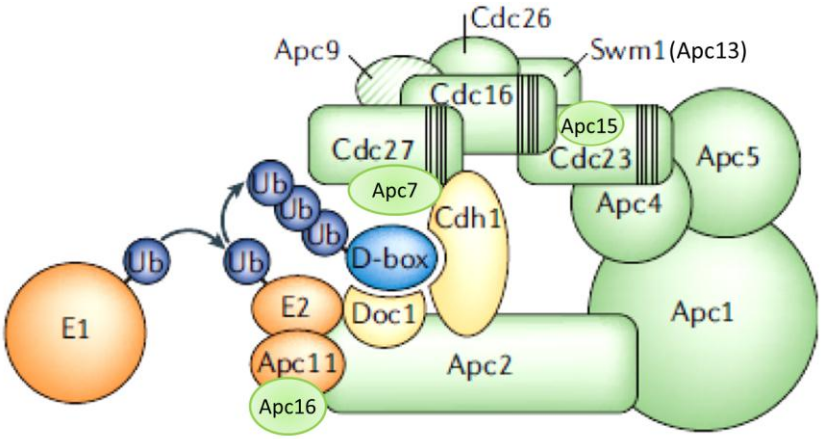

Figure 1.2. Model of the APC-dependent ubiquitination of substrate, picture adapted taken from (Peters, 2006). Protein ubiquitination begins with ubiquitin activation which is achieved through ATP-dependent covalent binding of ubiquitin to the ubiquitin-activating enzyme (E1). Then the ubiquitin is transferred to ubiquitin-conjugating enzyme (E2). The E2 enzyme interacts with the Apc11 subunit of the APC (E3 ubiquitin ligase). The APC facilitates transfer of the activated ubiquitin from the E2 enzyme to the target protein, containing a D-box or/and a KEN-box. The Doc1 (known also as Apc10) subunit together with an APC activator (Cdh1 or Cdc20) constitute a docking site for APC substrates [for a cryo-electron microscopy map of APC/C in complex with the Cdh1 co-activator (APC^{Cdh1}) see (da Fonseca et al., 2011)]. Position of Apc7, Apc15 and Apc16 is based on (Vodermaier and Gieffers, 2003; Vodermaier, 2004; Chibi et al., 2008; Kops et al., 2010; Schreiber et al., 2011; Uzunova et al., 2012). Apc7 and Apc16 has been detected only in human APC. Apc9 is hatched because so far it has been identified in budding yeast APC.

The APC complex targets cyclins, including cyclin B, for degradation at the end of mitosis promoting mitotic exit (Sudakin et al., 1995; King et al., 1995; Schwab et al., 1997). Securin is another mitotic substrate of the APC, whose degradation is essential for chromosome segregation and anaphase onset (Thornton and Toczyski, 2003). The APC complex is also involved in degradation of mitotic kinases, Polo-like kinase 1 (Plk1), Aurora B kinase (Stewart and Fang, 2005; Lindon and Pines, 2004), and other cell cycle regulators including Cdc20 (Robbins and Cross, 2010) and shugoshin (Salic et al., 2004).

APC activators

APC activity requires association of cell-cycle specific co-activators. The APC activators are characterized by the presence of sequence elements mediating APC binding, called the C-boxes and the IR-tails, as well as a C-terminal WD40 domain implicated in substrate recognition [for review see (Peters, 2006)]. Cdc20/Slp1 and Cdh1/Hct1/Swr1 are the most important APC activators (Schwab et al., 1997; Visintin, 1997). Cdc20 activates the APC prior to mitotic exit allowing chromosome segregation and cyclin B degradation. Cdh1 associates with the APC in late mitosis and in early G1 phase which leads to further cyclin destruction (Morgan 2007).

The association of both Cdc20 and Cdh1 with the APC is partly regulated by phosphorylation. The Cdc20 interaction with the APC requires Cdk-dependent phosphorylation of the APC (Kramer et al., 2000; Kraft et al., 2003) and protein phosphatase 2A-dependent dephosphorylation of Cdc20 (Labit et al., 2012). Late in mitosis Cdks activity drops which results in dissociation of Cdc20 from the APC followed by the APC inactivation until another metaphase-to-anaphase transition. Phosphorylation negatively regulates Cdh1 interaction with the APC. In this case phosphorylation of Cdh1 by Cdks blocks Cdh1-APC complex formation (Jaspersen et al., 1999; Zachariae, 1998).

Substrate recognition

A common feature of the APC substrates are amino-acid sequence motifs required for their ubiquitination. The most common motifs are the destruction box or D-box (a degenerated motif containing RXXLXXXXN) and the KEN box (KENXXXN) (Pfleger and Kirschner, 2000; Glotzer et al., 1991). Most APC substrates contain both motifs.

The two major APC activators, Cdc20 and Cdh1, seem to be required for substrate recognition. All the APC activators contain a C-terminal WD40 domain. The WD40 domain is thought to interact with APC substrates containing D-boxes and/or KEN-boxes (Kraft et al., 2005). In recent years the structure of the APC interacting with either Cdh1 or Cdc20 has been observed using cryo-EM which gave better

understanding of the APC activation and substrate recognition/binding (Herzog et al., 2009; Ohi et al., 2007; Chao et al., 2012; Dube et al., 2005). Selection of APC targets most likely involves a co-activator protein (either Cdc20 or Cdh1) together with core APC subunits (Burton and Solomon, 2001; da Fonseca et al., 2011). However, there are studies questioning this hypothesis. For example in *Xenopus* egg extract the APC complex can stably bind cyclin B's D-box in the absence of Cdc20 (Yamano et al., 2004).

1.1.2. The fission yeast *Schizosaccharomyces pombe* cell cycle

The fission yeast *Schizosaccharomyces pombe* is a single celled, free living archiascomycete fungus. The *S. pombe* genome, containing 13.8 Mb, is distributed between three chromosomes and it has been fully sequenced (Wood et al., 2002). *S. pombe* cells grow as stable haploids. Starved *S. pombe* cells form diploids with cells of the opposite mating type then undergo meiosis and sporulate.

Similar to higher eukaryotes, the *S. pombe* cell cycle is composed of four phases: G1, S, G2 and M phases (Figure 1.3). In exponentially growing cultures S phase occurs around the time of cytokinesis and G1 phase is very short, therefore the *S. pombe* cell cycle is extensively controlled at the G2/M transition (Fantes, 1977; Nasmyth et al., 1979). To enter mitosis a cell must complete DNA replication and reach a critical size. As in other eukaryotes, formation of the mitotic spindle occurs in late G2 phase and chromosomes condense early in mitosis. In contrast to the budding yeast, *Saccharomyces cerevisiae*, in which connection to a kinetochore is provided by a single microtubule, fission yeast kinetochores, as in metazoan cells, bind to multiple (usually 2-4) microtubules (McDonald et al., 1992; Ding et al., 1993; Winey et al., 1995). Cell division, as in most mammalian cell types, is symmetric [for review see (Gachet et al., 2006)]. In contrast to higher eukaryotes, in yeast the nuclear envelope does not breakdown which is called closed mitosis [for review see (Fosburg and Nurse 1991)].

In fission yeast the decision to enter the next cell cycle takes place at Start in G1 phase which can be defined as the point of commitment to the cell cycle (Hartwell et al., 1974). Start, called the restriction point in vertebrates, controls the G1/S

transition. To pass through the G1/S transition a cell must achieve a critical cell mass and its G1-phase is expanded to allow this (Nurse, 1975; Nasmyth et al., 1979). The *S. pombe* cell cycle is driven by a single Cdk, Cdc2, which is required both for the G1/S and G2/M transitions (Nurse et al., 1976). DNA replication and mitosis are initiated by association of Cdc2 with B-type cyclin Cig2 and Cdc13, respectively (Mondesert et al., 1996). Two other cyclins, Cig1 and Puc1, have minor roles in G1 phase. Interestingly, a minimal machinery capable of driving the cell cycle progression in *S. pombe* has been recently described (Coudreuse and Nurse, 2010). A protein fusion of Cdc13 and Cdc2 (Cdc13-linker-Cdc2 fusion) under control of the Cdc13 promoter was able to trigger both S and M phases in absence of endogenous Cdc2, Cdc13, Cig2, Cig1 and Puc1.

In addition to being regulated by association with cyclins, Cdc2 kinase activity is modulated via inhibitory phosphorylation by Wee1 and Mik1 kinases and activating dephosphorylation by Cdc25 phosphatase targeting conserved Thr14 and Tyr15 in the ATP binding site of Cdc2. The Cdc2 kinase is inactive in G2 phase as Cdc13 levels are low along with high activity of Wee1 kinase and low activity of Cdc25 phosphatase. Late in G2 phase the level of Cdc13 increases and Cdc25 phosphatase becomes active which results in assembly of an active Cdc2-Cdc13 complex. The Cdc2-Cdc13 complex can, in turn, phosphorylate Wee1 and Cdc25, inactivating and activating these enzymes, respectively. Cdc13 is degraded by the proteasome prior to mitotic exit leading to a drop in Cdc2 activity [for review see (Fosburg and Nurse 1991), (Morgan 2007)].

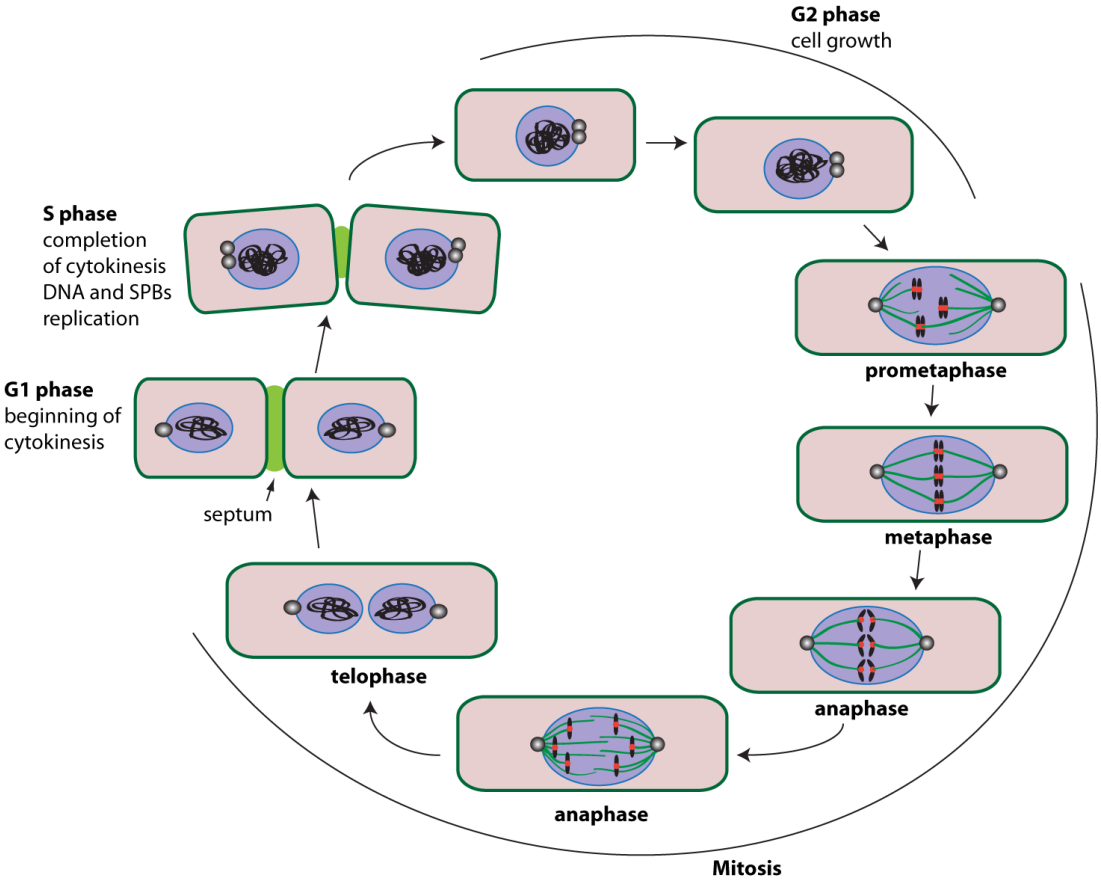

Figure 1.3. Model of the fission yeast cell cycle.
Note that fission yeast G2 phase is very long as it takes about 70 % of the cell cycle (which is not reflected in the model).

1.1.3. Cell cycle checkpoints

Cell cycle events are highly regulated by multiple mechanisms to ensure cell viability and unperturbed cell function. In addition to the regulatory mechanisms described in the previous sections cells evolved checkpoints which control transition from one stage of cell cycle to the next one. The checkpoints monitor completion of one event prior to entering the next one (Hartwell and Weinert, 1989). The checkpoints pathways are not constitutively active and they are not regular events in the cell cycle. Instead, checkpoints are 'turned on' in case of defects in a particular cell cycle event and they block cell cycle progression until the defects are eliminated.

S phase checkpoints: DNA damage and DNA replication checkpoints

Mechanisms ensuring the dependence of mitosis on successful DNA synthesis are called the DNA damage and replication checkpoints [for review see (Harrison and Haber, 2006; Labib and De Piccoli, 2011)]. DNA damage and DNA replication checkpoints delay mitotic entry in response to DNA damage or defects in chromosome replication and give the cell time for DNA repair.

RAD9 was the first identified checkpoint gene. Original studies on *RAD9* showed that this is gene is required to arrest cells in G2 phase in response to DNA damage caused by X-irradiation *S. cerevisiae* (Hartwell and Weinert 1989; Weinert and Hartwell 1988). Further analysis revealed that *RAD9* is not required for cell viability (it is not an essential gene), however chromosome segregation defects are elevated in *rad9* mutants. According to current models Rad9 is an adaptor protein which couples the activation of upstream checkpoint kinase Mec1 (vertebrate ATR, *S. pombe* Rad3), with downstream effector kinase Rad53/Chk2 (Vialard et al., 1998; Gilbert et al., 2001). Mec1 is a key component of DNA damage and DNA replication checkpoints since it senses single-stranded DNA (ssDNA) and defective replication forks, respectively. Yeast Tel1 (vertebrate ATM) is involved in the DNA damage checkpoint by responding to double-strand breaks in DNA via its downstream effector kinase Rad53/Chk2 (Vialard et al., 1998). In vertebrates, Chk2 acts downstream of ATM responding to double-strand breaks, whereas Chk1 acts

downstream of ATR sensing defects at the DNA replication forks [for review see (Labib and De Piccoli, 2011)].

Mitotic checkpoints

Mitosis is monitored by several checkpoints including: the spindle orientation checkpoint which was proposed for fission yeast, the spindle position checkpoint described in budding yeast, the NoCut pathway and the mitotic spindle checkpoint which is conserved from yeast to humans.

In fission yeast latrunculin treatment (actin depolymerising agent) results in maloriented spindle and abnormal astral microtubules which in turn lead to a delay in sister chromatid separation and cyclin B degradation (Tournier et al., 2004; Rajagopalan et al., 2004). This observation argued for the presence of a spindle orientation checkpoint (SOC) in fission yeast [for review see (Gachet et al., 2006)]. The spindle orientation checkpoint was proposed to rely on a subset of the mitotic spindle checkpoint proteins Bub1, Bub3, Mad3 and Mph1 (Tournier et al., 2004; Rajagopalan et al., 2004). Recently, the existence of the spindle orientation checkpoint has been questioned by studies showing that spindle orientation is determined by interphase microtubules prior to mitosis not, as had been proposed previously, by astral microtubules in mitosis (Vogel et al., 2007; Meadows and Millar, 2008).

In budding yeasts cell division occurs at the mother-bud neck. Therefore, budding yeast must move the spindle into the neck before dividing [for review see (Fraschini et al., 2008)]. Delay in spindle movement results in a delay in mitotic exit and cytokinesis (Yeh et al., 1995). This phenomenon is called the spindle position checkpoint which ensures that each daughter cell inherits a nucleus (Adames et al., 2001).

The NoCut pathway was originally described in budding yeast (Norden et al., 2006). The NoCut pathway represses cytokinesis in the presence of chromosomes on the cleavage plane preventing DNA from being damaged during abscission (Norden et al., 2006). In budding yeast the NoCut pathway depends on Ipl1/Aurora B kinase,

which is activated by the chromatin environment (Norden et al., 2006; Mendoza et al., 2009). Downstream effectors of the NoCut pathway are the anillin-like Boi1 and Boi2 proteins which inhibit cytokinesis upon their Ipl1-dependent tethering to the bud neck (Norden et al., 2006). A similar mechanism, which also depends on Aurora B, was observed in HeLa cells (Steigemann et al., 2009).

The mitotic spindle checkpoint called also the spindle assembly checkpoint (SAC) is a mechanism which delays anaphase onset until all kinetochores are attached and bi-oriented at the mitotic spindle (described in detail later).

1.2. Mitosis

The term ‘mitosis’ was coined by Walther Fleming in the 1880’s. The word ‘mitosis’ comes from Greek word ‘mitos’ which means ‘thread’ and refers to the thread-like chromatin seen during cell division (Mitchison and Salmon, 2001).

Chromosome segregation is the ultimate goal of mitosis. To ensure equal chromosome segregation to daughter cells, cells evolved the mitotic spindle checkpoint which monitors chromosome attachment to the spindle microtubules. In the early stages of mitosis the cell prepares machinery required for chromosome segregation (mitotic spindle) and chromosomes themselves. The completion of mitosis consists of sister-chromatid segregation and the formation of two identical daughter nuclei.

Vertebrate mitosis is composed of six sub-phases: prophase, prometaphase, metaphase, anaphase (anaphase A and B) and telophase. In yeast cells a distinction between prophase and prometaphase is not possible as in these organisms the nuclear envelope does not break down (closed mitosis).

In prophase chromosomes start to condense, centrosomes (spindle pole bodies in yeast) separate and the mitotic spindle starts to form. The nuclear envelope breaks down in the beginning of prometaphase. Prometaphase finishes with all the sister chromatids attached to the mitotic spindle at its central region via kinetochores. In metaphase all the sister chromatids are aligned on the metaphase plate awaiting to

separate. Chromosomes are known to oscillate during prometaphase and metaphase which reflects growth and shrinkage of the spindle microtubules connected to kinetochores in bi-polar fashion (each sister kinetochore is attached to microtubule/s emanating from opposite centrosomes/spindle pole bodies).

At this stage microtubule-kinetochore attachments are monitored by the mitotic spindle checkpoint and if they are correct the cell enters anaphase, however if they are improper the cell undergoes metaphase arrest.

In anaphase A the cohesion linkage between sister chromatids, established in S phase, is completely lost and sister chromatids can be pulled towards opposite poles of the spindle. During anaphase B the spindle poles move farther apart from each other segregating sisters into different halves of the cell. Mitosis finishes in telophase when two identical daughter nuclei are formed, the spindle disassembles and chromosomes start to decondense. In vertebrates the nuclear envelope reforms, in yeast the anaphase nucleus is halved during cytokinesis (Morgan, 2007).

1.2.1. Kinetochore

The kinetochore is a multiprotein structure assembled at the surface of the centromeric DNA. The fundamental function of kinetochore lies in providing a linkage between DNA (chromosome) and microtubule plus ends. Chromosome segregation must be extremely well controlled and coordinated with the cell cycle, hence the kinetochore regulatory machinery must also ensure precise and timely distribution of chromosomes to daughter nuclei (Cheeseman and Desai, 2008).

Centromere

The centromere is commonly defined as a specialized chromatin domain, which directs kinetochore assembly. CENP-A (Cse4 in S. *cerevisiae*, Cnp1 in *S. pombe*) is a histone H3 variant believed to be the hallmark of kinetochore identity. Centromeres contain specific CENP-A nucleosomes as well as ‘normal’ H3 nucleosomes (Blower et al., 2002). In fission yeast Cnp1 is deposited at centromere during S and G2

phases (Takahashi et al., 2005) whereas in human cells from telophase until G1 phase (Jansen et al., 2007).

The budding yeast centromere is the smallest and simplest centromere which has been studied so far. It consists of a specific 125 bp sequence divided into three domains: CDEI, CDEII and CDEIII, wrapped on a single nucleosome (point CEN). The CDEI and CDEIII regions are conserved between the yeast chromosome. A single point mutations in the CDEIII region abolish its function whereas mutations in CDEI, including complete deletion of this region, impair centromere function to various degrees (Saunders et al., 1988). Importantly, budding yeast centromere function depends critically on sequence specific DNA-protein interactions [for review see (Cleveland et al., 2003)].

In contrast, vertebrates and fission yeast centromeres can extend over many kilo- and megabases (regional CENs). They seem to be specified by epigenetic mechanisms rather than by sequence-specific binding proteins [for review see (Pidoux and Allshire, 2004)].

All three fission yeast centromeres have an unconserved central core (*cnt*) surrounded by innermost repeats (*imr*) and outer repeats (*otr*) (Figure 1.5) [for review see (Clarke, 1998)]. The central core and innermost repeats make up the central core domain and two outer repeat regions constitute the twin outer repeat domains. The central domain is occupied by Cnp1 and two other conserved proteins Mis6 and Mis12 (Saitoh et al., 1997; Goshima et al., 1999; Takahashi et al., 2000). Cnp1 loading at centromeres is facilitated by the Mis16-Mis18 complex in conjunction with Scm3 (human HJURP) (the most upstream factors in kinetochore recruitment of Cnp1) (Hayashi et al., 2004; Pidoux et al., 2009) , the Mis6-Sim4 complex (Pidoux et al., 2003; Takahashi et al., 2000) and the GATA-type transcription factor, Ams2 (Chen et al., 2003). Kinetochore proteins are assembled on central core chromatin containing Cnp1 (CENP-A).

The outer repeats domains are composed of heterochromatin. Centromeric heterochromatin recruits cohesin and ensures cohesion between sister centromers (Bernard et al., 2001; Nonaka et al., 2002). Moreover, distinct posttranslational

modifications of heterochromatin histones, including histone H3 methylation on lysine 9 (H3K9me), promote Swi6 (hererochromatin protein 1, HP1) binding (Bannister et al., 2001; Nakayama et al., 2001). Swi6 is required for gene silencing. In general, fission yeast and metazoans centromere structures are similar with kinetochore regions flanked by transcriptionally silent heterochromatin.

The molecular composition of kinetochores

In human cells CENP-A associates with CENP-C and 13 interacting proteins (CENP-H, CENP-I, CENP-K–U) (Foltz et al., 2006; Okada et al., 2006). This group of proteins is called the constitutive centromere-associated network (CCAN) as they persist on CENP-A containing nucleosomes throughout the cell cycle. Apart from the CCAN, kinetochore composition changes during the cell cycle [for review see (Fukagawa, 2004; Cheeseman and Desai, 2008)]. Mis18, HJURP (vertebrate homologue of *S. pombe* Scm3) and KNL2, required for CENP-A loading, associate with the centromere transiently from telophase until G1. Late in interphase the Mis12 complex and KNL1, both required for further kinetochore assembly and microtubule binding, localise to kinetochores. A number of proteins including: the Ndc80 complex, Bub1, BubR1, Bub3, CENP-F, the Chromosomal Passenger Complex (CPC, the CPC consists of Aurora B, INCENP, survivin and borealin) and Polo-like kinase (Plk1) accumulate at kinetochores in prophase. Mad1, Mad2, dynein, CENP-E are enriched at kinetochores early in prometaphase and upon microtubule attachment they delocalise along with BubR1. Before anaphase onset Bub1, Bub3, the CPC, Plk1 and CENP-F dissociate form kinetochores. Eventually in anaphase Ndc80 complex, followed by Mis12 and KNL1 delocalise.

S. pombe kinetochores also exhibit dynamic behavior not only in terms of composition but also in terms of localisation. During interphase fission yeast kinetochores are clustered in the vicinity of spindle pole bodies (Uzawa and Yanagida, 1992). Tethering kinetochores to SPBs might be direct as, according to electron microscopy studies, there are no microtubules present between the kinetochores and SPBs (Kniola et al., 2001). Early in mitosis kinetochores are translocated to the middle of the short spindle (Uzawa and Yanagida, 1992). The

molecular composition of kinetochores changes throughout the cell cycle. For example Mis6, Mis12, Sim4, Cnp1 and Spc7 are constitutively associated with kinetochores (Goshima et al., 1999; Takahashi et al., 2000; Pidoux et al., 2003; Kerres et al., 2004) whereas Dis1, Klp5 and Klp6 are transiently present at kinetochores during mitosis (Nakaseko et al., 2001; West et al., 2002).

Electron microscopy pictures of vertebrate kinetochore revealed that the kinetochore is a trilaminar structure on the surface of the centromeric heterochromatin [for review see (Craig et al., 1999)]. The three distinct layers consist of the inner kinetochore, the outer kinetochore and the fibrous corona (the most external part). Chromatin located between two sister kinetochores is called the inner centromere [for review see (Musacchio and Salmon, 2007; Cheeseman and Desai, 2008)]. The multilayer model of kinetochores was also confirmed by high resolution electron microscopy in fission yeast (Kniola et al., 2001).

Vertebrate inner kinetochores consist of CENP-A nucleosomes and CCAN proteins (Figure 1.4). The Ndc80 complex, Mis12 complex, KNL1 and Ska complex are localised in the outer kinetochore. Checkpoint proteins are assembled on the platform provided by outer kinetochore proteins, and together with microtubule motors, microtubule- plus-end-binding proteins (+TIPs) and subunits of the nuclear pore complex (NPC) they make up the corona. It has been also reported that the APC associates with checkpoint components at improperly attached kinetochores (Acquaviva et al., 2004). Aurora kinase, together with other components of the CPC (Chromosomal Passenger Complex) occupies the inner centromere.

The mitotic kinetochore is composed of many different proteins representing several different activities. Forming load-bearing attachments and chromosome segregation constitute primary functions of kinetochores. All other activities of the kinetochore ensure fidelity of these two processes. The kinetochore consists of proteins required for turnover of erroneous attachments and bi-orientation (shugoshin, Bub1, CENP-E etc.), proteins ensuring normal mitotic timing (Mad2, BubR1, Mps1) (Meraldi et al., 2004; Tighe et al., 2008), checkpoint proteins delaying anaphase when chromosome missegregation might occur (Mad1, Mad2, Mad3/BubR1, Bub3, Mps1) as well as

proteins whose activities are required to silence the checkpoint and enter anaphase (PP1 phosphatase, Spindly, dynein).

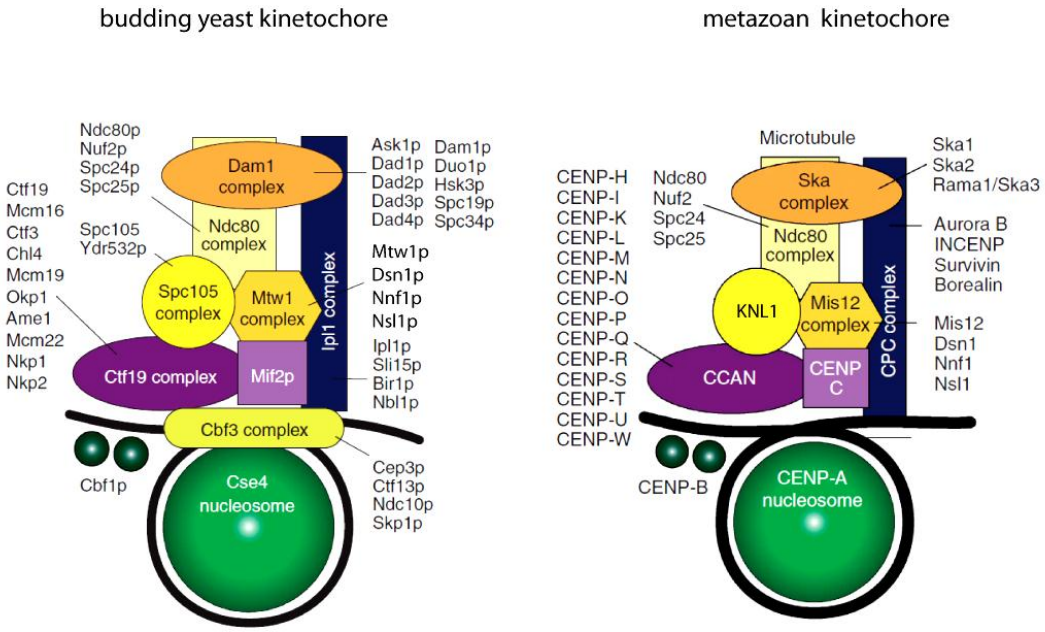

Figure 1.4. Models of *S. cerevisiae* and metazoan kinetochores adapted from (Santaguida and Musacchio, 2009). Although the budding yeast kinetochore is built on a point centromere whereas metazoan kinetochore assembles on regional centromere, the overall organization of the kinetochores is similar. The colours indicate the kinetochore components which have homologous functions in both systems (Santaguida and Musacchio, 2009). Three subunits of the Cbf3 complex (Ctf13, Cep3 and Ndc10) are present only in the organisms with point centromeres (Meraldi et al., 2006).

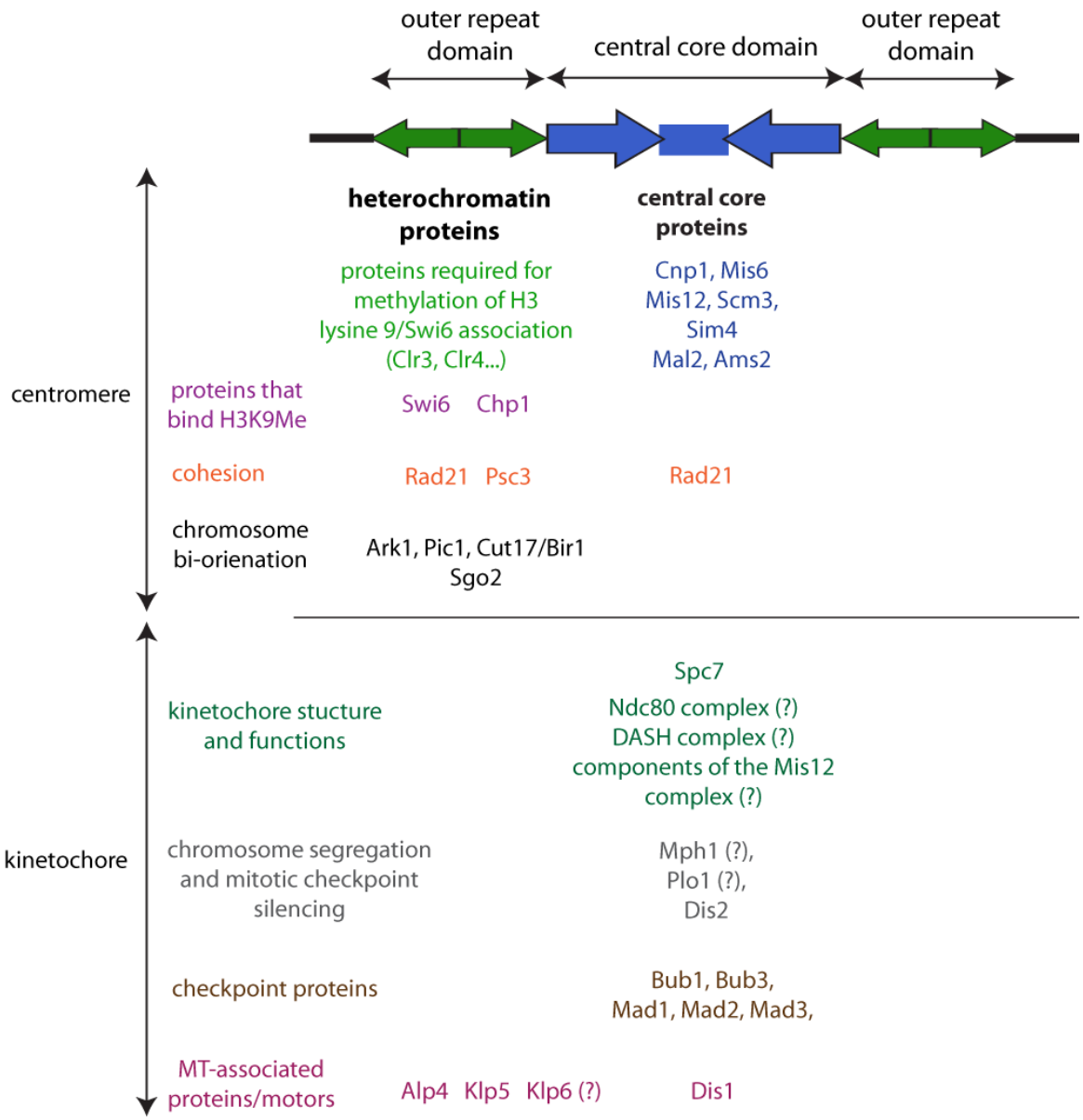

Figure 1.5. The centromere domains and kinetochore protein assembly in fission yeast. Based on (Garcia et al., 2002; Pidoux and Allshire, 2004; Vanoosthuyse et al., 2004; Kerres et al., 2004; Liu et al., 2005; Pidoux et al., 2009). Heterochromatin domain proteins are in the left column, whereas central core domain proteins are in the right column. Proteins are grouped according to role (indicated by colour). Question marks indicate that the association of a particular protein with the outer repeat domain or central core domain has not been verified by published ChIP experiment. Such proteins were allocated to columns based on functional analysis or biochemical data rather than ChIP.

1.2.2. Kinetochore-microtubule interactions

Providing a load-bearing attachment constitutes an essential function of the kinetochore. I will now describe how kinetochore-microtubule attachments are established and regulated.

1.2.2.1. Chromosome capture

Dynamic instability of microtubules, which causes either growth or shrinkage of microtubules (Mitchison and Kirschner, 1984), is proposed to facilitate a 'search and capture' process by which growing microtubules explore cellular space and ultimately bind a kinetochore (Kirschner and Mitchison, 1986).

The initial capture of microtubules by kinetochores takes place in prometaphase just after nuclear envelope breakdown in vertebrate cells. Observations made in living newt lung cells revealed that during initiation of kinetochore-microtubule interactions, the unattached chromosome is repeatedly probed by microtubules emanating from spindle poles which results in rapid movement of the chromosome towards the pole (Hayden et al., 1990). The initial kinetochore-microtubule interactions rely on the association of a single long microtubule with one of the kinetochores of the chromosome (Rieder and Alexander, 1990). In many cases the microtubule extends well past the kinetochore. These findings were confirmed in budding yeast and diatom cells showing that the mechanism is conserved. Taken together, the current model of kinetochore capture by microtubules proposes that capture occurs on the lateral surface of the microtubule and it is followed by poleward transport along the microtubule [for review see (Tanaka et al., 2005b), (Tanaka et al., 2005a; Tippit et al., 1980)].

The efficiency of kinetochore encounter and capture by microtubules is enhanced by the RanGTP-Importin-β complex gradient which is high in the vicinity of the chromosomes and low in the cytoplasm. A high concentration of the RanGTP-Importin-β complex promotes microtubule nucleation close to chromosomes which in turn facilitate the 'search and capture' process (Kalab et al., 2002; Caudron et al., 2005).

Kinetochore (or chromatin)-derived microtubules also contribute to kinetochore-microtubule interactions. The generation of microtubules from the kinetochore itself was first observed in chromosomes isolated from HeLa cells (Telzer et al., 1975). This phenomenon was soon confirmed by *in vivo* studies (Witt et al., 1980; De Brabander et al., 1981). The physiological importance of this process emerged from studies on vertebrate and *Drosophila melanogaster* cells. Studies have shown that kinetochore-derived microtubules were able to interact with microtubules coming from the spindle poles [for review see (Wittmann et al., 2001), (Maiato et al., 2004; Khodjakov et al., 2003).

Upon kinetochore capture by the lateral surface of microtubules chromosomes move towards the poles. In vertebrates and fission yeast kinetochores interact with additional microtubules (kinetochore fibers) during their poleward travel whereas in budding yeast kinetochores remain attached to a single microtubule (Rieder and Alexander, 1990; Hayden et al., 1990; Tanaka et al., 2005a). Kinetochore sliding along a microtubule relies on minus end-directed motors [for review see (Wittmann et al., 2001). In vertebrate cells dynein is involved in this process (Yang et al., 2007b; King et al., 2000). Interestingly, in budding yeast dynein localises outside the nucleus and Kar3, a kinesin-14 family member, which is a slow, non-processive motor causes kinetochore sliding (Tanaka et al., 2007). This difference between vertebrates and yeast might be an evolutionary consequence of the closed mitosis in yeast and the open mitosis in vertebrate cells. Studies in budding yeast showed that when the shrinking microtubules plus-ends reach the kinetochore two things can occur: kinetochores can be attached to the microtubule plus ends (conversion from lateral to end-on attachment) or the microtubule can re-grow (rescue-conversion from MT shrinkage to re-growth). The rescue is promoted by Stu2 (orthologue of vertebrate XMAP215/ch-TOG, *S. pombe* Dis1) transfer from kinetochore to microtubule tips [for review see (Gard et al., 2004), (Gandhi et al., 2011)].

End-on attachment to microtubules is thought to be more stable than lateral attachment and therefore it resists tension upon bi-orientation establishment [for review see (Tanaka, 2010), (Tanaka et al., 2005a)]. In budding yeast only one microtubule is embedded in the kinetochore upon end-on attachment whereas in

fission yeast and metazoans the interaction is provided by multiple microtubules (McDonald et al., 1992; Ding et al., 1993; Winey et al., 1995).

1.2.2.2. Chromosome bi-orientation on the mitotic spindle

Once end-on attachment is achieved a mono-oriented pair of sister chromatids oscillates near the spindle pole. The unoccupied kinetochore gets attached to a microtubules extending from opposite spindle pole leading to bi-orientation or amphitelic attachment (Figure 1.6). Tension applied upon bi-orientation moves kinetochores to the centre of the spindle where they align on the metaphase plate. In some cases aberrant kinetochore-microtubule attachments might occur (Figure 1.6) [for review see (Tanaka, 2010)]. A situation in which both sister kinetochores are attached to microtubules emanating from one spindle pole generating a tensionless interaction is known as a syntelic attachment. In organisms having multiple microtubules connected with a kinetochore (fission yeast, vertebrate), microtubules from opposite spindle poles can capture one kinetochore and this is called merotelic attachment.

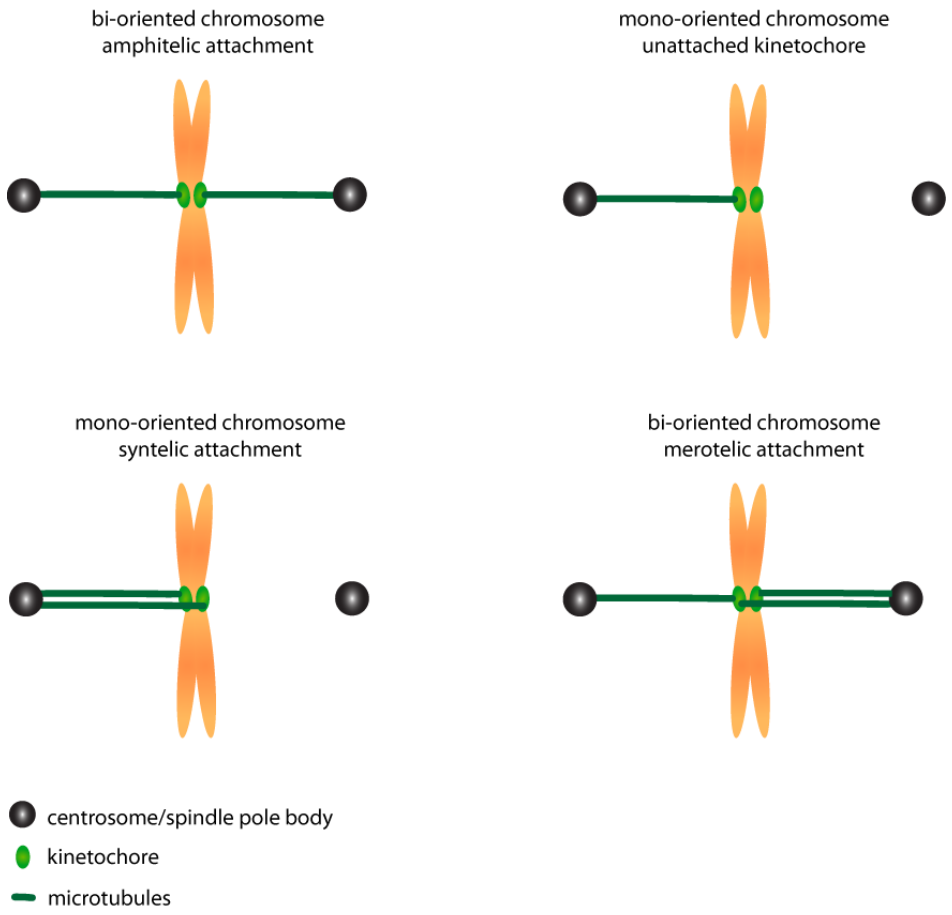

Figure 1.6. Different types of kinetochore-microtubule attachments. Unattached kinetochores and syntelic attachments do not generate tension across the kinetochores which leads to mitotic checkpoint activation. Merotelic attachment does not signal the spindle checkpoint and is corrected by an Aurora B-dependent mechanism [(Knowlton et al., 2006), for review see (Gregan et al., 2011)].

Two mechanisms promoting bi-orientation have been proposed: a kinetochore geometry-dependent mechanism and a tension dependent mechanism (error correction). The first mechanism is based on the back-to-back position of sister kinetochores [for review see (Tanaka et al., 2005b; Tanaka, 2010)]. In mitosis this position is provided by cohesion at centromeres. The geometry-dependent mechanism proposes that when one kinetochore is attached to the spindle microtubules from a given pole, the constraint in geometry makes the other kinetochore face the opposite direction (Ostergren, 1951). This situation promotes association of the unattached kinetochore only with microtubules from the opposite pole. The role of cohesin in kinetochore geometry has been recently investigated in fission yeast by visualizing concealed cohesion within the centromere along with

introducing artificial tethers that can influence kinetochore geometry (Sakuno et al., 2009). The study demonstrated that cohesion within the centromere regulates kinetochore geometry and that increased cohesion at the peri-centromere regions, relative to central core of the centromere, facilitates sister kinetochore geometry for bi-orientation. The kinetochore-geometry mechanism helps to avoid aberrant kinetochore-microtubule attachments but it is unable to correct them if they have already appeared. Improper kinetochore-microtubule interactions are removed by a tension-dependent mechanism [for review see (Tanaka, 2010; Tanaka et al., 2005b)].

The tension-dependent error correction mechanism was first observed in living grasshopper spermatocytes undergoing meiosis I [for review see (Nicklas, 1997), (Nicklas and Koch, 1969)]. During prometaphase bivalents, consisting of two homologous chromosomes, are attached to spindle microtubules via their kinetochores. Sometimes the kinetochores are attached to the same spindle pole which results in mono-polar attachment. In normal conditions these aberrant tensionless attachments are re-oriented to proper bi-polar attachments. This phenomenon indicates that lack of tension triggers the re-orientation process. Nicklas and Koch (1969) used a micromanipulation needle to apply artificial tension to mono-polar bivalents. When tension was applied the wrong attachment was maintained showing that tension stabilizes kinetochore microtubule interactions. The tension-dependent mechanism was confirmed in budding yeast mitosis (Dewar et al., 2004). In this case the experiment relied on an unreplicated circular minichromosome with two centromeres. Although the minichromosomal centromeres lacked the normal back-to-back geometry, tension should be still generated across the two centromeres upon bi-orientation. These minichromosomes were able to bi-orient implying that sister kinetochore geometry is dispensable for bi-orientation (Dewar et al., 2004). According to this study tension-dependent error correction is sufficient to bi-orient chromosomes in mitosis. However there is evidence that kinetochore geometry might assist bi-orientation as a redundant mechanism (Indjeian and Murray, 2007; Sakuno et al., 2009).

An additional mechanism for promoting chromosome bi-orientation was described in vertebrate cells (Kapoor et al., 2006). It was shown that mono-oriented chromosomes

can slide towards the middle of the spindle alongside kinetochore fibers attached to other already bi-oriented chromosomes. This mechanism depends on the kinetochore-associated, plus end-directed microtubule motor CENP-E (kinesin-7) (Kapoor et al., 2006).

1.2.2.3. At the interface of kinetochore-microtubule interactions

Both lateral and end-on attachments are provided by kinetochores [for review see (Joglekar et al., 2010; Cheeseman and Desai, 2008; Westermann et al., 2007)]. The Ndc80 and Dam1 complexes are thought to be the main kinetochore- microtubule linkers. Microtubule binding activities of the kinetochore components Ndc80, Dam1 and KNL1 are all regulated by phosphorylation. Aurora B kinase is known to disrupt kinetochore-microtubule attachments whereas the opposing PP1 phosphatase activity stabilizes the interactions.

Ndc80 complex and KNL1

The Ndc80 complex is evolutionarily conserved from yeast to human. It is composed of four proteins: Ndc80 (mammalian Hec1), Nuf2, Spc24 and Spc25 which was initially shown in budding yeast (Janke et al., 2001). Next, the structural organization of the Ndc80 complex was described. Electron microscopy, X-ray crystallography and biochemical methods demonstrated that the Ndc80 complex consists of two subcomplexes: the Spc24-Spc25 complex and the Ndc80p-Nuf2 complex which are stabilized by a parallel heterodimeric coiled-coil (Ciferri et al., 2005; Wei et al., 2005, 2006). These subcomplexes tetramerize via an interaction of the C- and N-terminal portions of the Ndc80-Nuf2 and Spc24-Spc25 coiled-coils forming the functional Ndc80 complex (Ciferri et al., 2005). The globular domain of Ndc80-Nuf2 interacts with microtubules whereas the globular domain of Spc24-25 makes contact with other kinetochore proteins (Wei et al., 2007; Ciferri et al., 2008; Wei et al., 2006). X-ray crystallography revealed that the Ndc80-Nuf2 globular domain is made of two calponin-homology (CH) domains (Wei et al., 2007; Ciferri et al., 2008). Positively charged residues in the CH domains are important for mediating an interaction with the negatively charged C-terminal tails of tubulin (Ciferri et al., 2008). Aurora B-dependent phosphorylation of an unstructured N-terminal 80- to

100-residue close to the CH domain is involved in regulating Ndc80-microtubule interactions (Ciferri et al., 2008; Cheeseman et al., 2006).

The Ndc80 complex is accompanied by KNL1 (human Blinkin/KNL1, *S. pombe* Spc7, *S. cerevisiae* Spc105) in providing the core of the kinetochore-microtubule interface. Initially *C. elegans* KNL-1 was described by Desai et al. as a kinetochore protein whose RNAi-mediated depletion resulted in a 'kinetochore-null' phenotype (Desai et al., 2003). The 'kinetochore null' phenotype is characterized by complete failure of mitotic chromosome segregation, inability to recruit other kinetochore components and to assemble a stable spindle (Oegema et al., 2001; Desai et al., 2003). Together with the Mis12 complex and the Ndc80 complex KNL1 forms the KNL1-Mis12-Ndc80 (KMN) network (Cheeseman et al., 2004, 2006). KNL1 binds microtubules with lower affinity than Ndc80 but is also highly regulated by phosphorylation during mitosis (Welburn et al., 2010; Espeut et al., 2012; Cheeseman et al., 2006).

Dam1 complex

The Dam1 complex has been proposed to act as a tool that can translate the force generated by microtubule depolymerisation into poleward kinetochore movement [for review see (Westermann et al., 2007)].

The Dam1 complex, also known as the DASH complex, was initially identified in budding yeast where it is essential for microtubule-kinetochore interactions and viability (Hofmann et al., 1998; Cheeseman et al., 2001). The Dam1 complex consists of ten subunits (Duo1, Dam1, Dad1, Spc34, Ask1, Spc19, Dad2, Dad3, Dad4, Hsk3) all of which, except for Dam1 and Duo1, were identified in yeast two hybrid assays followed by biochemical purification (Enquist-Newman et al., 2001; Cheeseman et al., 2001; Li et al., 2002). All ten subunits of the Dam1 complex are well conserved in *S. pombe*, however, in contrast to budding yeast, the fission yeast Dam1/DASH complex is not essential (Liu et al., 2005). Homologues of the Dam1 complex have not been identified outside of fungi. Its functions have been proposed to be carried out by the Ska complex in mammalian cells (see below) (Welburn et al., 2009).

All ten subunits of the Dam1 complex form a soluble heterodecamer *in vitro*, consisting of a single copy of each subunit. Sixteen Dam1 complexes can associate to form a large 50-nm ring complex, which encircles microtubules *in vitro* (Westermann et al., 2006, 2005). Although the Dam1 complex does not have a fixed binding site on the microtubule surface, the ring complex moves processively for several micrometres at the ends of depolymerising microtubules without detaching from the lattice (Westermann et al., 2006). These findings suggest that the Dam1 complex might couple microtubule depolymerisation with (its own) sliding along the microtubule lattice, facilitating chromosome segregation. However, clear evidence for existence of the Dam1 ring complex *in vivo* has not been found so far.

Ska complex

Recently, the Ska complex containing three subunits (Ska1, Ska2 and Ska3), has been identified in vertebrate cells (Hanisch et al., 2006; Gaitanos et al., 2009). The Ska complex has been suggested to complement the KMN network since it possesses microtubule binding activity (Gaitanos et al., 2009). Kinetochore recruitment of the Ska complex depends on the KMN network and the Ska complex was shown to interact with the Ndc80 and Mis12 complexes (Hanisch et al., 2006; Gaitanos et al., 2009; Chan et al., 2012). It has been proposed that metazoan Ska complex might be a functional homologue of the yeast Dam1/DASH1 complex (Welburn et al., 2009). Analysis of the Ska complex structure favours this hypothesis (Jeyaprakash et al., 2012).

1.2.2.4. Factors facilitating bi-orientation and error correction

Chromosome bi-orientation is crucial for the fidelity of cell division. A series of factors is responsible for establishment and maintenance of tension-generating attachment of kinetochores. I will now describe the most important of them.

Aurora B kinase

The evolutionarily conserved mitotic kinase Aurora B (*S. cerevisiae* Ipl1, *S. pombe* Ark1) is crucial for chromosome bi-orientation. The first observation that Aurora B could be involved in this process came from budding yeast. In *ipl1* mutants kinetochore bi-orientation is defective causing a high rate of chromosome missegregation (He et al., 2001; Biggins et al., 1999; Biggins and Murray, 2001). Circular minichromosomes with two centromeres (described above) often failed to bi-orient in the *ipl1* mutant background, suggesting that Ipl1 could facilitate bi-orientation (Dewar et al., 2004). Additionally, the *ipl1* mutant could not re-establish proper kinetochore-microtubule attachments, in contrast to will-type cells (Dewar et al., 2004; Tanaka et al., 2002). In mammalian cells Aurora B inhibition results in the presence of maloriented (syntelic and merotelic attachments) kinetochores (Lampson et al., 2004; Hauf et al., 2003; Ditchfield et al., 2003). Moreover, studies carried out in budding yeast have demonstrated that Ipl1 monitors tension at sister kinetochores (Biggins and Murray, 2001; Pinsky et al., 2006b). In the case of defective tensionless kinetochore-microtubule attachments, Ipl1 kinase activity causes disruption of aberrant attachments. This generates unattached kinetochores which are able to signal the mitotic spindle checkpoint (Pinsky et al., 2006b). Taken all together these results suggest that that Aurora B kinase activity facilitates turnover of the faulty tensionless kinetochore-microtubule interactions promoting establishment of bi-orientation at kinetochores. The mechanism of the Aurora B dependent error-correction has been extensively investigated over recent years, which has generated good understanding of the process.

Aurora B kinase localises to inner centromeres during prometaphase and metaphase (Vader et al., 2006; Klein et al., 2006; Honda et al., 2003). Three other proteins: INCENP, survivin and borealin are associated with Aurora B kinase, forming a

complex known as the Chromosomal Passenger Complex (the CPC) which is crucial for Aurora B activity and cellular localisation [for review see (Ruchaud et al., 2007; Carmena and Earnshaw, 2003)]. Aurora B is located in the vicinity of the kinetochore where it targets kinetochore components. This is thought to weaken kinetochore-microtubule attachments and facilitate their turnover. The most important kinetochore targets of Aurora B have been subsequently identified in many systems including both budding and fission yeast and human [for review see (Liu and Lampson, 2009)]. Key kinetochore associated substrates of Aurora B/Ipl1/Ark1 kinase include: Dam1 complex subunits in budding yeast (Cheeseman et al., 2002), KNL1 in yeast and mammalian cells (Welburn et al., 2010; Liu et al., 2010; Koch et al., 2011) and the Ndc80 complex in budding yeast and humans (Ciferri et al., 2008; Akiyoshi et al., 2009a; Cheeseman et al., 2006; DeLuca et al., 2006). Interestingly, mutants that mimic constitutive phosphorylation of Dam1, Ndc80 and KNL1 results in defective bi-orientation (Welburn et al., 2010; Cheeseman et al., 2002; DeLuca et al., 2006). Experiments that employed fluorescence resonance energy transfer (FRET)-based sensors of Aurora B kinase activity revealed a spatial phosphorylation gradient early in anaphase centred at the spindle midzone (Fuller et al., 2008). This finding suggested that upon anaphase onset Aurora B substrates are gradually dephosphorylated (Fuller et al., 2008). Further works demonstrated that once proper tension-generating kinetochore-microtubule attachments are established, Aurora B substrates including the KMN network, need to be dephosphorylated by PP1 in order to stabilize kinetochore-microtubule interactions (Welburn et al., 2010; Liu et al., 2010).

These results are consistent with the kinetochore stretching model which has been proposed recently (Maresca and Salmon, 2009; Uchida et al., 2009). The model is based on the observation that upon bi-orientation both the kinetochore and centromere are stretched satisfying the mitotic spindle checkpoint. The model suggests that kinetochore stretching moves Aurora B kinetochore substrates away from the kinase which is localised in the inner centromere so that they are no longer under influence of Aurora kinase and can be efficiently dephosphorylated promoting stable attachments and anaphase onset (Figure 1.7). Lately, kinetochore stretching has been investigated at the sub-molecular level. The structure of vertebrate

kinetochore was analysed by immunoelectron microscopy (EM) in the presence or absence of tension from spindle microtubules (Suzuki et al., 2011). The study revealed that under tension the inner kinetochore stretches but the outer kinetochore does not. Amongst the inner kinetochore proteins CENP-T has been show to undergo tension-dependent elongation (Suzuki et al., 2011).

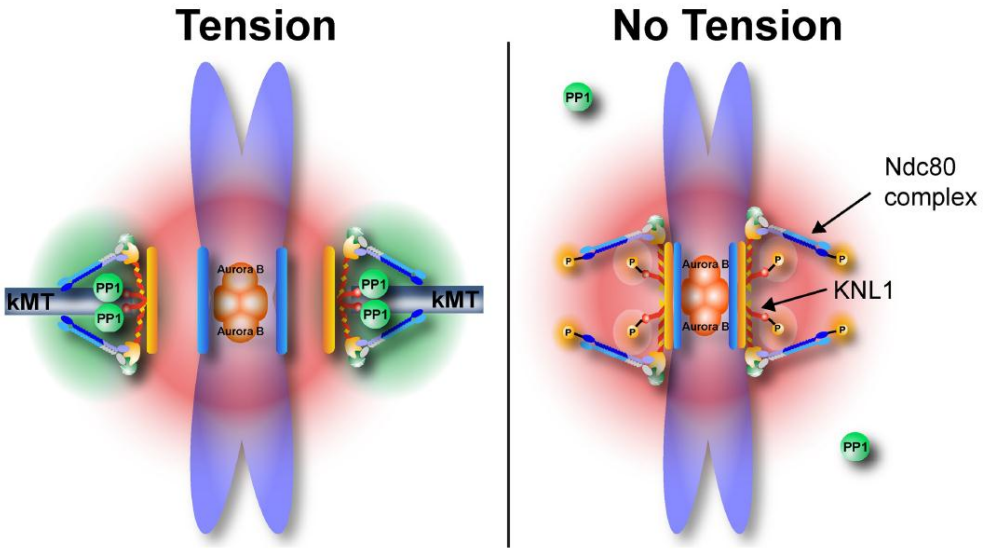

Figure 1.7. Model of Aurora B and PP1 opposing each other at the kinetochore taken from (Liu et al., 2010). When tension is applied to kinetochores (left panel), Aurora B is spatially separated from its kinetochore substrates and consequently they are dephosphorylated. This situation enhances the binding of PP1 and microtubules to kinetochores. In the absence of tension (right panel), Aurora B phosphorylates kinetochore proteins which reduces binding of both PP1 and microtubules to kinetochores.

However, a recent study on human Ndc80 (Hec1) revealed that a subpopulation of Aurora B kinase localised at the outer kinetochore even upon Ndc80 dephosphorylation which occurs as chromosomes bi-orient (DeLuca et al., 2011).

This result suggests that Ndc80 phosphorylation by Aurora B might not be regulated wholly by spatial positioning of the kinase.

Mps1 kinase

Mps1 (Mph1 in *S. pombe*) is an evolutionarily conserved protein kinase of many functions including role(s) in chromosome bi-orientation.

Inhibition of budding yeast Mps1 kinase activity by using the ATP analogue in *mps1-as* mutant background affects many spindle-associated processes including spindle pole body duplication, spindle formation and the spindle checkpoint. In addition, it impairs the positioning of kinetochores on the mitotic spindle and chromosome segregation (Jones et al., 2005). This suggested that Mps1 might be important for tension establishment between sister kinetochores and chromosome bi-orientation. This hypothesis was confirmed by the observation of GFP-marked mini-chromosome behaviour in the *mps1-as* mutant (Maure et al., 2007). Upon Mps1 inhibition the GFP-marked mini-chromosome remained mono-oriented in the vicinity of one SPB whereas in control *MPS1-WT* cells GFP signals were found halfway between two spindle pole bodies. This clearly showed that Mps1 has a crucial role in establishing sister-kinetochore bi-orientation of the mitotic spindle by promoting turnover of tensionless kinetochore-microtubule attachments in budding yeast (Maure et al., 2007).

Similar to Aurora B, Mps1 kinase targets several kinetochore components, which might be required for bi-orientation. Six Mps1 phosphorylation sites have been identified in the budding yeast Dam1 protein *in vitro* (Shimogawa et al., 2006). Loss of phosphorylation at two of these sites results in the localisation of chromosome clusters closer to spindle pole bodies than in wild-type cells. This suggests that Mps1-dependent phosphorylation of Dam1 contributes to efficient coupling of kinetochores to microtubule plus ends. However, impaired kinetochore coupling to microtubule plus ends did not result in bi-orientation defects (Shimogawa et al., 2006). Ndc80 is another budding yeast Mps1 kinetochore target and the *in vitro* and *in vivo* sites have been mapped (Kemmler et al., 2009). The importance of Mps1-dependent phosphorylation of Ndc80 has been mainly investigated with respect to

spindle checkpoint (see later). However, it has been demonstrated that Ndc80 phosphomimetic mutants bi-orient their chromosomes just as well as wild type cells (Kemmler et al., 2009), which is in opposition to hypotheses arguing for Mps1 destabilizing kinetochore-microtubule interactions. In mammalian cells borealin has been described as an Mps1 substrate (Jelluma et al., 2008a). Mps1-dependent phosphorylation of borealin enhances Aurora B activity specifically at centromeres. Consequently, activated Aurora B corrects incorrect kinetochore-microtubule attachments (Jelluma et al., 2008a). A recent study has shown that human Mps1 kinase activity is required for centromere localisation of Sgo1, probably by recruiting Bub1 kinase to kinetochores which in turn phosphorylates histone H2A (Maciejowski et al., 2010). The connection between Aurora B and Mps1 is controversial as some studies propose that Aurora B acts upstream of Mps1 (Santaguida et al., 2010; Hewitt et al.; 2010, Jelluma et al., 2010; Heinrich et al., 2012) and others argue for positive feedback between the two kinases (Saurin et al., 2011).

PP1 phosphatase

The observation that mimicking constitutive phosphorylation of Aurora B substrates *in vivo* is as devastating as preventing phosphorylation implicates the existence of a phosphatase opposing Aurora B kinase activity (Welburn et al., 2010; Cheeseman et al., 2002; DeLuca et al., 2006). The PP1 phosphatase (*S. cerevisiae* Glc7, *S. pombe* Dis2), which had been studied for many years in yeast (Francisco and Chan, 1994; Cheeseman et al., 2002; Pinsky et al., 2006; Vanoosthuyse and Hardwick, 2009; Meadows et al., 2011) and in mammalian cells (Trinkle-Mulcahy et al., 2006; Trinkle-Mulcahy, 2003), has been widely accepted as the main phosphatase which opposes Aurora B kinase activity.

It has been recently shown that PP1/Dis2 binds to KNL1 (Spc7 in *S. pombe*) via two very well conserved PP1 binding motifs SILK and RVSF (Liu and Lampson, 2009; Meadows et al., 2011). In HeLa cells the PP1 interaction with KNL1 is negatively regulated by Aurora B kinase (Liu et al., 2010). Recruitment of PP1 is required to

oppose Aurora B activity at kinetochores. PP1 dephosphorylates Aurora B substrates which in turn stabilizes microtubule attachments (Liu et al., 2010).

Shugoshin

The shugoshin proteins were originally identified in *Drosophila* as proteins required for proper chromosome segregation (Tang et al., 1998; LeBlanc et al., 1999). Members of the shugoshin family are important for protecting centromeric cohesion especially in meiosis [for review see (Watanabe and Kitajima, 2005)]. The observation that yeast shugoshins (Sgo1 in *S. cerevisiae*, Sgo1 and Sgo2 in *S. pombe*) mutants had elevated rates of chromosome missegregation raised the possibility that the shugoshins are required for chromosome bi-orientation. Initially, budding yeast Sgo1 was proposed to be a kinetochore tension sensor (Indjeian et al., 2005). Another study demonstrated that budding yeast Sgo1, together with Bub1 kinase domain (Bub1 is also a mitotic checkpoint protein), is required to ensure chromosome bi-orientation and proper segregation. However, the study did not determine if Bub1 phosphorylates Sgo1 directly (Fernius and Hardwick, 2007). Fission yeast Sgo2 was shown to promote chromosome bi-orientation by regulating localisation of the Chromosomal Passenger Complex in mitosis (Vanoosthuyse et al., 2007; Kawashima et al., 2007). Survivin (Bir1) was proposed as a Sgo2 interactor which promotes Aurora B and other components of the Chromosomal Passenger Complex to associate with the peri-centromeric region (Kawashima et al., 2007). Recently histone H2A has been identified as a Bub1 kinase substrate in *S. pombe* (Kawashima et al., 2010). Bub1-dependent phosphorylation of histone H2A is required to target Sgo2 to centromeres which in turn localises Aurora B at the centromere, where it facilitates chromosome bi-orientation (Kawashima et al., 2010).

Haspin

Haspin is a serine/threonine mitotic kinase well-conserved from yeast to human [for review see (Higgins, 2010)]. Recent studies demonstrated that haspin promotes chromosome bi-orientation.

In mitosis haspin phosphorylates histone H3 at threonine 3 (Dai et al., 2005). This phosphorylation generates a chromatin binding site for the Chromosomal Passenger Complex (CPC) at centromeres (Wang et al., 2010; Kelly et al., 2010; Yamagishi et al., 2010). It has been proposed that haspin-dependent phosphorylation of threonine 3 in histone H3 and Bub-1 dependent phosphorylation of serine 121 in histone H2A collaborate in targeting CPC to centromeres (Yamagishi et al., 2010).

1.2.3. Chromosome segregation

Long before entering mitosis cells need to prepare chromosomes for segregation which occurs in anaphase. Sister chromatid cohesion is crucial to ensure the proper structure of mitotic chromosomes, their bi-orientation and their segregation (Tanaka et al., 2000; Sonoda et al., 2001) .

Cohesion

Two mechanisms provide sister chromosome cohesion. The first one is called DNA catenation. It occurs when two replication forks encounter each other during DNA replication. Catenation causes intertwining of duplicated DNA molecules. This tangle needs to be removed by an enzyme called topoisomerase before metaphase so eventually catenation does not contribute much to sister chromosome cohesion [for review see (Shintomi and Hirano, 2010), (Morgan, 2007)].

The main mechanism ensuring sister chromatid cohesion relies on cohesin loading during S phase [for review see (Nasmyth, 2002)]. In eukaryotic cells the conserved cohesin complex mediates sister chromatid cohesion. The cohesin complex is composed of two SMC proteins (for Structural Maintenance of Chromosomes), Smc1 and Smc3, and two non-SMC proteins-Scc1and Scc3 (Figure 1.8) [for review see (Nasmyth and Haering, 2005; Nasmyth, 2011), (Haering et al., 2002)]. Smc1 and Smc3 are extended proteins in which 45 nm long coiled-coil regions separate two globular domains: one domain possessing ATPase activity (head domain) and another forming a ‘hinge’ domain. Heterodimerization of Smc1 and Smc3 via their ‘hinge’ domains followed by ATP-dependent interaction between the ATPase

domains results in formation of the ‘ring’ structure, which may encircle two sister chromatids (Haering et al., 2002; Anderson et al., 2002; Ivanov and Nasmyth, 2005).

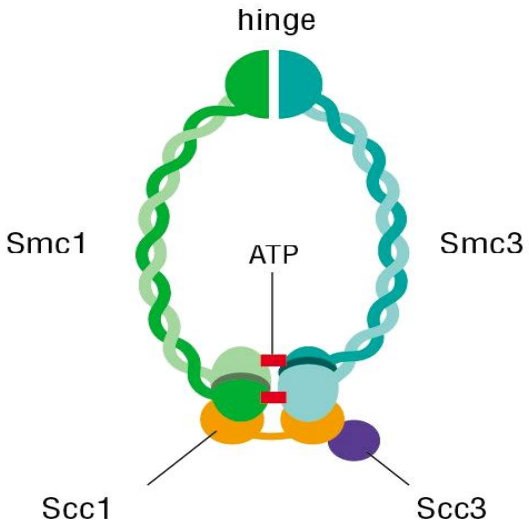

Figure 1.8. ‘Ring model’ of the cohesin complex taken from (Morgan, 2007). Two SMC (for Structural Maintenance of Chromosomes) proteins, Smc1 and Smc3 interact with each other via their globular ‘hinge’ domains creating a V-shape structure. ATP binding brings the two ATPase domains together closing ‘the ring’. The SCC1 subunit of the cohesin complex connects the two ATPase domains which results in formation of the ‘ring structure’. Then two non-SMC subunits of the cohesin complex, Scc1 and Scc3 bind the ring in the vicinity of the globular ATPase domains.

As mentioned above sister chromatid cohesion is established during DNA replication. The bulk of vertebrate cohesin dissociates from chromosomes between prophase, when chromosomes start to condense, and prometaphase when chromosome bi-orientation is achieved (Sumara et al., 2000; Losada et al., 2002). Cohesin is removed from chromosomes arms mainly in separase-independent manner in vertebrate cells (Waizenegger et al., 2000), whereas in budding yeast cohesin removal solely depends on separase (Pds1) and occurs at anaphase onset (Uhlmann et al., 1999, 2000). In vertebrate cells cohesin dissociation from chromosome arms is regulated by its Polo-like kinase (Plk1)- and Aurora B-dependent phosphorylation (Losada et al., 2002; Hauf et al., 2005). However, a fraction of cohesin persists on chromosomes until anaphase onset. This cohesin pool

is enriched mainly at centromeres providing the only linkage between sister chromatids in metaphase. The residual centromeric cohesin is protected by shugoshin protein (Sgo1 in human cells) (McGuinness et al., 2005) in collaboration with PP2A phosphatase, which associates with Sgo1 and counteracts Plk1 and Aurora B kinase activities at centromere (Kitajima et al., 2006; Tang et al., 2006). Upon anaphase onset the Scc1 subunit of the cohesin complex is cleaved by separase (Figure 1.9) (Uhlmann et al., 1999; Hauf et al., 2001). Cohesin cleavage leads to release of sister chromatids from the cohesin rings which enable them to segregate to opposite spindle poles. Anaphase is initiated by cohesin cleavage, as mentioned above, and by the APC-dependent destruction of cyclin B (Sudakin et al., 1995; King et al., 1995).

.If chromosome segregation might result in unequal distribution of chromosomes to daughter nuclei, which is the case in the presence of aberrant kinetochore-microtubule attachments, cohesion cleavage is inhibited. The inhibition of cohesin cleavage is a consequence of mitotic checkpoint activation.

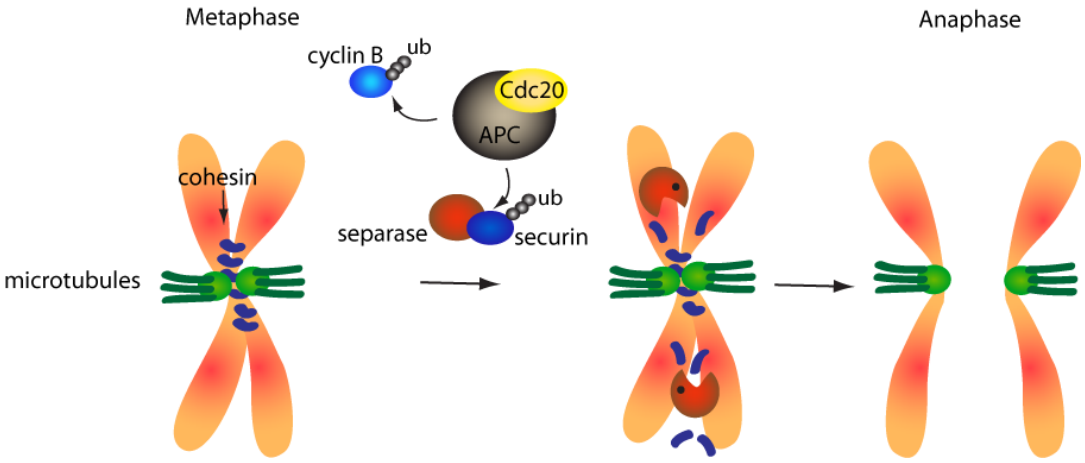

Figure 1.9. Metaphase to anaphase transition. The metaphase to anaphase transition is triggered by degradation of securin and cyclin B mediated by the APC^{Cdc20}. Separase is a cysteine protease responsible for triggering anaphase by hydrolysing cohesin. Securin is a separase inhibitor. Securin degradation liberates separase which cleaves centromeric cohesin. This allows the sister chromatids to separate and enter anaphase. See text for references.

Cytokinesis

Anaphase results in generation of two daughter nuclei, which are distributed into separate cells during cytokinesis [(Morgan 2007), for review see (Pollard, 2010)] . *S. cerevisiae* divides by forming a bud which increases in size throughout the cell cycle. Once mitosis is completed the bud detaches from the mother cell. The *S. pombe* cells divide by septation - a new cell wall (septum) is built at the midpoint of the cell. In vertebrate cells a cleavage furrow halves the cell. In the organisms mentioned, cytokinesis relies on a contractile ring which is positioned at the inner surface of cell membrane, at the site of cell division. This apparatus contains bundles of actin and the motor protein myosin II, whose gradual contraction pulls the cell membrane inward leading to cell division.

1.3. Mitotic spindle checkpoint

Overview

The mitotic spindle checkpoint is the last control mechanism before final and irreversible segregation of chromosomes to daughter nuclei. If kinetochore-microtubule attachments are missing or aberrant, the mitotic spindle checkpoint arrests cell in metaphase. This gives the cell time to establish/re-establish proper kinetochore-microtubule interactions which is crucial as chromosome missegregation might lead to aneuploidy.

The mitotic spindle checkpoint can sense two types of events: unattached kinetochores and lack of tension on sister kinetochores. Observations suggesting that the mitotic spindle checkpoint responds to unattached kinetochores came from experiments in which an unattached kinetochore was destroyed by laser ablation in rat kangaroo (Ptk) cells previously arrested in metaphase (Rieder et al., 1995). Upon removal of the unattached kinetochore, cells entered anaphase. This experiment demonstrated that the mitotic checkpoint signal is generated by unattached kinetochores and that one unattached kinetochore is enough to activate the checkpoint. The importance of tension in spindle checkpoint activation was tested by applying tension at improperly attached chromosomes with a micromanipulation

needle in praying mantid spermatocytes (Li and Nicklas, 1995). Artificially applied tension triggered anaphase onset showing that the lack of tension at faulty attached chromosomes signals the mitotic spindle checkpoint.

The anaphase delay, induced by checkpoint activation, is the result of Anaphase-Promoting Complex (APC) inhibition. Checkpoint proteins, directly and indirectly, target APC activity. Upon APC inhibition, the APC substrates whose degradation is required for the metaphase to anaphase transition, securin (separase inhibitor) and cyclin B, are stably maintained. High mitotic levels of securin and cyclin B result in metaphase arrest [for review see (Zich and Hardwick, 2010; Musacchio and Salmon, 2007)].

The spindle checkpoint proteins were originally identified in two budding yeast screens for mutants which were unable to arrest in mitosis in the presence of spindle depolymerising agents. The genes identified in these screens were: MAD1, MAD2 and MAD3 (for mitotic-arrest deficient) (Li and Murray, 1991) and BUB1, BUB2 and BUB3 (for budding uninhibited by benzimidazole) (Hoyt et al., 1991). All of them are core components of the mitotic checkpoint, except for BUB2 which is involved in the mitotic exit network (MEN) in budding yeast (Piatti et al., 2006). The mitotic spindle checkpoint pathway is highly conserved in eukaryotes, which was confirmed by identification of the checkpoint proteins homologues in other organism. Additionally, other proteins including mitotic kinases Mps1 (Mph1 in *S. pombe*) and Aurora B (Ipl1 in *S. cerevisiae*, Ark1 in *S. pombe*) are involved in checkpoint but they also regulate other processes and so were not identified in the Mad/Bub screens. The core components of the spindle checkpoint are not essential in yeast but they are essential in vertebrates as complete checkpoint gene knockouts are embryonic lethal in mice [for review see (Kops et al., 2005b), (Baker et al., 2004; Wang et al., 2004; Dobles et al., 2000)].

1.3.1. How does the mitotic checkpoint work?

The mitotic checkpoint signal originates from unattached kinetochores and from syntelic kinetochore-microtubule attachments (Figure 1.10). In both cases sister kinetochores lack tension. Aurora B kinase recognises and signals tensionless

kinetochores and recruits Mps1 kinase to kinetochores in human and fission yeast cells (Santaguida et al., 2010; Jelluma et al., 2010; Heinrich et al., 2012). Kinetochore-localised Mps1 kinase targets the core checkpoint components including Mad1, Mad2, BubR1 (Mad3), Bub1 and Bub3 to kinetochores (Millband and Hardwick, 2002; Maciejowski et al., 2010; Heinrich et al., 2012). Aurora B and Mps1 kinases act upstream of other checkpoint proteins. They are **signalers** of the checkpoint pathway as they initiate and transduce the checkpoint response (see section 1.3.1.1).

Upon checkpoint activation, checkpoint proteins are enriched at kinetochores in a hierarchical order (Heinrich et al., 2012). Kinetochore localization of Bub1-Bub3 is required to recruit Mad1, Mad2 and Mad3, and Bub1-Bub3 constitute a scaffold for Mad3 at kinetochores (Vanoosthuyse et al., 2004; Millband and Hardwick, 2002; Windecker et al., 2009; Rischitor et al., 2007). Mad1 is required for Mad2 kinetochore recruitment and the Mad1-Mad2 scaffold recruits more Mad2 (Vink et al., 2006). Mad2 undergoes a conformational change at the kinetochore which is crucial for Mad2 activation and its ability to inhibit the APC (the 'template model' described in section 1.3.1.3) (De Antoni et al., 2005). The presence of checkpoint proteins at tensionless kinetochores requires association of the checkpoint components with kinetochore proteins. In recent years KNL1 (Spc7 in *S. pombe*) has been shown to constitute a kinetochore binding site for Bub1-Bub3 complex (Kiyomitsu et al., 2007, 2011). Less is known about the interaction between Mad1-Mad2 complex and the kinetochore. The Ndc80 complex has been proposed to mediate this interaction but detailed biochemical analysis is still required to confirm this hypothesis (DeLuca et al., 2003; Martin-Lluesma et al., 2002). Bub1-Bub3, Mad1-Mad2 and KNL1/Spc7 **scaffolds** are described in section 1.3.1.2.

The ultimate goal of the checkpoint is to inhibit Cdc20, an APC activator, and arrest cells that have tensionless kinetochores in mitosis. Mad2, BubR1 (Mad3) and Bub3 bind transiently to tensionless kinetochores where they undergo activation (Howell et al., 2004). Once activated, these proteins can bind cytoplasmic Cdc20 and form the MCC (Mitotic Checkpoint Complex). The MCC associates with the APC which results in APC inhibition. Therefore the Mad2, BubR1 and Bub3 proteins constitute a

diffusible wait-anaphase signal or, in other words, they are **effectors** of the checkpoint signalling pathway (see section 1.3.1.3). Checkpoint-dependent inhibition of the APC leads to accumulation of APC substrates including cyclin B and securin which blocks cell cycle progression.

Once proper kinetochore-microtubule interactions are established, the spindle checkpoint is satisfied and the cell resumes the cell cycle (see section 1.3.1.5).

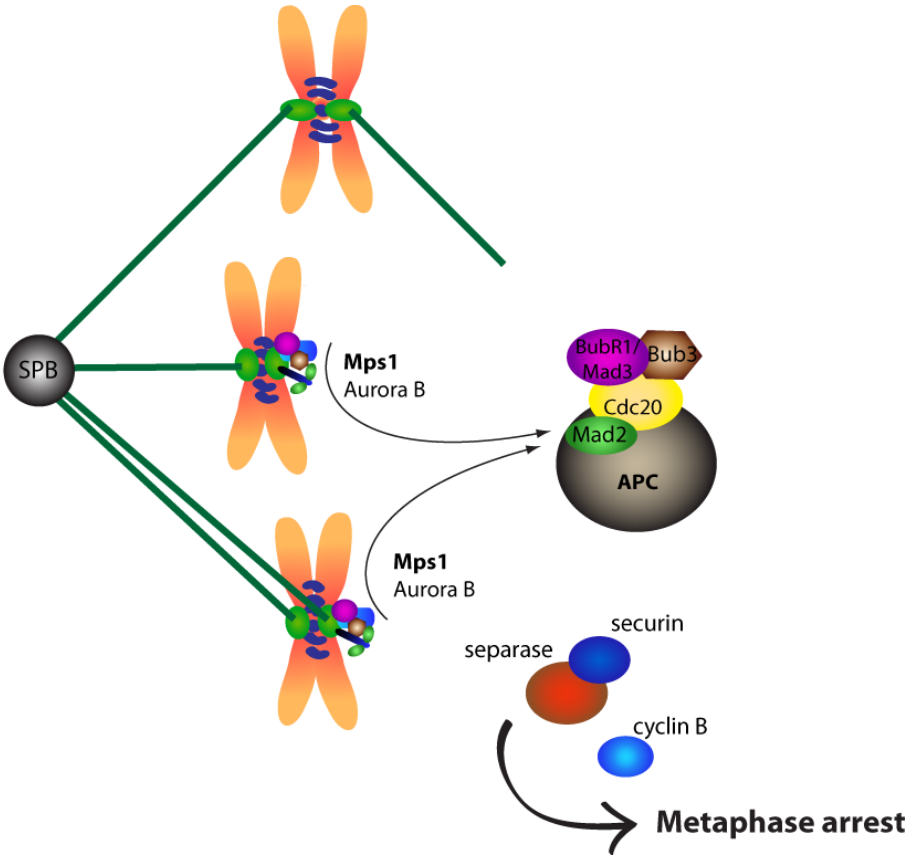

Figure 1.10. Spindle checkpoint activation - a simple model. Spindle checkpoint signaling is triggered by tensionless kinetochore-microtubule interactions, including lack of kinetochore attachment and syntelic attachment. Some checkpoint proteins (e.g. Mad1 and Bub1) stably bind to unattached kinetochores and provide scaffolds for other checkpoint proteins (effectors). Soluble effectors are activated at the kinetochores and then proceed to inhibit the APC. Mitotic kinases enhance checkpoint signaling by phosphorylating checkpoint proteins and other proteins required for an efficient checkpoint establishment (for example kinetochore proteins which recruit checkpoint proteins).

1.3.1.1. Signalers

The spindle checkpoint signal is transduced and amplified by phosphorylation. Mps1 and Aurora are the major checkpoint kinases whereas Bub1 kinase plays a minor role in this process. All checkpoint proteins are phosphorylated which might contribute to stabilization of protein-protein interactions and formation of active kinetochore scaffolds (Mad1-Mad2 and Bub1-Bub3).

Mps1 kinase

Mps1 is a dual-specificity kinase (able to phosphorylate serines/threonines and tyrosines), and is essential in budding yeast and vertebrates. Mps1 kinase is required for a functional spindle checkpoint in yeast and vertebrate cells [for review see (Zich and Hardwick, 2010)]

The *MPS1* (mono-polar spindle 1) gene was identified in *S. cerevisiase* (Winey et al., 1991). The original *mps1-1* mutant was unable to duplicate its spindle pole body which is critical to establish a bi-polar spindle. In addition, the *mps1-1* cells were unable to arrest in mitosis with their defective spindles and exhibited a high rate of chromosome missegregation (Winey et al., 1991).

Mps1 orthologs have been identified in fission yeast (He et al., 1998), humans (Lindberg et al., 1993; Mills et al., 1992), mice (Douville et al., 1992), *Xenopus* (Abrieu et al., 2001) and other systems including plants. Interestingly, an Mps1 homologue has not been identified in the nematode *Caenorhabditis elegans*. It was soon observed that Mps1 expression is correlated with cell proliferation (Mills et al., 1992) and cell cycle progression (Schmandt et al., 1994).

Mps1 consists of an N-terminal kinetochore binding region (Stucke et al., 2004) and a conserved C-terminal kinase domain (Lauzé et al., 1995). Both regions have been recently crystallized (Chu et al., 2008; Wang et al., 2009; Lee et al., 2011; Kwiatkowski et al., 2010). A TPR domain, similar to these in Bub1 and BubR1, was reported in the N-terminus of human Mps1 (Lee et al., 2011).

To exhibit full kinase activity Mps1 has to be autophosphorylated within the activation domain and the P+1 loops. Mps1 autophosphorylation occurs in mitosis.

The residue on which phosphorylation is required to obtain full Mps1 kinase activity has been mapped in mammalian cells and shown to be T676 in the activation loop (Jelluma et al., 2008b; Kang et al., 2007; Mattison et al., 2007). Mutating T676 to alanine causes only a 1.4-fold reduction in autophosphorylation (Mattison et al., 2007). A second important phosphosite, T686, was shown to be located in the P+1 loop (Mattison et al., 2007; Wang et al., 2009). Alanine substitution at this site decreases the kinase activity by at least 40 fold (Mattison et al., 2007). Moreover phospho-T686 antibody abrogates the Mps1 kinase activity (Wang et al., 2009). Therefore phospho-T686 has been proposed to be a feature of active Mps1 kinase whereas phosphorylation at T676 may be a priming event for phosphorylation at T686 (Wang et al., 2009).

Autophosphorylation at these sites is essential for Mps1functions. In human cells reducing Mps1 autophosphorylation affects the mitotic checkpoint and leads to chromosome missegregation (Kang et al., 2007; Jelluma et al., 2008b). Also, in budding yeast impaired Mps1 autophosphorylation results in a defective mitotic checkpoint (Mattison et al., 2007).

Kinase autophosphorylation might be achieved either by intermolecular (transphosphorylation) or intramolecular (cisphosphorylation) mechanisms. Mps1 kinase has been shown to use the first mechanism. Initially, Mps1 transphosphorylation was shown *in vitro* (Kang et al., 2007; Wang et al., 2009; Mattison et al., 2007), in parallel it has been demonstrated that induced dimerization of Mps1 is sufficient to activate the kinase *in vivo* (Kang et al., 2007). This mechanism can take advantage of high Mps1 concentrations at kinetochores during mitosis (Kang et al., 2007; Jelluma et al., 2010; Howell et al., 2004), but there is also the possibility that Mps1 undergoes autophosphorylation at the centrosome/spindle pole body where its local concentration is elevated as well. In mammalian cells Mps1, similarly to other proteins involved in the checkpoint response including Bub1, Bub3, Mad1, Mad2 and Cdc20, localises to unattached kinetochores in prophase. Mps1 persists at kinetochores throughout anaphase (Howell et al., 2004). Kinetochore localisation of Mps1 was also seen in budding yeast (Castillo et al., 2002). Human Mps1 kinetochore localisation requires the presence of the

Hec1/Ndc80-Nuf2 complex and the RNA processing 4 (PRP4) protein kinase at the kinetochore (Stucke et al., 2004; Montembault et al., 2007).

In budding yeast Mps1 is required for spindle pole duplication (Winey et al., 1991) whereas its role at vertebrate centrosome remains controversial. Studies in mouse confirmed a role for Mps1 in centrosome duplication and showed that in mouse Mps1 is regulated by Cdk2 for this process (Fisk and Winey, 2001). However there is also evidence which shows that human Mps1 is dispensable for centrosome duplication (Stucke et al., 2002; Kwiatkowski et al., 2010).
In contrast to the unclear function of Mps1 in centrosome duplication, the major role of Mps1 in mitotic checkpoint signaling has been consistently reported by different studies in different organisms (Stucke et al., 2004; Liu et al., 2003; He et al., 1998; Hardwick et al., 1996; Abrieu et al., 2001; Dorer et al., 2005; Winey et al., 1991).

In budding yeast Mps1 overexpression induces mitotic arrest in the absence of perturbed spindle (Hardwick et al., 1996). This phenomenon is correlated with Mad1 hyperphosphorylation. This suggests that Mad1 might be a true Mps1 substrate as Mps1 phosphorylates Mad1 *in vitro* (Hardwick et al., 1996). Moreover, it has been reported that Mad1 association with Bub1-Bub3 complex requires Mps1 (Brady and Hardwick, 2000). Surprisingly, budding yeast Mps1 overexpression is capable of activating the checkpoint independently of kinetochores, which has been demonstrated in *ndc10-1* strains (Fraschini et al., 2001a). *Ndc10-1* cells do not arrest in mitosis under normal condition due to lack of functional kinetochores, (*ndc10-1* mutation destroys kinetochores), which eliminates the kinetochore-dependent branch of the checkpoint signaling. Mps1 overexpression bypasses a requirement for the kinetochore pathway indicating a central role for Mps1 in the mitotic spindle checkpoint. A similar observation was recently made in human cells. Expression of the Mps1 kinase mutant that is unable to binds to kinetochores, generates a soluble pool of cytoplasmic kinase, which delays anaphase (Maciejowski et al., 2010). This suggests that Mps1 kinase phosphorylate the APC and that can make the APC sensitive to inhibition by MCC. However, this hypothesis remains unconfirmed. Recently Mps1 activity has been shown to facilitate formation of the Cdc20

inhibitory complexes (Mad2 and/or BubR1 or both associated with Cdc20), which are required for proper M-phase timing and spindle checkpoint signaling (Maciejowski et al., 2010) . The *S. pombe* homologue of Mps1, Mph1, is required to stabilize MCC-APC (Zich et al., 2012). Moreover, Mps1 activity is required for the association of O-Mad2 with the C-Mad2-Mad1 kinetochore scaffold (Hewitt et al., 2010).

In *Xenopus* Mps1 is crucial for spindle checkpoint activation and maintenance by recruiting CENP-E to kinetochore. Kinetochore-localised CENP-E in turn promotes Mad1 and Mad2 association with the kinetochore which is necessary for checkpoint response in this system (Abrieu et al., 2001). Also in human cells Mps1 activity targets checkpoint components to kinetochores, since inhibition of Mps1 leads to dissociation of Bub1, BubR1, Mad1, Mad2, and Zw10 from kinetochores (Maciejowski et al., 2010).

The levels of Mps1 are regulated during cell cycle. Budding yeast Mps1 is targeted for degradation by the APC^{Cdc20} and APC^{Cdh1} during anaphase and G1, respectively (Palframan et al., 2006). The APC dependent degradation of Mps1 and Mps1 removal from kinetochores were proposed to contribute to spindle checkpoint silencing (Palframan et al., 2006, Jelluma et al., 2010). In S phase Mps1 stability is regulated by Cdk2. Inhibition of Cdk2 prevents centrosome reduplication by destabilizing Mps1 which is then lost from centrosomes (Fisk and Winey, 2001).

The fission yeast Mps1 homologue Mph1 [Mps1-like pombe homologue] is, like Mps1 homologues in other organisms, a critical component of the mitotic spindle checkpoint (He et al., 1998). However, fission yeast Mph1 is not required for spindle pole duplication and this might explain why in this system Mph1 is not essential (He et al., 1998). The *S. pombe* homologue of Mps1 has been quite a mysterious protein until the publication of very recent studies revealing functions of Mph1. The first study focused on the role of Mph1 kinase in promoting binding of the MCC (which in fission yeast consists of Mad2-Mad3-Cdc20) to the APC (Zich et al., 2012). The Mph1-dependent phosphorylation sites in Mad2 were mapped and mutated leading to

reduced MCC-APC binding resulting in checkpoint defects. Moreover, this study showed that an *mph1-kinase dead* mutant exhibits a high rate of chromosome missegregation, which suggests that Mph1 is involved in this process and is consistent with results obtained in other systems. In addition Mph1 was shown to localise at fission yeast kinetochores during a mitotic arrest, caused by Mph1 overexpression (Ito et al., 2011). Interestingly, the *mph1-kinase dead* mutant was able to localise at kinetochores almost as well as the wild type kinase, but it was checkpoint deficient. Importantly centromere-tethered Mph1 kinase constitutively recruited Bub1 to kinetochores but not Mad1(Ito et al., 2011).

Aurora B

The Aurora protein kinase family consists of highly conserved serine/threonine kinases involved in many processes during cell division [for review see (Carmena and Earnshaw, 2003; Fu et al., 2007)].
An *aurora* allele was originally identified in a genetic screen in *Drosophila melanogaster* (Glover et al., 1995). The phenotype of aurora mutants is condensed chromosomes arranged on circular monopolar spindles resembling a glow in the sky seen in the polar zone (Glover et al., 1995). In mammalian cells three paralogues are present: Aurora A, Aurora B and Aurora C. Aurora A and B regulate: centrosome separation and maturation, spindle assembly, kinetochore microtubule interactions, chromosome condensation and cytokinesis [for review see (Carmena and Earnshaw, 2003; Fu et al., 2007)]. Aurora C, which is mainly expressed in the testis, plays a critical role in meiosis (Yang et al., 2010).

Both budding and fission yeast have single Aurora kinases. *S. cerevisiae* Aurora, called Ipl1 for ‘increase in ploidy’, was identified in a genetic screen for mutants with inappropriate kinetochore-microtubule attachments and chromosome segregation defects (Biggins et al., 1999; Chan and Botstein, 1993). *S. pombe* Ark1 kinase, which stands for ‘Aurora related kinase1’, was first described as a gene which rescued fission yeast mutants overexpressing *Xenopus* Aurora A (Petersen et al., 2001).

In budding yeast both expression levels and localisation of Ipl1 are, similar to mammalian Aurora B, regulated in the cell cycle. Ipl1 levels are low during G1 phase and then elevated in S and M phase (Biggins et al., 1999). Microscopy analysis of Ipl1 localisation showed that during S phase Ipl1 is enriched in nucleus whereas in mitosis it is concentrated on mitotic spindles (Biggins et al., 1999). In fission yeast Ark1 protein levels remain constant through the cell cycle with Ark1 concentrated in the nucleus in G1 phase (neither associated with spindle pole bodies nor with centromeres) and on centromeres/kinetochores upon entry to mitosis. Ark1 dissociates from centromeres/kinetochores during anaphase (Petersen et al., 2001).

Experiments in budding yeast that employed the temperature-sensitive *ipl1-321* allele showed that Ipl1 is required for proper chromosome segregation and the mitotic checkpoint response to tensionless kinetochore-microtubule attachments which suggested a possible role for Ipl1 in checkpoint signaling (Biggins and Murray, 2001). Several studies demonstrated that in budding yeast and in metazoans Aurora B kinase is required to disrupt improper kinetochore-microtubule attachments and thereby promotes bi-orientation (Tanaka et al., 2002; Lampson et al., 2004; Hauf et al., 2003; Pinsky et al., 2006b). The unattached kinetochores then signal the mitotic spindle checkpoint which suggests a rather indirect role of Aurora B in the spindle checkpoint signaling (Hauf et al., 2003; Pinsky et al., 2006b). However, since Ipl1-dependent phosphorylation of Mad3 is required for mitotic arrest in the absence of tension at sister kinetochores (King et al., 2007a), Ipl1 might be involved in both direct and indirect pathways of mitotic checkpoint activation.

In fission yeast Ark1 covers the functions of both mammalian Aurora A and Aurora B kinase. Ark1 has been shown to regulated chromosome condensation and chromosome segregation (Petersen and Hagan, 2003; Petersen et al., 2001; Leverson and Huang, 2002; Hauf et al., 2007). There is also evidence that Ark1, similar to budding yeast Ipl1, is required to resolve incorrect syntelic attachments (Hauf et al., 2007). Moreover, Ark1 has been also reported to be involved in checkpoint response to unattached kinetochores. A conditional *ark1*$^{+}$ shut off mutant failed to activate the

checkpoint in response to microtubule depolymerizing drugs (Petersen and Hagan, 2003). Other analyses showed that the inhibition of Ark1 activity with an ATP analogue (1-NMPP1; using the *ark1-as3* allele) allowed previously arrested cells to exit from the mitotic block. This suggests that Ark1 activity is required for the maintenance of the spindle checkpoint (Vanoosthuyse and Hardwick, 2009). These findings are consistent with a study in *Xenopus* which also reported that in this system Aurora B plays role in the checkpoint response to unattached kinetochore (Kallio et al., 2002). Moreover, Ark1 contributes to the APC inhibition as Mad2 kinetochore localisation and Mad2-Mad3 complex formation depend on Ark1 activity (Petersen and Hagan, 2003).

Ark1, as in other organisms, needs to be associated with survivin (Bir1), INCENP (Pic1; Inner centromere protein-related protein) and borealin (Nbl1; novel Borealin - like 1), components of the Chromosomal Passenger Complex (CPC), to be functional (Petersen and Hagan, 2003; Leverson and Huang, 2002; Bohnert et al., 2009).

Bub1 kinase

As described above, Bub1 was identified in a screen for proteins required for mitotic arrest upon microtubule depolymerisation (Hoyt et al., 1991). Yeast Bub1 mutants either lacking the C-terminal kinase domain or with inactivating mutations, are still able to arrest in metaphase upon complete microtubule depolymerisation (Vanoosthuyse et al., 2004; Fernius and Hardwick, 2007). However, there is some evidence for a minor role for Bub1 kinase in the spindle checkpoint response.

In *Xenopus* egg extracts kinase dead Bub1 was defective in maintaining the spindle checkpoint in low dose of nocodazole (microtubule depolymerising drug) whereas in higher doses the checkpoint was fully functional (Chen, 2004). This result indicates that Bub1 kinase activity is not required for the checkpoint response to a strong signal, but is required to support mitotic arrest in response to weak signals. In fission yeast Bub1 was suggested to be required for complete checkpoint functions (Yamaguchi et al., 2003). A minor role of Bub1 kinase activity in spindle checkpoint

signaling was also reported for HeLa cells (Klebig et al., 2009). Moreover the fact that Bub1 phosphorylates Mad1 and Bub3 *in vitro* suggests that Bub1 kinase activity might have some checkpoint functions (Seeley et al., 1999; Roberts et al., 1994).

Surprisingly, it has been demonstrated in HeLa cells that Bub1 kinase can contribute to the spindle checkpoint arrest by phosphorylating Cdc20, the APC activator (Tang et al., 2004). Bub1 can phosphorylate Cdc20 *in vitro* and *in vivo* and the role of this phosphorylation was tested using an *in vitro* ubiquitination assay. This study showed that Bub1 kinase activity is required to inhibit the APC dependent ubiquitination of cyclin B. Moreover *in vivo* experiments using a nonphosphorylatable Cdc20 mutant revealed spindle checkpoint defects (Tang et al., 2004). This discovery was followed by structural analyses which provided a better understanding of the mechanism of the Bub1 kinase activity dependent inhibition of the APC (Kang et al., 2008). Bub1 has two KEN boxes outside its kinase domain and these KEN boxes were shown to be docking sites for Cdc20. They were shown to be required for Bub1-dependent phosphorylation of Cdc20, which inhibits APC activity and thus contributes to checkpoint signaling (Kang et al., 2008).

Bub1 kinase activity is crucial for chromosome bi-orientation and segregation by facilitating shugoshin protein localisation to the peri-centromere which, along with haspin activity, results in the recruitment of Aurora B and other members of the Chromosomal Passenger Complex (Fernius and Hardwick, 2007; Kawashima et al., 2010; Yamagishi et al., 2010).

1.3.1.2. Scaffolds

The scaffolding proteins are stably associated with unattached kinetochores. Scaffolds recruit and activate effector proteins, which leads to the checkpoint signal generation and APC inhibition. We can distinguish two main scaffold complexes in spindle checkpoint signaling: Mad1-Mad2 and Bub1-Bub3.

Mad1

Mad1 belongs to the core components of mitotic spindle checkpoint. *mad1* mutants are sensitive to benomyl (spindle poison) and this sensitivity is rescued by hydroxyurea in budding yeast (Li and Murray, 1991; Hardwick and Murray, 1995). This observation can be explained by the fact that hydroxyurea slows down DNA synthesis which prolongs duration of mitosis (mimicking mitotic spindle checkpoint) and allows *mad1* mutant to grow on benomyl which otherwise would kill the cells. This applies to relatively low levels of benomyl, which allow the cell to form a functional spindle but the process needs more time.

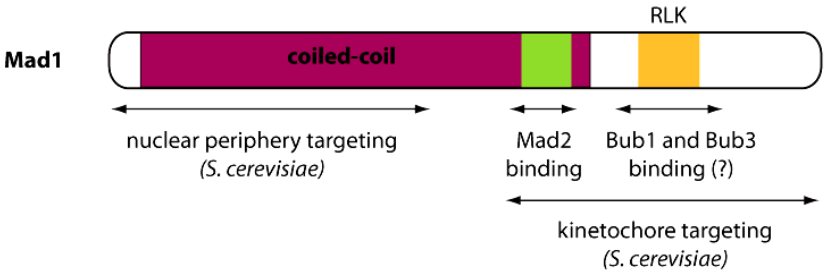

Figure 1.11. Domain organization of Mad1.

Mad1 is predominantly a coil-coiled protein (Figure 1.11). Two N-terminal coiled-coils target *S. cerevisiae* Mad1 to the NPCs (Scott et al., 2005). In budding yeast the C-terminal half of Mad1 is required for its kinetochore localisation (Scott et al., 2005), whereas in *Xenopus* the N-terminus of Mad1 is implicated in its kinetochore targeting (Chung and Chen, 2002). Jin et al. (1998) demonstrated by yeast two

hybrid assay that in human Mad1 residues 465-584 mediate the Mad2 binding. The Mad1 region required for Bub1 and Bub3 binding has not been mapped. However, Brady and Hardwick (2000) showed that a conserved RLK motif in the Mad1 C-terminus is required for Bub1 and Bub3 binding.

During interphase Mad1 and Mad2 accumulate at the nuclear periphery where they associate with the Nuclear Pore Complex (NPC) (Chen et al., 1998; Campbell et al., 2001; Iouk et al., 2002; Shah et al., 2004). The Mad1 interaction with the NPC is mediated by nucleoporin Nup53 and Nup60-Mlp1-Mlp2 complex where the Mlps, Myosin-like proteins, connect the NPC with the nuclear interior (Iouk et al., 2002; Scott et al., 2005). It has been shown that the NPC binding is not required for checkpoint functions of Mad1 (Scott et al., 2005). In *S. cerevisiae* the Mad1 localisation to NPC is largely maintained during spindle checkpoint activation whereas the vast majority of Mad2 relocates to kinetochores (Iouk et al., 2002). FRAP analysis of Mad1 dynamics in budding yeast revealed that the majority of Mad1 rapidly cycles between the Mlp proteins and kinetochores in an energy dependent manner (Scott et al., 2005). Further investigation demonstrated that Mad1 contains a nuclear export signal (NES) which is recognized by exportin Xpo1 (Scott et al., 2009). Consistently, the Mad1 movement onto kinetochores during checkpoint signalling depends on exportin Xpo1, RanGTP and hydrolysis of GTP by Ran (Scott et al., 2009). However, a Mad1 mutant, which was unable to accumulate at kinetochores, remained checkpoint proficient (Scott et al., 2009).

In mammalian cells, which unlike yeast undergo open mitosis, Mad1 is enriched at the nuclear envelope in interphase whereas during prophase and prometaphase most of Mad1 (about 80%) is immobilized on unattached kinetochores where it colocalises with Mad2 (Shah et al., 2004; Chen et al., 1998). The Ndc80 complex has been proposed to serve as a kinetochore docking site for Mad1 (DeLuca et al., 2003; Martin-Lluesma et al., 2002). Upon microtubule attachment Mad1 is redistributed along microtubules to the spindle poles where it is released in anaphase and telophase (Shah et al., 2004).

In human and *Xenopus* Mad1 kinetochore localisation depends on Mps1 kinase (Abrieu et al., 2001; Liu et al., 2003). A study carried out in *Xenopus* egg extracts demonstrated that kinetochore localisation of Mad1 requires Bub1 independently of its kinase activity (Sharp-Baker and Chen, 2001).

Upon spindle checkpoint activation Mad1 becomes hyperphosphorylated which requires Bub1, Bub3 and Mad2 in yeast cells (Hardwick and Murray, 1995). Both Mps1 and Bub1 kinases phosphorylate Mad1 *in vitro* (Seeley et al., 1999; Hardwick et al., 1996) but the physiological relevance of this phosphorylation still needs to be determined.

Mad1 is a component of two complexes which are involved in the checkpoint response. The Mad1-Bub1-Bub3 complex is present during the formation of stable kinetochore-microtubule attachments in *S. cerevisiae* and its levels dramatically increase once spindle checkpoint is activated (Brady and Hardwick, 2000). Formation of this complex is Mad2- and Mps1-dependent whereas Mad3 is dispensable for the interaction (Brady and Hardwick, 2000). *In vitro* reconstitution experiments using mammalian proteins confirmed the results obtained in budding yeast (Seeley et al., 1999). However, there is no *in vivo* evidence for Mad1-Bub1-Bub3 complex formation outside budding yeast, so far.

Mad1 also interacts with Mad2 at kinetochores (Chen et al., 1999) and this interaction is crucial for Mad2 activation and in turn the APC inhibition (De Antoni et al., 2005). The mechanism of this interaction is called the ‘template model’ (De Antoni et al., 2005) (see the Mad2 section below). Tethering Mad1 to bi-oriented kinetochores is sufficient to arrest cell in mitosis and this depends on Mad1 association with Mad2 (Maldonado and Kapoor, 2011).

Bub1

Bub1 has essential functions in spindle checkpoint signaling [for review see (Elowe, 2011)]. Studies in yeast and vertebrates consistently showed that Bub1 is crucial for spindle checkpoint establishment due to its scaffolding properties (Vanoosthuyse et al., 2004; Bernard et al., 1998; Hoyt et al., 1991; Taylor and McKeon, 1997).

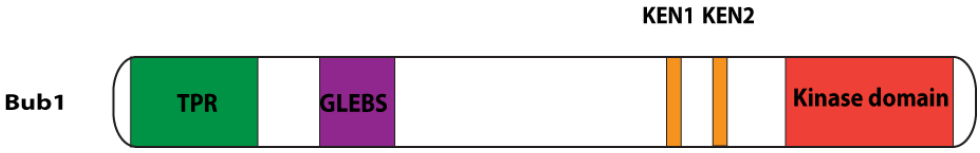

Figure 1.12. Domain organization of Bub1. Bub1 contains an N-terminal TPR region (green), whose role in Bub1 kinetochore targeting has recently become controversial (see below). The GLEBS domain (purple) mediates Bub3 binding. Two KEN boxes (orange) present in human Bub1 are required for its APC^{Cdh1} dependent degradation in G1. The C-terminal kinase domain plays a role in chromosome segregation. See text for references.

In vertebrate cells Bub1 appears mainly at the kinetochore outer plate in early prophase, prior to the kinetochore recruitment of BubR1, and it remains there until anaphase onset (Jablonski et al., 1998; Taylor et al., 2001). In fission yeast Bub1 is associated with kinetochores from metaphase until telophase (Bernard et al., 1998). At misaligned chromosomes the Bub1 concentration is higher (Jablonski et al., 1998) and Bub1 becomes phosphorylated (Taylor et al., 2001). Measurements of fluorescence recovery after photobleaching (FRAP) in mammalian cells showed that Bub1 is a stable component of the mitotic kinetochore, similar to Mad1 (Howell et al., 2004; Shah et al., 2004). Similar experiment in *S. pombe* cells confirmed stable binding of Bub1 to kinetochores (Rischitor et al., 2007). Moreover, tethering Bub1 to telomeres is sufficient to recruit both Mad3 and Bub3 independently of its kinase activity (Rischitor et al., 2007). Two properties of Bub1, being stably bound to kinetochores and ability to recruit other checkpoint proteins, makes Bub1 a kinetochore scaffold for checkpoint signaling.

Phosphorylation of Bub1, which in human cells is induced by challenging the spindle checkpoint (Sharp-Baker and Chen, 2001; Chen, 2004; Taylor et al., 2001), is also important for the efficient arrest (Chen, 2004; Yamaguchi et al., 2003). Bub1 is phosphorylated by mitogen-activated protein kinase (MAPK) and Cdk1 (Chen, 2004; Yamaguchi et al., 2003) as well as undergoing autophosphorylation, but these have only been demonstrated *in vitro* (Roberts et al., 1994; Seeley et al., 1999).

Two KEN boxes, which mediate the APC^{Cdh1} dependent degradation of Bub1 in G1, were mapped in human Bub1 (Figure 1.12) (Qi and Yu, 2007). The Bub1 C-terminal kinase domain is dispensable for checkpoint signaling (Vanoosthuyse et al., 2004; Fernius and Hardwick, 2007) (see below).

The N-terminus of Bub1 and BubR1(Bub Related 1)/Mad3 are highly conserved and contain a triple-tandem arrangement of the tetratricopeptide repeat (TPR) motif revealed by crystallographic studies (Figure 1.12 and 1.13) (Bolanos-Garcia et al., 2005, 2009; D'Arcy et al., 2010). The TPR contains a degenerate 34-amino acid sequence present in tandem arrays of 3-16 repeat elements. Each individual 34-amino acid repeat forms a helix-turn-helix structure (Das et al., 1998). TPR motifs are known to mediate protein-protein interactions (Das et al., 1998; Bolanos-Garcia et al., 2005). Over recent years, a large body of data has been published uncovering the role of Bub1 and BubR1 TPRs.

It was demonstrated that the N-terminus of Bub1 is required for kinetochore targeting and checkpoint functions of Bub1 in fission yeast (Vanoosthuyse et al., 2004). Kiyomitsu et al.(2007) showed using a yeast two hybrid assay that human Bub1 (residues 1-150), containing a TPR motif, binds the N-terminus of Blinkin/KNL1 and this interaction is critical for Bub1 kinetochore localisation and its checkpoint functions. Klebig et al. (2009) also demonstrated that the N-terminal TPR region of human Bub1is required for its kinetochore targeting. The KI1 motif in the N-terminus of Blinkin/KNL1 was proposed to act as a Bub1 kinetochore binding site in Blinkin/KNL1 (Kiyomitsu et al., 2011). Recently, the crystal structure of human Bub1(1-150)-Blinkin/KNLl (150-200) complex, where the Bub1 and Blinkin/KNL1fragments contain the TPR region and KI1 motif, respectively, was determined (Krenn et al., 2012). However, direct interaction between the Bub1 TPR domain and KI1 motif in Blinkin/KNL1 seems to have a marginal role in Bub1 kinetochore targeting (Krenn et al., 2012). Structural analyses also suggest that the Bub3 binding region of Bub1, called the GLEBS motif (for GLE2p-binding sequence, Wang et al., 2001), is necessary and sufficient for recruitment of Bub1 kinetochores (Krenn et al., 2012), which is consistent with previous observations

(Taylor et al., 1998). Thus it was proposed that the interaction of Bub1 with Blinkin/KNL1 might be mediated by Bub3 (Krenn et al., 2012).

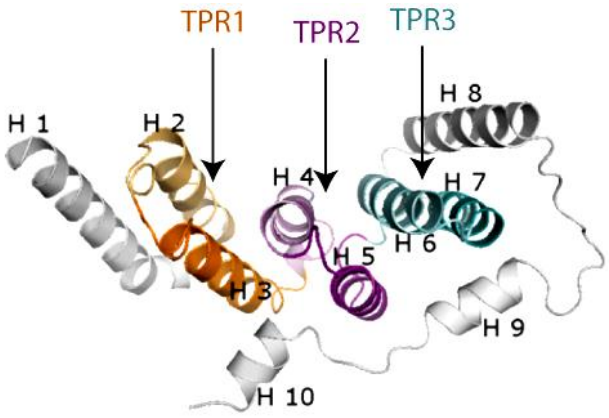

Figure 1.13. Ribbon model showing that the N-terminus of the *S. cerevisiae* Bub1 (residues 29-230) has a tetratricopeptide-like fold adapted from (Bolanos-Garcia et al., 2009). The N-terminus of Bub1 contains 10 α helices of which helices 2 and 3 constitute TPR1 (orange), helices 4 and 5-TPR2 (magenta) and helices 6 and 7-TPR3 (cyan).

Both Mad3 (human BubR1) and Bub3 are recruited to kinetochore by Bub1(Basu et al., 1998; Chen, 2004; Sharp-Baker and Chen, 2001; Johnson et al., 2004; Kadura et al., 2005). A study in fission yeast showed that Bub1 and Bub3 are interdependent for their kinetochore localisation and formation of the Bub1-Bub3 complex does not depend on Mad3 (Vanoosthuyse et al., 2004). The Bub1-Bub3 complex can be found in different systems (Taylor et al., 1998), whereas in budding yeast the Bub1-Bub3 complex associates with Mad1forming the Mad1-Bub1-Bub3 complex (Brady and Hardwick, 2000).

In addition to Bub3 and Mad3 (vertebrate BubR1), Bub1 recruits other proteins to kinetochores independently of its kinase activity including Mad2, CENP-E and CENP-F in human cells (Johnson et al., 2004) and Mad1, Mad2, and CENP-E in *Xenopus* egg extracts (Sharp-Baker and Chen, 2001).

Bub3

Bub3 acts both as a spindle checkpoint scaffold and effector (in vertebrate cells). Its effector function will be described later, in combination with Mad2.

Bub3 was originally identified in budding yeast as a multi copy-suppressor of Bub1. The crystal structure of the budding yeast protein has been solved revealing that Bub3 is a seven-blade β-propeller and each blade is a four-stranded β-sheet (Figure 1.14) (Larsen and Harrison, 2004).

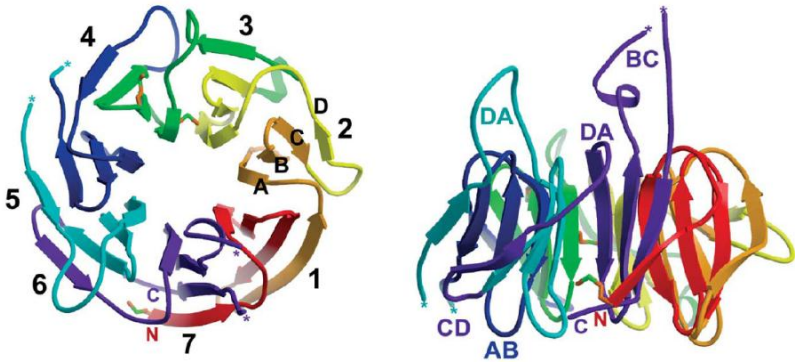

Figure 1.14. Structure of Bub3, picture taken from (Larsen and Harrison, 2004). Left-top view, right-side view. Numbers (1-7) indicate the blades; letters (A-B) refers to the strands of β-sheets.

Bub3 localises to kinetochores from prometaphase until metaphase (Taylor et al., 1998; Howell et al., 2004) but it is not stably bound to kinetochores as it cycles between the cytoplasm and kinetochores (Howell et al., 2004). Interactions between Bub3 and Bub1 as well as Bub3 and Mad3 were first shown in budding yeast (Roberts et al., 1994; Hardwick et al., 2000) and levels of these complexes are stable during cell cycle (Hardwick et al., 2000; Brady and Hardwick, 2000). In mammalian cells Bub3 was demonstrated to recruit both Bub1 and BubR1 to kinetochores (Taylor et al., 1998).

In many systems Bub3 is required for spindle checkpoint signaling (Hoyt et al., 1991; Kalitsis et al., 2000; Lopes et al., 2005), but its role in fission yeast spindle checkpoint signaling is controversial. Although previous studies reported an important role of Bub3 in checkpoint signaling due to its scaffolding properties (Vanoosthuyse et al., 2004), more recent studies showed that *bub3* mutants are able to establish reasonably good mitotic arrests (Tange and Niwa, 2008; Vanoosthuyse et al., 2009; Windecker et al., 2009). Further analysis of *bub3* mutants has revealed that Bub3 is also required for chromosome bi-orientation (Logarinho et al., 2008; Windecker et al., 2009) and spindle checkpoint silencing in fission yeast (Vanoosthuyse et al., 2009).

KNL1/Spc7

KNL1 (Spc7 in *S. pombe*, Spc105 *in S. cerevisiae*) was originally described as a protein essential for kinetochore assembly in *C. elegans* (Desai et al., 2003). Further studies confirmed the crucial role for KNL1 in this process in other organisms including yeast. Over the last few years a body of evidence showed that KNL1 serves also as a kinetochore platform for checkpoint proteins including Bub1-Bub3 and BubR1. Yeast two-hybrid interactions between the TPR motif of human Bub1 and BubR1 and the N-terminus of KNL1 were first reported by Kiyomitsu et al., (2007). Due to its ability to bind Bub1 and BubR1, the authors proposed to rename human KNL1 Blinkin for bub-linking kinetochore protein. The important role of KNL1 in checkpoint signaling was confirmed by the observation that KNL1 depletion in human cells prevents Bub1 and BubR1 from binding to kinetochores and checkpoint activation (Kiyomitsu et al., 2007). Another study by Kiyomitsu et al. (2011) revealed two minimal Bub1 and BubR1 binding sites containing a consensus KI motif, KI[D/N]XXXF[L/I]XXLK, in the N-terminus of KNL1 (residues 151-250) which are conserved in vertebrates but not in yeast. Recently, two studies determined the crystal structure of the KI1-Bub1 complex (Krenn et al., 2012) and KI2-BubR1 (Bolanos-Garcia et al., 2011) revealing the molecular details of these interactions (Figure 1.15). Interestingly, Krenn et al. (2012) showed that the interactions between the TPR domains of Bub1 and BubR1 and the KI1 and KI2

motifs of KNL1, respectively, are dispensable for localisation of Bub1 and BubR1 to kinetochores. However, the role of KNL1 in the recruitment of Bub1 and BubR1 to kinetochores is clear, which suggests other modes of KNL1 interaction with Bub1 and BubR1. The interaction between KNL1 and Bub1 and BubR1 can be mediated by Bub3 (Krenn et al., 2012). This is consistent with older findings that Bub3 is required for Bub1 kinetochore localisation (Taylor et al., 1998; Vanoosthuyse et al., 2004).

In non-vertebrates the KI motifs are absent (Vleugel et al., 2012). Nevertheless, the *D. melanogaster* homologue of KNL1, Spc105, interacts with Bub1 in a yeast two-hybrid assay (Schittenhelm et al., 2009).

The scaffolding function of KNL1 seems not to be limited to recruiting Bub1, BubR1 and Bub3. In vertebrates the C-terminal region of KNL1 interacts with the kinetochore protein Zwint-1 (Kiyomitsu et al., 2011). Zwint-1 is required to recruit the RZZ complex to kinetochores which, in turn, promotes the association of Mad1 with kinetochores (Karess, 2005). Moreover, KNL1 binds PP1 phosphatase which in yeast and *C. elegans* facilitates checkpoint silencing (Liu et al., 2010; Vanoosthuyse and Hardwick, 2009; Espeut et al., 2012).

In addition to being an essential kinetochore component and a kinetochore scaffold for checkpoint activation and silencing, KNL1 has microtubule binding activity (Cheeseman et al., 2004). Thereby KNL1 might coordinate microtubule attachment status with checkpoint signaling.

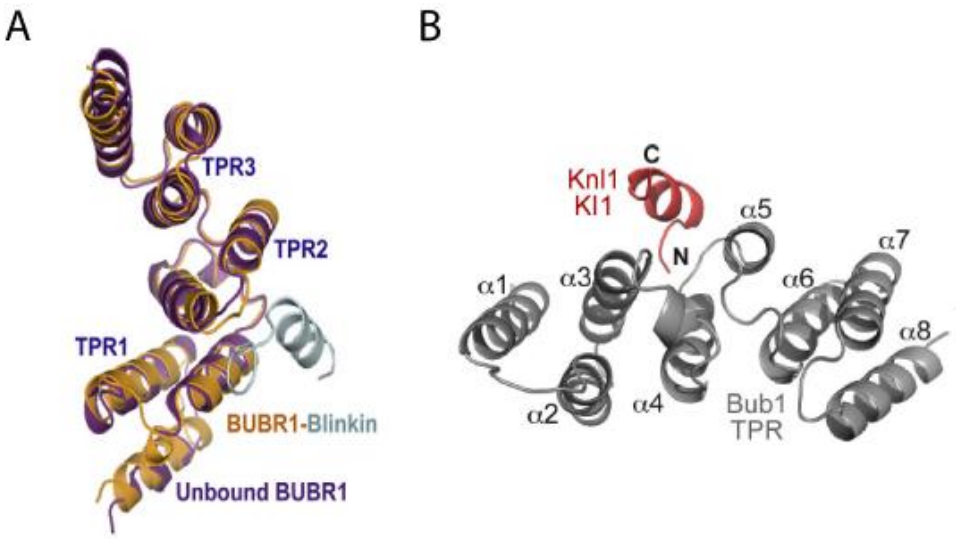

Figure 1.15. A. Structure of KNL1-BubR1 complex taken from (Bolanos-Garcia et al., 2011). The TPR-containing domain of human BubR1 (57-220) interacts with the KI2 motif of KNL1 (residues 208-226). **B. Structure of KNL1-Bub1 complex taken from (Krenn et al., 2012).** The TPR-containing domain of human Bub1 (residues 1-150) interacts with the KI2 motif of KNL1 (residues 150-200).

Rod-ZW10-Zwilch (RZZ) complex

All checkpoint proteins initially identified in yeast (Bub1, Bub3, Mad1, Mad2, Mad3 and Mps1) have clear orthologous proteins in metazoans. However, in higher eukaryotes checkpoint signaling requires additional players which do not have homologues in yeast. Rod, Zw10 and Zwilch are examples of such proteins [for review see (Karess, 2005; Lu et al., 2009)].

Zeste-White 10 (ZW10) and Rough deal (Rod) were originally identified in *Drosophila* (Smith et al., 1985; Karess and Glover, 1989). The ZW10 and Rod homologues were subsequently found in other multicellular eukaryotes (Starr et al., 1997; Chan et al., 2000; Okamura et al., 2001). Zwilch was identified in *Drosophila* and demonstrated to be a binding partner of ZW10 and Rod in HeLa cells (Williams et al., 2003).

Checkpoint function of Rod and ZW10 was first reported for human cells and *Drosophila* neuroblasts (Chan et al., 2000; Basto et al., 2000). Injection of antibodies against ZW10 and Rod abolished mitotic arrest in human cells treated with

nocodazole demonstrating that Rod and ZW10 are spindle checkpoint components (Chan et al., 2000).

Drosophila cells lacking either Rod or ZW10 were unable to arrest in metaphase in response to spindle damage (Basto et al., 2000). Further studies demonstrated that Rod and ZW10 are required for recruitment of Mad1-Mad2 to kinetochores. In *Xenopus* extract immunodepletion of Rod and ZW10 caused disassociation of the Mad1-Mad2 complex and BubR1 from kinetochores (Kops et al., 2005a). Dependency of the Mad1-Mad2 complex on ZW10 for their kinetochore localisation was confirmed in HeLa cells by ZW10 siRNA experiment (Kops et al., 2005a).

Consistently Buffin et al. (2005) showed that Rod-ZW10 is required for Mad2 localisation at unattached kinetochores in the *Drosophila* larval neuroblast cells.

1.3.1.3. Effectors

Effectors, upon their activation at kinetochores, bind and inhibit APC^{Cdc20}. APC inhibition prevents cyclin B and securin from being degraded which arrests cells in metaphase.

Mad2

Mad2 is a key component of spindle checkpoint signaling (He et al., 1997; Chen et al., 1999) and bound to Cdc20, together with Mad3 and Bub3 (not in fission yeast), acts as the APC inhibitor (see Figure 1.10).

Mad2 localises to the nuclear envelope and the nucleus during interphase (Campbell et al., 2001; Ikui et al., 2002) and unattached kinetochores during mitosis (Chen et al., 1996; Waters et al., 1998; Ikui et al., 2002). Both Mad2 association with the nuclear periphery and unattached kinetochores depend on Mad1 (Chen et al., 1998; Ikui et al., 2002). Interestingly, Mad1-independent kinetochore localisation of Mad2 has been recently demonstrated in human cells (Westhorpe et al., 2011). The authors provided some evidence for Cdc20-mediated Mad2 kinetochore binding (Westhorpe et al., 2011).

Mad2 tightly associates with Mad1 independently of cell cycle stage and the presence or absence of other checkpoint components, and this interaction is crucial for the spindle checkpoint (Hwang et al., 1998; Chen et al., 1999). The crystal structure of Mad1(485-584)-Mad2 complex was solved (Sironi et al., 2002).

Mad2 forms a complex with Cdc20 and the complex formation is enhanced in mitosis, which probably reflects elevated levels of Cdc20 during this stage of the cell cycle (Hardwick et al., 2000; Hwang et al., 1998; Kim et al., 1998). The observation that the interaction between Mad2 and Cdc20 depends on Mad1 (Hwang et al., 1998) suggested the current 'template' model of Mad1-Mad2 complex catalyzing formation of Mad2-Cdc20 complex, which in turn inhibits the APC (De Antoni et al., 2005; Chung and Chen, 2002). Mad2 exist in two distinct conformations: 'open Mad2' (O-Mad2) and 'closed' Mad2 (C-Mad2) (Figure 1.16 A and B). Upon binding to Mad1, Mad2 adopts the closed conformation. Kinetochore bound Mad1-C-Mad2 functions as a checkpoint signaling scaffold (Figure 1.16.B) (De Antoni et al., 2005). Free O-Mad2 molecules can interact with the Mad1-C-Mad2 template via Mad2 dimerization and adopt the closed conformation. The new C-Mad2 molecule is then liberated from the scaffold to the cytoplasm exchanging with another O-Mad2 molecule. Importantly, the crystal structure of the O-Mad2-C-Mad2 dimer confirms the 'template' model (Mapelli et al., 2007).

Interestingly, the 'template' model is reflected by the results of FRAP experiments (Howell et al., 2000; Shah et al., 2004), which revealed two population of Mad2 at kinetochores. One population rapidly exchanges at the kinetochore, and the second is stably associated with kinetochores being a part of the Mad1-C-Mad2 scaffold. In yeast, the APC inhibitory complexes, including Mad2-Cdc20 can be formed in the absence of functional kinetochores (Fraschini et al., 2001b; Sczaniecka et al., 2008). However, they are not sufficient to inhibit the APC complex, suggesting that the kinetochore might serve as an important source of post-translational modifications (Sczaniecka et al., 2008).

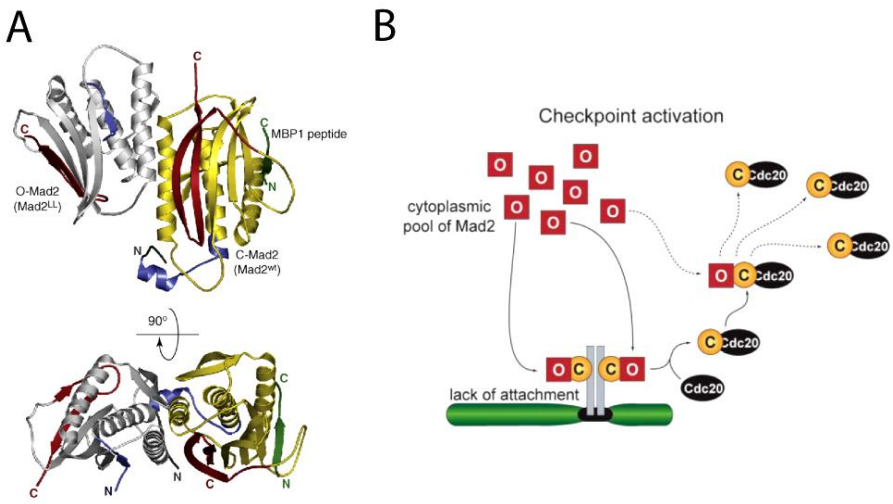

Figure 1.16. A. Ribbon model of a Mad2 dimer adapted from (Mapelli et al., 2007). The Mad2 dimer is formed by 'open' Mad2 (O-Mad2 in grey) and 'closed' Mad2 (C-Mad2 in yellow). The presence of a Mad2-Binding Peptide 1 (MBP1 in green), which mimics the consensus Mad2-binding motifs of Mad1 and Cdc20, allowed them to obtain C-Mad2 for crystallographic experiments (Mapelli et al., 2007). The N- and C-terminal regions of Mad2, whose topology differs between C-Mad2 and O-Mad2, are in blue and red, respectively (Mapelli et al., 2007). The C-terminal tail of Mad2 (in red), sometimes called the 'safety belt', wraps around the binding partner (Cdc20 or Mad1).
B. The 'template' model of Mad2 activation proposed by Musacchio and co-workers taken from (De Antoni et al., 2005). The Mad1-C-Mad2 scaffold is stably associated with unattached kinetochores catalyzing conformational change of O-Mad2 to C-Mad2 (see text for details and references).

Mad3/BubR1

Mad3, an essential checkpoint protein, was originally identified in budding yeast (Hardwick et al., 2000; Li and Murray, 1991). The mammalian orthologue was found in human cells via its homology to Bub1 (Cahill et al., 1998) and it was called BubR1 (Bub Related1). The checkpoint functions of BubR1 were confirmed in mammalian cells (Taylor et al., 1998; Chan et al., 1999).

Mad3/BubR1 persists at kinetochores from early prometaphase until anaphase during an unperturbed mitosis (Millband and Hardwick, 2002; Taylor et al., 2001).

Mad3/BubR1 kinetochore localisation depends on other checkpoint proteins including Bub1 and Bub3 (Vanoosthuyse et al., 2004; Taylor et al., 2001) and Mph1 in fission yeast (Millband and Hardwick, 2002). Mad3 is not stably associated with kinetochores as its turnover at kinetochores is high (Howell et al., 2004). BubR1 is implicated in the response to a lack of tension across sister kinetochores, whereas Mad2 seems to sense the lack of attachment to microtubules. This idea is supported by observations in HeLa cells where BubR1 and Bub1 are enriched specifically at tensionless kinetochores, whereas Mad2 accumulates at unattached kinetochores (Skoufias et al., 2001). Similar behavior of BubR1 and Mad2 is seen in *Drosophila melanogaster* S2 cells (Logarinho et al., 2004). BubR1 kinetochore localisation in the absence of tension depends on Aurora B activity (Ditchfield et al., 2003). In budding yeast Mad3 levels do not change during the cell cycle (Rancati et al., 2005; Hardwick et al., 2000), whereas human BubR1 concentration increases in late S phase, G2 phase and upon spindle checkpoint activation (Li et al., 1999)

Mad3/BubR1 undergoes post-translational modifications which are important for BubR1 functions.

Mad3/BubR1 is phosphorylated during mitosis (Taylor et al., 2001; Li et al., 1999). Moreover, phosphorylation of different residues by different kinases regulates BubR1 functions (Huang et al., 2008). Polo like kinase (Plk1), Aurora B kinase (Ipl1) and Mps1 kinase phosphorylate Mad3/BubR1 (Rancati et al., 2005; King et al., 2007a; Huang et al., 2008; Ditchfield et al., 2003). Cdk1 mediated phosphorylation of BubR1 is thought to prime its Plk1-dependent phosphorylation (Wong and Fang, 2007). BubR1 is also acetylated in prometaphase and this modification protects BubR1 from ubiquitin-dependent degradation during checkpoint activation (Choi et al., 2009). Recently, BubR1 was reported to be sumoylated and this was required for its removal from kinetochores and anaphase onset, was reported (Yang et al., 2011, 2012)

In terms of spindle checkpoint signaling Mad3/BubR1 has a dual role. Mad3/BubR1 is a component of the Mitotic Checkpoint Complex (MCC; Mad2–Mad3/BubR1–Bub3–Cdc20) which binds and inhibits the APC (Fang, 2002; Chan et al., 1999;

Sudakin et al., 2001; Sczaniecka et al., 2008). The *Xenopus* BubR1 also exhibits checkpoint scaffolding function at kinetochores by recruiting Bub1, Bub3, Mad1, Mad2, and CENP-E checkpoint proteins (Chen, 2002; Abrieu et al., 2000).

In addition to checkpoint functions vertebrate BubR1 is involved in monitoring chromosome attachment/alignment and mitotic timing (Jablonski et al., 1998; Lampson and Kapoor, 2005; Huang et al., 2008; Meraldi et al., 2004).

The vertebrate BubR1 homologues have a C-terminal kinase domain (Figure 1.17) (Suijkerbuijk et al., 2012). The kinase domain is absent in yeast. The role of the BubR1 kinase domain in checkpoint signaling is debatable. A study, based on inactive version of *Xenopus* BubR1 kinase (BubR1 kinase-dead) and truncated BubR1 lacking its kinase domain, demonstrated that BubR1 kinase activity was dispensable for the checkpoint (Chen, 2002). However, other studies, which also used an inactive version of BubR1, reported that kinase activity of BubR1 contributed to the checkpoint signaling (Kops et al., 2004; Mao et al., 2005; Huang et al., 2008). A recent study showed that the vertebrate BubR1 kinase domain lost its kinase activity in the course of evolution and became a pseudokinase (Suijkerbuijk et al., 2012). The kinase activity observed in BubR1 immunoprecipitates (Fang, 2002) was caused by other kinases, most likely Bub1 and Cdk1, co-precipitating with BubR1 (Suijkerbuijk et al., 2012). Moreover, it was shown that the spindle checkpoint defects observed in the BubR1 kinase domain mutants probably reflected a reduced conformational stability of the mutated BubR1 (Suijkerbuijk et al., 2012). In these BubR1 mutants amino acid substitutions were introduced to the ATP binding pocket which resulted in a decrease in BubR1 levels (Suijkerbuijk et al., 2012). A similar phenomenon was reported for kinase domain-mutants of BubR1 detected in the cancer predisposition syndrome mosaic variegated aneuploidy (MVA) (Suijkerbuijk et al., 2010).

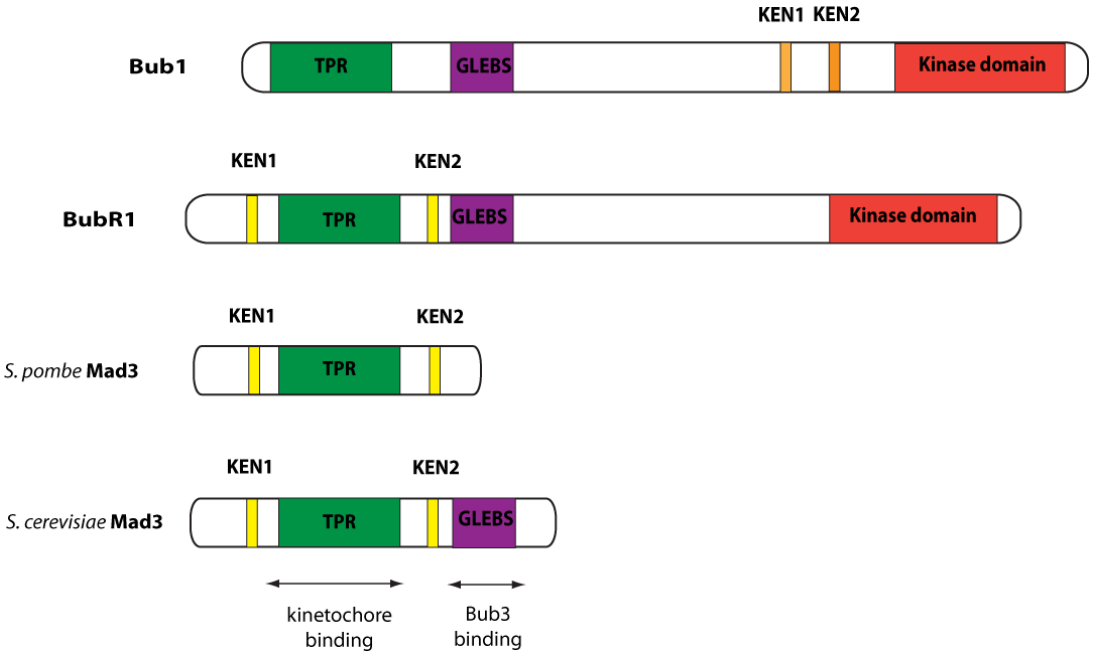

Figure 1.17. Domain organization of Bub1, BubR1, fission yeast Mad3 and budding yeast Mad3. The presence of a N-terminal TPR region (green) is a common feature Bub1, BubR1 and yeast Mad3 (Bolanos-Garcia et al., 2005). Interactions between Bub1 and BubR1 might depend on a region C-terminal to their TPR motifs (D'Arcy et al., 2010). The N-terminus of Bub1 and Mad3/BubR1 was proposed to mediate interaction of these proteins with Blinkin/KNL1 (D'Arcy et al., 2010; Kiyomitsu et al., 2007). The GLEBS motif (purple), required for Bub3 binding and kinetochore targeting of Bub1(Taylor et al., 1998; Krenn et al., 2012), is present in vertebrate and yeast Bub1, vertebrate BubR1 and budding yeast Mad3. The Mad3/BubR1 homologues contain two conserved KEN boxes (yellow) required for spindle checkpoint signaling (King et al., 2007b; Sczaniecka et al., 2008). Human Bub1 contains non-conserved KEN boxes (orange) which are required for its degradation in G1 (Qi and Yu, 2007). The kinase domain (red) present in Bub1 and BubR1 proteins has been very recently showed to be an inactive pseudokinase domain in BubR1 proteins (Suijkerbuijk et al., 2012).

1.3.1.4. Mitotic Checkpoint Complex

The main function of the spindle checkpoint effectors is to inhibit Cdc20, the APC activator. Checkpoint proteins and Cdc20 form the Mitotic Checkpoint Complex (MCC), consisting of BubR1, Bub3, Cdc20 and Mad2 in budding yeast and vertebrates, which binds to the APC leading to its inhibition (Figure 1.18 A and B)

(Sudakin et al., 2001; Fraschini et al., 2001b). In fission yeast Bub3 is not stably associated with the MCC because fission yeast Mad3 lacks a GLEBS domain which is necessary for Bub3 binding (Sczaniecka et al., 2008). The MCC complex was shown to be formed every mitosis, not only when the spindle checkpoint is active (Sczaniecka et al., 2008). It has been reported that BubR1 alone can inhibit APC^{Cdc20} in reconstituted ubiquitination assay as well as in *Xenopus* egg extracts (Tang et al., 2001). However, results obtained in yeast and humans show that Mad2 and Mad3/BubR1 are interdependent for binding to the APC and they act synergistically to form a more potent inhibitor *in vitro* (Davenport et al., 2006; Sczaniecka et al., 2008; Fang, 2002). Later in mitosis Mad2 can dissociate from vertebrate MCC-APC leaving bound Mad3 (BubR1) as a final inhibitor of the APC (Nilsson et al., 2008; Kulukian et al., 2009), but there is no evidence for this in yeast.

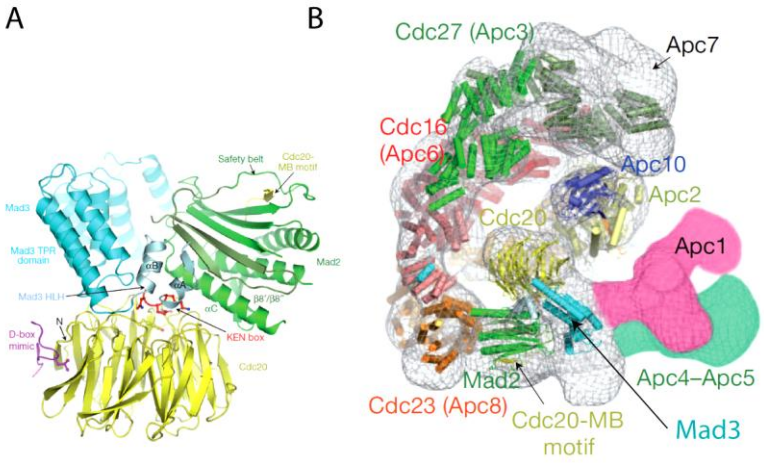

Figure 1.18. A. Crystal structure of the *S. pombe* MCC, taken from (Chao et al., 2012). The MCC components Mad2, Mad3 and Cdc20 are in green, cyan and yellow respectively. Mad2 is in the closed conformation with its safety belt wrapped around Cdc20-Mad2 binding (MB) motif. The N-terminal KEN box (red), critical for MCC formation is located in the Mad3 helix-loop-helix (HLH) motif (Chao et al., 2012). The interaction between Mad2 and Mad3 is mediated by the Mad2 αC helix and β8'-β8'' hairpin and the HLH motif of Mad3 (Chao et al., 2012). The D-box mimic (magenta) is bound to Cdc20 (Chao et al., 2012). **B. Pseudo-atomic structure of human MCC-APC adapted from (Chao et al., 2012).** The model shows the position of MCC associated with the APC [the APC cryo-EM model, (Herzog et al., 2009)].

Four mechanisms of APC inhibition have been proposed [for review see (Zich and Hardwick, 2010; Barford, 2011)].

The first two are based on the observation that there are two populations of inactive APC in human mitotic cells: the APC with bound MCC and the APC on its own (not associated with its activator, Cdc20) (Herzog et al., 2009). The first pool is kept inactive by forming a tight complex with MCC. It is possible that MCC components act as pseudo-substrates preventing real substrates from being ubiquitinated. In this respect Mad3 is a good candidate for the pseudo-substrate as it contains two KEN boxes-degron motifs which can be recognized by the APC (Burton and Solomon, 2007; King et al., 2007b; Lara-Gonzalez et al., 2011). The second model proposes that Cdc20 can be simply sequestered by Mad2 and this is consistent with the observation that in budding yeast the amount of Mad2-Cdc20 is much higher than that of the MCC (Poddar et al., 2005).

The third mechanism relies on Cdc20 destabilization/degradation caused by spindle checkpoint activation. This idea is supported by a study demonstrating that budding yeast Cdc20 is destabilized in a checkpoint- and APC-dependent manner (Pan and Chen, 2004). Cdc20 binding to Mad2 and Mad3 is required for a decrease in Cdc20 levels, whereas Cdh1 is not involved in this process (Pan and Chen, 2004). A similar mechanism was described in human cells. Nilsson et al. (2008) showed that human Cdc20 is ubiquitinated by the APC in response to the checkpoint signaling. A non-ubiquitinatable 'K-less' mutant of Cdc20 was unable to maintain spindle checkpoint suggesting that the Cdc20 degradation contributes to the spindle checkpoint signaling (Nilsson et al., 2008).

The last mechanism implicates Bub1 kinase in inhibitory phosphorylation of Cdc20 (Tang et al., 2004) (described in the 'Bub1 kinase' section).

1.3.1.5. Spindle checkpoint silencing

Upon the establishment of correct, stable bi-polar kinetochore-microtubule attachments leading to spindle checkpoint satisfaction, spindle checkpoint signaling has to be silenced to allow cell cycle progression. Complete inactivation of the spindle checkpoint requires inhibition of Mad2-Cdc20 generation at kinetochores and termination of APC inhibitor formation in the cytoplasm. In various model organisms, the kinetochore and cytoplasmic pathways contribute to checkpoint silencing to different extents. Several mechanisms of spindle checkpoint silencing have been proposed [for review see (Hardwick and Shah, 2010)].

p31^{comet} - a checkpoint antagonist

The first checkpoint-silencing mechanism targets Mad1- or Cdc20- bound Mad2. p31^{comet} was originally identified as a Mad2 binding partner in HeLa cells (Habu and Kim, 2002) . Overexpression of p31^{comet} in human cells bypasses the spindle checkpoint whereas p31^{comet} RNAi prolongs mitosis after release from nocodazole (Habu and Kim, 2002; Xia et al., 2004).

p31^{comet}, the checkpoint antagonist, adopts a structure which mimics Mad2 and binds at the dimerization interface of C-Mad2 (Yang et al., 2007a). This mechanism blocks recruitment of O-Mad2 to Mad1-C-Mad2 template inhibiting 'production' of active Mad2 molecules (the 'capping model') and promotes dissociation of Mad2-Cdc20 complexes (Yang et al., 2007a). It has been recently demonstrated that depletion of p31^{comet} prevents cells, having unperturbed kinetochore-microtubule attachments, from entering anaphase (Hagan et al., 2011). This finding shows that p31^{comet} is required for mitotic exit each cell cycle suggesting that p31^{comet} serves as a mitotic timer (Hagan et al., 2011). Further investigation demonstrated that p31^{comet} causes disassembly of the MCC (Teichner et al., 2011). In human cells arrested in nocodazole and taxol p31^{comet} interacts with BubR1, Cdc20 and the APC (Westhorpe et al., 2011), however this interaction is most likely mediated by closed Mad2 (Xia et al., 2004). Comparing amounts of Mad2 bound to the MCC in nocodazole arrested cells (many unattached kinetochores) and taxol arrested cells (few unattached kinetochores) revealed that more Mad2 is bound to MCC upon nocodozole treatment

(Westhorpe et al., 2011). Moreover, depletion of p31^{comet} increases the levels of Mad2 bound to BubR1-Cdc20 (Westhorpe et al., 2011). Taken together, the study showed the amount of Mad2 bound to BubR1–Cdc20 is variable during SAC signalling, and is positively regulated by unattached kinetochores and negatively regulated by p31^{comet} (Westhorpe et al., 2011). Interestingly, Westhorpe et al. generated a Mad2 mutant which was capable of MCC binding but unable to bind Mad1 and p31^{comet}. The mutant was defective in checkpoint silencing showing that the p31^{comet}-mediated Mad2 dissociation from the MCC promotes checkpoint silencing (Westhorpe et al., 2011). It has been recently proposed that the MCC disassembly is promoted by Cdk-dependent phosphorylation of Cdc20 (Miniowitz-Shemtov et al., 2012). The Cdk-dependent phosphorylation of Cdc20 is stimulated by p31^{comet} which implies that p31^{comet} might be required to trigger conformational changes in Cdc20 promoting its Cdk-dependent phosphorylation and thereby MCC disassembly (Miniowitz-Shemtov et al., 2012). Note however that yeast homologues of p31^{comet} have not been identified so other silencing mechanism must exist.

Dynein-dependent ‘stripping’ of Mad2

The behaviour of Mad2 upon chromosome alignment on the metaphase plate suggested another silencing mechanism called dynein-dependent ‘stripping’ of Mad2 (Howell et al., 2000). Dynein is a minus-end-directed motor which requires dynactin, also called the dynein activator complex. The dynactin complex regulates dynein association with cargo which is transported along microtubules. It has been observed that the dynein-dynactin complex removes Mad2 molecules from kinetochores that are attached to microtubules, takes them along kinetochore fibres and releases then at spindle poles in mammalian cells (Howell et al., 2000, 2001). Similarly, Rod and ZW10 checkpoint protein, components of Rod-ZW10-Zwilch complex (RZZ), are removed from kinetochores upon microtubule attachment in *D. melanogaster* (Wojcik et al., 2001; Basto et al., 2004).

Spindly has been identified as a protein required for kinetochore localisation of dynein in *Drosophila* and in human cells (Griffis et al., 2007). Spindly promotes removal of Mad2 and Rod from kinetochores by targeting dynein to kinetochores

which is proposed to facilitate checkpoint silencing in these organisms (Griffis et al., 2007). However, a recent study suggests that the Spindly-dependent kinetochore targeting of dynein is dispensable for spindle checkpoint silencing in humans, since Spindly depletion mutants can inactivate checkpoint signaling (Gassmann et al., 2010). Surprisingly, Spindly motif mutants, which are unable to recruit dynein and thereby remain constitutively associated with kinetochores, are defective in checkpoint silencing (Gassmann et al., 2010). Taken together, it seems that the dynein-dependent removal of Spindly from kinetochores *per se* is required for efficient checkpoint silencing (Gassmann et al., 2010). As mentioned above, the absence of Spindly does not affect checkpoint silencing which suggests the existence of an additional dynein-independent checkpoint silencing mechanism (Gassmann et al., 2010), which might be conserved from yeast to higher eukaryotes.

Interestingly, the *C. elegans* homologue of Spindly, SPDL-1, interacts with Mad1 and this is required for Mad1 and Mad2 kinetochore loading (Gassmann et al., 2008; Yamamoto et al., 2008).

CUEDC2

Recently, CUEDC2, a CUE domain-containing protein, has been reported as a cell cycle regulator. Cdk1-phosphorylated CUEDC2 binds Cdc20 and facilitates dissociation of Mad2 from Cdc20-APC activating the complex which results in the metaphase to anaphase transition in human cells (Gao et al., 2011).

Phosphatases

A fission yeast gene encoding PP1, *dis2* (dis-defective in sister chromatid disjoining), was identified in mutants that blocked mitotic chromosome disjunction (Ohkura et al., 1989, 1988). Fission yeast Dis2 phosphatase is implicated in spindle checkpoint silencing. Upon Ark1 inhibition in a *dis2Δ* background *S. pombe* cells cannot degrade cyclin B and enter anaphase (Vanoosthuyse and Hardwick, 2009). In fission yeast spindle checkpoint silencing relies on the Dis2 interaction with Spc7 (KNL1), but also on Dis2 association with kinesins Klp5 and Klp6 independently of their motor activities (Meadows et al., 2011). Fission yeast expresses another PP1

phosphatase encoded by *sds21* gene (Ohkura et al., 1989). Dis2 and Sds21 have very similar amino acid sequence (79% identity in amino acid sequence) and overlapping functions (Ohkura et al., 1989). However, only Dis2 can silence the checkpoint (Vanoosthuyse and Hardwick, 2009). Similar PP1-dependent spindle checkpoint silencing mechanisms has also been described in budding yeast (Pinsky et al., 2009; Rosenberg et al., 2011) and in *C. elegans* (Espeut et al., 2012). In both systems, like in fission yeast, PP1 homologues (Glc7 in *S. cerevisiae*) are targeted to kinetochores via KNL1/Spc7 family proteins (Rosenberg et al., 2011; Espeut et al., 2012).

Vanoosthuyse and Hardwick (2009) proposed that the Dis2-silencing mechanism targets proteins which were previously phosphorylated by Ark1. Recently, a role for Bub3 in checkpoint silencing has been reported (Vanoosthuyse et al., 2009). According to Vanoosthuyse et al. (2009), kinetochore-localised Bub3 might enrich for other checkpoint proteins at the kinetochore where they can be effectively dephosphorylated by Dis2. Therefore, checkpoint proteins, especially the Bub3 interactors Bub1 and Mad3, are strong candidates for being both Ark1 and Dis2 substrates. Apart from checkpoint proteins, KNL1, Ndc80, and dynein might be PP1 substrates, whose dephosphorylation is required specifically for checkpoint silencing (Liu et al., 2010; Whyte et al., 2008; Kemmler et al., 2009; DeLuca et al., 2006). However, this needs to be further investigated to fully understand the process of checkpoint silencing.

Phosphatase specificity, localisation and activity are modulated by association of a catalytic subunit with accessory subunits. Highly conserved Sds22, which is involved in regulation of mitosis in yeast and metazoans, is an example of such an accessory subunit (Ohkura and Yanagida, 1991; Peggie et al., 2002; Posch et al., 2010; Pinsky et al., 2006a). Recently, budding yeast Fin1 was identified as a Glc7 regulatory subunit required for Glc7 spindle/kinetochore recruitment (Akiyoshi et al., 2009b). From their analyses, Akiyoshi et al. (2009b) proposed a model of Glc7 regulation by Fin1 where Cdk1-dependent phosphorylation of Fin1 promotes Fin1 association with 14-3-3 proteins. This prevents premature Fin1-Glc7 localisation to the spindle maintaining kinetochore balance between Glc7 and Ipl1 during metaphase. In anaphase Fin1 is dephosphorylated by Cdc14 phosphatase which disrupts binding

between Fin1 and 14-3-3 proteins. ‘Free’ Fin1 can interact with Glc7 and recruit it to the spindle in order to dephosphorylate Ipl1 substrates at kinetochores and thereby contribute to spindle checkpoint silencing (Akiyoshi et al., 2009b). However, a checkpoint silencing defect was not detected in *fin1Δ* cells, suggesting that an additional regulatory subunit controls Glc7 (Akiyoshi et al., 2009b).

The mechanism of spindle checkpoint activation is quite well conserved between species but the checkpoint silencing pathways are different variable in different systems. Therefore, it would be interesting to determine why different organisms developed different ways to inhibit checkpoint signaling.

1.3.2. Main aims of this thesis

In recent years significant progress in understanding how the checkpoint signal is generated, amplified and silenced has been achieved. Nevertheless, many important questions remain to be addressed. The role of the mitotic kinases Mps1 and Aurora B in checkpoint signaling has been extensively investigated. However, it is unclear how these kinases are activated in the response to unattached kinetochores. What are their major substrates in the mitotic checkpoint signaling pathway, and how do the kinases regulate each other? It is known that one unattached kinetochore is enough to produce a checkpoint signal, however it remains to be determined how the signal is amplified to inhibit the total pool of APC. Also, the interaction between the MCC and APC needs to be further investigated. What is the mechanism that the MCC utilizes to inhibit the APC and how is APC inhibition released after establishing correct kinetochore-microtubule attachments?

We decided to investigate how checkpoint proteins are recruited to unattached kinetochores. First, we asked whether, similar to the KNL1 homologue in humans (Kiyomitsu et al., 2007, 2011), the fission yeast kinetochore protein Spc7 interacts with the checkpoint proteins Bub1 and Bub3. We also aimed to determine how kinetochore recruitment of the Bub1-Bub3 complex is regulated. To address these questions we developed an assay which allowed us to reconstitute the interaction between checkpoint proteins and Spc7 *in vitro.*

In addition, we attempted to analyze the mechanism that regulates the binding of PP1/Dis2 phosphatase to Spc7 to further dissect the mechanism of spindle checkpoint silencing. Finally, we showed that Spc7 has microtubule binding activity and tested whether this could be regulated by Aurora B/Ark1.

Chapter 2

Material and Methods

Chapter 2

Material and Methods

2.1. General Information

2.1.1 Supplier Information

Chemical used in this study were supplied by Sigma, Melford, Gibco BRL and Fisher unless stated otherwise. Reagents for yeast and bacteria growth media were purchased from Sigma Sigma, Formedium, Difco and Biogene. Restriction enzymes were provided by New England BioLabs.

2.1.2. Sterilization

Majority of solutions was filter sterilized using bottle top filters (Nalgene or Helena Biosciences) or 0.45 μm syringe filters (Millipore). Non-temperature sensitive solutions (e.g. salts) were autoclaved (120^0C, 15 pounds/inch^2, 15 min). All glassware was sterilized by baking at 250°C for 16 hours.

2.2. *Escherichia coli* methods

2.2.1. Bacteria strains

Table 2.1. *E. coli* strains used in this study

strain name	genotype
DH5α (prepared in the lab)	*F⁻ ϕ80dlacZΔM15 Δ(lacZYA-argF)U169 deoR recA1 endA1 hsdR17(rk⁻ mk⁺) phoA supE44 λ- thi-1 gyrA96 relA1*

SoloPack Gold (Stratagene)	*Tet^r Δ(mcrA)183 Δ(mcrCB-hsdSMR-mrr)173 endA1 supE44 thi-1 recA1gyrA96 relA1 lac Hte [F′ proAB lacI^{q}ZΔM15 Tn10 (Tet^r) Amy Cam^r]*
XL1-Blue MRF′ (Stratagene)	*Δ(mcrA)183 Δ(mcrCB-hsdSMR-mrr)173 endA1 supE44 thi-1 recA1 gyrA96 relA1 lac [F′ proAB lacI^{q}ZΔM15 Tn10 (Tet^r)]*
BL21-CodonPlus RIL	*E. coli B F$^-$ ompT hsdS(r_B^- m_B^-) dcm$^+$ Tet^r gal endA The [argU ileY leuW Cam^r]*

DH5α cells were used for gateway cloning and plasmid propagation. XL1-Blue MRF' Supercompetent Cells and SoloPack Gold Competent cells were used for site-directed mutagenesis.

BL21-CodonPlus RIL cells, which enhance expression of AT-rich genes, were used for expression of recombinant proteins.

2.2.2. *E. coli* media

2.2.2.1. LB

Bacto-tryptone	1 % (w/v)
Bacto-yeast extract	0.5 % (w/v)
NaCl	0.5 % (w/v)

pH adjusted to pH 7.2 with NaOH

2.2.2.2. SOC

Bacto-tryptone	2 % (w/v)
Bacto-yeast extract	0.5 % (w/v)
NaCl	0.5 % (w/v)
glucose	20 mM
$MgCl_2$	10 mM
$MgSO_4$	10 mM
KCl	10 mM

2.2.3. Antibiotics

The following antibiotics were used for plasmid selection and maintenance:

- Ampicillin at a final concentration of 100 μg/ml (100 mg/ml stock solution in water)
- Kanamycin at a final concentration of 50 μg/ml (10 mg/ml stock solution in water)
- Chloramphenicol at a final concentration 50-170 μg/ml (34 mg/ml stock solution in ethanol)

2.2.4. Bacteria growth conditions

Bacteria were typically grown on LB plates or in liquid LB at 37°C unless stated otherwise. An appropriate antibiotic was added to media for plasmid selection.

2.2.5. *E. coli* storage

Bacterial strains were kept on LB plates at 4°C up to 10 days. For long-term storage bacterial strains were resuspended in LB containing 20 % glycerol in cryotubes and stored at -80^{0}C.

2.2.6. *E. coli* transformation

2.2.6.1. Transformation of DH5α and BL21-CodonPlus RIL cells

In order to transform competent DH5α or BL21-CodonPlus RIL cells, plasmid DNA and DMSO (1 μl of DMSO per 100 μl of cell suspension) were added to cell suspension. The mixture was incubated on ice for 30 min. Then cells were heat shocked at 42°C for 90 s. Cells were cooled down (2 min on ice), resuspended in LB and incubated at 37°C with shaking for 45 min to recover. Cells were plated on LB solid medium containing appropriate antibiotic and incubated at 37^{0}C overnight.

2.2.6.2. Transformation of SoloPack Gold and XL1-Blue MRF´ cells

Transformations of SoloPack Gold and XL1-Blue MRF´ cells were carried out according to the manufacturer's protocol (Stratagene).

2.2.7. Expression of recombinant proteins in *E. coli*

To obtain MBP or GST tagged protein of interest the pHMGWA- or pHGGWA-based expression vector was transformed into *E. coli* BL21-RIL cells. The cells were grown in 10 ml pre-culture containing ampicillin (100 μg/ml) and chloramphenicol (optional, 50-170 μg/ml) at 37^0C overnight. The presence of chloramphenicol is required to maintain a pACYC-based plasmid containing extra copies of the *argU*, *ileY* and *leuW* tRNA genes in the BL21-Codon Plus strains. Next, 1 litre culture (1:100 dilution of an overnight culture containing 100 μg/ml ampicilin) was grown in LB medium at 37°C. Then the culture was induced with 0.5 mM IPTG (Melford) (at OD_{600}= 0.4-0.8) and shifted to 18°C for 8-15 hours. Then cells were pelleted, frozen and ground in a mortar under liquid nitrogen. The cell powder was stored at -80^0C.

2.3. Fission yeast methods

Table 2.2. Fission yeast strains used in this study

strain	genotype	source
RA1645 (wild type)	h+ *ade6-210 leu1-32 ura4-D18 his3-D1 arg3-D4*	R. Allshire
AS268	*nmt41 mph1:natR leu1-32::nmt41-HFG-spc7 1-283:leu1*	This study
AS261 and AS 262	h+ *nda3-KM311 leu1-32::nmt41-HFG-spc7 1-283:leu1*	This study
YJZ157	mad3::*ura4*	This lab
VV1170	h- *bub1::natR*	This lab
AS504 and AS505	h- *spc7::natR lys1::spc7:kanMX6*	This study
AS235 and AS236	h- *spc7::natR lys1::spc7-S108A S114A:kanMX6*	This study
AS230 and AS231	h- *spc7::natR lys1::spc7-S9A S108A S114A:kanMX6*	This study
AS286 and AS287	h- *spc7::natR lys1::spc7-S28A:kanMX6*	This study
AS288.1 and AS288.2	h- *spc7::natR lys1::spc7-S9A S28A:kanMX6*	This study
AS292 and AS293	h- *spc7::natR lys1:spc7-S9A:kanMX6*	This study
AS310 and AS311	h- *spc7::natR lys1::spc7-S9D:kanMX6*	This study
AS312 and AS313	h- *spc7::natR lys1::spc7-S108D S114D:kanMX6*	This study
AS344 and AS345	h- *spc7::natR lys1::spc7-S9D S28D:kanMX6*	This study
YJZ24	*mph1-kd-SZZ:leu1 ura4-D18 leu1-32 ade6-210*	This lab
YLM223	*mph1-SZZ:kanMX6 nda3-KM311*	This lab

AS304	*leu1-32::nmt41-HFG-spc7 1-283:leu1 bub1-SZZ:kanMX6*	This study
SJ636	*h- bub1-SZZ:kanMX6*	This lab
JM7027	h+ *bub1-GFP:kanMX6 spc7::natR lys1::spc7:ura4 sid4-tdTomato:hygR nda3-KM311*	J. Millar
JM7029	h+ *bub1-GFP:kanMX6 spc7::natR lys1::spc7-T9A:ura4 sid4-tdTomato:hygR nda3-KM311*	J. Millar
JM7031	h+ *bub1-GFP:kanMX6 spc7::natR lys1::spc7-T9E:ura4 sid4-tdTomato:hygR nda3-KM311*	J. Millar
SJ687	h- *bub1-GLEBSΔ-SZZ:kanMX6*	This lab
KP258	*bub3-GFP*	This lab
KP332	*bub3-GFP mad3Δ*	This lab
KP333	*bub3-GFP bub1Δ*	This lab
AS501	h- *spc7::natR lys1::spc7-R6A K24A R25A (BP 1&2)::kanMX6*	This study
AS247	*spc7::natR lys1::spc7::kanMX6 cdc13-GFP:LEU2 nda3-KM311*	This study
AS300 and AS301	*spc7::natR lys1::spc7-S9A S28A:kanMX6 cdc13-GFP:LEU2 nda3-KM311*	This study
AS302 andAS303	*spc7::natR lys1::spc7-S9A:kanMX6 cdc13-GFP:LEU2 nda3-KM311*	This study
AS299	*spc7::natR lys1::spc7-S28A:kanMX6 cdc13-GFP:LEU2 nda3-KM311*	This study
AS357	*spc7::natR lys1::spc7-S9D S28D:kanMX6*	This study

	cdc13-GFP:LEU2, nda3-KM311	
AS127	h- *mad3::ura4 cdc13-GFP:LEU2 nda-KM311*	This study
VV429	*cdc13-GFP:LEU2 cut12-CFP:kanMX6 nda3-KM311*	This lab
AS483	*leu1-32::nmt41-HFG-spc7 1-283:leu1*	This study
AS491	*leu1-32::nmt41-HFG-spc7-R6A (BP1) 1-283:leu1*	This study
AS477	*leu1-32::nmt41-HFG-spc7-K24A R25A (BP2) 1-283:leu1*	This study
AS481	*leu1-32::nmt41-HFG-spc7-R6A K24A R25A (BP 1&2) 1-283:leu1*	This study
JM5667	h+ *GFP-dis2:ura4 ark1-as3:hygR nda3-KM311*	J. Millar
VV1440	*GFP-dis2:ura4 bub3Δ:ura4 nda3-KM311*	This lab

2.3.1. Fission yeast media

2.3.1.1. YES (yeast extract supplemented) (liquid and solid)

yeast extract	0.5 % (w/v)
D-glucose, anhydrous	3 % (w/v)
1 x supplements	

For solid media 2 % (w/v) agar was added.

2.3.1.2. PMG (pombe minimal growth)

phtalic acid	3 g/l
di-sodium hydrogen orthophosphate, anhydrous	2.2 g/l
L-glutamic acid, monosodium salt	3.75 g/l

D-glucose, anhydrous	20 g/l
1 x vitamins	
1x minerals	
1 x salts	

For solid media 2 % (w/v) agar was added.

2.3.1.3. SPA (synthetic sporulation agar)

D-glucose, anhydrous	10 g/l
KH_2PO_4	1 g/l
agar	20 g/l (2 % w/v)

1 x vitamins and 1 x supplements were added after medium autoclaving.

2.3.1.4. FOA plates

5-Fluoroorotic Acid (5-FOA) (Toronto Research Chemicals) at concentration of 2 g/l was dissolved in sterile water at 50°C, with occasional mixing and filter sterilized. The 5-FOA solution was mixed with equal volume of autoclaved 2 x YES [1 % (w/v) yeast extract, 6 % (w/v) D-glucose, anhydrous, 4 % (w/v) agar]. Then 1 x supplements were added.

2.3.1.5. Thiamine plates

For maintenance of strains overexpressing proteins under nmt41 promoter PMG media (liquid and solid) were supplemented with thiamine at final concentration of 15 μM (1000 x stock solution-5mg/ml thiamine stored at 4°C in dark)

2.3.1.6. Supplements

20 x supplement stock:

adenine, arginine, histidine, leucine, lysine, uracil	1.5 g/l

Filter sterilized

2.3.1.7. Minerals

10000 x mineral stock:

Boric acid	80.9 mM
$MnSO_4$	23.7 mM
$ZnSO_4 \times 7\ H_2O$	13.9 mM
$FeCl_3 \times 6\ H_20$	7 mM
Molybdic acid	2.47 mM
KI	6.02 mM
$CuSO_4 \times 5\ H_2O$	1.6 mM
Citric acid	47.6 mM

2.3.1.8. Vitamins

1000 x vitamin stock:

biotin	10 mg/l
pantothenic acid	1 g/l
nicotinic acid	10 g/l
inositol	10 g/l

Filter sterilized

2.3.1.9. Salts

50 x salt stock

$CaCl_2$	1 g/l
Na_2SO_4	2 g/l
KCl	50 g/l
$MgCl_2$	53.5 g/l

2.3.1.10. Drugs

G418 (Geneticin)

G418 (from Calbiochem) was dissolved in ddH_2O and added to YES agar to a final concentration of 150 μg/ml.

Clonat (Nourseothricin)

Clonat (from Werner Bioagents) (stock solution 200 mg/ml in ddH_2O; kept at -20^{0}C) was added to YES agar to a final concentration of 100 μg/ml.

Hygromycin

Hygromycin (from Formedium) (stock solution 50 mg/ml in ddH_2O; kept at 4°C in dark) was added to YES agar to a final concentration of 100 μg/ml.

Benomyl

Benomyl was used at different concentrations (stock solution 30mg/ml in DMSO; kept at -20°C)

2.3.2. Fission yeast transformation

2.3.2.1. Electroporation

Strains to be transformed were grown in YES to an OD_{600} of 0.5-1.0. Cells were centrifuged at 3 000 rpm for 3 min at RT and washed once in ice-cold water and once ice-cold 1 M sorbitol. Cells were resuspended in ice-cold 1 M sorbitol to a final density of 1-5 x 10^9 cells per ml. 40 µl of the suspension was transferred to a pre-chilled eppendorf tube containing the DNA. After short incubation on ice (about 5 min) cell suspension was added to a pre-chilled electroporation 2 mm cuvette (EquiBio) and pulsed using BioRad electroporator set as follows: 1.5 kV, 200 Ohm, 15 µF. Immediately after electroporation 400 µl of ice-cold 1 M sorbitol was added to the cuvette and then cells suspension was plated onto YES plates. After 1-2 days of growing on YES plates, cells were replica plated onto selective media.

2.3.2.2. Lithium acetate

Cells were grown to a density of 0.5 -1 x 10^7 cells/ml (OD_{600} 0.2-0.5) in YES. 50 ml of cell culture was centrifuged at 2 500 rpm for 3 min and then washed two times with sterile water and once with 0.1 M lithium acetate in 1 x TE pH 4.9 (adjusted with acetic acid). Cells were resuspended to a final concentration of 1 x 10^9 cells/ml in 0.1 M lithium acetate in 1 x TE pH 4.9. 150 µl of the cell suspension was aliquoted into eppendorf tubes and incubated at 30°C with shaking for 60-120 min. Then, cells were mixed with the DNA and 370 µl of fresh 50 % (w/v) PEG (3350, Sigma) in 1 x TE prewarmed to 30°C. After 60 min incubation at 30^0C with shaking cells were subjected to a 15-min heat shock at 42^0C. Cells were left at RT for 10 min to cool down, then centrifuged (4 000 rpm, 1 min), resuspended in 1 ml of YES and incubated at 30^0C with shaking for 1 hour to recover. After incubation cells were centrifuged (4 000 rpm, 1 min), supernatant was removed and cells were resuspended in 400 µl of YES and plate onto YES plates. After 1-2 days of incubation, cells were replica plated onto selective media

2.3.3. Fission yeast storage

Fission yeast strains were resuspended in YES containing 40 % glycerol in cryotubes and stored at -80^{0}C.

2.3.4. Fission yeast cell biology methods

2.3.4.1. Benomyl sensitivity assay

4-fold serial dilutions of tested strains were plated on YES plates containing following concentrations of benomyl: 0, 3.5, 5.0 or 6.0 and 7.5 µg/ml. Plates were incubated at 30°C for 3-4 days.

2.3.4.2. Protein overexpression under nmt41 promoter

The *S. pombe nmt41-mph1* and *nda3KM311* cells were transformed with the pDUAL *-nmt41-HFG-spc7 (1-283)* constructs which integrated the first 283 amino acids of Spc7, N-terminally tagged with 6xHis-FLAG-GFP (HFG), into the *leu1* locus.
Similarly, the wild type cells were transformed with the pDUAL *-nmt41-HFG-spc7 (1-283),* pDUAL-*nmt41- HFG-spc7 R6A (BP1) (1-283),* pDUAL-*nmt41- HFG-spc7 K24A R25A (BP2) (1-283) and* pDUAL-*nmt41-HFG-spc7 R6A K24A R25A (BP 1&2) (1-283)* constructs.

Expression of the HFG-Spc7 (1-283) proteins and Mph1 was induced by the absence of thiamine in media as the transgene was under control of the nmt41 promoter. Among nmt (no message in thiamine) promoters the nmt41 provides moderate overexpression of target protein (Basi et al., 1993).

Pre-culture were grown overnight in YES containing thiamine to repress the nmt41 promoter. The next day cells were harvested (3 000 rpm, 3 min) and washed five times with sterile water to remove all thiamine. Then cells were resuspended, (to a low OD), in PMG plus supplements and incubated at 30°C for 12-14 hours to allow the HFG-Spc7 (1-283) proteins and Mph1 overexpression.

Mph1 overexpression resulted in metaphase arrest as reported previously (Hardwick et al., 1996b; He et al., 1998).

2.3.4.3. Mitotic arrest using *nda3-KM311* strains

To arrest *nda3-KM311* strains in mitosis cells were grown overnight at the permissive temperature of 32°C. Mid-log cell cultures were then shifted to the restrictive temperature of 18°C for 8-10 hrs. Samples were taken at the 2-hour intervals starting from 4th hour of the incubation. Cells were fixed in methanol prior to microscopic analysis.

2.3.4.4. Microscopy

Microscopy was performed with an Intelligent Imaging Innovations Marianas microscope, CoolSnap CCD, and Slide- Book software.

2.3.4.4.1. Methanol fixation

To visualize Cdc13-GFP dots in the *nda3* arrest experiment and overexpressed GFP-Spc7 1-283 proteins cells were briefly fixed in ice-cold 100 % methanol. 4 µl of the cell suspension and 1µl DAPI solution (0.5 µg/ml in PEM) was applied on onto a slide.

2.3.4.4.2. Immunofluorescence - TAT1 spindle staining

Buffers

PEM buffer
100 mM PIPES pH 7.6,
1 mM $MgSO_4$,
1 mM EGTA

PEMS buffer
1 M sorbitol
100 mM PIPES pH 7.6,
1 mM $MgSO_4$,
1 mM EGTA

PEMBAL

BSA 1 %

L-lysine 0.1 %

sodium azide 0.1 %

100 mM PIPES pH 7.6,

1 mM $MgSO_4$,

1 mM EGTA

TAT1 is an anti-tubulin antibody. TAT1 spindle staining was used to determine whether cells overexpressing HFG-Spc7 (1-283), wild type and basic patch mutants, exhibit an elevated number of mitotic cells characterized by a short spindle.

Cells were fixed in ice-cold methanol. Cell pellets were resuspended in PEM and centrifuged for 1 min at 5 000 rpm at RT. This step was repeated once again and then cell pellets were resuspended in 1 ml PEMS containing 0.4 mg/ml zymolyase (Seikagaku Biobusiness). Samples were incubated at 30°C for 45 min with occasional mixing. After incubation, cells were washed twice with PEMS (1 min at 5 000 rpm at RT). Next cells were resuspended in 500 μl of PEMS containing 1 % Triton X-100 and then immediately washed twice with PEM. Cells were blocked in PEMBAL for 1 hour at RT. Following the blocking of unspecific antibody binding, cells were resuspended in PEMBAL containing primary TAT1 antibody (1:50) and incubated overnight at 4^0C. The next day, cells were washed twice with PEM and incubated with secondary anti-mouse (Alexa Fluor 594, Invitrogen) for 1 hour at RT in dark. Prior to microscopic analysis cells were washed with PEM and then resuspended in 20-50 μl of PEM.

2.4. DNA methods

Table 2.3. Plasmids used in this study

name	description	source
pGBDT7-*spc7*$^{+}$	Yeast two-hybrid bait expression vector, pGBDT7, contatining full lenght Spc7	J. Millar
pBSSK-*ura4-spc7-S108A S114A*	pBluescript SK containing 350bp of upstream promoter region and an N-terminal fragment of Spc7 (residues 1-666) with serines 108 and 114 substituted for alanines	J. Millar
pHGGWA-*spc7 1-283*	Backbone: pHGGWA expression vector (Busso et al., 2005); contains: Spc7 residues 1-283; marker: ampicillin	This study
pHGGWA-*spc7-S108A S114A 1-283*	Backbone: pHGGWA expression vector (Busso et al., 2005); contains: Spc7 residues 1-283; mutations: S108, S114A; marker: ampicillin	This study
pHGGWA-*spc7-S9A S108A S114A 1-283*	Based on pHGGWA-*spc7-S108A S114A 1-283;* contains: Spc7 residues 1-283; mutations: S9A 108A 114A; marker: ampicillin	This study
pHGGWA-*spc7-S9A S28A S108A S114A 1-283*	Based on pHGGWA-*spc7-S9A S108A S114A 1-283;* contains: Spc7 residues 1-283; mutations: S9A S28A 108A 114A;	This study

	marker: ampicillin	
pHGGWA-*spc7-S108D S114D 1-283*	Based on pHGGWA-*spc7*$^{+}$ *1-283;* contains: Spc7 residues 1-283; mutations: 108D 114D; marker: ampicillin	This study
pHGGWA-*spc7-S9A S28A 1-283*	Based on pHGGWA-*spc7*$^{+}$ *1-283;* contains: Spc7 residues 1-283; mutations S9A S28A; marker: ampicillin	This study
pHGGWA-*spc7-S9D 1-283*	Based on pHGGWA-*spc7*$^{+}$ *1-283;* contains: Spc7 residues 1-283; mutations S9D; marker: ampicillin	This study
pHGGWA-*spc7-S28D 1-283*	Based on pHGGWA-*spc7*$^{+}$ *1-283;* contains: Spc7 residues 1-283; mutations S28D; marker: ampicillin	This study
pHGGWA-*spc7-S9D S28D 1-283*	Based on pHGGWA-*spc7S9D 1-283;* contains: Spc7 residues 1-283; mutations S9D S28D; marker: ampicillin	This study
pHGGWA-*spc7-R6A (BP1) 1-283*	Based on pHGGWA-*spc7*$^{+}$ *(1-283);* contains: Spc7 residues 1-283; mutations: R6A; marker: ampicillin	This study
pHGGWA -*spc7-K24A R25A (BP2) 1-283*	Based on pHGGWA-*spc7*$^{+}$ *1-283;* contains: Spc7 residues 1-283; mutations: K24A R25A; marker: ampicillin	This study
pHGGWA -*spc7-R6A K24A R25A (BP 1&2) 1-283*	Based on pHGGWA -*spc7-K24A R25A (BP2) 1-283;* contains: Spc7 residues 1-283;	This study

	mutations: R6A K24A R25A; marker: ampicillin	
pHMGWA-*spc7 1-666*	Backbone: pHMGWA expression vector (Busso et al., 2005); contains: Spc7 residues 1-666; marker: ampicillin	This study
pHMGWA-*spc7-T9A 1-666*	Backbone: pHMGWA expression vector (Busso et al., 2005); contains: Spc7 residues 1-666; mutations: T257A, T338A, T366A, T395A,T422A, T453A, T507A, T529A, T552A; marker: ampicillin	This study
pHMGWA-*spc7-T9E 1-666*	Backbone: pHMGWA expression vector (Busso et al., 2005); contains: Spc7 residues 1-666; mutations: T257E, T338E, T366E, T395E,T422E, T453E, T507E, T529E, T552E; marker: ampicillin	This study
pDUAL-*nmt41-HFG-spc7 1-283*	backbone: pDUAL HFG41c (kind gift of Prof. K.Sawin) (Matsuyama et al., 2004); contains: Spc7 residues 1-283; marker: *leu1*	This study
pDUAL-*nmt41-HFG-spc7-R6A (BP1) 1-283*	Based on pDUAL-*nmt41-HFG-spc7 1-283*; contains: Spc7 residues 1-283; mutations: R6A; marker: ampicillin	This study
pDUAL-*nmt41-HFG- spc7-K24A R25A (BP2) 1-283*	Based on pDUAL-*nmt41-HFG-spc7 1-283*; contains: Spc7 residues 1-283; mutations:	This study

	K24A, R25A; marker: ampicillin	
pDUAL-*nmt41-HFG- spc7-R6A K24A R25A (BP 1&2) 1-283*	Based on pDUAL-*nmt41-HFG-spc7-R6A 1-283*; contains: Spc7 residues 1-283; mutations: R6A, K24A, R25A; marker: ampicillin	This study
pLYS1K-*spc7*$^{+}$	pLYS1K vector (Matsuyama et al., 2008) containing full length Spc7 with 500 bp of 5'UTR and 200bp of 3'UTR; marker: kanMX6	J. Millar
pLYS1K-*spc7-S108A S114*	Based on pLYS1K-*spc7*$^{+}$; contains containing full length Spc7 with 500 bp of 5'UTR and 200bp of 3'UTR; mutations: S108A S114A; marker: kanMX6	This study
pLYS1K-*spc7-S9A S108A S114A*	Based on pLYS1K-*spc7-S108A S114*; contains containing full length Spc7 with 500 bp of 5'UTR and 200bp of 3'UTR; mutations: S9A S108A S114A; marker: kanMX6	This study
pLYS1K-*spc7-S9A*	Based on pLYS1K-*spc7*$^{+}$; contains containing full length Spc7 with 500 bp of 5'UTR and 200bp of 3'UTR; mutations: S9A; marker: kanMX6	This study
pLYS1K-*spc7-S28A*	Based on pLYS1K-*spc7*$^{+}$; contains containing full length Spc7 with 500 bp of 5'UTR and 200bp of 3'UTR; mutations:	This study

	S28A; marker: kanMX6	
pLYS1K-*spc7- S9A S28A*	Based on pLYS1K-*spc7-S9A*; contains containing full length Spc7 with 500 bp of 5'UTR and 200bp of 3'UTR; mutations: S9A S28A; marker: kanMX6	This study
pLYS1K-*spc7-S9D*	Based on pLYS1K-*spc7*$^{+}$; contains containing full length Spc7 with 500 bp of 5'UTR and 200bp of 3'UTR; mutations: S9D; marker: kanMX6	This study
pLYS1K-*spc7-S9D S28D*	Based on pLYS1K-*spc7- S9D*; contains containing full length Spc7 with 500 bp of 5'UTR and 200bp of 3'UTR; mutations: S9D S28D; marker: kanMX6	This study
pLYS1K-*spc7-S108D S114D*	Based on pLYS1K-*spc7*$^{+}$; contains containing full length Spc7 with 500 bp of 5'UTR and 200bp of 3'UTR; mutations: S108D S114D; marker: kanMX6	This study
pLYS1K-spc7-*R6A K24A R25A (BP 1&2)*	Based on pLYS1K-*spc7- K24A R25A*; contains containing full length Spc7 with 500 bp of 5'UTR and 200bp of 3'UTR; mutations: *R6A K24A R25A* marker: kanMX6	This study
pLYS1K-*spc7-T9A*	pLYS1K vector (Matsuyama et al., 2008) containing full length Spc7 with 500 bp of 5'UTR and 200bp of 3'UTR; mutations: : T257A, T338A, T366A,	J. Millar

	T395A,T422A, T453A, T507A, T529A, T552A; marker: kanMX6	
pLYS1K-*spc-T9E*	pLYS1K vector (Matsuyama et al., 2008) containing full length Spc7 with 500 bp of 5'UTR and 200bp of 3'UTR; mutations: : T257E, T338E, T366E, T395E,T422E, T453E, T507E, T529E, T552E; marker: kanMX6	J. Millar
pHGGWA-Pic1 IN box	Backbone: pHGGWA expression vector (Busso et al., 2005); contains: Pic1 residues 925-1018; marker: ampicillin	This study
pHGGWA-160 Pic1 IN box	Backbone: pHGGWA expression vector (Busso et al., 2005); contains: Pic1 residues 765-1018; marker: ampicillin	This study
pHMGWA-Pic1 IN box	Backbone: pHMGWA expression vector (Busso et al., 2005); contains: Pic1 residues 925-1018; marker: ampicillin	This study
pHMGWA-160 Pic1 IN box	Backbone: pHMGWA expression vector (Busso et al., 2005); contains: Pic1 residues 765-1018; marker: ampicillin	This study
pITRu-*spc7*$^{+}$	Episomal expression of full length Spc7 with 500 bp of 5'UTR and 200bp of 3'UTR, marker: *ura4*	J. Millar
pDONR201	Donor vector in Gateway	

	Technology (Invitrogen); marker tetracycline and chloramphenicol	

Table 2.4. Primers used in this study

name	sequence (5'→3')	purpose
Spc7 FW gateway	GGGGACAAGTTTGTACAAA AAAGCAGGC TTCATGCCA ACATCGCCTCGTCGC	pHGGWA-*spc7 1-283* pHGGWA-*spc7-S108A S114A 1-283* pHMGWA-*spc7 1-666* pHMGWA-*spc7-T9A 1-666* pHMGWA-*spc7-T9E 1-666*
Spc7 REV 1-283 gateway	GGGGACCACTTTGTACAA GAAAGCTGGGTCCTAAGT ACCTTGCTCGCTAGAGCT	pHGGWA-*spc7 1-283* pHGGWA-*spc7-S108A S114A* 1-283
Spc7 REV 1-666 gateway	GGGGACCACTTTGTACAA GAAAGCTGGGTCCTAATT CAAAGTTGAAATTGATTT TCG	pHMGWA-*spc7 1-666* pHMGWA-*spc7-T9A 1-666* pHMGWA-*spc7-T9E 1-666*
Pic1 REV gateway	GGGGACCACTTTGTACAA GAAAGCTGGGTCCTATAA AAAACCCATGTTTTTCTTA TAGTTATC	pHGGWA-Pic1 IN box pHGGWA-160 Pic1 IN box pHMGWA-Pic1 IN box pHMGWA-160 Pic1 IN box
IN box FW gateway	GGGGACAAGTTTGTACAAA AAAGCAGGCTTCGATTAT	pHGGWA-Pic1 IN box

	TCGGATGATTCAGATGA	pHMGWA-Pic1 IN box
160aa+IN box FW gateway	GGGGACAAGTTTGTACAAA AAAGCAGGCTTCGCTGAG GACATGTCATTGGCATT	pHGGWA-160 Pic1 IN box pHMGWA-160 Pic1 IN box
Spc7 S108A S114A FW (J. Millar)	AACAGAAGAGTTGCCTTTG CTAGTCAT	pLYS1K-*spc7-S108A S114A*
Spc7 S108A S114A REV (J. Millar)	CAAAGCTTTTCTAGACGTC TC	pLYS1K-*spc- S108A S114A*
Spc7 S9A FW	ACATCGCCTCGTCGCAATG CCATAGCGACGACCG	pHGGWA-*spc7-S9A S108A S114A 1-283* pLYS1K-*spc- S9A* pLYS1K-*spc7-S9A S108A S114A*
Spc7 S9A REV	CGGTCGTCGCTATGGCATT GCGACGAGGCGATGT	pHGGWA-*spc7-S9A S108A S114A 1-283* pLYS1K-*spc7 S9A* pLYS1K-*spc7 S9A S108A S114*
Spc7 S9D FW	ACATCGCCTCGTCGCAATG ATATAGCGACGACCG	pHGGWA-*spc7-S9D 1-283* pLYS1K-*spc7-S9D*
Spc7 S9D REV	CGGTCGTCGCTATATCATT GCGACGAGGCGATGT	pHGGWA-*spc7-S9D 1-283* pLYS1K-*spc7-S9D*
Spc7 S28A FW	TAGGAAGCGTCCACACGC GCTTGGAGGACCTGGT	pHGGWA-*spc7-S9A S28A S108A S114A 1-283*

		pHGGWA-*spc7-S9A S28A 1-283* pLYS1K-*spc7-S28A* pLYS1K-*spc7-S9A S28A*
Spc7 S28A REV	ACCAGGTCCTCCAAGCGC GTGTGGACGCTTCCTA	pHGGWA-*spc7-S9A S28A S108A S114A 1-283* pHGGWA-*spc7-S9A S28A 1-283* pLYS1K-*spc7-S28A* pLYS1K-*spc7-S9A S28A*
Spc7 S28D FW	TAGGAAGCGTCCACACGA TCTTGGAGGACCTGGT	pHGGWA-*spc7-S28D 1-283* pHGGWA-*spc7-S9D S28D 1-283* pLYS1K-*spc7-S9D S28D*
Spc7 S28D REV	ACCAGGTCCTCCAAGATCG TGTGGACGCTTCCTA	pHGGWA-*spc7-S28D 1-283* pHGGWA-*spc7-S9D S28D 1-283* pLYS1K-*spc7-S9D S28D*
Spc7 S108D S114D FW	GACGTCTAGAAAAGATTTGA ACAGAAGAGTTGATTTTGCT AGTCA	pHGGWA-*spc7-S108D S114D 1-283* pLYS1K-*spc7-S108D S114D*
Spc7 S108D S114D REV	TGACTAGCAAAATCAACTCT TCTGTTCAAATCTTTTCTAGA CGTC	pHGGWA-*spc7-S108D S114D 1-283* pLYS1K-*spc7-S108D*

		S114D
Basic patch R6A FW	ATGCCAACATCGCCTGCCCG C AATAGTATAGCGA	pHGGWA-*spc7-R6A (BP1)1-283 pDUAL-nmt41-HFG-spc7-R6A (BP1) 1-283*
Basic patch R6A REV	TCGCTATACTATTGCGGGCA GG CGATGTTGGCAT	pHGGWA-*spc7-R6A (BP1)1-283* pDUAL-*nmt41-HFG-spc7-R6A (BP1) 1-283*
Basic patch K24A R25A FW	AGAAACAAAAGTAGGGCCG CC CCACACTCGCTTGG	pHGGWA -*spc7-K24A R25A (BP2) 1-283* pHGGWA -*spc7-R6A K24A R25A (BP 1&2) 1-283* pLYS1K-*spc7-R6A K24A R25A (BP 1&2)* pDUAL-*nmt41-HFG-spc7-K24A R25A (BP2) 1-283* pDUAL-*nmt41-HFG-spc7-R6A K24A R25A (BP 1&2) 1-283*
Basic patch K24A R25A REV	CCAAGCGAGTGTGGGGCGGC C CTACTTTTGTTTCT	pHGGWA -*spc7-K24A R25A (BP2)* 1-283 pHGGWA -*spc7-R6A K24A R25A (BP 1&2) 1-283* pLYS1K-*spc7-R6A K24A R25A (BP 1&2)* pDUAL-*nmt41-HFG-spc7-K24A R25A (BP2) 1-283*

		pDUAL-*nmt41-HFG-spc7-R6A K24A R25A (BP 1&2) 1-283*
TM A	AACAATAAACACGAATGCCTC	specific to the central core (ChIP)
TM B	ATAGTACCATGCGATTGTCTG	specific to the central core (ChIP)
OTR A	CACATCATCGTCGTACTACAT	specific to the outer repeats (ChIP)
OTR B	GATATCATCTATATTTAATGACTACT	specific to the outer repeats (ChIP)
fbp A	AATGACAATTCCCCACTAGCC	euchromatic control primer
fbp B	ACTTCAGCTAGGATTCACCTGG	euchromatic control primer

2.4.1. Buffers

2.4.1.1. 10 x TE buffer

100 mM Tris-HCl pH 8.0
10 mM EDTA

2.4.1.2. Smash buffer

2 % Triton X-100,
1 % SDS
100 mM NaCl
10 mM Tris-HCl (pH 8.0)

2.4.1.3. 10 x TBE buffer

445 mM Tris base
455 mM Boric acid
100 mM EDTA (pH 8.0)

2.4.2. *E. coli* plasmid mini prep

For plasmid isolation bacteria cells were grown overnight in 3 ml LB containing appropriate antibiotic. Cells were collected by centrifugation and processed using GeneJET™ Plasmid Miniprep Kit (Fermentas) according to the provided protocol.

2.4.3. Genomic DNA extraction from fission yeast

10 ml cell cultures were grown to an OD_{600} of 0.5-1.0. Cells were harvested (4000 rpm, 1 min, RT), resuspended in sterile water and transferred to screw cap tubes and then centrifuged again (14 000 rpm, 1 min, RT). The cell pellets were resuspended in 200 µl of Smash buffer and 200 µl of phenol:chloroform:isoamyl alcohol (25:24:1) (Sigma). 300 mg of glass beads was added to each sample and then the mixtures were vortexed for 4 min. After vortexing, 200 µl of TE pH 8.0 was added and samples were centrifuged at 14 000 rpm for 5 min at RT. The aqueous, upper phase was transferred to a fresh tube and 1 ml of 96 % ethanol was added. Samples were centrifuged at 14 000 rpm for 2 min at RT. Pellets were resuspended in 400 µl of TE pH 8.0 containing 30 µg of RNase A and incubated at 37°C for 5 min. After incubation 10 µl of 4 M ammonium acetate plus 1 ml of 96 % ethanol was added. Samples were mixed by inversion and centrifuged at 14 000 rpm for 5 min at RT. The DNA pellets were air-dried and resuspended in 200 µl of TE pH 8.0. For PCR reaction, 1-2 µl of the genomic DNA suspension was used.

2.4.4. Polymerase Chain Reaction

DNA was amplified by Polymerase Chain Reaction (PCR). For cloning, diagnostic and ChIP purposes Phusion High-Fidelity DNA Polymerase (New England BioLabs) and the Expand High Fidelity PCR system (Roche Diagnostics GmbH) were used.

PCR reactions were carried out in DNA Engine Thermal Cycler (BioRad) or in PTC-200 Thermo Cycler (MJ Research).

2.4.4.1. Phusion High-Fidelity-PCR reaction mixture

Component	Final concentration
5 x Phusion GC Buffer	1 x Phusion GC Buffer
10 x dNTPs (2.5 mM dATP, dGTP, dCTP and dTTP)	1 x dNTPs
Forward Primer	0.5 µM
Reverse Primer	0.5 µM
Phusion DNA Polymerase	1 unit per 50 µl reaction
Template	plasmid DNA, genomic DNA, yeast and *E.coli* colonies

For all templates routine PCR programme was used:

1. Initial denaturation	98°C	30 sec
2. Denaturation	98°C	10 sec
3. Annealing	*	20 sec
4. Extension	72°C	15-30 sec/1 kb
5. Got to 2. 30 times		
6. Final extension	72°C	5 min

*annealing temperature was determined using online TM calculator-Finnzymes

2.4.4.2. Expand High-Fidelity-PCR reaction mixture

Component	Final concentration
10 x PCR Buffer	1 x PCR Buffer
10 x dNTPs (2.5 mM dATP, dGTP, dCTP and dTTP)	1 x dNTPs
Forward Primer	0.5 µM
Reverse Primer	0.5 µM
Polymerase	3 unit per 50 µl reaction
Template	plasmid DNA, genomic DNA, yeast and *E.coli* colonies

For all templates routine PCR programme was used:

1. Initial denaturation	94°C	2 min
2. Denaturation	94°C	30 sec
3. Annealing	53°C -60°C	30 sec
4. Extension	72^{0}C	1min/1 kb
5. Got to 2. 30 times		
6. Final extension	72^{0}C	5 min

2.4.4.3. Colony PCRs

Yeast colony PCR: a small amount of yeast was transferred to the PCR tube and the yeast was heated at 98^{0}C for 5 min in thermal cycler. Then the reaction mixture was added to the tube and PCR reaction was carried out.

E. coli colony PCR: a small amount of bacteria was introduced to the PCR tube containing the reaction mixture and PCR reaction was carried out.

2.4.5. Site-directed mutagenesis

- Site directed mutagenesis was typically performed using the QuikChange II Site-Directed Mutagenesis Kit (Stratagene).

Site-directed mutagenesis-PCR reaction mixture:

Component	Amount used
10 x reaction buffer	1 µl (1 x reaction buffer)
dNTPs	0.2 µl
Template (plasmid DNA)	5-10 ng
Forward Primer	25 ng
Reverse Primer	25 ng
PfuUltra HF DNA polymerase	0.2 µl (0.5 unit)
ddH_2O	Top up to 10 µl

Site-directed mutagenesis-PCR programme:

1. Initial denaturation	95°C	30 sec
2. Denaturation	95°C	30 sec
3. Annealing	55°C	1 min
4. Extension	68^0C	1 min/1 kb
5. Got to 2. 16-18 times		
6. Final extension	68^0C	5 min

- To introduce the S108A S114A mutations into Spc7 Phusion Site-Directed Mutagenesis kit (Finnzymes) was used according to the provided protocol.

2.4.6. Sequencing reaction

Sanger sequencing was carried out by 'The GenePool' (the University of Edinburgh) on samples already processed with BigDye reagents. Analysis of the samples was performed on the ABI 3730 capillary sequencing instrument.

Sequencing reaction mixture:

Component	Amount used
BigDye Terminator kit v3.1	2 µl
Template (plasmid DNA)	200-500 ng for plasmid DNA 40-100 ng for PCR product
Sequencing Primer	1.6 pmol
ddH_2O	Top up to 10 µl

Sequencing reaction-PCR programme:

1. Initial denaturation	95°C	5 min
2. Denaturation	95°C	30 sec
3. Annealing	55°C	15 sec
4. Extension	60^0C	4 min

5. Got to 2. 25 times

2.4.7. PCR product purification

PCR product purification was performed using the PCR Purification kit (Qiagen) according to the manufacturer's protocol

2.4.8. DNA electrophoresis

Separation of DNA fragments was typically carried out in 0.8 % agarose gel (0.8 % agarose in 1 x TBE) containing 0.5 µg/ml ethidium bromide. 6 x sample loading buffer was added to the sample prior to electrophoresis.

2.4.9. DNA digestion with restriction enzymes

Restriction digest was performed prior to fission yeast transformation to linearize plasmid DNA. Endonucleases and appropriate restriction buffers were purchased from New England BioLabs. The digest reactions were carried out according to the New England BioLabs guideline. Efficiency of DNA digestion was checked by electrophoresis.

2.4.10. Gateway Cloning

- To generate GST-Spc7 (1-283) fusion proteins a gene fragment encoding Spc7 residues 1-283 was amplified from pGBDT7-*spc7*$^{+}$ and *pBSSK-ura4-spc7-S108A S114A* plasmids using high fidelity polymerase (Roche Diagnostics GmbH) and primers Spc7 FW gateway and Spc7 REV 1-283 gateway.

- To generate MBP-Spc7 (1-666) fusion proteins a gene fragment encoding Spc7 residues 1-666 was amplified from pLYS1K-*spc7*$^{+}$, pLYS1K-*spc7-T9A* and pLYS1K-*spc7-T9E* using high fidelity polymerase (Roche Diagnostics GmbH) and primers Spc7 FW gateway and Spc7 REV 1-666 gateway.

- To generate MBP- and GST- tagged Pic1 IN box and Pic1 160-IN box proteins gene fragments encoding Pic1 residues 925-1018 and 765-1018, respectively, were amplified from pDONR-Pic1 (generated by S. van der Sar) using high fidelity polymerase (Roche Diagnostics GmbH) and following primer pairs: Pic1 REVgateway/IN box FW gateway and Pic1 REVgateway/160aa+IN box FW gateway.

- To generate the pDUAL HFG41c- based constructs containing *spc7 1-283*, a gene fragment encoding Spc7 residues 1-283 was amplified from

pGBDT7-*spc7*$^{+}$ using high fidelity polymerase (Roche Diagnostics GmbH) and primers Spc7 FW gateway and Spc7 REV 1-283 gateway.

The PCR products were cloned into pDONR201 donor vector using Gateway BP Clonase II enzyme mix (Invitrogen) and then transferred to pHGGWA Gateway-based destination vector (Busso et al., 2005) using Gateway LR Clonase II enzyme mix (Invitrogen) according to the manufacturer's instructions.

2.5. Protein Biochemistry

2.5.1. Buffers and Solutions

2.5.1.1. SDS-PAGE gel running buffer

50 mM Tris base

384 mM Glycine

2 % SDS

2.5.1.2. Nitrocellulose membrane semi-dry transfer buffer

25 mM Tris base

130 mM Glycine

20 % methanol

2.5.1.3. 2 x SDS gel-loading buffer

62.5 mM Tris-HCl base pH 6.8

5 % SDS

10 % glycerol

5 % β- mercaptoethanol

0.2 % bromophenole blue

2.5.1.4. Ponceau S stain

0.1 % Ponceau S

2 % acetic acid

2.5.1.5. PBS+Tween 20

1 x PBS

0.05 % Tween 20

2.5.1.6. Blocking solution

1 x PBS

0.05 % Tween 20

4 % milk powder (Marvel)

2.5.2. SDS Polyacrylamide Gel

‘Regular’ 10 % SDS-PAGE resolving gel:

1.5 M Tris-HCl pH 8.8	3.75 ml
40 % acrylamide (29:1)	3.7 ml
2 % bisacrylamide	0.98 ml
10 % SDS (optional)	150 µl
10 % Ammonium Persulfate (APS)	75 µl
TEMED	7.5 µl
dd H_2O	to 15 ml

gel was overlaid with isopropanol

10 % SDS-PAGE resolving gel for mobility shift detection of phosphorylated proteins

1.5 M Tris-HCl pH 9.2	3.75 ml
40 % Acrylamide	3.5 ml
2 % Bisacrylamide	0.5 ml
10 % SDS (optional)	150 µl
10 % Ammonium Persulfate (APS)	150 µl
TEMED	6.0 µl
dd H_2O	to 15 ml

gel was overlaid with isopropanol

5 % Stacking gel (1 x stock solution, stored at 4°C)

1 M Tris-HCl pH 6.8	6.25 ml
40 % Acrylamide	6.25 ml
2% Bisacrylamide	3.33 ml
dd H_2O	to 50 ml

-50 µl of 10 % APC per 5 ml of stacking gel was added prior to use
-5 µl of 10 % TEMED per 5 ml of stacking gel was added prior to use

2.5.3. Protein electrophoresis and transfer

Proteins were typically separated by 10 cm x 20 cm SDS-PAGE gels for 90 min at constant voltage of 160 -180 volts in 1 x SDS-PAGE running buffer.

Proteins were transferred form SDS Polyacrylamide gels to nitrocellulose membranes (GE Water & Process Technologies) using a semi-dry transfer blotter (Hoefer , TE77) at 125 mA for 90 min in semi-dry transfer buffer according to the manufacturer's instructions.

2.5.4. Western blotting

After transfer membranes were washed briefly with sterile water and incubated for 2-5 min with Ponceau S stain solution to check transfer quality. Ponceau S stain was washed off with sterile water and membranes were subjected to 30 min incubation in blocking solution. Following blocking, membranes were incubated with the appropriate primary antibody diluted in blocking solution for 3-5 hours at RT or overnight at 4°C depending on the antibody. Next, membranes were washed 3 times in PBS+Tween 20 for 15 min and incubated with the appropriate secondary antibody for 1 hour at RT. Unbound antibody was removed by washing membranes in PBS+Tween 20 (3 times, 15 min).

2.5.5. Protein detection

Proteins were visualized by chemiluminescence using an ECL detection kit (SuperSignal West Pico or SuperSignal West Femto from Pierce) according to provided protocol. Then membranes, wrapped in cling foil, were exposed to X-ray films (CP-Bu new Agfa HealthCare). Films were developed using Konica-Minolta SRX-101A Film Processor.

Table 2.5. Antibodies used for western blots in this study

antibody	species	working concentration	origin
anti-GFP	sheep	1:1 000	This lab
anti-Spc7	sheep	1:1 000	This study
anti-Spc7 p108	rabbit	1:500	Eurogentec (gift from J.Millar)
anti-Spc7 p114	rabbit	1:500	Eurogentec (gift from J.Millar)
anti-Dis2	rabbit	1:1 000	Bio Academia
anti-PK	mouse	1:1 000	Serotec
PAP (peroxidase anti peroxidase)		1:1 000	Sigma
anti-tubulin (TAT1)	mouse	1:1 000	gift from Keith Gull
sheep-HRP*	donkey	1:10 000	Jackson Immuno Research
rabbit-HRP*	sheep	1:5 000	GE-Healthcare
mouse-HRP*	donkey	1:5 000	GE-Healthcare

*Horseradish Peroxidase

2.5.6. Protein extracts

Protein extracts were prepared from 5-10 ml cultures grown till saturation (an OD_{600} of 0.5-1.0). Cells were collected by centrifugation (4000 rpm 3 min), washed once with ice-cold water and transferred to the screw cap tubes. Then, 200-300 µl of SDS gel-loading buffer containing protease and phosphatase (optional) inhibitors [1 mM Pefabloc (Roche), 10 µg/ml LPC (Leupeptin/Pepstatin/Chymostatin; Roche) and 0.1 µM microcystin, respectively] and 200 µl Zirconia/Silica beads (BioSpec Products) were added to the cells. Cell walls and membranes were disrupted

by bead-beating (twice, 20 sec). Extracts were boiled at 95°C-100°C for 3-5 min and directly loaded onto SDS-PAGE gel or stored at -80°C.

2.5.7. Recombinant protein purification

Buffers

Lysis buffer

PBS containing

0.5 M NaCl
0.5 % Tween 20
1 mM Pefablock (Roche)
10 µg /ml LPC (leupeptin/pepstatin/chymostatin, Roche)
Complete Mini EDTA-free Protease Inhibitor Cocktail Tablets (Roche)
(1 tablet per 10 ml of buffer)

Wash buffer

PBS containing

0.25 M KCl
0.5 mM DTT

Lysate preparation

Cell powder (obtained as described in 2.2.7.) was resuspended in five pellet volumes of ice-cold lysis buffer. The suspension was then sonicated (20 sec pulse, 20 sec interval, three cycles) (Sonics, Vibra-Cell) and DNase and lysozyme were added. Lysate was incubated at RT for 15-20 minutes and then centrifuged at 17 500 rpm for 15 min. Supernatant was filtered through a 25 mm GD/X syringe filters, pore size 1.6 µM (Whatman).

GST protein purification

Clarified lysate was passed through Glutathione Agarose (Sigma) slurry three times. After two washes with wash buffer containing 0.05 % Tween 20 and one wash without Tween 20, GST-fusion proteins were eluted with 10 mM reduced glutathione (Sigma) in 50 mM Tris-HCl pH 9.0.

MBP protein purification

Clarified lysate was passed through Amylose resin (New England BioLabs) slurry three times. After two washes with wash buffer containing 0.05 % Tween 20 and one wash without Tween 20, MBP-fusion proteins were eluted with 10 mM maltose, 0.25 M KCl, 50 mM Tris-HCl pH 8.0.

Dialysis

Following purification, recombinant proteins were dialysed overnight into buffer containing 50 mM Hepes pH 7.6, 50 mM KCl, 20 % glycerol SnakeSkin Dialysis Tubing (Thermo Scientific).

Protein concentration

Protein concentration assay was typically carried out using Protein Assay Dye Reagent Concentrate (BioRad) diluted five times with ddH_2O and different BSA concentrations (1 μg/ml-8 μg/ml) as standards. Absorbance was measured at 595 nm. Protein solutions were assayed in duplicate.

2.5.8. Anit-Spc7 antibody generation and purification

Antigen column preparation

Antigen column was prepared by coupling 8 mg of GST-Spc7 1-283 to AminoLink Plus Coupling Resin according to the manufacturer's protocol (Pierce)

Anti-Spc7 antibody purification

Ant-Spc7 antibody was produced in sheep and rabbit. The antigen injection and blood collection was performed by Scottish National Blood Transfusion Service, Pentlands Science Park.

Purification was carried out together with Dr. Kevin Hardwick.

Buffers

PBS-High salt
PBS containing 0.5 M NaCl

PBS-T
PBS containing 0.1 % Tween 20

Wash
PBS containing 0.1 % Tween 20 and 0.5 M NaCl

Elution buffer T
100 mM triethylamine pH 11.5

Elution buffer G
100 Glycine pH 2.5

Column preparation

Before using the column was washed three times with PBS High salt and once with Elution Buffer G or Elution buffer T to remove any proteins which could be non-covalently bound to the column. Then the cloumn was washed with PBS-T until the pH of flow-through went back to neutral (monitored using indicator sticks) and connected to a Miniplus 3 peristaltic pump (Gilson).

Serum preparation

Serum was centrifuged at 4 500 rpm for 10 min at 4°C and sodium azide was added to 0.04 %.

Purification

The serum was loaded onto column with the pump speed set at 10 and left for overnight binding at 4^0C. The next day, the column was washed twice with 0.2 x PBS. Antibody was first eluted with Elution buffer T by pipetting 1/5 column volume aliquots of elution buffer directly onto the top of the column bed. Fractions were collected into eppendorf tubes conatining enough of 1 M Tris-HCl to neutralize the pH of eluates. Then the pH of the column was brought back to neutral using PBS. The second elution was carried out using Elution buffer G in the same way.

Fractions were assayed on nitrocellulose membrane stained with Ponceau S. Following purification, fractions positive by Ponceau S were pooled and dialysed against PBS containing 50 % (v/v) glycerol.

Antibody was stored at -20^0C. The column was equilibrated with PBS and stored at 4 ^{0}C with addition of sodium azide (0.04 %).

2.5.9. Crosslinking Immunoprecipitation

Buffers

Cross buffer

20 mM Hepes pH 7.6
100 mM Potassium acetate

Stop solution

1 M Tris-HCl pH 7.4

IP buffer

PBS containing

50 mM Hepes pH 7.6
75 mM KCl
1 mM $MgCl_2$
1 mM EGTA
0.1 % Triton X-100
1 mM Na_3VO_4
0.1 μM microcystin
1 mM Pefablock (Roche)
10 μg /ml LPC (leupeptin/pepstatin/chymostatin, Roche)
Complete Mini EDTA-free Protease Inhibitor Cocktail Tablets (Roche)
(1 tablet per 10 ml of buffer)

Intracellular crosslinking

Mid-log phase cultures of *bub1-SZZ* cells overexpressing HFG-Spc7 1-283 under nmt41 promoter were harvested at 3 000 rpm for 4 minutes at RT. Cells were washed twice with Cross buffer and resuspended in Cross buffer containing 2 mM DSP crosslinker (Thermo Scientific). Following 30 min incubation at RT on rocker, crosslinking reactions were stopped by addition of Stop solution to final concentration of 20 mM. Cells were washed twice with IP buffer.

Preparation of IgG Dynabeads

300 mg of IgG Dynabeads (Invitrogen) was used per sample. Prior to use, the beads were washed twice with PBS and once with IP buffer.

Immunoprecipitation

Zirconia/Silica beads (BioSpec Products) (200 μl) and 300 μl of ice-cold IP buffer were added to cell pellets. Samples were subjected to 20 sec beat-beating and then centrifuged at 14 000 rpm for 5 min at 4^0C. Supernatant was transferred to fresh

tubes and centrifuged (14 000 rpm, 4^0C) for another 5 min. 50 µl of the extract was mixed with SDS gel-loading buffer and kept for further analysis. Remaining extract was transferred to the tubes containing 300 mg of IgG Dynabeads. Extracts were incubated with IgG Dynabeads for 30 min at 4 ^{0}C on spinning wheel. After incubation the beads were washed three times with ice-cold IP buffer . 50 µl of SDS gel-loading buffer (containing 5 % β-mercaptoethanol) was added to each sample. Samples were boiled at 100°C for 5 minutes to cleave DSP and remove the immunoprecipitated proteins from the beads.

2.5.10. Mph1 WT-SZZ and Mph1 KD-SZZ purification

The purification protocol was developed by Dr. Judith Zich.

Buffers

1 x Hyman buffer
50 mM bis-Tris propane (pH 7.0)
100 mM KCl
5 mM EGTA
5 mM EDTA
10 % glycerol

2 x Hyman buffer
100 mM bis-Tris propane (pH 7.0)
200 mM KCl
10 mM EGTA
10 mM EDTA
20 % glycerol
1 mM Pefablock
10 µg/ml leupeptin/pepstatin/chymostatin (Roche)
Complete Mini EDTA-free Protease Inhibitor Cocktail Tablets (Roche)
(1 tablet per 10 ml of buffer)

TST buffer

50 mM Tris-HCl (pH 7.4)
150 mM NaCl
0.1 % Tween-20

Preparation of IgG Dynabeads

10 mg of IgG Dynabeads (Invitrogen) was used for 20 g of yeast powder. Prior to use, the beads were washed three times in TST buffer.

Lysate preparation

Cycling cells expressing either Mph1WT-SZZ or Mph1 KD-SZZ were grown in 4 x YES to an OD_{600} below 10. Then the cells were pelleted (4 000 rpm, 5 min) and washed once with ice-cold water. Cells, resuspended in 1/5 pellet volume of water, were drop-frozen in liquid nitrogen and then ground in a mortar under liquid nitrogen. Cell powder was stored at - 80°C. Cell powder was resuspended in one cell powder weight of 2 x Hyman buffer. Triton X-100 was added to 1 % final concentration (v/v) and then the cell suspension was sonicated for 30 sec (Sonics, Vibra-Cell). Lysed cells were centrifuged for 10 min, 4500 rpm at 4°C to remove cell debris. Supernatant was filtered through a 25 mm GD/X syringe filters (Whatman), pore size 2.6 μM and a 25 mm GD/X syringe filters (Whatman), pore size 1.6 μM.

IgG Dynabeads Binding

For IgG Dynabeads binding, clear lysate was mixed with the beads and incubated for 30 min at 4°C on rocker. Following incubation, the beads were washed 3 times with 15 ml 1 x Hyman buffer and then 3 times with 15 ml 1 x Hyman containing 1 mM DTT and 0.1 % Tween-20 using a magnet (MagnaBot, Promega).

TEV cleavage

The SZZ-tagged proteins were cleaved off the beads using 100 units of AcTEV protease (Invitrogen) in 1 ml of 1 x Hyman buffer containing 1 mM DTT and 0.1 % Tween-20. The cleavage was carried overnight with rotating at 4°C. The supernatant was collected into a fresh tube. The beads were washed with 1 ml of 1 x Hyman buffer containing 1 mM DTT and 0.1 % Tween-20.

S-protein agarose binding

The supernatant containing cleaved proteins was mixed with S-protein agarose (Novagen) and incubated with rolling for 4 hours at 4°C. Following incubation, the resin was washed five times with 1 x Hyman buffer. Purified proteins (on S-protein agarose beads) were stored at -80°C in 50 µl aliquots.

Purity of Mph1-SSZ and Mph1 KD-SZZ preps was checked by silvers staining. Samples were run on NovexNuPAGE 4-12 % Bis-Tris gel (Invitrogen) and the gel was processed using Silver Stain Kit (Pierce).

2.5.11. *In vitro* kinase assays

2 x Kinase buffer

100 mM Hepes pH 7.6
100 mM KCl,
20 mM $MgCl_2$
20 mM $MnCl_2$
50 mM β-glycerophosphate
1 mM DTT

Mph1 kinase reaction

Purified Mph1 kinase coupled to the S-protein agarose beads was washed twice with 1 x kinase buffer. Reaction was carried out in 25 µl of 1 x Kinase buffer containing 3-4 µg of recombinant protein, 20 µM ATP and 50 µCi [γ-32P] ATP mixed with the beads. The reaction mix was incubated at 30°C for 30 min. Reaction was stopped by adding 4 x SDS gel-loading buffer (Invitrogen).

Ark1 kinase reaction

Recombinant MBP-Ark1 (1.5 µg), Ark1 kinase activator (1.0 µg; GST-IN box, MBP-IN box, GST-160 IN box or MBP-160 IN box) and recombinant substrate (2-4 µg; GST-Spc7 1-283 proteins) were incubated in 25 µl of 1 x Kinase buffer containing 20 µM ATP and 50 µCi [γ-32P] ATP for 30 minutes at 30°C. Reactions were stopped by adding 4 x gel loading buffer (Invitrogen).

Autoradiography

Samples were separated by NovexNuPAGE 4-12 % Bis-Tris gel (Invitrogen). The gel was stained with Instant*Blue* (Expedeon) then dried onto Whatman paper and exposed to X-ray film.

2.5.12. *In vitro* Spc7 binding assay

MBP-Spc7 1-666 beads preparation

Recombinant proteins, MBP-Spc7 1-666 and GST-Spc7 1-283 (WT and mutants), were incubated with amylose resin (New England BioLabs) or Glutathione Agarose (Sigma), respectively, in lysis buffer (see 2.2.7.) for 30 min at 4^0C on rocker. Then the beads were washed once in lysis buffer and twice with IP buffer (without protease/phosphatase in inhibitors) (see 2.5.9). Beads were resuspended in a small amount of IP buffer and 50 µl aliquots were distributed into eppendorf tubes.

Spc7 binding

Log phase *bub1-SZZ, bub1-GLEBSΔ-SZZ* and *bub3-GFP* cell frozen pellets (200 mg) were resuspended in IP buffer (see 2.5.9.) and immediately bead-beaten twice for 20 sec with a 30 sec incubation on ice between the pulses. Extracts were centrifuged at 14 000 rpm for 5 min at 4^0C and transferred to fresh tubes. Extracts were centrifuged again with the same settings. 50 µl of extracts were mixed with SDS gel-loading buffer and kept for further analysis. Remaining extracts were added to the Spc7-coated beads and incubated with rolling for 30 min at 4^0C. Beads were then washed three times in IP buffer, and proteins were eluted by boiling in SDS gel-loading buffer.

Samples were analyzed by SDS-PAGE and western blotting with appropriate antibodies.

2.5.13. Chromatin Immunoprecipitation (ChIP)

Buffers

ChIP lysis buffer:

50 mM Hepes-KOH, pH 7.5
140 mM NaCl
1 mM EDTA
1% (v/v) Triton-X100
0.1% (w/v) Sodium deoxycholate

ChIP wash buffer

10 mM Tris-HCl, pH 8.0
0.25M LiCl
0.5% NP-40
0.5% (w/v) Sodium deoxycholate
1 mM EDTA

TE

10 mM Tris-HCl pH 8.0
1 mM EDTA

PEMS

100 mM PIPES pH 7.0
1mM $MgCl_2$
1 mM EDTA
1.2 M Sorbitol

Cell preparation

Mid-log phase *nda3-KM311* cells were either metaphase-arrested for 6 hr at 18°C or allowed to process through the cell cycle by incubation at permissive temperature 32°C. The cells were then fixed by addition of paraformaldehyde to 1 % final concentration (Sigma) and 30 min incubation at 18°C with shaking. Fixation was stopped by addition of 1/20 volume of 2.5 M glycine. Medium containing paraformaldehyde was removed and cells were washed twice with PBS (centrifugation 3 000 rpm for 2 min at 4^0C). Cells were resuspended in PEMS containing 0.4 mg/ml zymolyase (Seikagaku Biobusiness) to a final concentration of 10^8 cells/ml. Cells were incubated with zymolyase 100T at 37^0C for 30-40 min. Following the cell walls digestion, cells were washed twice with PEMS and then the cell pellets were frozen in eppendorf tubes and stored at -80^0C.

Beads preparation

10 µl of Protein A (Dynal) beads was used per one IP sample. Prior to experiment, beads were washed three times with PBS containing 0.02 % Tween 20 and then coated with 4 µg of anti-GFP antibody (Molecular Probes) by 1 hour incubation with the antibody dilution in PBS-0.02 % Tween 20 at 4°C. After incubation, the beads were washed twice with PBS-0.02 % Tween 20 and once with ice-cold lysis buffer and transferred to screw cap tubes.

Extract preparation and immunoprecipitation

The cell pellets were resuspended in ice-cold lysis buffer containing protease inhibitors [1 mM Pefablock, 10 µg/ml leupeptin/pepstatin/chymostatin (Roche), Complete Mini EDTA-free Protease Inhibitor Cocktail Tablets (Roche) (2 tablets per 10 ml of buffer)]. Samples were sonicated in the Diagenode Bioruptor Twin for 15 min with 30 sec pulse in 30 sec intervals. Samples were centrifuged at 14 000 rpm for 15 min at 4^0C. Supernatants were transferred to fresh tubes and centrifuged (14 000 rpm, 4^0C) for another 5 min. 15 µl of each supernatant, (Whole Cell Extract, WCE), was kept at -80^0C for furthe analysis whereas remaining supernatants

were mixed with the Protein A beads coated with anti-GFP antobody and incubated overnight at 4^0C on spinning wheel.

DNA recovery

Following immunoprecipitation, the beads were washed once with lysis buffer containing protease inhibitores, once with lysis buffer conataing 0.5 M NaCl, once with wash buffer and once with TE. After final wash all supenatants were carefully aspirated, and the beads were mixed with Chelex-100 resin (Bio Rad) (200 µl of 10 % slurry in sterile water). Chelex-100 resin was also added to thawed WCE samples. All samples were boiled at 100^0C for 10 min and the tubes were then cooled down to RT and centrifuged at 2 000 rpm. 2.5 µl of 10 mg/ml of Proteinase K was added to each sample and the samples were incubated at 55^0C for 30 min with occasional mixing. The samples were boiled at 100^0C for 10 min to inactivate Proteinase K. Supernatant containing immunoprecipitated DNA was collected by centrifugation and store at -20^0C.

PCR

1 µl of undiluted IP DNA was typically used in PCR. WCE DNA was diluted 100 times and 1 µl of the dilution was used in PCR.

The reaction was carried out using Phusion DNA Polymerase (New England BioLabs) and primer pairs: TM A and TM B, OTR A and OTR B, fbp A and fbp B (see table 2.4). PCR products were separated by 1.5 % agarose gel.

Component	Final concentration
5 x Phusion GC Buffer	1 x Phusion GC Buffer
10 x dNTPs (2.5 mM dATP, dGTP, dCTP and dTTP)	1 x dNTPs
TM A	0.5 µM
TMB	0.5 µM
OTR A	0.375 µM
OTR B	0.375 µM
fbp A	0.5 µM
fbp B	0.5 µM
Phusion DNA Polymerase	0.4 unit per 20 µl reaction
Template (IP DNA or WCE DNA)	1 µl per 20 µl

PCR programme:

1. Initial denaturation	98^{0}C	30 sec
2. Denaturation	98^{0}C	10 sec
3. Annealing	55^{0}C	20 sec
4. Extension	72^{0}C	30 sec
5. Got to 2. 28 times		
6. Final extension	72^{0}C	5 min

2.5.14. Microtubule coprecipitation assay

Microtubule coprecipitation experiment was performed according to protocol from Prof. H. Ohkura lab with Dr. Heather Syred's help (Ohkura lab)

BrB80 buffer

80 mM PIPES-KOH (pH 6.8)
1 mM $MgCl_2$
1 mM Na_3EGTA
1 mM DTT

Mixture (50 µl) containing following components:

- 4 µg of recombinant GST-Spc7 protein (WT and mutants)
- 1 mM GTP
- 10 µM tubulin (Cytoskeleton) (+T samples) or 0 µM tubulin (-T samples)
- 30 µM taxol
- 0.3 x BrB 80 (14.5 µl of 1 x BrB80) containing protease inhibitors
  [1 mM Pefablock (Roche) and Complete Mini EDTA-free Protease Inhibitor Cocktail Tablets (Roche) (1 tablet per 10 ml of buffer)]

was incubated at RT for 30 min and then centrifuged at 14 000 rpms for 10 min. Supernatant was transferred to a new tube. Pellet was washed twice with BRB80. SDS gel-loading buffer was added to the pellet and supernatant samples to the same volume.

Samples were separated by 10 % SDS-PAGE gel and the gel was then stained with Instant*Blue* (Expedeon).

2.5.15. Mass spectrometry

Initial mass spectrometry experiments were carried out in the Wellcome Trust Centre for Gene Regulation and Expression in Dundee in collaboration with Prof. Mike Stark under supervision of Dr. Sara Ten Have and Kelly Hodge. Majority of data presented in this sudy was obtained in collaboration with Prof. Juri Rappsilber under supervision of Dr. Juan Zou in the Wellcome Trust Centre for Cell Biology in Edinburgh.

Mass-spectrometry

Prior to MS experiment, *in vitro* Ark1 and Mph1 kinase assays were performed as described above without addition of [γ-32P] ATP.

2.5.15.1. Solutions

	Alkylating solution
ABC	
	55 mM Iodoacetamide
50 mM Ammonium bicarbonate	50 mM Ammonium bicarbonate
Reducing solution	Trypsin buffer
10 mM DTT	13 ng/µl trysin
50 mM Ammonium bicarbonate	10 mM ammonium bicarbonate
	10 % (v/v) acetonitrile

2.5.15.2. In gel protein digestion

[Rappsilber lab protocol based on (Shevchenko et al., 1996)]

4 µg of recombinant MBP- and GST-Spc7 fusion proteins (in the kinases assay mixture) was electroporated through NuPAGE 4-12 % Bis-Tris gel (Invitrogen) in MOPS buffer (Invitrogen). Proteins were stained with Instant*Blue* (Expedeon).

Washing

Bands were excised, cut into small pieces, moved to the eppendorf tube and incubated with ABC solution at RT for 5 min. ABC solution was removed and replaced with acetonitrile. Pieces were incubated in acetonitrile until they became white and shrunk. Incubation with ABC solution and acetonitrile was repeated at least once.

Reduction/alkylation

Reducing solution was added to the tube and the reaction was carried out at 37°C for 30 min. Reducing solution was removed and the gel pieces were washed in acetonitrile. Alkylating solution was added to the gel pieces and then the pieces were incubated at RT for 20 min in dark. Alkylating solution was removed and the gel pieces were washed as described above.

Tryptic digestion

The gel pieces were covered with trypsin buffer, left on ice for 15 min and then transferred to 37^0C for overnight incubation.

2.5.15.3. Stage tip extraction

[according to (Rappsilber et al., 2003)]

The supernatant of digested samples was acidified by addition of 0.1 % trifluoroacetic acid (TFA).

The samples were desalted on a C18 Stage Tip containing manually cut Empore Disk C18.
First methanol was passed through the Stage Tip. The Stage Tip was equilibrated to acidic conditions with 0.1 % TFA and the sample was then passed through the Stage Tip. Peptides bound to the C18 disk were washed with 0.1 % TFA. The Stage Tips for all samples were stored at -20°C.

Prior to MS analysis peptides were eluted in 20 µl of 80 % acetonitrile, 0.1 % TFA. The acetonitrile was allowed to evaporate down to 5 µl (Concentrator 5301, Eppendorf AG, Hamburg, Germany) and the samples were subjected to LC-MS/MS analysis.

2.5.15.4. Phosphoenrichment

(Dr. J. Zou's protocol, Rappsilber lab)

Buffers

Acidic elution buffer

1 % trifluoroacetic acid (TFA)
20 % acetonitrile

Titanium Dioxide loading buffer

5 % TFA
80 % acetonitrile

Basic elution buffer

5 % NH_4OH pH 11.6

Trypsin digested proteins were desalted on a C18 Stage Tip and eluted with 80 % acetonitrile, 0.1 % TFA acid. The acetonitrile concentration was reduced to 50 % with 0.1 % TFA. Then the IMAC beads (washed with 0.1 % trifluoroacetic acid, 50 % acetonitrile) were added to the peptide solution.

After 30 min incubation at RT with gentle shaking suspension was transferred to a C8 Stage Tip to make IMAC Tip column (Sigma). The IMAC flow-through was collected (peptides that have not bound to the IMAC resins). The C8 Stage Tip was washed with 0.1 % TFA acid, 50 % acetonitrile and the wash was pooled with the IMAC flow-through in a tube.

Acidic elution buffer was pushed through the IMAC Tip column slowly and the eluate containing mono and non-phosphorylated peptides was collected in the same

tube as IMAC flow-through. Then the solution of pooled IMAC flow-through, IMAC wash and acidic eluate was vacuum-dried in a concentrator and reconstituted in Titanium Dioxide loading buffer for Titansphere Phos-TiO Spin Tip step.

Basic elution buffer was pushed through the IMAC Tip column slowly and the eluate containing multiple phosphorylated peptides was collected in a low peptide binding tube. The basic elution buffer containing 50 % acetonitrile was pushed through the IMAC Tip column again and the eluate was collected in the same low peptide binding tube containing basic eluate from previous step. The eluate was stored at 4^0C.

Titansphere Phos-TiO Spin Tip (GL Sciences) was equilibrated with 5 % TFA, 80 % acetonitrile and next with 25 % lactic acid, 5 % TFA, 80 % acetonitrile. Then the fraction from the IMAC step containing peptides that have not bound to IMAC resins, mono and non-phosphorylated peptides was applied and pushed through the Titansphere Phos-TiO Spin Tip. Flow-through was collected and pushed through the Spin Tip once again. The column was washed with 25 % lactic acid, 5 % TFA, 80 % acetonitrile and then with 5% TFA, 80 % acetonitrile and then twice with 0.1 % TFA. Elution was performed with basic elution buffer and then with 30 % acetonitrile to the low peptide binding tube containing basic elution from IMAC step. The sample was dried in a concentrator and reconstituted in 0.1 % TFA acid, 2 % acetonitrile. Next the sample was desalted on a C18 StageTips and stored at -20°C for LC MS/MS analysis.

2.5.15.5. Mass spectrometry analysis

Mass spectrometry analysis was performed by Dr. Juan Zou (the Wellcome Trust Centre for Cell Biology, Edinburgh).

Peptides were analyzed using an LTQ Orbitrap Velos (Thermo Fisher Scientific) coupled with a nano-ACQUITY UPLC system (Waters) and a 250 mm long self-packed analytical column with a self-assembled particle frit. Peptides were loaded at 0.7 µl/min and separated at a flow rate of 0.3 µl/min. Mobile phase A consisted of water, 0.1 % formic acid; Mobile phase B consisted of acetonitrile, 0.1 % formic

acid. A linear gradient was increased from 5 % to 35 % acetonitrile in 0.1 % formic acid to elute peptides. Mass spectra were recorded at 100,000 resolution. The ten peaks with the highest intensity were selected in each cycle for higher energy collisional activated dissociation (HCD) with 40 % normalized collision energy and detected by the Orbitrap at 7,500 resolution. Dynamic exclusion was set to 90 s and repeat count was one. Raw files were processed using Mascot software with phosphorylation as variable modification (Perkins et al., 1999).

Chapter 3

Spc7 is substrate of Ark1 and Mph1 mitotic kinases

Chapter 3

Spc7 is substrate of Ark1 and Mph1 mitotic kinases

3.1. Introduction

Protein phosphorylation is the main post-translational modification regulating cell cycle progression [for review see (Nigg, 2001)]. Consistently, the mitotic spindle checkpoint, a surveillance mechanism that delays anaphase onset in presence of maloriented kinetochores, also depends on phosphorylation. In fission yeast two conserved protein kinases have been implicated in the checkpoint signalling cascade: Mph1 (monopolar spindle 1 like pombe homologue) which is homologous to vertebrate Mps1 (monopolar spindle1) and Ark1 (Aurora related kinse1) - a homologue of Aurora kinases.

The Mps1 kinase role in spindle checkpoint signalling is evolutionarily conserved from yeast (Winey et al., 1991; He et al., 1998) to vertebrates (Abrieu et al., 2001; Stucke et al., 2002; Dorer et al., 2005; Kwiatkowski et al., 2010). Budding yeast Mps1 kinase activity against exogenous substrates and itself (autophosphorylation) was originally demonstrated *in vitro* by Lauzé et al. (Lauzé et al., 1995). The same study identified the C-terminal kinase domain which contained the consensus sequences for the 11 subdomains of a protein kinase defined by Hanks et al. (1988). Further, budding yeast Mps1 was shown to be a dual specificity kinase that is able to phosphorylate both serine and threonine residues, similar to its mouse (Douville et al., 1992) and human (Lindberg et al., 1993) homologues (Lauzé et al., 1995). A 'kinase dead' allele of Mps1 was generated by substituting an aspartic acid residue with alanine within the consensus sequence DFG present in a highly conserved subdomain VII (Lauzé et al., 1995). A similar mutation, (D459A), was introduced into fission yeast Mph1 kinase resulting in expression of catalytically inactive Mph1 (*mph1-kd* mutant) (Zich et al., 2012) (Figure 3.1). Recently, autophosphorylation sites in human Mps1 have been mapped (Jelluma et al., 2008b; Dou et al., 2011). The autophosphorylation sites showed a close resemblance to Plk1 consensus motif, [D/E]X[S/T]φ (φ-a hydrophobic amino acid), therefore it has been suggested that these two kinases can phosphorylate common substrates (Dou et al., 2011).

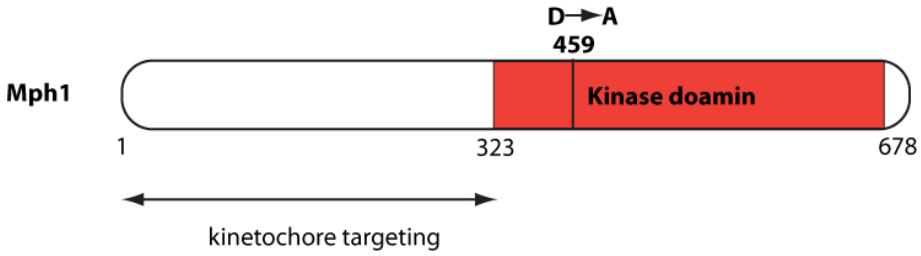

Figure 3.1. Domain organization of Mph1 kinase. The C-terminal half of the protein constitutes a conserved kinase domain (in red) (Zich et al., 2012; He et al., 1998). Aspartic acid residue substitution with alanine in the highly conserved DFG motif abolished kinase activity of Mph1 (Zich et al., 2012). The N-terminus of Mph1 is required for its kinetochore targeting, perhaps through binding to phosphorylated Ndc80 (Kemmler et al., 2009).

He et al. (1998) demonstrated that fission yeast Mph1 kinase shares sequence similarity with budding yeast Mps1; the sequence identity between Mph1 kinase domain and that of *S. cerevisiae* Mps1 was estimated to be 52%. Moreover, Mph1 is required for a functional spindle checkpoint and Mph1 overexpression results in mitotic arrest (He et al., 1998) which is consistent with analyses of Mps1 made in budding yeast (Hardwick et al., 1996a). Budding yeast Mps1 kinase is essential for viability as it also has a crucial role in spindle pole body duplication (Winey et al., 1991) whereas in fission yeast Mph1 is not required for spindle pole body duplication and hence is not essential (He et al., 1998).

Recently the role of Mph1 in the checkpoint signalling has been revealed by a study showing that Mph1 kinase activity drives the MCC binding to the APC (Zich et al., 2012). Mph1-dependent phosphorylation sites in *S. pombe* Mad2 have been mapped. The physiological relevance of these phosphosites was proved by generating Mad2 phosphomutants which were defective in Mad2 and Mad3 binding to the APC (Zich et al., 2012). Fission yeast Mad3 turned out to be an Mph1 substrate and 18 Mph1-dependent phosphorylation sites have been mapped in Mad3 (J. Zich, personal communication).

Fission yeast Aurora kinase, termed Ark1 (Aurora related kinase1), was initially described as a protein which could suppress the lethal consequences of *Xenopus* Aurora A overexpression (Petersen et al., 2001). Ark1 is a dual specificity kinase

containing 356 amino acids. This kinase is essential as it is regulates sister chromosome condensation, chromatid segregation, spindle formation, cytokinesis (Petersen and Hagan, 2003; Leverson et al., 2002; Petersen et al., 2001) and kinetochore-microtubules interactions (Hauf et al., 2007). It has been also demonstrated that Ark1 is involved in spindle checkpoint signalling since Ark1 inhibition leads to an inability to activate and maintain checkpoint arrest in the presence of unattached kinetochores (Petersen and Hagan, 2003; Vanoosthuyse and Hardwick, 2009).

Ark1 belongs to the Aurora kinase family and shares common structure with other members of the family as described by Giet and Prigent (1999). Aurora-related kinases consist of a well conserved C-terminal kinase domain and an N-terminal domain which varies in size and amino acid composition. The most conserved motif was identified between subdomains VII and VIII in a potential activation loop (Giet and Prigent, 1999). Similarly to other members of the family, Ark1 has a KEN box localised in its N-terminus and D-box in the C-terminus (Giet and Prigent, 1999; Leverson et al., 2002) (Figure 3.2). The non-conserved N-terminal domain was proposed to localise Ark1 to centromeres (Leverson et al., 2002).

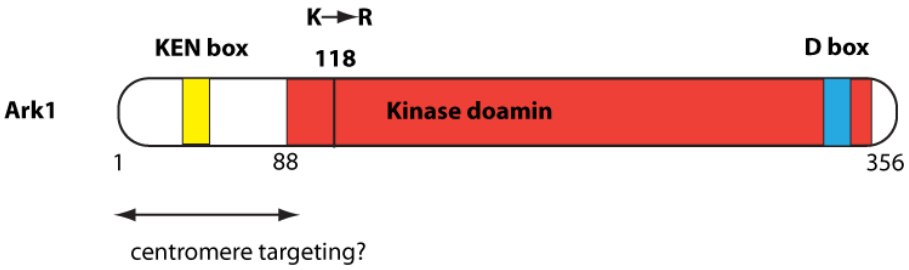

Figure 3.2. Domain organization of Ark1 kinase. The C-terminal Ark1 kinase domain (red) constitutes about 75% of the protein (Leverson et al., 2002; Giet and Prigent, 1999; Petersen and Hagan, 2003). Ark1 has a KEN box (yellow) in its N-terminus and D-box (blue) in its C-terminus (Giet and Prigent, 1999; Leverson et al., 2002). The N-terminus of Ark1 might be involved in centromere targeting of the protein.

Ark1 levels are constant throughout the cell cycle (Petersen et al., 2001; Leverson et al., 2002). However, Ark1 activity seems to be regulated as phosphorylation of histone H3, previously showed to be positively correlated with Aurora B activity (Adams et al., 2001), is elevated in mitosis (Petersen et al., 2001). An Ipl1 (*S. cerevisiae* Aurora related kinase) consensus sequence [R/K]X[T/S][I/L/V] (X-any amino acid) was proposed by Cheeseman et al. (2002). Recently, results of a proteome-wide screen for fission yeast Ark1 substrates revealed that the kinase does not have a strong preference for the suggested sequence, nevertheless a high proportion of the identified sites contained [R/K]X[S/T] (X-any amino acid) (Koch et al., 2011).

In vertebrate cells, Aurora B binds to the C-terminus of INCENP which contains a highly conserved region called the IN box (Adams et al., 2000; Kaitna et al., 2000). This interaction is thought to activate Aurora B from yeast to human (Kang et al., 2001; Bishop and Schumacher, 2002; Honda et al., 2003; Sessa et al., 2005). Moreover, Aurora B phosphorylates a highly conserved TSS motif in the IN box close to the C-terminus of INCENP further stimulating its own activity in a positive feedback loop (Honda et al., 2003; Bishop and Schumacher, 2002; Sessa et al., 2005).

Ark1 also interacts with an INCENP homologue in *S. pombe* known as Pic1 (Vanoosthuyse et al., 2007; Leverson et al., 2002). Yeast two hybrid assays revealed that Pic1 fragments containing residues 925-1018, corresponding to the IN box, bind to Ark1. Further analysis showed that Pic1 residues 925-972 are necessary and sufficient for Ark1 binding and most likely make contact with the kinase domain (Leverson et al., 2002). Functional analysis of different Ark1 truncation mutants combined with yeast two hybrid data indicated that the interaction between Ark1 and Pic1 is physiologically relevant (Leverson et al., 2002). Therefore, we decided to utilize the recombinant fragments of Pic1 containing IN box as the Ark1 activator. Additionally, recombinant Pic1 fragments can serve as an internal control for Ark1 activity in an *in vitro* kinase assays.

In addition to INCENP, Aurora B interacts with survivin (Bolton et al., 2002) and borealin (Gassmann et al., 2004; Klein et al., 2006), which are required for

localization, stability and enzymatic activity of the Chromosomal Passenger Complex (CPC). Consistently, in *S. pombe* Ark1 interacts with the survivin homologue, Bir1, and with the recently identified borealin homologue, Nbl1 (novel borealin-like protein 1) and both proteins contribute to Ark1 activity (Petersen and Hagan, 2003; Bohnert et al., 2009).

Recently, Aurora B kinase was demonstrated to phosphorylate the human kinetochore protein KNL1/Blinkin which regulates kinetochore-microtubule attachment (Welburn et al., 2010). Another study revealed that Aurora B-dependent phosphorylation of KNL/Blinkin opposes PP1 activity at kinetochores (Liu et al., 2010). Interestingly, Blinkin/KNL1 has been suggested to serve as a binding platform for vertebrate checkpoint proteins Bub1 and BubR1 (Kiyomitsu et al., 2011, 2007; Krenn et al., 2012). The multiple functions of KNL1/Blinkin must be tightly regulated.

Overall, previous analyses demonstrated that Mps1 kinase is essential for checkpoint signaling in all model organisms investigated, except for *C. elegans* which does not have the Mps1 homologue. It is known that Mps1 kinase activity is required to recruit checkpoint components to kinetochores. It has been also proposed that human KNL1/Blinkin serves as a kinetochore docking site for checkpoint proteins. The Mps1/Mph1-dependent phosphorylation of KNL1 and its homologues has not been analysed before. Aurora dependent sites in KNL1 have been mapped for human, chicken, *C. elegans* and *X. laevis*. Ark1-dependent phosphorylation sites in Spc7 have been identified in a proteome-wide screen for mitotic Ark1 substrates but the role for Ark1-dependent phosphorylation has not been described. Moreover, due to the large scale of this experiment some Ark1-dependent sites might not have been identified. The aim of the experiments presented in this chapter is to identify Mph1- and Ark1-dependent phosphorylation sites in Spc7. It is likely that checkpoint kinases Ark1 and Mph1 phosphorylate Spc7 and therefore play an important role in checkpoint signaling.

Such analyses address the following questions in this chapter:

- Is the fission yeast homologue of KNL1/Blinkin, Spc7, phosphorylated during mitosis?
- Which kinases phosphorylate Spc7?
- What are the phosphorylation sites in Spc7 and is their phosphorylation important for cell cycle progression?

In order to investigate Spc7 phosphorylation *in vitro* Mph1 and Ark1 kinase assays were employed. Recombinant Ark1 kinase and yeast-purified Mph1 kinase wild type and kinase-dead versions were used in the experiment described. Identification of the Ark1 and Mph1 substrates was followed by mass spectrometry analysis which allowed mapping of the phosphorylated residues. Phosphomutants were generated and their phenotypes characterised.

3.2. Construction of pHGGWA-*spc7 1-283* and pDUAL-*nmt41-HFG-spc7 1-283*

A recombinant fragment of Spc7 containing residues 1-283 was used in *in vitro* Ark1 kinase assays (Figure 3.3). To generate GST-Spc7 fusion proteins a gene fragment of Spc7 encoding residues1-283 was amplified from pGBDT-*spc7 WT* and pBSSK-*ura4-spc7 S108A S114A*, (provided by Prof. J. Millar, University of Warwick) (Meadows et al., 2011), using primers compatible with the Gateway Cloning system (Invitrogen). The PCR products were cloned into pDONR201 donor vector using Gateway BP Clonase II enzyme mix (Invitrogen) and then transferred to pHGGWA Gateway-based destination vector using Gateway LR Clonase II enzyme mix (Invitrogen) according to the manufacturer's instructions (Busso et al., 2005). The pHGGWA-*spc7 1-283*, pHGGWA-*spc7 S108A S114A 1-283* were subjected to site-directed mutagenesis (QuikChange II Site-Directed Mutagenesis, Stratagene) to obtain a series of Spc7 phosphomutants. The pHGGWA-*spc7* expression vectors were transformed to BL21-CodonPlus-RIL *E. coli* cells, which enhance expression of AT-rich genes.

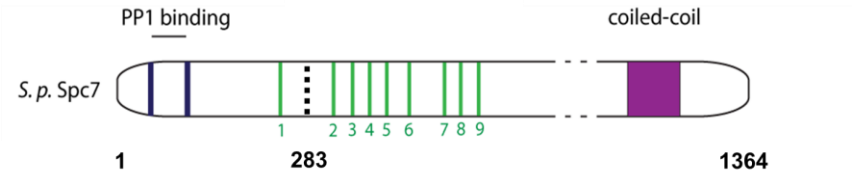

Figure 3.3. Schematic representation of *S. pombe* Spc7.This diagram shows the invariant N-terminal PP1 binding motifs (dark blue), the N-terminal MELT repeats (numbered in *S. pombe* Spc7) (green), and the C-terminal coiled-coil domain (purple).

Due to difficulties with detection of full length endogenous Spc7, a construct which allowed overexpression of 6xHis-FLAG-GFP-Spc7 (residues 1-283) from the *leu1* locus in yeast cells was generated (Matsuyama et al., 2004). The Spc7 gene fragment encoding residues 1-283 was amplified from pGBDT-*spc7 WT* expression vector with primers compatible with Gateway Cloning system (Invitrogen). The PCR products were cloned into pDONR201 donor vector using Gateway BP Clonase II enzyme mix (Invitrogen) and then transferred to pDUAL HFG41c Gateway-based destination vector, (kind gift of Prof. Kenneth Sawin, University of Edinburgh),

using Gateway LR Clonase II enzyme mix (Invitrogen) according to the manufacturer's instructions forming pDUAL-*nmt41-HFG-spc7 1-283* construct.

3.3. Spc7 is phosphorylated upon mitotic arrest

In order to determine whether Spc7 undergoes mitosis-specific posttranslational modifications, including phosphorylation, the following experiment was performed.

HFG-Spc7 (1-283) was overexpressed under the nmt41 promoter in fission yeast cells along with Mph1 overexpression (14 hours overexpression in minimal media lacking thiamine). The cells arrested in mitosis as Mph1 overexpression leads to checkpoint-dependent arrest (He et al., 1998; Hardwick et al., 1996a). HFG-Spc7 (1-283) was also overexpressed in *nda3-KM311* cells which were shifted to 18^0C for the last 6 hours of the overexpression. The *nda3-KM311* mutant arrests in mitosis at its non-permissive temperature (18^0C) due to microtubule depolymerisation (Hiraoka et al., 1984). Additionally, HFG-Spc7 (1-283) was overproduced in cycling cells. Then the cells were pelleted and processed to obtain cell extracts. The cell extracts were separated by 10% SDS-PAGE gel (Tris pH 9.2) and probed with antibodies against Spc7 and Mph1.

Figure 3.4 shows that arresting cells in mitosis by Mph1 overexpression causes a gel mobility shift of HFG-Spc7 (1-283). The shift manifests itself as double band in samples obtained from cells overexpressing Mph1 kinase (Figure 3.4 upper panel). In samples obtained from *nda3-KM311* arrested cells the shift is far less pronounced. These results indicate that Spc7 is likely to be phosphorylated upon checkpoint activation and Mph1 can contribute directly or indirectly to this phosphorylation. However, the possibility that the observed shift is a consequence of other posttranslational modification/s cannot be excluded.

The hypothesis that Spc7 is phosphorylated by mitotic kinases was further tested by *in vitro* Ark1 and Mph1 kinase assays.

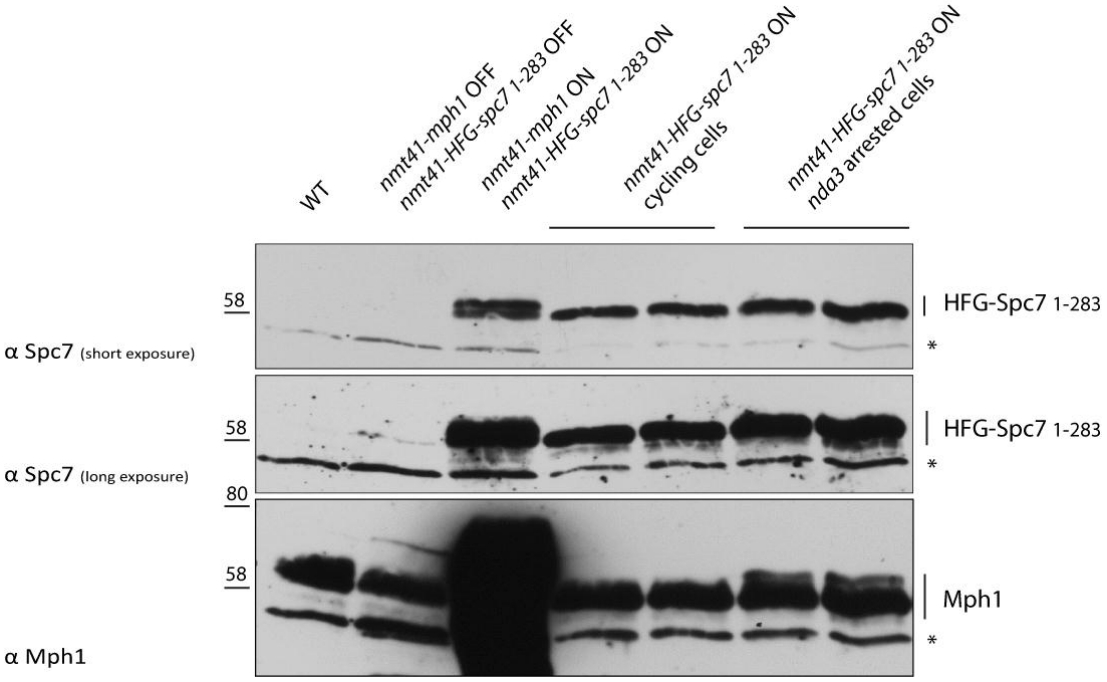

Figure 3.4. Spc7 gel mobility shift upon mitotic arrest. Western blot analysis of protein extracts from metaphase arrested cells (Mph1 overexpression or microtubule depolymerisation in *nda3-KM311* background) overexpressing HFG-Spc7 (1-283) and from cycling cells overexpressing HFG-Spc7 (1-283). HFG-Spc7 (1-283) was overexpressed from the nmt41 promoter. WT-protein extract from wild type cells. The blot was probed with anti-Spc7 antibody and then reprobed with anti-Mph1 antibody.

3.4. Analysis of Ark1-dependent phosphorylation of Spc7

In order to identify Ark1-dependent sites in the N-terminus of Spc7 *in vitro* Ark1 kinase assays were performed. In the assay a recombinant fragment of Pic1 containing the IN box was used as the Ark1 activator. The sites were identified by mass spectrometry which allowed the generation of a series of yeast Ark1 phosphorylation mutants. Phosphomutants were then assayed for mitotic defects in the presence of the microtubule destabilizing drug benomyl.

3.4.1. Developing *in vitro* Ark1 kinase assay - the C-terminal fragment of Pic1 containing conserved IN box enhances Ark1 kinase activity *in vitro*

In order to identify Ark1 substrates *in vitro* an Ark1 kinase assay was developed.

It had been shown that wild-type Ark1 purified as a GST-fusion protein is able to autophosphorylate itself in the absence of other components of the CPC *in vitro* (Leverson et al., 2002). However, as a conserved IN box present in the C-terminus of INCENP was demonstrated to activate Aurora B kinase (Bishop and Schumacher, 2002; Honda et al., 2003) and recombinant Sli15 (S. *cerevisiae* homologue of INCENP) enhanced Ipl1 kinase activity *in vitro* (King et al., 2007a), different GST- and MBP-Pic1 fusions were tested in the Ark1 kinase assay.

MBP-Ark1 was incubated with the artificial substrate, myelin basic protein, with or without the addition of the Pic1-IN box fragment to the buffer containing γ^{32}-P-ATP. Two different truncations of Pic1 were used: the first contained only the IN box whereas the second contained the IN box together with 160 amino acid extending to the N-terminus from the IN box (Figure 3.5). Both truncations were tagged at their N-terminus with GST and MBP. Kinase assay samples were run on a 10% SDS-PAGE gel and phosphorylation visualised by autoradiography.

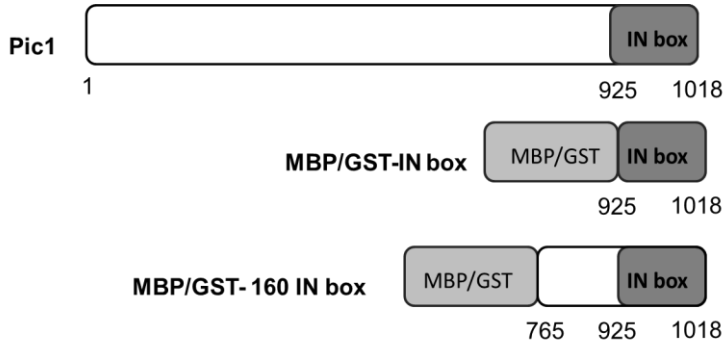

Figure 3.5. Two C-terminal fragments of *S. pombe* Pic1 that were used as Ark1 activators in *in vitro* Ark1 kinase assays.

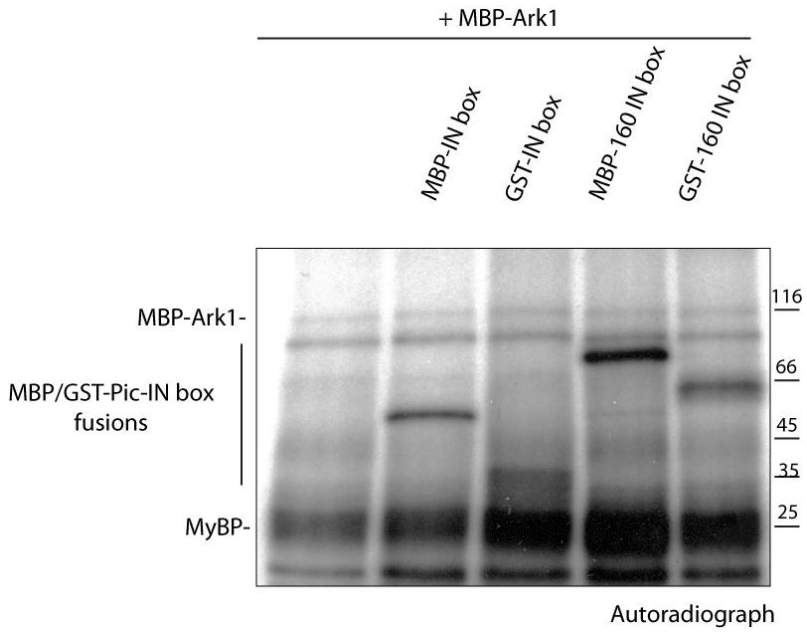

Figure 3.6. *In vitro* kinase assay of MBP-Ark1 with myelin basic protein (MyBP) and different recombinant MBP/GST-Pic1-IN box fusions. Each lane contains the same amount of the proteins (1.5 µg MBP-Ark1, 1 µg Ark1 activator, 1.5 µg MyBP). (MBP-maltose binding protein, GST- glutathione S-transferase)

Figure 3.6 shows that that recombinant MBP-Ark1 kinase alone is able to autophosphorylate and phosphorylate myelin basic protein. However, addition of

recombinant Pic1-IN box increases the incorporation of ^{32}P by about 50% on average. This finding indicates that MBP-Ark1 should be use along with its Pic1-IN box activator in order to enhance Ark1 kinase activity *in vitro*. Additionally, Ark1 phosphorylates different MBP/GST-Pic1-IN box fusions.

3.4.2. Spc7 is an *in vitro* substrate of Ark1

Human Blinkin/KNL1 has been recently demonstrated to be an Aurora B substrate (Welburn et al., 2010). In order to investigate, whether Ark1 phosphorylates *S. pombe* Spc7 *in vitro* Ark1 kinase assays were performed. A bacterially expressed GST-Spc7 containing residue 1-283 (GST-Spc7 1-283) was incubated with MBP-Ark1 and MBP-IN box in buffer containing γ-^{32}P-ATP. Kinase assay samples were run on a 4 - 12 % precast NuPAGE gradient gel (Invitrogen) and subjected to autoradiography (Figure 3.7).

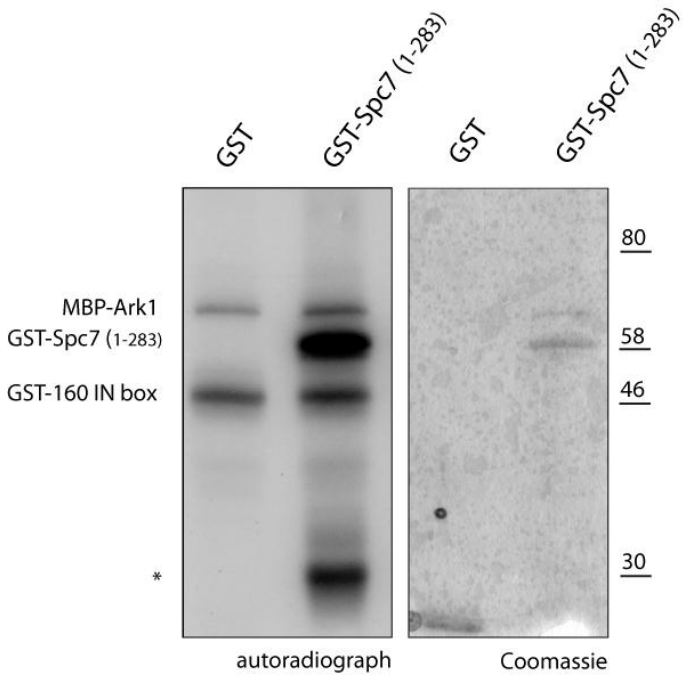

Figure 3.7. Spc7 is an *in vitro* substrate of Ark1. *In vitro* kinase assay of MBP-Ark1 against GST-Spc7 (1-283) and GST (negative control). MBP-IN box was used as Ark1 activator. The Spc7 signal is specific as no signal can be detected for GST on the autoradiograph.*-degradation product of GST-Spc7 (1-283).

3.4.3. Identification of phosphorylation sites

The experiment presented in Figure 3.7 shows that Spc7 is an *in vitro* substrate of Ark1 kinase. In order to determine the physiological relevance of Spc7 phosphorylation phosphomutants need to be generated in yeast. However, first the *in vitro* phosphorylation sites were mapped by mass spectrometry.

In vitro kinase assays were performed as described above using recombinant MBP-Ark1 kinase, GST/MBP-Pic1-IN box and two different Spc7 fragments: GST-Spc7 (1-283) and a longer fragment MBP-Spc7 (1-666) generated more recently. The kinase buffer did not contain γ-^{32}P-ATP in these experiments. Kinase assay samples were processed differently depending on where the experiments were performed.

The first two experiments were carried out in the Wellcome Trust Centre for Gene Regulation and Expression in Dundee in collaboration with Prof. Mike Stark under kind supervision of Dr. Sara Ten Have and Kelly Hodge. In the first experiment a tryptic digestion of the samples was performed in solution, in the second experiment samples were first separated by SDS-PAGE gel and then in gel digestion was employed. Phosphopeptide enrichment was employed on some samples prior to mass spectrometric analysis.

Another two experiments were carried out in collaboration with Prof. Juri Rappsilber with help from Dr. Juan Zou in the Wellcome Trust Centre for Cell Biology in Edinburgh. Here, all the samples were trypsinised in gel. Again, phosphopeptide enrichment was carried out on some samples prior to mass spectrometric analysis (see Material and Methods for details). The mass spectrometry data was analysed by Dr. Sara Ten Have and Kelly Hodge in Dundee and Dr. Juan Zou in WTCCB, Edinburgh.

Five *in vitro* Ark1 sites were mapped in the N-terminal half of Spc7: S9, S28, S114, S148, and S638. The identified phosphopeptides are shown in Table 3.1. All phosphopeptides were identified in multiple experiments with high confidence except for the peptide containing pS148 which was seen only once. Peptides containing pS9 and pS28 were the strongest hits in all experiments.

Peptides identified	phosphorylated residue	Aurora B consensus	ions score**
RNpSIATTDNVIGR(7_19)	S9*	+	66
RPHpSLGGPGALQELKEHTNPAK(24_46)	S28*	-	26
RVpSFASHAR(112_120)	S114*	+	42
TFApSDAK(145_151)	S148	-	
LRYpSTSSFDQSTLRR(635_648) _YpSTSSFDQSTLRR_(637_648)	S638*	+	36

Table 3.1. Ark1 phosphorylation sites identified in Spc7 *in vitro*.
*-sites identified with high confidence in at least two experiments
**- Mascot ions scores obtained for the peptides identified in the representative experiment carried out in WTCCB, Edinburgh.

3.4.4. Is serine 108 targeted by Ark1?

Serine 108 is located in an Aurora B consensus site adjacent to the highly conserved RVXF (X-any amino acid) PP1 phosphatase binding motif described by Egloff et al. (1997). In *Xenopus* KNL1 Aurora B phosphorylates serine located at position -1 from this motif (Rosenberg et al., 2011) which might correspond to serine 108 in fission yeast (position -3 from the motif) (Figure 3.15). However, while phosphorylation at S114 was detected by mass spectrometry, putative phosphorylation on S108 has not been seen. In order to validate these mass spectrometry results additional kinase assays were performed. The samples from these experiments were then separated by 10% SDS PAGE gel and immunoblotted using anti-Spc7 phospho-S108 and anti-Spc7 phospho-S114 antibodies (Eurogentec, gift from J. Millar).

The western blot analysis shown in Figure 3.8 revealed that S108, although not detected by mass spectrometry, is phosphorylated by Ark1 kinase *in vitro.* No signal was observed for the 'loss' of phosphorylation mutant, GST-Spc7-108A 114A, after incubation in an Ark1 kinase reaction. This confirmed that both antibodies are specific to phospho-S108 (Eurogentec) and to phospho-S114 (Eurogentec). Interestingly, the antibodies also detected the phosphomimetic mutant of Spc7,

GST-Spc7-108D 114D. In the case of the anti-Spc7 phospho-S114 antibody, the detection level of the phosphomimetic mutant was comparable to that of the phosphorylated wild type.

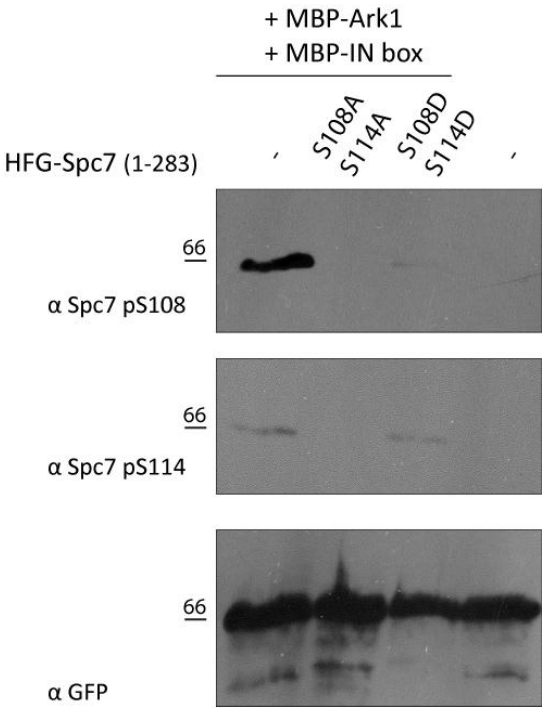

Figure 3.8. Phosphorylation at serine 108 and serine 114 detected by phospho-specific antibodies in *in vitro* Ark1 kinase assay. Western blot analysis on the *in vitro* kinase assay samples was performed using anti Spc7 phospho-S108 and anti Spc7 phospho-114 antibodies (Eurogentec).

3.4.5. Phosphorylation at serine 9 and 28 contributes the most to the total phosphorylation of the N-terminus of Spc7 *in vitro*

In order to determine which sites are the main *in vitro* Ark1 targets in the N-terminus of Spc7 a series of phosphomutants was generated. The phosphorylated residues that had been previously mapped by mass spectrometry, together with serine 108 detected by the anti-Spc7 phospho-S108 antibody (Eurogentec), were mutated to alanine to prevent their phosphorylation in the *in vitro* kinase assay. The phosphomutants were then used as substrates in the Ark1 assay. Incorporation of ^{32}P was measured using ImageJ software for each mutant and normalized against the protein loading and GST-Spc7 (1-283) control (100% of phosphorylation)

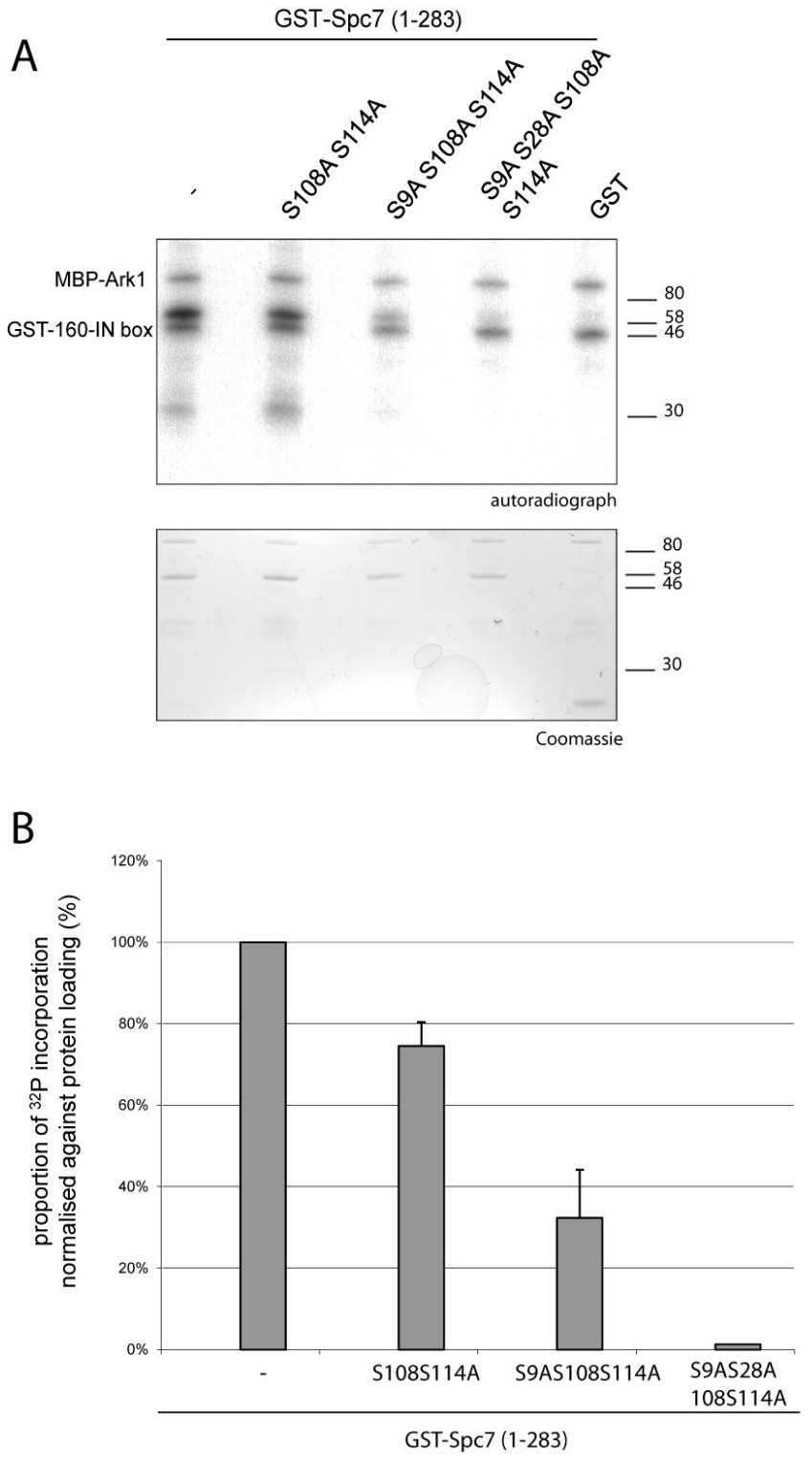

Figure 3.9. Serine 9 and 28 are the main *in vitro* Ark1 phosphorylation sites. **A**. *In vitro* Ark1 kinase assay with different serine to alanine substitution mutants **B.** Quantification of phosphorylation levels in each mutant, in comparison to GST-Spc7 (1-283) (100% of phosphorylation)

The analyses shown in Figure 3.9 revealed that serine 9 in combination with serine 28 constitute about 70% of the GST-Spc7 (1-283) phosphorylation, whereas serine 108 in combination with serine 114 about 30%. This result might help explain why few phosphopeptides containing pS114 and no phosphopeptides containing pS108 were detected in the mass spectrometry experiments. Alternatively those phosphopeptides may just not be detected by mass spectrometer.

3.4.6. Construction of Spc7 phosphorylation mutants

In order to determine physiological importance of the Spc7 phosphorylation sites mapped by mass spectrometry a series of *S. pombe* phosphomutants was generated.

The wild-type construct that I used to generate mutant alleles was obtained from the Millar Lab (University of Warwick). A 5 kb fragment of DNA containing full length *spc7* with 500 bp of 5' UTR (promoter) and 200 bp of 3'UTR had been amplified from genomic DNA and inserted into the *lys1* gene in the plasmid pLYS1K forming pLYS1K-*spc7* (Meadows et al., 2011). Point mutations, resulting either in 'loss' of phosphorylation sites (S/T substituted to A) or mimicking constitutive phosphorylation (S/T substituted to D), were introduced to pLYS1K-*spc7* by site-directed mutagenesis (QuikChange II Site-Directed Mutagenesis, Stratagene). The constructs were sequenced and after linearization, were transformed into haploid strains in which endogenous *spc7*$^{+}$ gene was deleted (*spc7::natMX6*) and Spc7 wild-type protein was expressed from the episomal plasmid pIRT2u-*spc7* (also obtained from the Millar Lab). After transformation pIRT2u-*spc7* was lost from the strains by counter-selection on 5-Fluoroorotic Acid (5-FOA), which kills cells with an active *ura4* gene.

3.4.7. Some Spc7 phosphorylation mutants are sensitive to microtubule depolymerizing agents

Benomyl is a microtubule depolymerizing agent which interferes with kinetochore-microtubule attachments and disrupts the mitotic spindle. Wild type cells, having a functional spindle checkpoint, are able to grow on plates containing low doses of benomyl whereas checkpoint mutants divide rapidly and lose chromosomes, which eventually leads to cell death. However, sensitivity to benomyl might be also caused by an inability to silence the checkpoint.

In order to determine whether mutation of the identified phosphorylation sites in Spc7 affects sensitivity to benomyl, the growth of Spc7 phosphomutants was compared with the known spindle checkpoint mutants *mad3Δ* and *bub1Δ*. The *mad3Δ* mutation results in impaired checkpoint only, whereas *bub1Δ* is also defective in chromosome segregation hence its growth on benomyl is severely impaired (Vanoosthuyse et al., 2004).

This benomyl sensitivity assay (Figure 3.10 and 3.11) revealed that the *spc7-S9A S28A* and *spc7-S9A S108A S114A* cells were sensitive to benomyl to a similar extent as *mad3Δ*. The *spc7-108A S114A*, *spc7-S28A* and *spc7-S9A* cells showed an intermediate phenotype. Interestingly, phosphomimetic mutants, *spc7-S9D* and *spc7-108D S114D,* do not exhibit benomyl sensitivity indicating that these phosphomimetic mutants can support Spc7 functions that are defective in the corresponding alanine mutants. All phosphomutants grew normally on the YES plates with no benomyl added indicating that the way the strains were generated did not affect cell functions (Figure 3.10).

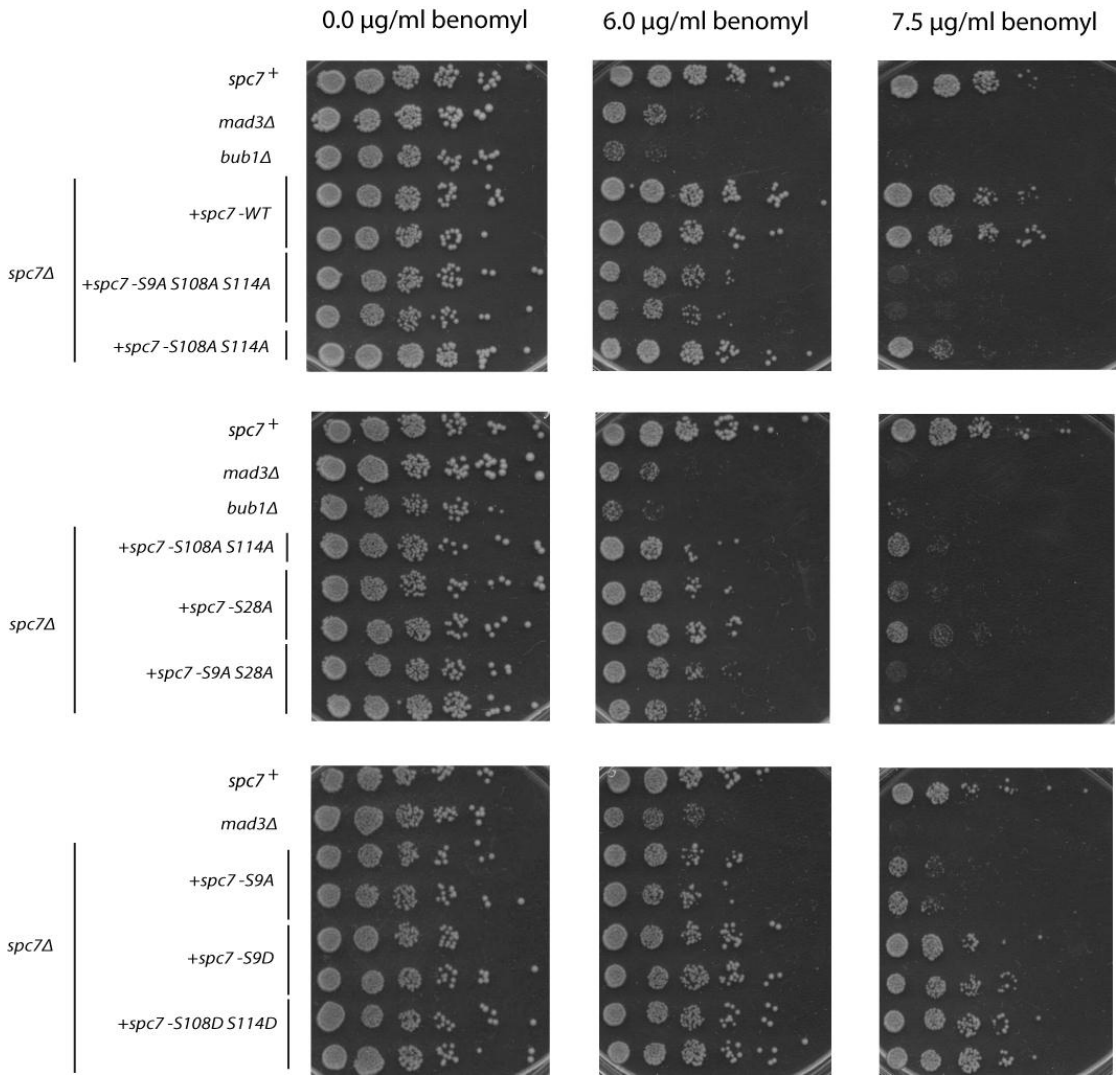

Figure 3.10. Some of the 'loss of phosphorylation' mutants exhibit an increased sensitivity to benomyl and a reduced growth on the drug. 4-fold serial dilutions of wild type, *mad3Δ*, *bub1Δ*, *spc7::natMX6 lys1::spc7-WT, spc7::natMX6 lys1::spc7-S9A S108A S114A, spc7::natMX6 lys1::spc7-108A S114A, spc7::natMX6 lys1::spc7-S9A, spc7::natMX6 lys1::spc7-S28A, spc7::natMX6 lys1::spc7-S9A S28A, spc7::natMX6 lys1::spc7-S9D, spc7::natMX6 lys1::spc7-108D S114D* (two isolates for each newly generated strain) were spotted on YES plates containing 0.0, 3.5, 5.0 or 6.0 and 7.5 µg/ml. Plates were incubated at 30°C for 3-4 days.

These results indicate that phosphorylation at the identified Spc7 residues might be relevant for spindle checkpoint function. However, as benomyl sensitivity is not a specific indicator of checkpoint defects, the observed phenotype might be the result of impaired chromosome segregation, defective spindle checkpoint silencing or a combination of these possibilities.

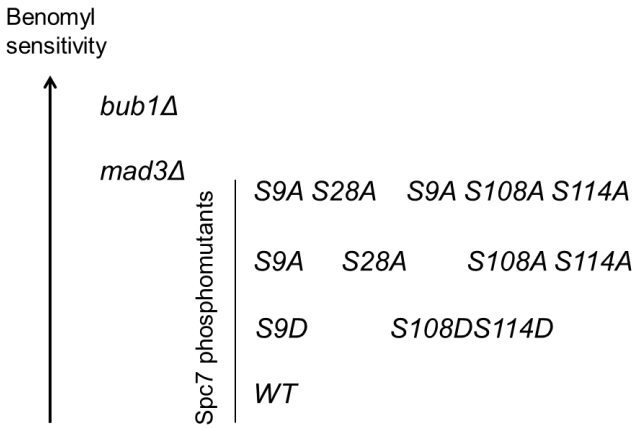

Figure 3.11. Benomyl sensitivity of control and Spc7 phosphomutant strains. Control strains (*mad3Δ*, *bub1Δ*) and the Spc7 phosphomutant strains were ranked according to their sensitivity to benomyl.

3.5. *In vitro* Mph1 kinase assays

An *in vitro* Mph1 kinase assay was developed by Dr. J. Zich (the Hardwick Lab). In the assay tandem affinity purified Mph1 kinase was used (see Material and Methods for details). To rule out the possibility that Mph1-SZZ co-purified with other yeast protein/s having kinase activity an Mph1-kd-strain was generated. In the *mph1-kd-SZZ* allele aspartic acid residue at position 459 was substituted for alanine (D459A) which abolished Mph1 kinase activity (Zich et al., 2012). The analysis shown in Figure 3.12.B demonstrates that Mph1-kd-SZZ is unable to autophosphorylate itself, demonstrating that indeed the kinase activity is lost whereas wild-type Mph1-SSZ remains catalytically active.

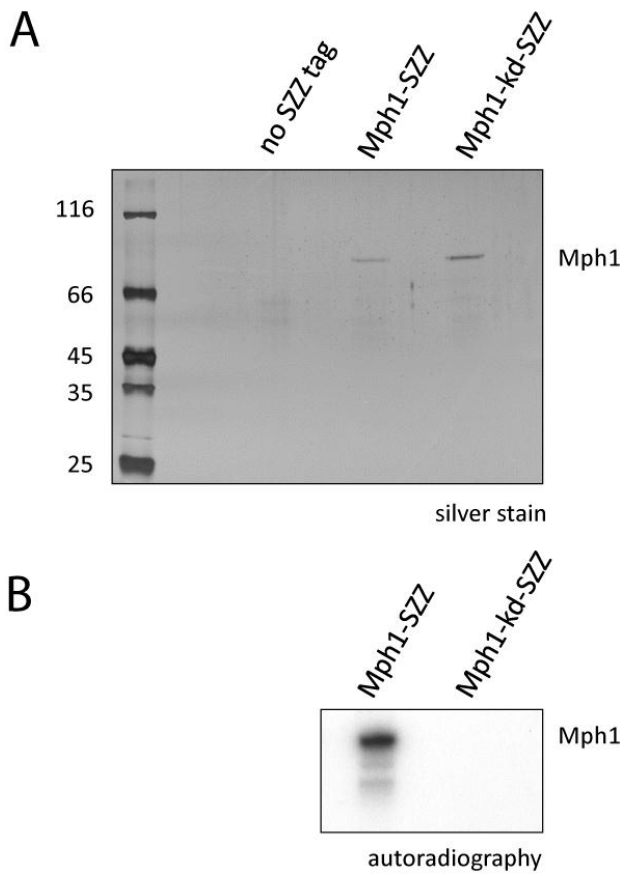

Figure 3.12. A. Tandem affinity purification of Mph1-SZZ and Mph1-kd-SSZ carried out together with Dr. J. Zich. Silver-stained 4 - 12 % precast NuPAGE gradient gel (Invitrogen) with Mph1-SSZ and Mph1-kd-SZZ preps demonstrates that the pull down experiment works and no contaminants are present in the samples. **B. *In vitro* Mph1 kinase assay.** Yeast purified Mph1-SSZ and Mph1-kd-SSZ were incubated in kinase buffer containing γ-^{32}P-ATP. Samples were separated by 4 - 12 % precast NuPAGE gradient gel (Invitrogen) and autophosphorylation of Mph1 was visualized by autoradiography.

3.6. Spc7 is *in vitro* substrate of Mph1 kinase

To determine whether Spc7 is also an Mph1 substrate, *in vitro* Mph1 kinase assays were performed. A recombinant fragment of Spc7 containing residues 1-666 was purified from *E. coli* as a fusion with MBP (MBP-Spc7 1-666) (for construction of pHMGWA-Spc7 (1-666) expression vector see chapter 4.2.). MBP-Spc7 (1-666) and MBP were incubated with yeast purified Mph1-SZZ or Mph1-kd-SZZ in kinase

buffer containing γ-^{32}P-ATP. After incubation the samples were run on a SDS-PAGE gel and subjected to autoradiography.

Figure 3.13 demonstrates that Spc7 phosphorylation was detected in samples containing active Mph1. Phosphorylation of GST-Spc7 (1-666) was detected in the Mph1-wt-SZZ lane but not in the lane containing Mph1-kd-SZZ.

Mass spectrometry mapping of Mph1-dependent phosphorylation sites in Spc7 resulted in the identification of four phosphopeptides (see Table 3.2 below). These results reveal phosphorylation of threonine residues 168, 283 and 507 and weakly phosphorylation of threonine 453 since this peptide was identified only in one experiment with a low score.

Peptides identified	phosphorylated residue	ions score*
NETQSSPHSHSASIISDGSDMDIASPIR(166-193)	T168	12/36
GLSSSEQGTVYSLK(275-288)	T283	-/71
SMEEQIMDLTQPISSTNAPTHLNED DLNQFTSNISSSSKPR(444-484)	T453	8/-
TANSSKPIPDSEDFMDITRPFNILSPSK(490-517)	T507	7/19

Table 3.2. Mph1 phosphorylation sites identified in Spc7 *in vitro*. *- Mascot ions scores obtained for peptides identified in two experiments carried out in WTCCB, Edinburgh.

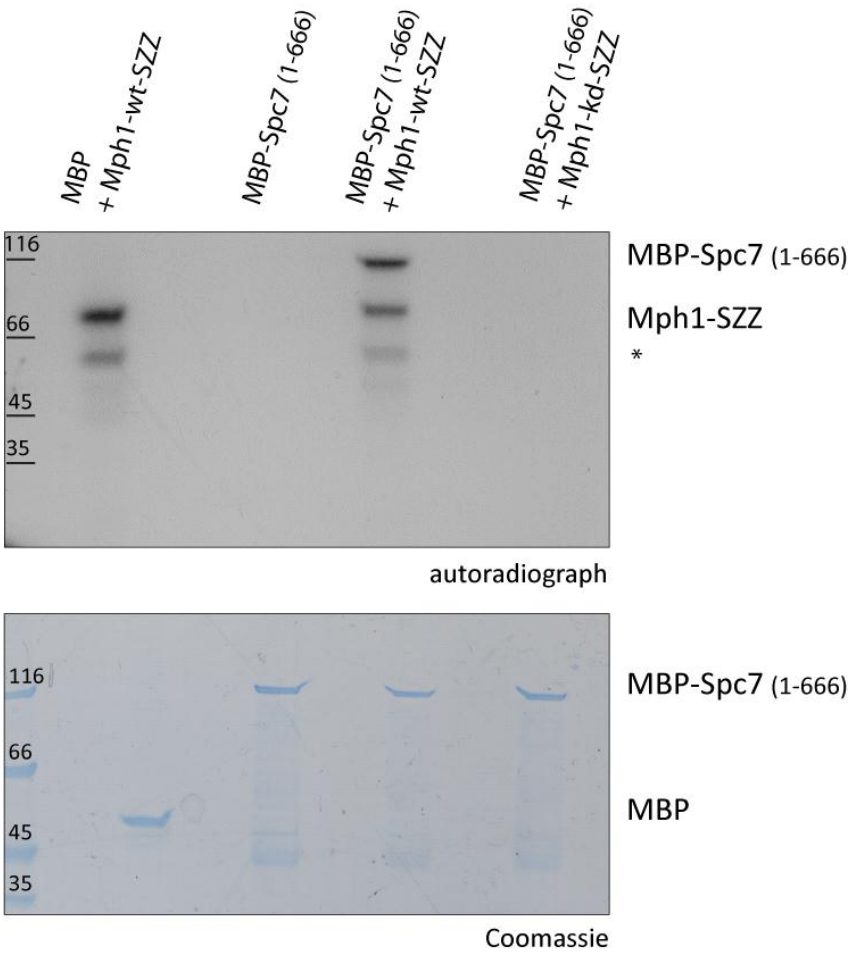

Figure 3.13. The N-terminal half of Spc7 is phosphorylated by Mph1. *In vitro* Mph1 kinase assay. Purified Mph1-SSZ and Mph1-kd-SSZ were incubated with MBP-Spc7 (1-666) and MBP in kinase buffer containing γ-^{32}P-ATP for 30 min at 30°C. Samples were separated by 4 - 12 % precast NuPAGE gradient gel (Invitrogen) and the incorporation of ^{32}P was visualized by autoradiography.

3.7. Summary and discussion

KNL1/Blinkin is a multifunctional kinetochore protein whose functions and structural organization is conserved from yeast to human. KNL1/Blinkin binds microtubules (Cheeseman et al., 2006; Welburn et al., 2010) via its very N-terminus (Espeut et al., 2012). The C-terminal half of KNL1/Blinkin contains a coiled-coil motif (Cheeseman et al., 2004) which is required for KNL1/Blinkin kinetochore binding (Kiyomitsu et al., 2007, 2011). There are two highly conserved PP1 binding motifs, SILK and RRVSF in the N-terminus of KNL1/Blinkin (Cheeseman et al., 2004) . The RRVSF motif is required for PP1 targeting to kinetochores in human and chicken cells (Liu et al., 2010). Similarly, the *S. pombe* homologue of KNL1/Blinkin, Spc7 (*S. pombe* centromere) has all the functions described above (Kerres et al., 2007, 2004; Meadows et al., 2011) (Figure 3.14).

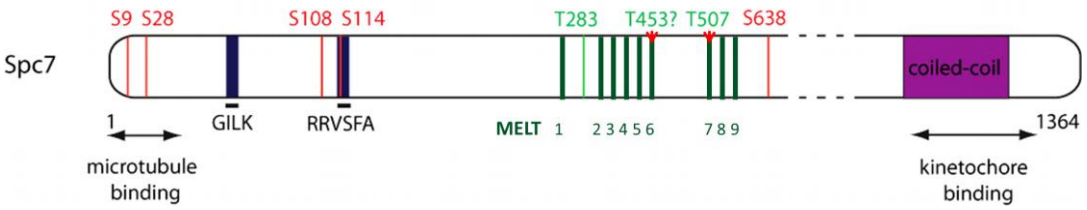

Figure 3.14. Schematic representation of Spc7 domain organization with *in vitro* Ark1 and Mph1 sites. Ark1-dependent phosphorylation sites identified in this study are in red, whereas Mph1 phosphorylation sites are in green. The Dis2 binding sequences, GILK and RRVSFA, are present in the N-terminus of Spc7 (dark blue) (Meadows et al., 2011). Conserved MELT motifs (dark green) are located in the N-terminal half of Spc7. Red arrows indicate phosphorylation event detected in the MELT motif of Spc7 in this study. The C-terminus consists of a coiled-coil motif (purple) which is required for kinetochore targeting of Spc7 via its interaction with the Mis12 complex (Kerres et al., 2007; Kiyomitsu et al., 2011).

In vertebrates, microtubule and PP1 binding to KNL1/Blinkin are regulated by Aurora B (Welburn et al., 2010, Liu et al., 2010). Considering the conservation and complexity of the KNL1/Blinkin family proteins, we wanted to test whether fission yeast Spc7 is also regulated by phosphorylation.

In this chapter results demonstrating that Spc7 is phosphorylated by Ark1 and Mph1 have been presented. Data obtained *in vivo* suggests that the N-terminus of Spc7 (HFG-Spc7 1-283) is likely to be phosphorylated specifically in mitosis, as the Spc7 gel mobility shift was observed in cells arrested in metaphase by Mph1 overexpression (Figure 3.4). The Spc7 gel mobility shift was far more pronounced upon Mph1 overexpression than upon *nda3-KM311* arrest indicating that Mph1 activity, directly or indirectly, affects Spc7 phosphorylation. A similar experiment was carried out with *nda3-KM311* arrested cells overexpressing HFG-Spc7 (1-666) under the nmt41 promoter, however the longer fragment was hardly detected by anti-Spc7 and anti-GFP antibodies after 48-36 hours of overexpression. Consistent with low expression, the GFP signal of HFG-Spc7 (1-666) was not detected by fluorescent microscopy whereas HFG-Spc7 (1-283) signal was visible after 8-12 hour overexpression (data not shown). This difference may indicate that the longer Spc7 fragment is degraded. The efficient degradation of the longer fragment might be promoted by the presence of a putative KEN box (residues 569-571). Interestingly, the nuclear localisation of GFP-tagged Spc7 containing residues 1-820 was observed in a study by Kerres et al. (2007) when it was overexpressed under the strongest nmt promoter, nmt1. This suggests that higher expression levels of the N-terminal half of Spc7 might overcome its sensitivity to degradation.

Ark1- and Mph1-dependent phosphorylation of Spc7 was demonstrated by *in vitro* kinase assays (Figures 3.7 and 3.13). Further, *in vitro* Ark1 and Mph1 kinase assay samples containing recombinant the N-terminal fragment of Spc7 were subjected to mass spectrometry analysis. The following Ark1 sites were identified: S9, S28, S114 and S638 (Table 3.1). Moreover, serine 108 was detected by anti-Spc7 pS108 antibody, but not by mass spectrometry (Figure 3.8). This might be explained by the technical difficulty with generating a tryptic peptide which would be long enough to support efficient detection. Serine 108 is located in an environment that is rich in arginine and lysine residues, thus the use of trypsin, which cleaves carboxy-terminal of arginine or lysine residues, will result in a 4-amino acid fragment containing S108. A solution to this would be to use a different protease to digest samples, for example Lys C which only cleaves peptide bonds on the carboxyl side of lysine residues.

According to the quantification of ^{32}P labelling of Spc7 (1-283) and Spc7-S108A S114A (1-283), Spc7-S9A S108A S114A (1-283) and Spc7-S9A S28A S108A S114A (1-283) mutants, serine 9 and 28 together constitute the major *in vitro* Ark1-dependent phosphorylation sites in recombinant Spc7 containing residues 1-283 (about 70% of the total phosphorylation) (Figure 3.9). All the identified sites are located within consensus motif for Aurora B-dependent phosphorylation except for serine 28.

In parallel with our identification of *in vitro* Ark1-dependent sites in Spc7 Koch et al. (2011) also mapped *in vivo* sites in a proteome-wide screen for Ark1 substrates in fission yeast. In their analyses serine 4 and serine 9 were identified as sites which phosphorylation was downregulated upon Ark1 inhibition with 1-NMPP1 in an *ark1as-3* strain (Koch et al., 2011). The *ark1-as3* allele encodes Ark1 kinase whose gatekeeper residue in a protein kinase pocket is mutated which creates a new pocket. The new pocket can bind both the ATP analogue (1-NMMP1) and ATP, so that the kinase can be selectively inhibited in the presence of the inhibitor (Hauf et al., 2007; Cipak et al., 2011).

Phosphorylation of serine 28 was downregulated upon *ark1*$^{+}$ cells treatment with 1-NMPP1 which indicates that in this experiment 1-NMPP1 might have had off-target effects and phosphorylation at serine 28 might have been a result of a distinct kinase activity (Koch et al., 2011). However, serine 28 together with serine 9 but not serine 4 were also identified using *in vitro* Ark1 kinase assays by Koch et al. (2011) which is consistent with the data obtained in our study.

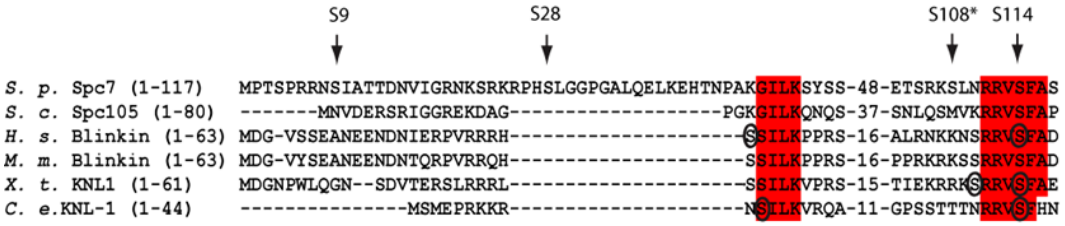

Figure 3.15. Sequence alignment of *S. pombe* (*S.p.*), *S. cerevisiae* (*S. c.*), *H. sapiens* (*H. s.*), *M. musculus* (*M. m.*), *X. tropicalis* (*X. t.*), *C. elegans* (*C. e.*), KNL1 homologues showing conservation of the N-terminal [S/G]ILK and RVSF motifs (highlighted in red). Arrows indicate *in vitro* Ark1 phosphorylation sites mapped in this study. Ovals indicate phosphorylation identified in other species [*H. s.*and *C. e.* -(Welburn et al., 2010), *X. l.*-(Rosenberg et al., 2011)], * - residue detected by specific anti-phospho antibody only**.**

In order to confirm the physiological significance of the identified Ark1 phosphorylation sites, yeast Spc7 phosphomutants were generated. Impaired growth on benomyl was observed for mutants having serine 9 and 28 substituted to alanine alone or in combination with the other sites (Figure 3.10). The strongest growth defect was exhibited by *spc7::natMX6 lys1::spc7-S9A S28A* mutant which agrees with the results of *in vitro* Ark1 kinase assay indicating that S9 and S28 are the major Ark1 sites in Spc7 (Figure 3.9). The localisation of the identified Ark1 phosphorylation sites suggests possible roles of these sites (Figure 3.14, red colour). Serines 9 and 28 are located in the extreme N-terminus of Spc7 which has been implicated in microtubule binding (Kerres et al., 2007). Two other putative Ark1 phosphorylation sites, serine 108 and 114, are situated in the close proximity to and inside, respectively, a highly conserved RRVSF motif (Figure 3.15). The RRVSF and [G/S]ILK sequences have been reported to be PP1 binding motifs (Egloff et al., 1997; Hendrickx et al., 2009). Aurora B was shown to negatively regulate PP1 kinetochore targeting by phosphorylating the serine adjacent to the SILK motif and the serine inside the RRVSF motif in human KNL1 (Liu et al., 2010). This raises the possibility that in *S. pombe* Ark1 might also control Dis2 phosphatase (the *S. pombe* homologue of PP1) localisation to kinetochores. Microtubule and Dis2 binding activities of Spc7 are described in Chapter 6.

Phosphorylation of serine 638 has not been further investigated. Nevertheless, the Ark1-dependent phosphorylation at this residue was strongly supported by mass spectrometry analysis. Therefore, it would be interesting to know whether phosphorylation of serine 638 has any functional role and this question will be addressed by future studies.

Spc7 was also shown to be an *in vitro* substrate of Mph1 [(Figure 3.13) and (Shepperd et al., 2012)]. Along with our observations two other studies have reported Mps1/Mph1-dependent phosphorylation of *S. cerevisiae* Spc105 and *S. pombe* Spc7 (London et al., 2012; Yamagishi et al., 2012). Three putative Mph1 sites, T283, T453, T507, have been identified by mass spectrometry, however T453 has been mapped with low confidence (this study, Figure 3.14). Phosphorylation at threonine T507 was confirmed by *in vitro* Mph1 kinase assay followed by mass spectrometry (Yamagishi et al., 2012). Mph1-phosphorylation of three other residues including T77, T338, and T552 was also reported (Yamagishi et al., 2012).

Interestingly T338, T507, T453 and T552 are located in MELT (M[E/D] [L/I] [S/T]) repeat sequences, conserved in KNL1/Blinkin family proteins (Cheeseman et al., 2004). Similarly, budding yeast Mps1 kinase targets three out of six MELT motifs which are present in Spc105 (London et al., 2012). Figure 4.1 shows the location of the MELT motifs in the N-terminal region of *S. pombe, S. cerevisiae* and *H. sapiens* KNL1/Blinkin proteins.

Taken together, the analysis presented in this chapter revealed that Spc7/KNL1, in addition to being an Aurora B substrate, is also phosphorylated by Mph1/Mps1. The Mph1/Mps1-dependent phosphorylation of Spc7/KNL1 is a new finding in the checkpoint field. Interestingly, we showed that at least two out of nine conserved MELT motifs are phosphorylated by Mph1 *in vitro*. The function of the MELT motifs is unknown. We hypothesise that Mph1-dependent phosphorylation of Spc7, possibly at threonines of the MELT motifs, might be involved in checkpoint signalling. The experiments which address these questions are presented in the next chapter.

Our study confirmed that Ark1, the fission yeast Aurora kinase, phosphorylates Spc7 *in vitro.* We identified five *in vitro* Ark1-dependent sites in Spc7 and three of them (S108, S114 and S638) have not been reported in fission yeast before. Previous reports suggest that that Ark1-phosphorylation of Spc7 might regulate checkpoint silencing and/or microtubule binding activity of Spc7.

Chapter 4

Kinetochore recruitment of Bub1 and Bub3 is promoted by Spc7 phosphorylation

Chapter 4

Kinetochore recruitment of Bub1-Bub3 is promoted by Spc7 phosphorylation

4.1. Introduction

In the previous chapter I demonstrated that Mph1 phosphorylates the fission yeast kinetochore protein Spc7 *in vitro*. The candidate phosphosites have been mapped and two of them, T453 and T507, are located in the MELT motifs which are highly conserved within KNL1/Blinkin family proteins (Cheeseman et al., 2004) (Figure 4.1).

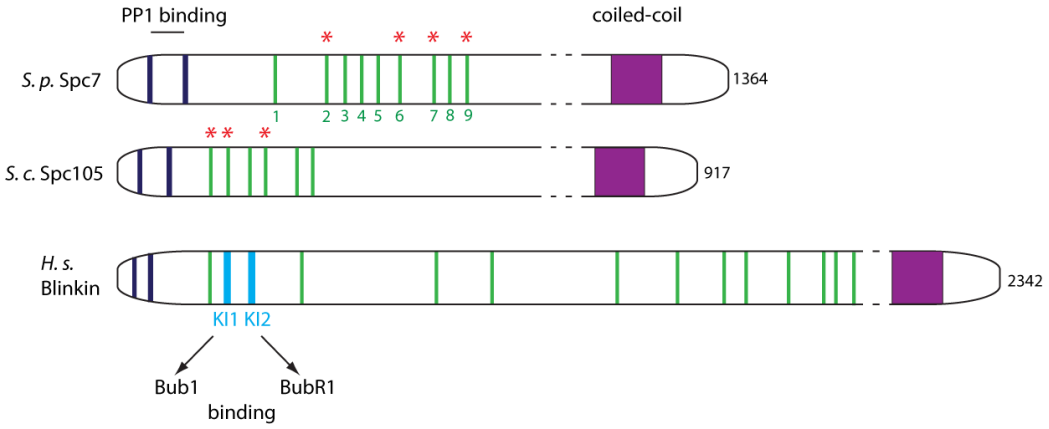

Figure 4.1. Schematic representation of *S. pombe* Spc7, *S. cerevisiae* Spc105 and *H. sapiens* Blinkin. This diagram shows the invariant N-terminal PP1 binding motifs (dark blue), the N-terminal MELT repeats (numbered in *S. pombe* Spc7) (green), and the C-terminal coiled-coil domain (purple) and the KI motifs 1 and 2 (light blue), which are required for human Bub1 and BubR1 interaction with Blinkin, respectively (Kiyomitsu et al., 2011). Asterisks indicate Mph1kinase phosphorylation sites mapped in MELT motifs by three independent studies including T453 and T507 of MELT 6 and MELT 7, respectively, mapped in this study (see Chapter 3) (London et al., 2012; Yamagishi et al., 2012).

Checkpoint signalling includes the recruitment of checkpoint scaffolds, Bub1-Bub3 complex and Mad1-Mad2 complex, to unattached kinetochores. It is well established that Mph1 kinase is required for checkpoint protein recruitment to unattached kinetochores. However, the exact mechanism that recruits checkpoint components to kinetochores is not known. Moreover, the role of checkpoint proteins at kinetochores is debatable as several studies demonstrated that kinetochore recruitment of checkpoint components is dispensable for checkpoint activation (Fraschini et al., 2001; Tange and Niwa, 2008; Vanoosthuyse et al., 2009). Here, we addressed the question of how the interaction between the Bub1-Bub3 complex and the kinetochore is promoted and what is the role for Mph1 kinase in this process. After considering previous reports, we decided to test the hypothesis that Spc7/KNL1 is a kinetochore platform that recruits the Bub1-Bub3 complex to unattached kinetochores upon checkpoint activation.

A crucial role for Mps1/Mph1 kinase in checkpoint signalling is supported by many studies. Selective inhibition of human Mps1-as activity by 23dMB-PP1 (an ATP analogue) resulted in reduced levels of Mad1, Mad2, Bub1 and Cdc20 at unattached kinetochores whereas BubR1 and CENP-E kinetochore localisation was marginally affected (Sliedrecht et al., 2010). Another study, also based on chemical genetic inhibition of human Mps1, confirmed that kinetochore enrichment of Mad1, Mad2 and Bub1 is abolished upon Mps1 inactivation (Maciejowski et al., 2010). Interestingly, this study also demonstrated that the kinetochore localisation of Mps1 is required for the Bub1 recruitment to kinetochores. An Mps1 mutant, which did not localise to kinetochores, failed to recruit Bub1 to kinetochores but was capable of facilitating Mad2-Cdc20 complex formation (Maciejowski et al., 2010). In fission yeast tethering Mph1 to kinetochores is sufficient for constitutive Bub1 localisation at kinetochores (Ito et al., 2011). These analyses imply that Mps1 activity at kinetochores is required for the recruitment of Bub1 to kinetochores and suggest that Mps1 might phosphorylate some kinetochore components which in turn promotes Bub1 association with kinetochores.

The analyses that I presented in Chapter 3 demonstrated that Spc7 is phosphorylated *in vitro* by Mph1 and at least two of the phosphorylation sites are located in a MELT motif (T453 and T507). This finding allowed us to hypothesise that Mph1-dependent phosphorylation of the MELT motifs might direct Bub1 association with Spc7 and thereby mediate the recruitment of Bub1 to kinetochores upon spindle checkpoint activation. To test this hypothesis various biochemical experiments including *in vitro* kinase assay, co-immunoprecipitation (Co-IP*), in vitro* binding assays and chromatin immunoprecipitation (ChIP) have been performed. Additional microscopy supporting the analysis of MELT phosphomutants was carried out in the J. Millar Laboratory (University of Warwick).

4.2. Construction of MBP-Spc7 (1-666), MBP-Spc7-T9A (1-666) and MBP-T9E (1-666) expression vectors

In the majority of experiments described in this chapter recombinant Spc7 fragments containing 1-666 residues of Spc7 tagged with MBP were used. *S. pombe* Spc7 contains nine MELT motifs (Table 4.1). We decided to express two Spc7 (1-666) phosphorylation mutants in *E. coli.* The mutants contain threonine residues that are present in all nine MELT motifs substituted either to alanine residues, which results in non-phosphorytable Spc7 mutant [Spc7-T9A (1-666)] or to glutamic acid residues which mimics constitutive phosphorylation [Spc7-T9E (1-666)].

To generate MBP-Spc7 fusion proteins a gene fragment of Spc7 encoding residues (1-666) was amplified from pLYS1K-*spc7*, pLYS1K-*spc7-9TA* and pLYS1K-*spc7-9TE* plasmids using primers compatible with the Gateway Cloning system (Invitrogen). The pLYS1K plasmids were provided by Prof. J. Millar (University of Warwick) (Shepperd et al., 2012). The PCR products were cloned into pDONR201 donor vector using Gateway BP Clonase II enzyme mix (Invitrogen) and then transferred to pHMGWA Gateway-based destination vector using Gateway LR Clonase II enzyme mix (Invitrogen) according to the manufacturer's instructions. The pHMGWA-*spc7 (1-666)*, pHMGWA-*spc7-T9A (1-666)*, pHMGWA-*spc7-T9E (1-666)* expression vectors were transformed to BL21-CodonPlus-RIL *E. coli* cells, which enhance expression of AT rich genes.

MELT motif	Residues
1	254-257
2	335-338
3	363-366
4	392-395
5	419-422
6	450-453
7	504-507
8	526-529
9	549-552

Table 4.1. The MELT motifs in the *S. pombe* Spc7

4.3. Phosphorylation of the MELTS motifs constitutes the majority of Mph1-dependent phosphorylation in the N-terminus of Spc7

In order to assess how much phosphorylation of the MELT motifs contributes to total Mph1-depentent phosphorylation of the N-terminus of Spc7, threonines in all nine MELTs were substituted to alanines to prevent phosphorylation specifically at the MELT motifs. Both proteins, MBP-Spc7 (1-666) and the alanine mutant MBP-Spc7-T9A (1-666), were subjected to an *in vitro* Mph1 kinase assay (described in section 3.4).

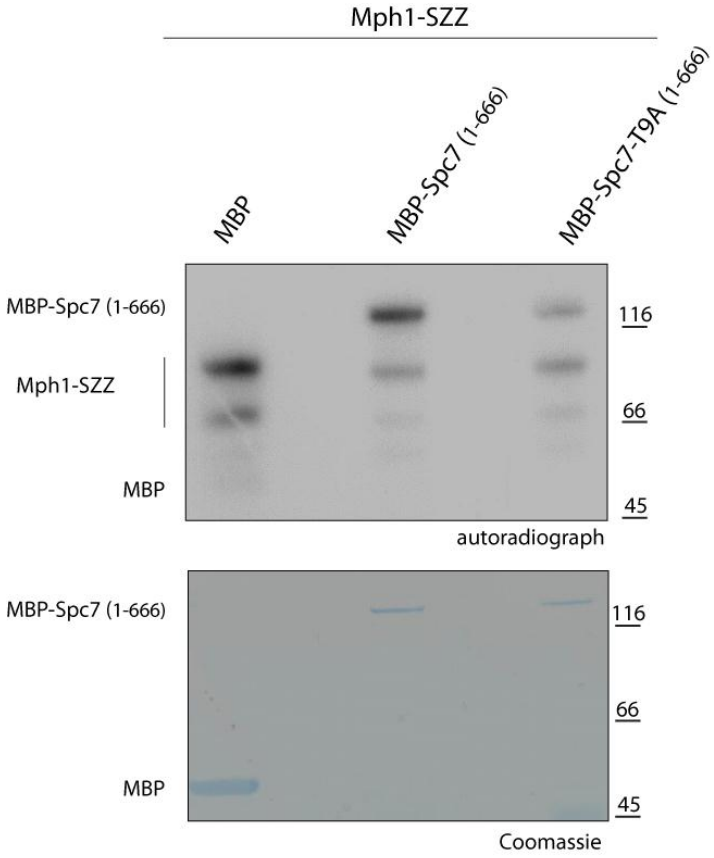

Figure 4.2. The MELT motifs are targeted by Mph1 activity. Yeast purified Mph1-SSZ and Mph1-kd-SSZ were incubated with MBP-Spc7 (1-666), MBP Spc7-T9A (1-666) and MBP in kinase buffer containing γ-^{32}P-ATP. Samples were separated by 4 - 12 % precast NuPAGE gradient gels (Invitrogen) gel and the incorporation of ^{32}P was visualized by autoradiography.

Alanine substitution of threonines in all nine MELT motifs reduced Mph1 kinase-dependent phosphorylation of Spc7 *in vitro* by about 60% (Figure 4.2). However, mutation of T453 and T507 alone did not substantially affect the Spc7 phosphorylation in *in vitro* Mph1 kinase assay (data not shown). These results suggest that Mph1 kinase phosphorylates more than one threonine in the MELT motifs.

4.4. Interaction between Spc7 and Bub1

At the initiation of this study, evidence for an interaction between human Bub1 and KNL/Blinkin interaction was provided by yeast two hybrid assays and structural studies (Kiyomitsu et al., 2007; Bolanos-Garcia et al., 2009). In order to investigate the interaction between Bub1 and Spc7 in yeast an immunoprecipitation approach was initially employed. However due to technical difficulties with Co-IPs, caused probably by proteolytic cleavage of endogenous Spc7 and loss of posttranslational modification on Spc7 in yeast cell extracts, alternative approaches were employed.

4.4.1. Bub1 interacts with Spc7 *in vivo*

The first approach was to trap the Spc7-Bub1 association by crosslinking (Figure 4.3). We used cells that express high levels of 6xHis-Flag-GFP-Spc7 (1-283) [(HFG-Spc7 1-283)] and endogenous levels of Bub1-SZZ. HFG-Spc7 (1-283) was overexpressed from the nmt41 promoter for 24 hours in minimal medium lacking thiamine. Subsequently, intracellular crosslinking with DSP (dithiobis[succinimidyl propionate]), which is a membrane permeable, homobifunctional and amine-reactive crosslinker, was carried out. Control cells were treated with DMSO only (-DSP lanes) as DSP was dissolved in DMSO. Bub1-SZZ was immunoprecipitated from yeast extracts made from crosslinked and control cells. Samples were separated by SDS-PAGE gel and immunoblotted with anti-Spc7 antibody and anti-Mad1 antibody which binds the SZZ tag.

Interestingly, Bub1 and Spc7 (1-283) co-immunoprecipitated only in the presence of the crosslinker (Figure 4.3). However, even in the crosslinked sample Spc7 signal was very weak suggesting that the Bub1-Spc (1-283) interaction was not well maintained in those conditions. This suggests that the short N-terminal fragment of

Spc7 may not contain the whole Spc7 region required for efficient Bub1 binding. This result also suggests that some posttranslational modification might be involved in mediating the Bub1-Spc7 interaction as crosslinking is likely to additionally preserve proteins modifications.

Overexpression of a longer HFG-Spc7 (1-666) fragment containing all the MELT motifs in yeast cells is very inefficient so another approach had to be used to investigate the Bub1 association with Spc7.

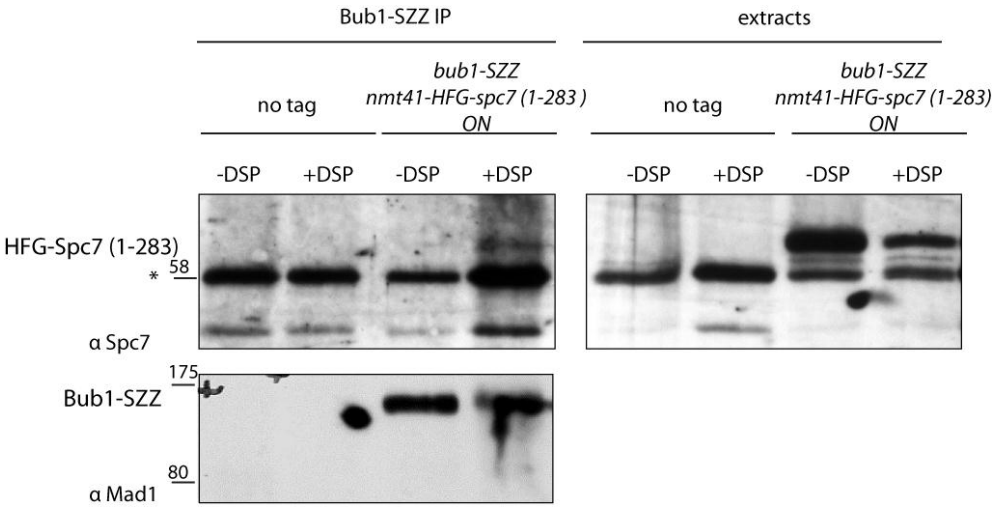

Figure 4.3. Bub1 and the N-terminus of Spc7 (residues 1-283) interact *in vivo*. Bub1-SZZ was immunoprecipitated from yeast extracts made from crosslinked (+DSP) and not-crosslinked (-DSP) cells. Samples were separated by 10% SDS-PAGE and subjected to western blot analysis with anti-Spc7 and anti-Mad1, (polyclonal rabbit anti-Mad1 antibody generated in Dr. K. Hardwick Laboratory cross-reacts with the SZZ tag), antibodies. Asterisk indicates an unspecific band (cross-reactivity with anti-Spc7 antibody)

4.4.2. Mph1-dependent phosphorylation of the MELT motifs in Spc7 promotes Bub1-Spc7 association *in vitro*

To confirm that Bub1 associates with Spc7 and examine whether phosphorylation of MELT motifs contributes to this interaction an *in vitro* Spc7 binding assay was developed. Bacterially expressed MBP-Spc7 (1-666), MBP-Spc7-T9A (1-666) and MBP-Spc7-T9E (1-666) were immobilized on amylose resin (NEB). Then the beads were incubated with yeast cell extract containing Bub1-SZZ and then split into two sets. Each set was run on a 10% SDS-PAGE gel, one gel was immunoblotted with PAP antibody to detect Bub1-SZZ whereas second gel was stained with Instant*Blue* (Expedeon) to visualize recombinant proteins.

Figure 4.4 demonstrates that neither Spc7 (1-666) nor Spc7-T9A (1-666) precipitated Bub1-SZZ from the yeast extract. However, the phosphomimetic MELT mutant, Spc7-T9E, was able to associate with Bub1-SSZ. Importantly, no interaction was observed in a sample containing MBP-Pic1-IN box which additionally confirmed that the observed interaction between Spc7-T9E (1-666) is specific.

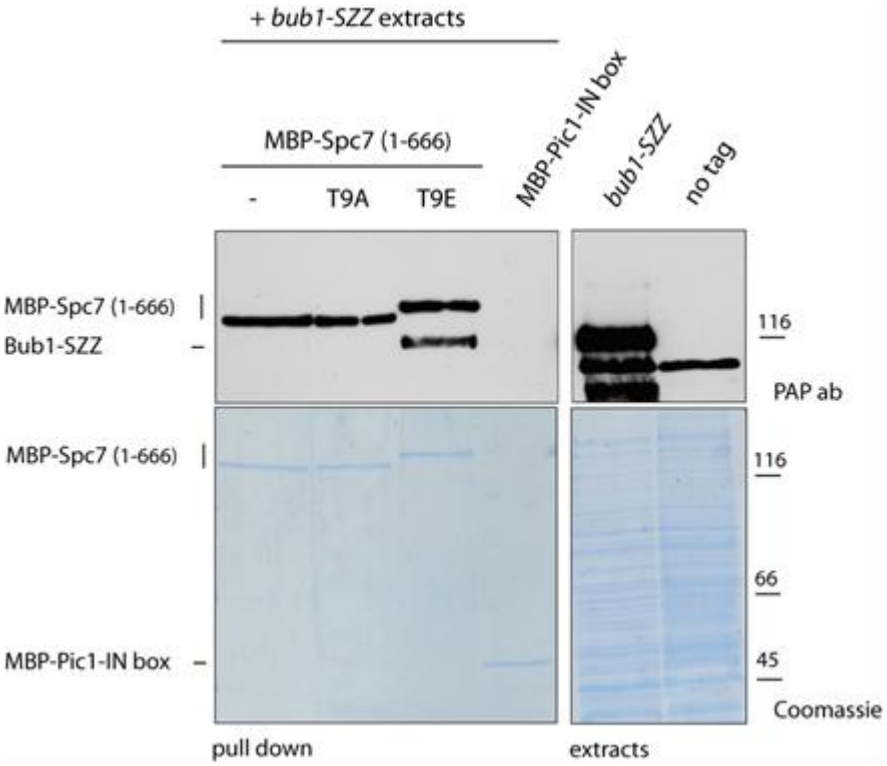

Figure 4.4. Bub1 interaction with Spc7 depends on phosphorylation of the MELT motifs. Beads coated with recombinant, MBP tagged Spc7 (1-666), Spc7-T9A (1-666) and Spc7-T9E (1-666) and Pic1-IN box (negative control) were incubated with *bub1-SZZ* cell extract. Pull downs and extracts were separated by 10% SDS-PAGE gel and probed with PAP antibody which recognises the SZZ tag. Note that PAP antibody cross-reacts with the MBP-Spc7 (1-666) proteins.

4.4.3. Phosphorylation of MELTS in Spc7 targets Bub1 to kinetochores

The previous result showed that mimicking phosphorylation at the MELT motifs is necessary for the Bub1-Spc7 association *in vitro*. To examine the influence of mimicking constitutive phosphorylation of the MELT motifs on Bub1 localisation during the cell cycle, chromatin immunoprecipitation (ChIP) experiment was carried out using *bub1-GFP spc7Δ nda3-KM311 lys1:: spc7-WT/T9A/T9E* strains.

Metaphase arrested or cycling cells were fixed with paraformaldehyde. Cell fixation was followed by zymolyase treatment in order to remove cell walls. Cell pellets were

frozen at -80° C. Protein A beads (Dynal) were coated with anti-GFP antibody (Molecular Probes) and used to immunoprecipitate Bub1-GFP from crude extracts obtained by sonicating the cell pellets. After washing, the beads were mixed with Chelex-100 resin (Bio-Rad) to capture co-immunoprecipitated DNA. The beads were treated with Proteinase K to remove proteins from the samples. The samples were then centrifuged and the supernatant containing co-precipitated DNA was collected to be amplified by PCR reaction. Three pairs of primers were used in the PCR reaction to test for enrichment of centromeric DNA relative to control probes

- primers specific to the central core (cnt), which is the site of kinetochore assembly,
- primers specific to centromeric outer repeats (otr)
- and control primers that amplify a noncentromeric, euchromatic negative control (fbp)

The PCR samples were run on a 1.5% agarose gel containing ethidium bromide and visualized by exposure to ultraviolet. Kinetochore enrichment of Bub1-GFP was quantified for a representative experiment.

This ChIP experiment demonstrated that Bub1 is specifically enriched with the central kinetochore region during a metaphase arrest caused by microtubule depolymerisation in *spc7*$^{+}$ *nda3-KM311* cells. In cycling cells Bub1 is not significantly enriched over the central core domain relative to the outer repeats or the fbp locus. Strikingly, in the *spc7-T9E* mutant a strong kinetochore enrichment of Bub1 was detected both in cycling and *nda3-KM311* arrested cells. The kinetochore signal of Bub1 is severely reduced but not eliminated in *spc7-T9A* cells upon metaphase arrest.

These analyses show that the constitutive phosphorylation of the MELT motifs (as mimicked by the *spc7-T9E* mutant) results in accumulation of Bub1 at kinetochores throughout the cell cycle. This finding was confirmed by microscopy carried out in the Millar Lab (Figure 4.8) (Shepperd et al., 2012).

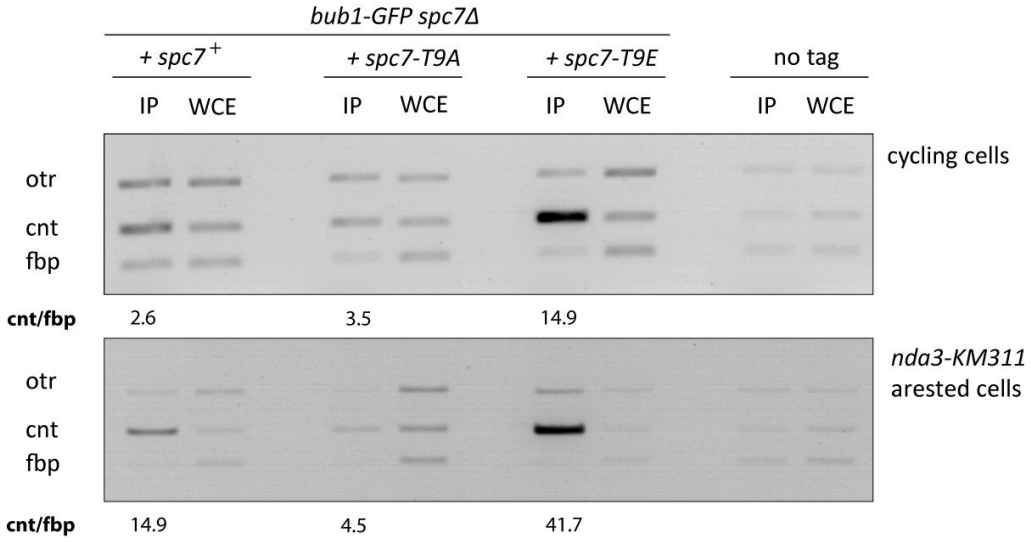

Figure 4.5. Bub1 is constitutively enriched at kinetochores in *spc7 9TE* cells. Bub1-GFP ChIP from *nda3* arrested and cycling *spc7*$^{+}$, *spc7-T9A* and *spc7-T9E* cells. The PCR reaction was performed on co-immunoprecipitated DNA using primers specific to the central core of centromere (cnt), centromeric outer repeats (otr) and euchromatin (fbp). Kinetochore enrichment factor for Bub1-GFP - tm/fbp.

4.4.4. Bub3 is required for Bub1 association with Spc7 phosphorylated on the MELT motifs *in vitro*

The above analyses indicate that the association of Bub1 with kinetochores is promoted by the phosphorylation status of Spc7. Previous studies have demonstrated that the recruitment of Bub1to kinetochores depends on Bub3 (Taylor et al., 1998; Vanoosthuyse et al., 2004; Krenn et al., 2012). The GLEBS domain in Bub1, (residues 264-289 in fission yeast), is required for Bub3 binding and thereby for the localisation of Bub1 to kinetochores (Taylor et al., 1998; Wang et al., 2001; Vanoosthuyse et al., 2009). It has been demonstrated that Bub1 and Bub3 localisation to kinetochores does not depend on Mad proteins, including Mad3 (Vanoosthuyse et al., 2004). To investigate whether Bub1 association with Spc7 depends on Bub3 and/or Mad3, *in vitro* Spc7 binding assays were performed using the MBP-Spc7 (1-666) proteins. Cell extracts were prepared from *mad3Δ bub1-SZZ*, *bub3Δ bub1-SZZ* and *bub1-GLEBSΔ-SZZ* cells. No tag cells were used as controls. The extracts were incubated with beads coated with MBP-Spc7 (1-666) and

MBP-Spc7-T9E (1-666). Co-precipitation of Bub1-SZZ was analysed by western blotting with PAP antibody.

This *in vitro* binding experiment confirms that Bub1 associates with the Spc7 phosphomimetic mutant Spc7-T9E (1-666) but not with Spc7 (1-666) suggesting that the phosphorylation of MELT motifs (as mimicked by T9E) mediates Bub1 association with Spc7 (Figure 4.6.A and B). The fact that the interaction between Bub1 and Spc7-T9E (1-666) is lost in cell extracts lacking Bub3 (Figure 4.6.A) or expressing a Bub1-GLEBSΔ (Figure 4.6.A) indicates that the interaction between Bub1 and Spc7-T9E (1-666) is mediated by Bub3. This experiment also indicates that Mad3 is dispensable for Bub1 association with Spc7-T9E (1-666) (Figure 4.6.A).

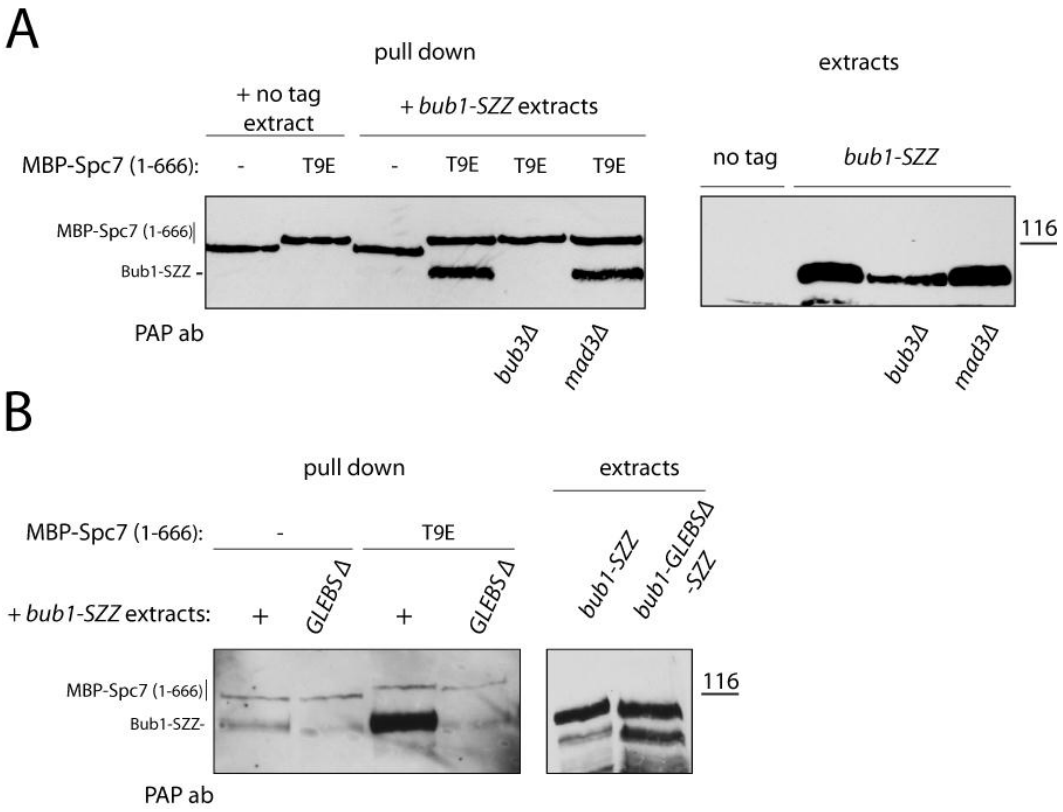

Figure 4.6. The Bub1-Spc7-T9E association depends on Bub3. *In vitro* Spc7 binding assays. A. Beads coated with recombinant, MBP tagged Spc7 (1-666) and Spc7-T9E (1-666) were incubated with *bub1-SZZ*, *bub1-SZZ bub3Δ* and *bub1-SZZ mad3Δ* cell extract. Pull downs and extracts were separated by 10% SDS-PAGE gel and probed with PAP antibody to detect Bub1-SZZ. **B.** Spc7 (1-666) and Spc7-T9E (1-666) beads were incubated with *bub1-SZZ* and *bub1-GLEBSΔ-SZZ* cell extracts. Pull downs and extracts were separated by 10% SDS-PAGE gel and probed with PAP antibody to detect Bub1-SZZ. Note that PAP antibody cross-reacts with the MBP-Spc7 (1-666) proteins.

4.4.5. Bub3 interacts *in vitro* with Spc7-T9E (1-666)

Since Bub3 is required for the interaction of Bub1 with the phosphomimetic mutant of Spc7, Spc7-T9E (1-666) *in vitro*, a Spc7 binding assay was employed to investigate whether Bub3 interacts with Spc7 T9E (1-666) and if it is so, what directs this interaction.

Amylose resins coated with MBP-Spc7 (1-666), MBP-Spc7-T9A (1-666), MBP-Spc7-T9E (1-666) and MBP-Pic1-IN-box were incubated with *bub3-GFP bub1Δ*, *bub3-GFP mad3Δ* and no tag cell extracts. The samples were run on a 10 % SDS-PAGE and immunoblotted with anti-GFP antibody to visualize Bub3-GFP.

These analyses demonstrate that the constitutive phosphorylation of the MELT motifs in Spc7 (as mimicked by the Spc-T9E mutant) is required for the interaction between Spc7 (residues 1-666) and Bub3 (Figure 4.7). Moreover, our experiment revealed that both Bub1 and Mad3 are dispensable for the association of Bub3 with Spc7-T9E (1-666).

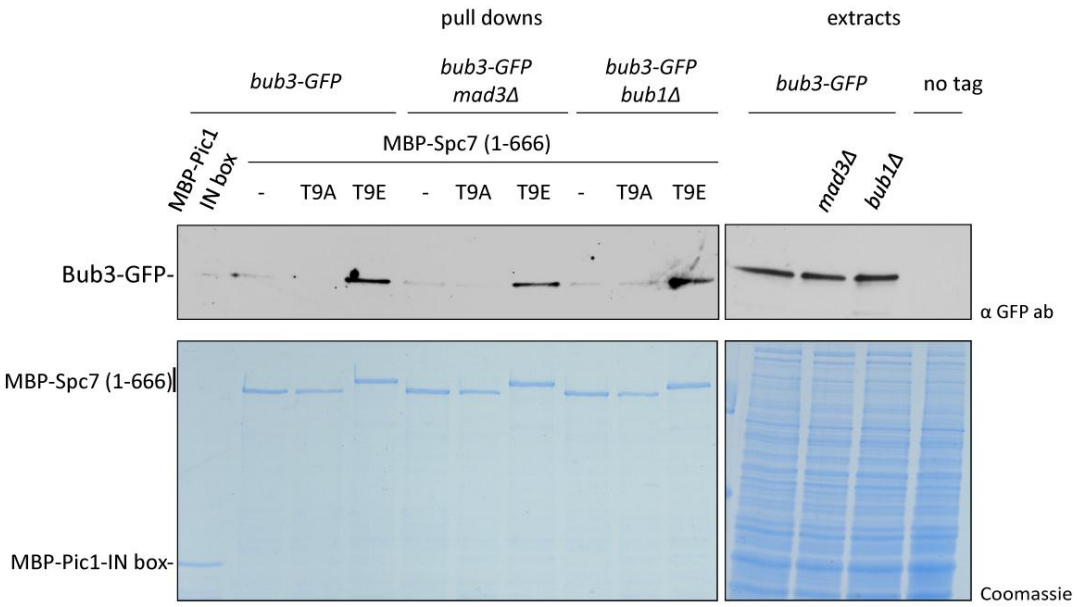

Figure 4.7. The Bub3 interaction with Spc7 depends on MELT phosphorylation but not on Bub1 and Mad3. Beads coated with recombinant, MBP tagged Spc7 (1-666), Spc7-T9A (1-666) and Spc7-T9E (1-666) were incubated with *bub3-GFP bub1Δ*, *bub3-GFP mad3Δ* and no tag cells extracts. Pull downs and extracts were separated by 10% SDS-PAGE gel and probed with GFP antibody to detect Bub3-GFP. Note that PAP antibody cross-reacts with the MBP-Spc7 (1-666) proteins.

4.6. Summary and discussion

The previous chapter demonstrated that the N-terminus of Spc7 is extensively phosphorylated by Mph1 and Ark1 kinases. In this chapter the role of Mph1-dependent Spc7 phosphorylation was investigated using *in vitro* and *in vivo* biochemical assays. Microscopy analysis of the interaction between Bub proteins and Spc7 has been carried out by the Millar Lab (Warwick University) and recently published together with experiments described in this chapter (Shepperd et al., 2012).

Our results have contributed to the checkpoint field by revealing the molecular mechanism for Bub1-Bub3 complex recruitment to unattached kinetochores. We demonstrated that the conserved checkpoint kinase Mph1 phosphorylates the MELT motifs of Spc7 and that this phosphorylation is sufficient to recruit Bub1-Bub3 complex to the Spc7 scaffold. In addition, our *in vitro* reconstitution assays suggest that Bub3 might mediate the interaction of Bub1 with Spc7. As all components of this pathway are evolutionarily conserved, we propose that this described mechanism might be employed by other organisms to maintain checkpoint signaling.

Spc7 is an Mph1 substrate

We demonstrated that the fission yeast kinetochore protein Spc7 is an *in vitro* and possibly *in vivo* substrate of Mph1 (see sections 3.3 and 3.6). Mass spectrometry analysis, performed in this study has identified T507 and T453, the latter one with a low confidence, as *in vitro* phosphorylation sites in Spc7 for the Mph1 kinase. Interestingly both threonines are located in conserved MELT motifs present in KNL1/Blinkin family proteins (see Figure 4.1). Threonines present in all nine MELT motifs in Spc7 were mutated to alanine resulting in the 'loss' of phosphorylation site Spc7 mutant [Spc7-T9A (1-666)] and to glutamic acid resulting in a phosphomimetic Spc7 mutant [Spc7-T9E (1-666)] to enable functional analysis of MELT motif phosphorylation. Phosphorylation of the MELT motifs constitutes about 60% of Mph1-dependent phosphorylation of Spc7 residues (1-666) *in vitro* (see Figure 4.2). The relevance of the MELT motifs phosphorylation was investigated in different biochemical experiments.

In addition to T453 and T507, T168 and T283 were identified as *in vitro* Mph1 kinase phosphorylation sites in Spc7. These two threonines are not located in the MELT motifs and therefore might account for the remaining 40% of the Mph1-dependent phosphorylation of Spc7 residues 1-666 *in vitro.* The importance of these phosphorylation events remains to be determined.

Mps1/Mph1 activity is required for recruitment of Bub1 and Bub3 proteins to kinetochores in human cells (Maciejowski et al., 2010; Sliedrecht et al., 2010). Very recent studies in fission and budding yeast confirmed that Mps1/Mph kinase activity is required for recruitment of Bub1 and Bub3 to kinetochores and therefore for efficient checkpoint signaling (Yamagishi et al., 2012; Shepperd et al., 2012; London et al., 2012).

Mph1-dependent phosphorylation of the Spc7 MELT motifs recruits Bub1 and Bub3 to kinetochores

This study has identified the MELT motifs of Spc7 as substrates for Mph1 at kinetochores. Therefore the hypothesis that Mph1-dependent phosphorylation of the MELT motifs recruits Bub1 and Bub3 to kinetochores was tested. Microscopic analysis performed in the Millar Lab revealed that Bub1 and Bub3 are enriched at kinetochores throughout the cell cycle in the *spc7-T9E* mutant whereas the kinetochore signal of Bub1and Bub3 was abolished in *spc7Δ spc7-T9A* cells (Figure 4.8.A and 4.9) (Shepperd et al., 2012). These results were confirmed by an *in vitro* Spc7 binding assay which showed that Bub1 and Bub3 associate with recombinant Spc7-T9E (1-666) protein but not by Spc7 (1-666) nor Spc7-T9A (1-666) (Figure 4.4 and 4.7). Moreover, both Bub1 and Bub3 localised to kinetochores in the *spc7Δ spc7-T9E* cells in the absence of Mph1 kinase activity (*mph1-kd* background) which demonstrates that the MELT motifs of Spc7 are the only Mph1 kinase targets required for the association of the Bub1-Bub3 complex with kinetochores (Figure 4.8.B and 4.9) (Shepperd et al., 2012).

Nevertheless, other kinases, including Ark1 (Aurora B) and Plk1 (Polo kinas), might phosphorylate Spc7 and/or other kinetochore components to facilitate recruitment of Bub1 and Bub3 to kinetochores. This possibility is supported by the finding that

Aurora B is required for efficient recruitment of Bub1 to kinetochores in mammalian cells (Hauf et al., 2003) and the observation that Plk1 and Mps1 share similar substrate consensus sites (Dou et al., 2011). All the Spc7 MELT motifs have aspartic or glutamic acid residue at position -2 which is also a feature of the Plk1 consensus sequence [D/E]X[S/T]φ (φ-a hydrophobic amino acid). Additionally, two out of nine MELT motifs (MELT 1 and MELT 9) in Spc7 constitute perfect Plk1 consensus sites. Mass spectrometry data provide evidence for Mph1-dependent phosphorylation of four MELT motifs (MELT 2, 6, 7, 9) (Shepperd et al., 2012; Yamaguchi et al., 2003) thus phosphorylation of the remaining MELT motifs by other kinase(s) cannot be excluded. Therefore it would be interesting to test whether Plk1 and/or other kinase(s) can contribute to the phosphorylation of MELT motifs in Spc7 in the future.

Are there any other kinetochore-associated substrates for Mph1 kinase that are required for spindle checkpoint signaling?

The constitutive association of Bub1 with kinetochores mediated by Spc7-T9E observed by microscopy (Figure 4.8) has been verified by Bub1-GFP ChIP from cycling and mitotically *nda3-KM311* arrested cells (Figure 4.5). The Bub1-GFP ChIP demonstrated a strong enrichment of Bub1 at centromeric central core, which corresponds to region of kinetochore assembly, in both cycling and metaphase arrested *spc7-T9E* cells. This result is consistent with the finding that tethering of an Mph1-Ndc80-GFP fusion protein to kinetochores results in Bub1 binding to kinetochores throughout the cell cycle (Ito et al., 2011). Additionally their study reported a constitutive Mad2-dependent arrest upon expression of Mph1-Ndc80-GFP from the native *mph1* locus. Mitotic arrest was not obtained upon weak overexpression of soluble Mph1-GFP suggesting an important role for a kinetochore-bound Mph1 in spindle checkpoint signalling in fission yeast (Ito et al., 2011). In contrast to the cells expressing Mph1-Ndc80-GFP, the *spc7-T9E* mutant did not block cell cycle progression as the mutant cell culture was not enriched in mitotic cells (see Figure 4.8. A). This difference suggests that the role of kinetochore-bound Mph1in spindle checkpoint signalling is not only limited to Spc7 phosphorylation and Bub1 loading to kinetochores. It has been recently demonstrated by Zich et al.

(2012) that Mph1 kinase activity against Mad2 is required for the MCC-APC complex formation. However, this checkpoint function of Mph1 might be exerted by soluble cytoplasmic pool of Mph1, as reported for mammalian cells (Maciejowski et al., 2010). Consequently, the findings discussed above raise the possibility that other kinetochore protein(s), apart from Spc7, may need to be phosphorylated by kinetochore-associated Mph1 in order to arrest the cell in mitosis.

According to current knowledge fission yeast Ndc80 would to be a good candidate for another kinetochore-associated substrate for Mph1 kinase. Both Ndc80 and Spc105 have been identified as Mps1 substrates in *S. cerevisiae* (Kemmler et al., 2009; London et al., 2012). Interestingly, mimicking phosphorylation of Mps1 sites in Ndc80 (*ndc80-14D*) causes a constitutive metaphase arrest in presence of stable bi-polar kinetochore microtubule attachments (Kemmler et al., 2009). Moreover Ndc80 has been proposed to serve as a binding site for the Mad1-Mad2 complex at human kinetochores (DeLuca et al., 2003; Martin-Lluesma et al., 2002). Taken together, the cited findings support the idea that targeting of checkpoint proteins to Spc7 and Ndc80 might be regulated by Mph1 kinase-dependent phosphorylation of these proteins. It would be interesting to test whether Mph1 can phosphorylate Ndc80 in fission yeast and if so, how this phosphorylation influences the checkpoint response.

A central role of Bub3 in the Bub1-Bub3 complex kinetochore targeting

Microscopic analysis of Bub1 localisation at kinetochores and *in vitro* Spc7 binding assays revealed that Bub1 targeting to Spc7-T9E depends on Bub3, but not on Mad3 (Figure 4.8.B and Figure 4.6). Like Bub1, Bub3 localised to the kinetochore throughout the cell cycle in *spc7-T9E* but not in *spc7*$^{+}$ and *spc7-T9A* cells (Figure 4.9) (Shepperd et al., 2012). This is consistent with *in vitro* Spc7 binding assays showing that Bub3 associates with the phosphomimetic Spc7-T9E (1-666) mutant but not with the 'loss' of phosphorylation Spc7 T9A (1-666) mutant or Spc7 (1-666) protein. According to microscopic analysis, Bub3 localisation to kinetochores depends on the presence of Bub1 (Figure 4.9). These data suggest that Bub1 and Bub3 are dependent on each other for Spc7 binding and Mph1-dependent phosphorylation of the MELT motifs in Spc7 recruits the Bub1-Bub3 complex to

kinetochores. The interaction between Bub1 and Bub3 might be important for the stability of the complex. These findings are consistent with previous reports which demonstrated that Bub1 and Bub3 are interdependent for their kinetochore localisation (Taylor et al., 1998; Vanoosthuyse et al., 2004; Sharp-Baker and Chen, 2001). Consistently, very recent data obtained by using *in vitro*-translated Spc7-12A, Spc7-12E, Bub1 and Bub3 in a pulldown assay confirmed the requirement for Bub1 and Bub3 being in complex in order to bind Spc7-12E (Yamagishi et al., 2012). However *in vitro* Spc7 binding assays carried out in this thesis demonstrate that Bub3 can bind Spc7-T9E (1-666) in the absence of Bub1 (Figure 4.7) which contradicts the dependency of Bub3 on Bub1 for its interaction with Spc7 "phosphorylated" at the MELT motifs described above.

The discrepancy between microscopy analysis and the *in vitro* binding assay could be explained by Bub1 being a binding partner of Bub3 which is required for Bub3 nuclear localisation and Bub3 stability but is dispensable for its association with kinetochores *per se*. This conclusion supports the model in which Bub1 facilitates nuclear localisation and retention of Bub3. Once Bub3 is targeted to nucleus it interacts with Spc7 phosphorylated by Mph1 and this interaction is necessary to dock Bub3-bound Bub1 to kinetochores via Spc7 (see Figure 4.10). However, the *in vitro* pulldown experiments carried out by Yamagishi et al. (2012) showed that Bub1 and Bub3, obtained by *in vitro* transcription/translation in rabbit reticulocyte lysate, are interdependent for Spc7-12E binding. The binding assays presented in the analysis presented here employ yeast cell extracts containing endogenous yeast proteins of interest tagged either with the SZZ tag (Bub1-SZZ) or GFP (Bub3-GFP). The proteins in the yeast cell extracts are presumably properly folded. They can undergo posttranslational modifications and interact with other yeast proteins present in the extract, which is not the case in *in vitro* transcription/translation system. Thus, the yeast extract might contain an unknown factor (the X protein in Figure 4.10) and promote posttranslational modifications of Bub3 and/or Spc7 which facilitates the Bub1-independent interaction of Bub3 with Spc7-T9E (1-666). Alternatively, the large amount of Spc7 immobilized on beads promotes Bub1-independent Bub3 binding because it is much easier to 'find' Spc7 on the beads than the small amount

of Spc7 at real kinetochores. We are planning to address these issues in future experiments (see below).

According to current models in budding and fission yeast cells the conserved MELT motifs are critical for Bub1 and Bub3 binding at kinetochores (London et al., 2012; Yamagishi et al., 2012; Shepperd et al., 2012). The MELT motifs are also present in human Blinkin, however yeast two hybrid analysis of Blinkin fragments containing 150 amino acids negated their role in Bub1 binding (Kiyomitsu et al., 2011). Instead, Kiyomitsu et al. identified minimal Bub1 and BubR1 binding sites in Blinkin located in the N-terminus of Blinkin that contain KI motifs (see Figure 4.1). However, the relevance of the KI motifs for Bub1and BubR1 kinetochore targeting was questioned by a study demonstrating a critical role of Bub3 in this process (Krenn et al., 2012). Moreover, a very recent study, which used full-length KNL1 with mutated MELT motifs (KNL1-8A/E), showed that the phosphorylation of the MELT motifs in HeLa cells faciltates Bub1 association with KNL1 (Yamagishi et al., 2012). Comparing these findings to the result of the yeast two hybrid assay described above suggests that MELT and KI motifs may collaborate in binding to Bub1 therefore the short Blinkin fragments used by Kiyomitsu et al. might have not contained enough MELT motifs to bind Bub1 and, most importantly, they were lacking phosphorylation or phosphomimetic mutations which could have completely abolished their putative Bub1 binding properties.

Results presented in this study confirm that Bub3 is necessary for Bub1 interaction with Spc7 containing phosphomimetic mutations in the MELT motifs (Figure 4.6 and 4.8.B). It would be informative to perform the Bub1-GFP ChIP experiment in *bub3Δ* mutant to precisely assess the Bub3 contribution to Bub1 kinetochore targeting in *spc7-T9E* cells.

Interestingly, Bub1-GFP signal is not completely abolished in *spc7-T9A* cells arrested in metaphase in Bub1-GFP ChIP (Figure 4.5). Moreover, a weak interaction between Bub1 and Spc7 residues 1-283 containing only one MELT motif stabilised by addition of cross-linker (DSP), was observed in a Co-IP experiment (Figure 4.3). These results suggest existence of other mechanism(s) which contribute to

Bub1-Spc7 association independently of the MELT motif phosphorylation. However, its putative role in the recruitment of Bub1 to kinetochores seems to be marginal.

The experiments presented in this thesis cannot completely determine whether the interaction between Bub1 or Bub3 and Spc7 is direct or indirect because the proteins of interest, tagged Bub1 and Bub3, are components of yeast cell extract where they can interact with other proteins. However, Bub3 seems to be a prime candidate for being a direct interactor of phosphorylated Spc7. Bub3 contains seven WD40 repeats which form β-propeller (Larsen and Harrison, 2004). Cdc4, as a part of SCF complex, is required for proteolysis of the Cdk inhibitor, Sic1, facilitating G1/S transition in *S. cerevisiae*. Cdc4 also contains WD40 repeats (8 of them) and interacts with Sic1 upon its phosphorylation by G1 and S phase Cyclin/Cdk1 complexes (Skowyra et al., 1997; Orlicky et al., 2003). Similarly the β-propeller of Bub3 might constitute an interface which binds Spc7 only upon its phosphorylation of the MELT motifs by Mph1.

Future experiments

Future experiments will further examine the mechanism which targets Bub1 and Bub3 proteins to Spc7. The *in vitro* Spc7 binding assay with modifications described below (see Supplementary Figure 1A, B and C), will be combined with the Stable Isotope Labelling by Amino acids in Cell culture (SILAC) approach (Ong et al., 2002) to 'hunt' for new Spc7 interactors which might be involved in Bub1-Bub3 targeting to Spc7 or in other processes that Spc7 may coordinate. The Spc7 (1-666) and Spc7-T9E (1-666) beads will be incubated with mitotic cell extract containing either heavy or light isotope of arginine and lysine which will enable to quantify the enrichment of a particular protein interacting specifically with one species of Spc7 (1-666), for example with Spc7-T9E (1-666).

In order to ensure high detection level of yeast proteins, the amount of recombinant Spc7 (1-666) in sample subjected to mass spectrometry analysis must be reduced to a minimum. The amylose resin used so far, takes advantage of the non-covalent interaction between MBP and amylose affinity matrix (NEB). Upon addition of gel loading buffer containing SDS, the binding between MBP and amylose is disrupted

resulting in the presence of MBP-Spc7 which is visible on SDS page gels stained with Coomassie or immunoblotted gels. In mass spectrometry analysis large amounts of recombinant Spc7 might mask peptides coming from yeast cell extracts. Therefore, recombinant Spc7 (1-666) and Spc7-T9E (1-666) will be covalently cross-linked to AminoLink resin (Thermo Scientific). Stable, permanent immobilization helps to avoid the presence of MBP-Spc7 in the final samples without decreasing the ability of Spc7 to bind its interactors from yeast extract (Supplementary Figure 1.B and C).

In order to look at the molecular mechanism of the Bub1-Bub3 complex association with Spc7 a 3D proteomics experiment is being considered. Proteins of interest including Spc7, Bub1, Bub3 and putative interactors, identified in the SILAC experiments, will be expressed in the Baculovirus Expression Vector System (BEVS) which allows production of high levels of proteins. The co-expressed proteins will be cross-linked and then subjected to mass spectrometry analysis to identify all cross-linked peptides. The results should provide information about protein domains /motifs involved in the interactions. This experiment will be carried out by Onur Sen, a PhD student in the Hardwick Lab. Both mass spectrometry experiments will be performed in collaboration with Prof. Juri Rappsilber and his laboratory (Edinburgh University).

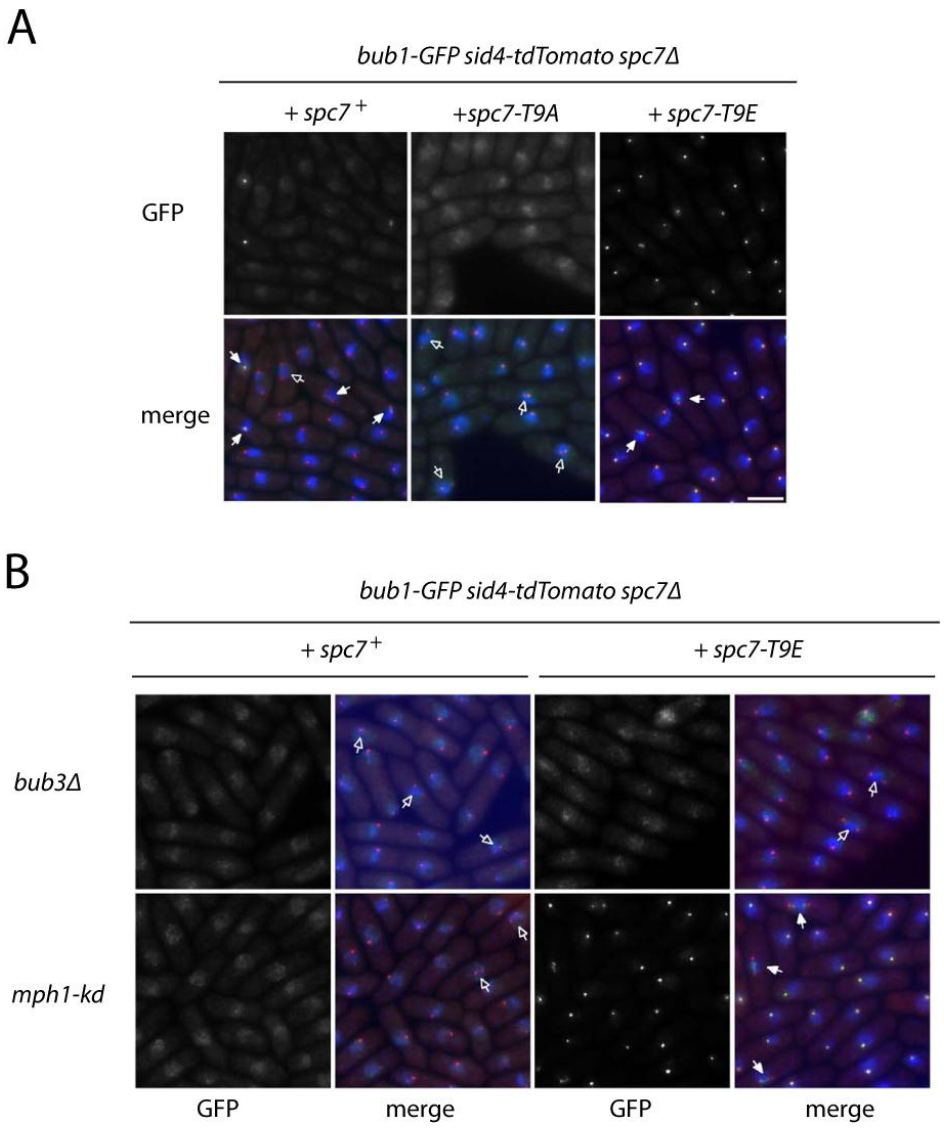

Figure 4.8. Bub1 kinetochore recruitment is promoted by Mph1-dependent phosphorylation of Spc7 [microscopy analysis carried out in the Millar Lab, images adapted from (Shepperd et al., 2012)]. A. cycling population of *spc7Δ spc7*$^{+}$, *spc7Δ spc7-T9A* and *spc7Δ spc7-T9E* cells expressing Bub1-GFP Sid4-tdTomato (Sid4 is a spindle pole body, SPB, marker). Cells with separated SPBs represent mitotic cells. Closed arrowheads indicate mitotic cells with Bub1 foci, open arrowheads-mitotic cells lacking Bub1 foci. Bar, 5µm. Bub1 is constitutively associated with kinetochores in *spc7Δ spc7 T9E* cells. **B.** cycling population of *spc7Δ spc7*$^{+}$ and *spc7Δ spc7-T9E* cells expressing Bub1-GFP Sid4-tdTomato in *mph1-kd* background. The *spc7Δ spc7-T9E* cells bypass requirement for Mph1 kinase activity to load Bub1 to kinetochores. Bar, 5µm.

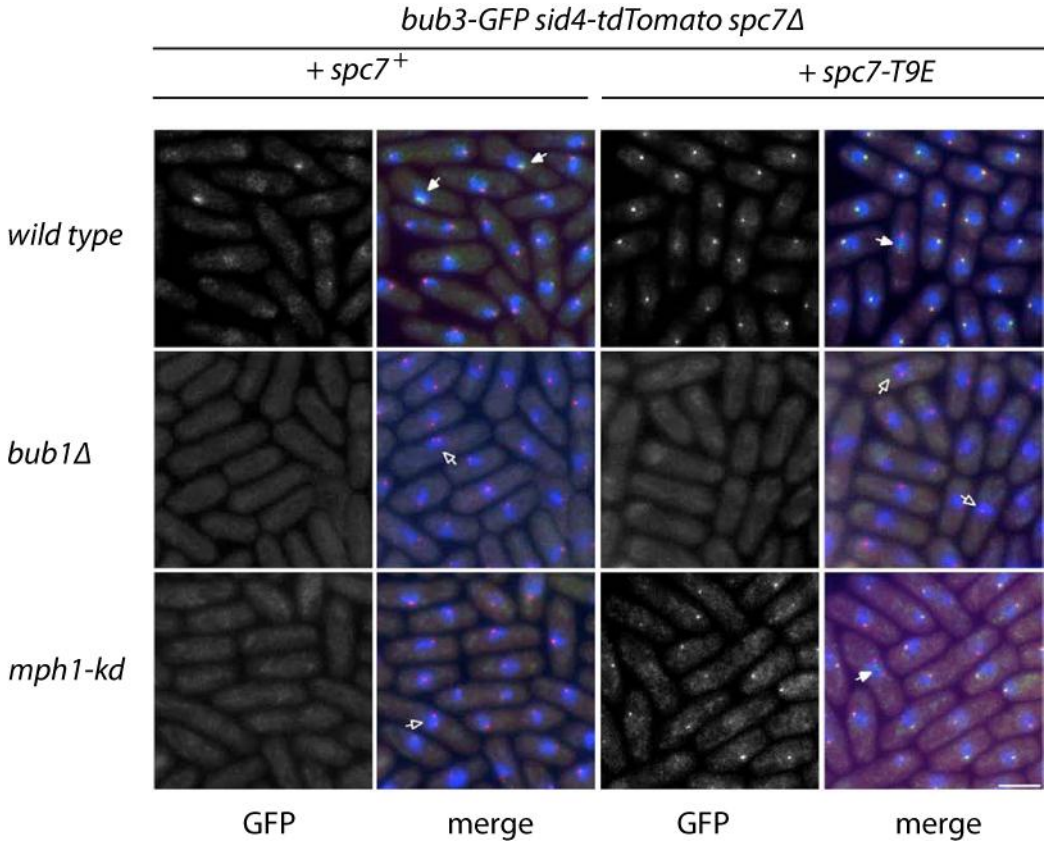

Figure 4.9. Bub3 kinetochore recruitment is promoted by Mph1-dependent phosphorylation of Spc7 [microscopy analysis carried out in the Millar Lab, images adapted from (Shepperd et al., 2012)]. Cycling population of *spc7Δ spc7*$^{+}$ and *spc7Δ spc7-T9E* cells expressing Bub3-GFP Sid4-tdTomato (Sid4 is a spindle pole body, SPB, marker). Cells with separated SPBs represent mitotic cells. Closed arrowheads indicate mitotic cells with Bub3 foci, open arrowheads-mitotic cells lacking Bub3 foci. Bar, 5µm. Bub3 is constitutively associated with kinetochores in *spc7Δ spc7-T9E* cells, which bypass the requirement for Mph1 kinase activity to load Bub3 to kinetochores.

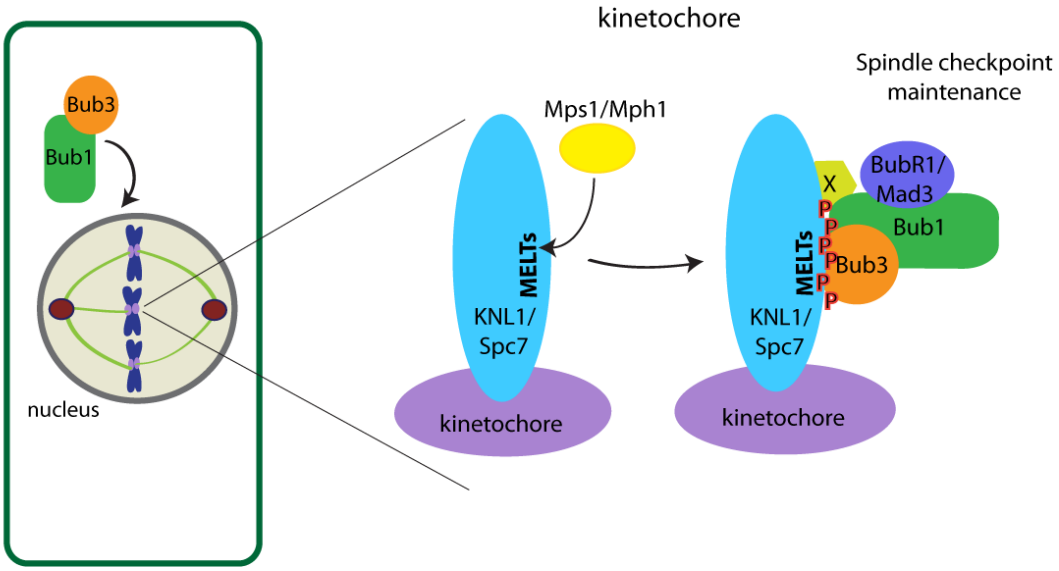

Figure 4.10. Model of Mph-1 dependent recruitment of the Bub1-Bub3 complex to kinetochore. In early in mitosis the Bub1-Bub3 complex is enriched in nucleus and binds to kinetochore via interaction with KNL1/Spc7. According to results presented here Bub1-Bub3 binding to Spc7 requires Mps1/Mph-dependent phosphorylation of the conserved MELT motifs in KNL1 family protein. Bub3 binding to Spc7 does not required Bub1, but interaction between Bub1-Bub3 might be necessary for Bub3 nuclear transport. However, Bub1 targeting to Spc7 is dependent of Bub3 and most likely Bub3 makes the Spc7 contact. The X protein is an unknown protein that may facilitate the interaction between Bub3 and Spc7 in the absence of Bub1 at kinetochores in *S. pombe*. Hypothetically, the X protein may be a protein kinase that phosphorylates Spc7 and/or Bub3 and thus can complement the lack of Bub1 kinase activity.

Chapter 5

Spc7 as a microtubule binding protein and Dis2 phosphatase docking site at kinetochores

Chapter 5

Spc7 as a microtubule binder and Dis2 kinetochore docking site

5.1. Introduction

The checkpoint-related function of the KNL1/Spc7 family proteins is not limited to being a binding platform for Bub1-Bub3 complex. The KNL1/Spc7 proteins exhibit microtubule binding activity and an ability to bind PP1 phosphatase, which is required for spindle checkpoint silencing (see Chapter 1). These properties of Spc7 make it a good candidate for coordinating checkpoint activation with checkpoint silencing and kinetochore-microtubule attachment status.

KNL-1 together with Mis12 and Ndc80 complexes constitute the KMN (KNL-1-Mis12-Ndc80) network which serves as a core microtubule binding site in the vertebrate kinetochore [for review see (Cheeseman and Desai, 2008), (Cheeseman et al., 2004, 2006)] (Figure 5.1). Within the KMN network three proteins have microtubule binding activity: Ndc80, Nuf2 (components of the Ndc80 complex) and KNL-1 (Cheeseman et al., 2006; Wei et al., 2007; Powers et al., 2009; Pagliuca et al., 2009). Both the Ndc80-Nuf2 dimer and KNL-1 have a weak microtubule binding affinity, however once associated with other components of the KMN network (Ndc24, Ndc25, Mis12 complex) the microtubule-binding affinity is synergistically increased (Cheeseman et al., 2006). The KMN network is conserved throughout eukaryotes including fission and budding yeasts have it (Kerres et al., 2004; Liu et al., 2005; Joglekar et al., 2006, 2008; Maskell et al., 2010; Meraldi et al., 2006).

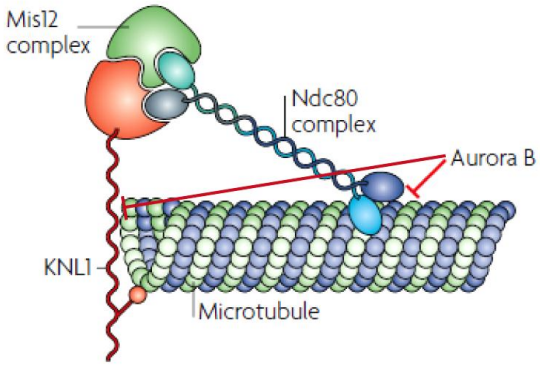

Figure 5.1. Model of the KMN network adapted form (Cheeseman and Desai, 2008). Association between KNL1 and Mis12 complex provides a docking site for the Ndc80 complex. The Ndc80 complex and KNL1 interact directly with microtubule plus ends (Cheeseman et al., 2006). Aurora B inhibits the Ndc80 complex and KNL1 microtubule binding activities (Cheeseman et al., 2006; Ciferri et al., 2008).

In fission yeast Spc7 is a part of Ndc80-Mis12-Spc7 complex which is a functional homologue of the vertebrate KMN network (Liu et al., 2005; Kerres et al., 2007; Meraldi et al., 2006). In yeast, like in higher organisms, the KNL1 homologue is essential (Kerres et al., 2004). Conditional mutants of Spc7 show severe defects in chromosome segregation along with aberrant structure of the spindle (Kerres et al., 2007). Experiments employing overexpression of N-terminal (residues1-820) and C-terminal (residues 821-1364) fragments of Spc7 revealed that the C-terminus is required for Spc7 kinetochore localisation whereas the N-terminal fragment binds to the mitotic spindle (Kerres et al., 2007). Moreover, overexpression of the C-terminal fragment resulted in severe chromosome segregation defects, increase of mitotic index and the presence of kinetochores which were not associated with the mitotic spindle suggesting that Spc7 plays an important role in regulating kinetochore-microtubule attachments (Kerres et al., 2004). Yeast two hybrid assay and immunoprecipitation experiments performed by Kiyomitsu et al., (2011) demonstrated that the C-terminus of human Blinkin/KNL1, containing a coiled-coil motif, can directly interact with Mis14, a component of the Mis12 complex. This is

consistent with previously described kinetochore localisation of the C-terminal part of fission yeast Spc7 (Kerres et al., 2007, 2004). However, *S. pombe* Spc7 is more likely to interact with Mis12 as the Spc7-GFP kinetochore localisation is diminished in the *mis12* mutant (Kerres et al., 2007).

It has been well established that KNL1 proteins provide a linkage between microtubule plus ends and other kinetochore proteins (Cheeseman et al., 2006; Pagliuca et al., 2009). The microtubule binding activity of *C. elegans* KNL-1 is exerted by its extreme N-terminus (Welburn et al., 2010; Espeut et al., 2012). Interestingly, Aurora B phosphorylation sites were mapped in this region in human, chicken and *C. elegans* KNL-1 (Welburn et al., 2010). The identified phosphosites were located adjacent to the first PP1 binding motif (human, chicken) or inside the motif (*C. elegans*) and in the second PP1 binding motif (all species) (see Figure 5.2).

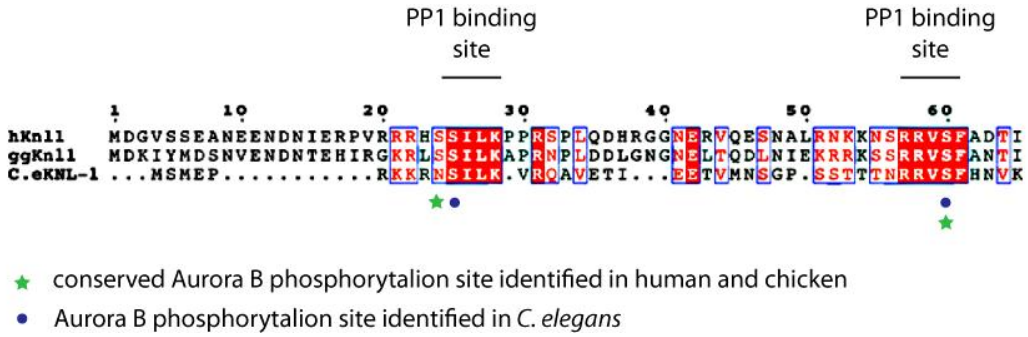

Figure 5.2. Aurora B phosphorylation sites mapped in the N-terminus of human (hKnl1), chicken (ggKnl1) and *C. elegans* (C.e KNL-1) KNL1 family proteins. Picture adapted from (Welburn et al., 2010).

A phosphomimetic mutant of Aurora B phosphorylation sites in *C. elegans* KNL-1 completely lost its microtubule binding activity (Welburn et al., 2010). Similarly, Aurora B-dependent phosphorylation of the N-terminus of Ndc80 disrupts the interaction between Ndc80 and microtubules (Cheeseman et al., 2006; Ciferri et al., 2008). These results show that Aurora B activity regulates the core of the kinetochore-spindle microtubule interface.

Recently Liu et al. (2010) showed that an N-terminal fragment of human KNL1 (residues 1-86), containing two PP1 binding motifs (described in chapter 3), interacts with PP1γ phosphatase *in vitro*. This interaction was significantly abolished when phosphorylation at Aurora B sites (S24 and S60), previously described by Welburn et al. (2010), was mimicked (Liu et al., 2010). Taken together, these studies. show that Aurora B negatively regulates KNL1 association with microtubules and KNL1 interaction with PP1 phosphatase by phosphorylating the same residues in KNL1.

It has been suggested that microtubule association with kinetochores is facilitated by stretches of basic residues (lysine and arginine) present in the N-terminus of Ndc80 (Ciferri et al., 2008). These basic patches are thought to electrostatically interact with negatively charged C-terminal tails of tubulin (Ciferri et al., 2008). Interestingly, the extremely N-terminal region of KNL1 family proteins (except for the *S. cerevisiae* Spc105) is enriched in basic residues (see Figure 5.3).

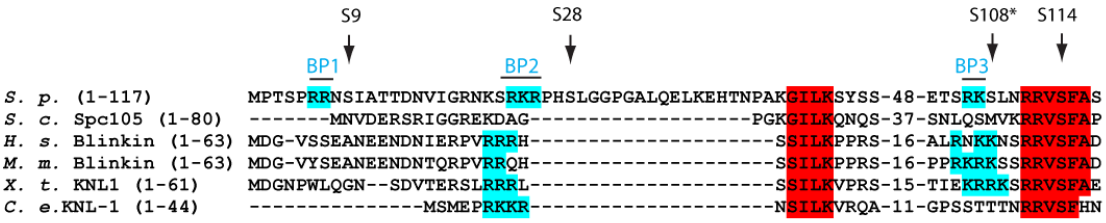

Figure 5.3. Sequence alignment of *S. pombe* (*S.p.*), *S. cerevisiae* (*S. c.*), *H. sapiens* (*H. s.*), *M. musculus* (*M. m.*), *X. tropicalis* (*X. t.*), *C. elegans* (*C. e.*), KNL1 homologues. The N-terminal [S/G]ILK and RRVSF PP1 binding motifs are highlighted in red. The basic patches are highlighted in blue and annotated: BP 1, BP 2, BP 3 for *S. pombe* Spc7. Arrows indicate *in vitro* Ark1 phosphorylation sites mapped in this study. * - residue detected by specific anti-phospho antibody only

The analysis of phosphorylation sites in Spc7 (see chapter 3) indicated that serines 9, 28, 108, 114 and 638 are substrates for Ark1 kinase. This indicates that in fission yeast phosphoregulation of Spc7 by Ark1 might be more extensive than in human or *C. elegans*, where only two residues were shown to be phosphorylated Aurora B (Figure 5.2).

The identified residues are located in the vicinity of the basic patches (S9, S28 and S108), in vicinity of the second PP1 binding motif (S108) and inside this motif (S114). The localisation of these Ark1 phosphorylation sites suggests that they might be involved in regulating microtubule binding activity of Spc7 and the recruitment of the protein phosphatase Dis2 to kinetochores.

This chapter addresses the question of how the interaction between Spc7 and microtubules is regulated. The related mechanism has been described in higher eukaryotes (Ciferri et al., 2008) and our study attempts to test model which proposes that it is the electrostatic interfaces between Spc7 and microtubules that are important for microtubule binding to kinetochores. In addition the model suggests central role for Aurora B kinase in regulating kinetochore-microtubule attachments. We tested different Spc7 mutants that might have impaired microtubule binding activity, using microtubule co-precipitation assays. We also analysed whether, similar to other species, fission yeast PP1 phosphatase (Dis2) interacts with Spc7/KNL1. This was tested using *in vitro* Spc7 binding assays.

5.2. The N-terminus of Spc7 interacts with microtubules

In order to investigate Spc7 microtubule binding activity and its regulation, microtubule co-sedimentation assays were used according to the Ohkura Lab protocol (see Material and Methods). Recombinant GST-Spc7 (residues1-283) wild type and mutant variants were incubated with taxol-stabilized microtubules for 30 minutes at room temperature and then subjected to centrifugation at high speed. Next, fractions containing supernatant and precipitated tubulin were separated by 10% SDS-PAGE gel and then the gel was stained with Instant*Blue* (Expedeon). The tested protein binds to microtubules if it is detected in the tubulin pellet.

The observation that recombinant GST-Spc7 (1-283) interacts with *in vitro* assembled microtubules (Figure 5.4. and data not shown) confirmed that in fission yeast, as in vertebrates, Spc7 provides a microtubule binding site at kinetochores.

5.2.1. Ark1-dependent phosphorylation at serines 9 and 28 negatively regulates the Spc7 microtubule binding activity

Knowing that Spc7 WT (residues 1-283) can bind microtubules in co-sedimentation assays we decided to test the Spc7 phosphorylation mutants for their microtubule binding activities. The mass spectrometry analysis revealed Ark1-dependent phosphorylation of serines 9 and 28 in the N-terminus of Spc7 with high scores (see Chapter 3). Interestingly, these residues are located near the basic patches (BP 1 and BP 2), which are candidates for being microtubule interacting regions (Figure 5.3).

These observations, along with the findings demonstrating that Aurora B-dependent phosphorylation of kinetochore proteins disrupts kinetochore-microtubule attachments in human cells (Welburn et al., 2010), suggest that serine 9 and 28 might be involved in regulating the Spc7 microtubule binding activity.

The Spc7 (1-283) phosphomimetic single mutants (S9D and S28D) and double mutant (S9D S28D) were used in microtubule co-sedimentation assays. Additionally,

GST-Spc7 (1-283) and GST-Spc7-S9A S28A S108A S114A (1-283) were employed as positive controls (see Figure 5.4).

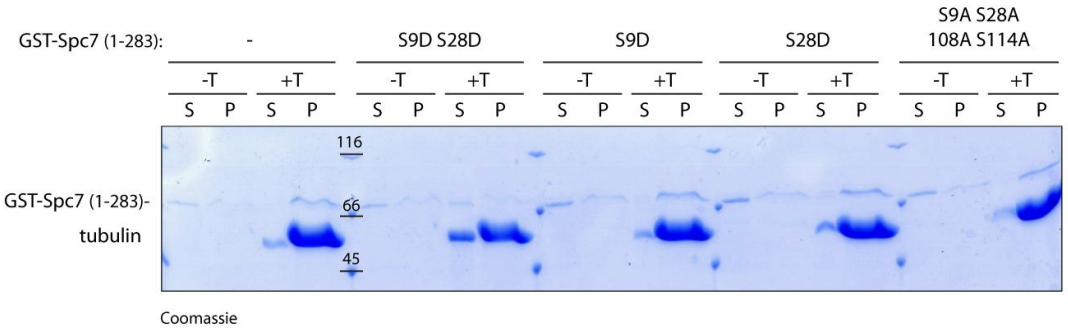

Figure 5.4. Ark1-dependent phosphorylation of the extreme N-terminus of Spc7 may reduce its ability to bind microtubules. Microtubule binding assays were performed in the presence of taxol-stabilized microtubules (+T) or the presence of free tubulin not subjected to taxol treatment (-T). The recombinant Spc7 proteins were incubated with the microtubules (+T) and with free tubulin (-T) for 30 minutes at room temperature. After centrifugation, the supernatant (S) and pellet (P) samples were run on a 10% SDS-PAGE gel and stained with Instant*Blue* (Expedeon).

The microtubule co-sedimentation assay showed that microtubules co-precipitated, as expected, with the Spc7 (1-283) and the Spc7-S9A S28A S108A S114A (1-283) quadruple mutants. On the contrary the phosphomimetic double mutant, Spc7-S9D S28D (1-283), exhibited 35% reduction in its microtubule binding activity. Interestingly, both single mutants, Spc7-S9D (1-283) and Spc7-S28D (1-283), bound microtubules at wild type level.

These results suggest that Ark-dependent phosphorylation of both serines, 9 and 28, in the vicinity of the basic patches may diminish the interaction between Spc7 and microtubules. However, to confirm that Ark1-dependent phosphorylation regulates microtubule binding activity of Spc7 *in vitro* we will have to titrate tubulin concentration to perform reliable quantitative analysis.

5.2.2. Positive charges in the N-terminus of Spc7 contribute to the interaction between Spc7 and microtubules

To examine the role of basic patches present in the N-terminus of Spc7 in microtubule binding, basic patch mutants were generated. In the mutants, arginine 6, lysine 24 and arginine 25 were mutated to alanines resulting in the Spc7-BP 1(R6A) (1-283), Spc7-BP 2 (K24A R25A) (1-283), and Spc7-BP 1&2 (R6A K24A R25A) (1-283) mutants, N-terminally tagged with GST.

The Spc7-BP 1, Spc7-BP 2, Spc7-BP 1&2 recombinant proteins were used in the microtubule co-sedimentation assay, which was carried out as described above.

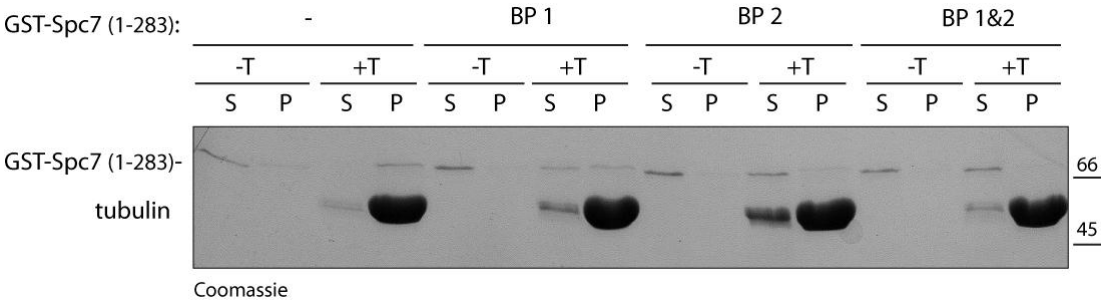

Figure 5.5. The N-terminal basic patches in Spc7 contribute to microtubule binding activity of Spc7. Supernatant (S) and pellet (T) samples were separated by 10% SDS-PAGE gel and stained with Instant*Blue* (Expedeon).

The experiment revealed that the stretches of positively charged residues might promote Spc7-microtubule association (Figure 5.5). Mutating the first basic patch (BP 1) in Spc7 leads to reduction of its microtubule binding activity by about 70%. Similar effect is observed when the second basic patch (BP 2) was mutated. The double basic patch mutant of Spc7 (BP 1&2) exhibits about 50% decrease in microtubule binding activity. This result implies that the basic patches contribute to

microtubule binding activity of Spc7, but quantitative assays with tubulin titration need to be carried out to confirm this hypothesis.

5.3. Mutants defective in microtubule binding are sensitive to microtubule depolymerising drugs

To examine whether the mutations reducing the Spc7 association with microtubules affect sensitivity to benomyl (see chapter 3.4.7), serial 4-fold dilutions of wild type, *mad3Δ, bub1Δ, spc7::natMX6 lys1::spc7 WT, spc7::natMX6 lys1::spc7 S9A S28A, spc7::natMX6 lys1::spc7 S9D S28D, spc7::natMX6 lys1::spc7 BP 1&2* were spotted on YES plates containing 0.0, 5.0 and 6.0 µg/ml benomyl. Plates were incubated at 30^0C for 3-4 days.

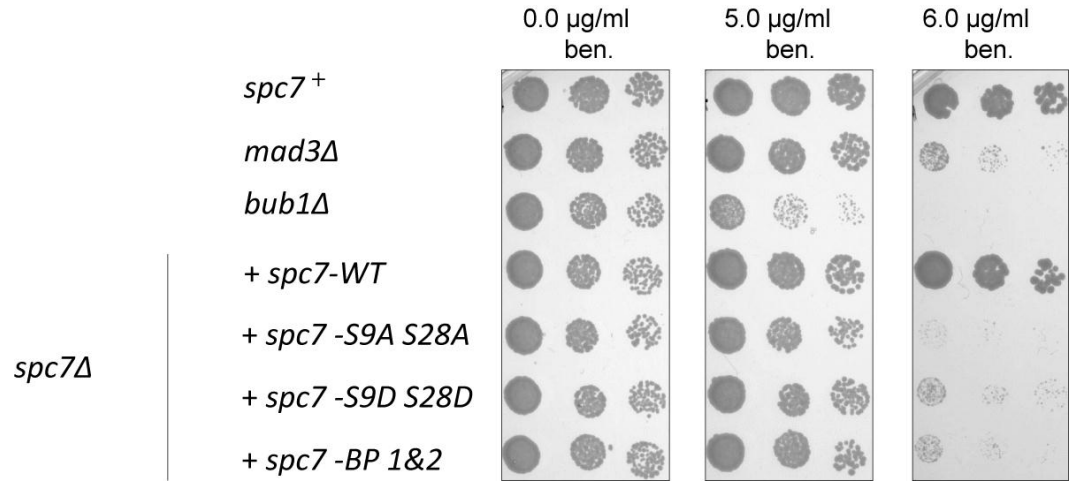

Figure 5.6. Mutations affecting Spc7 microtubule activity (S9D S28D and BP 1&2) result in an impaired growth on benomyl. The Spc7 phosphomutants (S9A S28A and S9D S28D) and the basic patch double mutant (BP 1&2) and controls-wild type strain (WT), *mad3Δ* and *bub1Δ* were spotted on plates containing different concentration of benomyl ranged from 0.0-6.0 µg/ml.

Figure 5.6. shows that the Spc7 mutants affecting its interaction with microtubules in microtubule co-sedimentation assays, *spc7Δ spc7-S9D S28D and spc7Δ spc7-BP 1&2,* have increased sensitivity to benomyl which is comparable to that of

mad3Δ. Interestingly, growth of the phosphomimetic mutant, *spc7Δ spc7-S9D S28D*, was less affected by benomyl than the growth of the corresponding alanine mutant, *spc7Δ spc7-S9A S28A*. That is surprising, as the alanine quadruple mutant, (Spc7-S9A S28A S108A S114A), did not affect microtubule binding *in vitro* (Figure 5.4).

Benomyl inhibits microtubule polymerisation and thereby slows down the mitotic spindle assembly. Elevated sensitivity to benomyl of the *spc7Δ spc7-S9D S28D* and *spc7Δ spc7 BP 1&2* cells might reflect their problems with establishing stable bi-oriented kinetochore-microtubule attachments. This situation promotes a high rate of chromosome missegregation which eventually leads to cell death. Alternatively, checkpoint activation or checkpoint silencing might be defective in these mutants. Additionally, the possibility that mutating the Ark1 phosphorylation sites or the basic patches interferes with more the one function of Spc7 cannot be ruled out.

5.4. Checkpoint activation and maintenance in the Spc7 phosphomutants

To assess possible checkpoint defects in the Spc7 phosphomutants of serine 9 and 28, *spc7Δ spc7-WT, spc7Δ spc7-S9A, spc7Δ-spc7 S28A, spc7Δ spc7-S9A S28A* and *spc7Δ spc7-S9D S28D* cells in *nda3-KM311* background were used. The *nda3-KM311* is a tubulin mutation which triggers microtubule depolymerisation at 18°C (Hiraoka et al., 1984). Microtubule depolymerisation activates the checkpoint which leads to metaphase arrest. In metaphase arrested cells high levels of cyclin B accumulate on spindle pole bodies (SPBs). This was scored using strains expressing Cdc13-GFP.

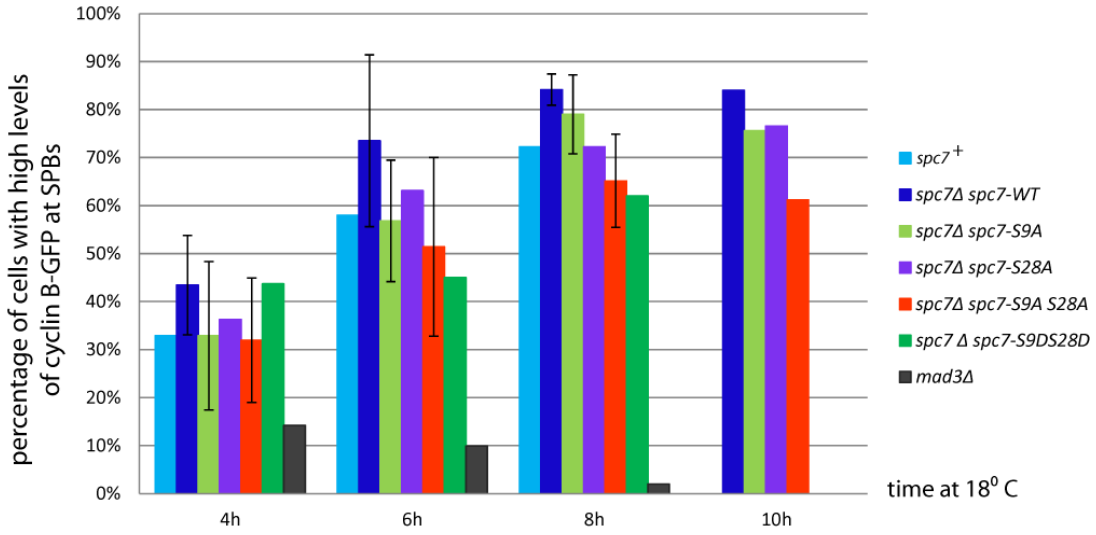

Figure 5.7. The Spc7 phosphomutants of serine 9 and serine 28 exhibit minor checkpoint activation/maintenance defects. Log-phase *nda3-KM311* cultures of indicated Spc7 phosphomutants, wild type (WT) positive control and *mad3Δ* negative control were shifted to 18ºC for 8-10 hours. Samples were taken at the 2-hour intervals starting from 4th hour of the incubation. Cells were fixed in methanol prior to microscopy analysis. Error bars represent standard deviation (SD) where n≥3; 200 cells were scored in each experiment. Note that not for the *spc7-S9D S28D* and *mad3Δ* experiment was performed only once (n=1) with the last time point at 8 hours and therefore it lacks error bars.

The *nda3-KM311* assay showed that the Spc7 phosphomutants of serine 9 and serine 28 are reasonably competent to activate and maintain metaphase arrest in response to microtubule depolymerisation. Similar observations were made for the *spc7Δ spc7-S108A S114A nda3-KM311* (data not shown), *spc7Δ spc7 S9A S108A S114A nda3-KM311* (data not shown) and *spc7Δ spc7-S9D S108D S114D nda3-KM311* (Prof J. Millar-personal communication) cells.

Among the tested mutants *spc7Δ spc7-S9A S28A nda3-KM311* and *spc7Δ spc7-S9D S28D nda3-KM311* were slightly checkpoint defective as about 60% of the cells accumulated high levels of cyclin B-GFP at SPBs after 8 hours of the arrest in comparison to about 80% in the *spc7Δ spc7-WT nda3-KM311* cells. However, this result cannot fully explain the elevated benomyl sensitivity of these mutants. The *mad3Δ* mutant does not arrest in *nda3-KM311* as the mitotic checkpoint is completely abolished in these cells yet they exhibit a similar sensitivity to benomyl as the *spc7Δ spc7-S9A S28A* and *spc7Δ spc7-S9D S28D* cells (see Figure 3.8. and 5.6). This indicates that the minor defects in spindle checkpoint

activation/maintenance in these mutants must be accompanied by defects in other mitotic process, for example in establishment of proper kinetochore-microtubule attachments consistent with the results of the microtubule co-sedimentation assays (Figure 5.4 and 5.5).

5.5. The second basic patch facilitates Spc7 nuclear transport

The microtubule binding activity of the Spc7 mutants cannot be relevant in the *nda3-KM311* experiment described above, because microtubules are absent in the *nda3-KM311* mutant at non-permissive temperature (Vanoosthuyse and Hardwick, 2009). A strong overexpression of the C-terminal half of Spc7 resulted in aberrant spindle formation and improper kinetochore-microtubule attachments which elevated the number of mitotic cells, indicating spindle checkpoint activation (Kerres et al., 2004, 2007). Similar experiments were carried out with the N-terminal fragments of Spc7 (residues 1-283). Upon moderate overexpression of HFG-Spc7-(1-283), HFG-Spc7-BP 1 (1-283), HFG-Spc7-BP 2 (1-283), HFG-Spc7-BP 1&2 (1-283) and HFG-Spc7-S9D S28D (1-283) no increase in mitotic index was observed. About 2-5% of the wild type and mutant cells were in mitosis (data not shown).

Interestingly, overexpression of the Spc7 (1-283) and Spc7-BP 1 (1-283) fragments resulted in accumulation of these fragments in nucleus, the GFP-signal of Spc7-BP 2 and Spc1-BP 1&2 was spread throughout the cells with a slight nuclear enrichment (Figure 5.8. A). Importantly, the HFG-Spc7 (1-283) fragments were expressed at the same levels (Figure 5.8. B). These results suggest that the second basic patch constitutes a nuclear localisation signal (NLS).

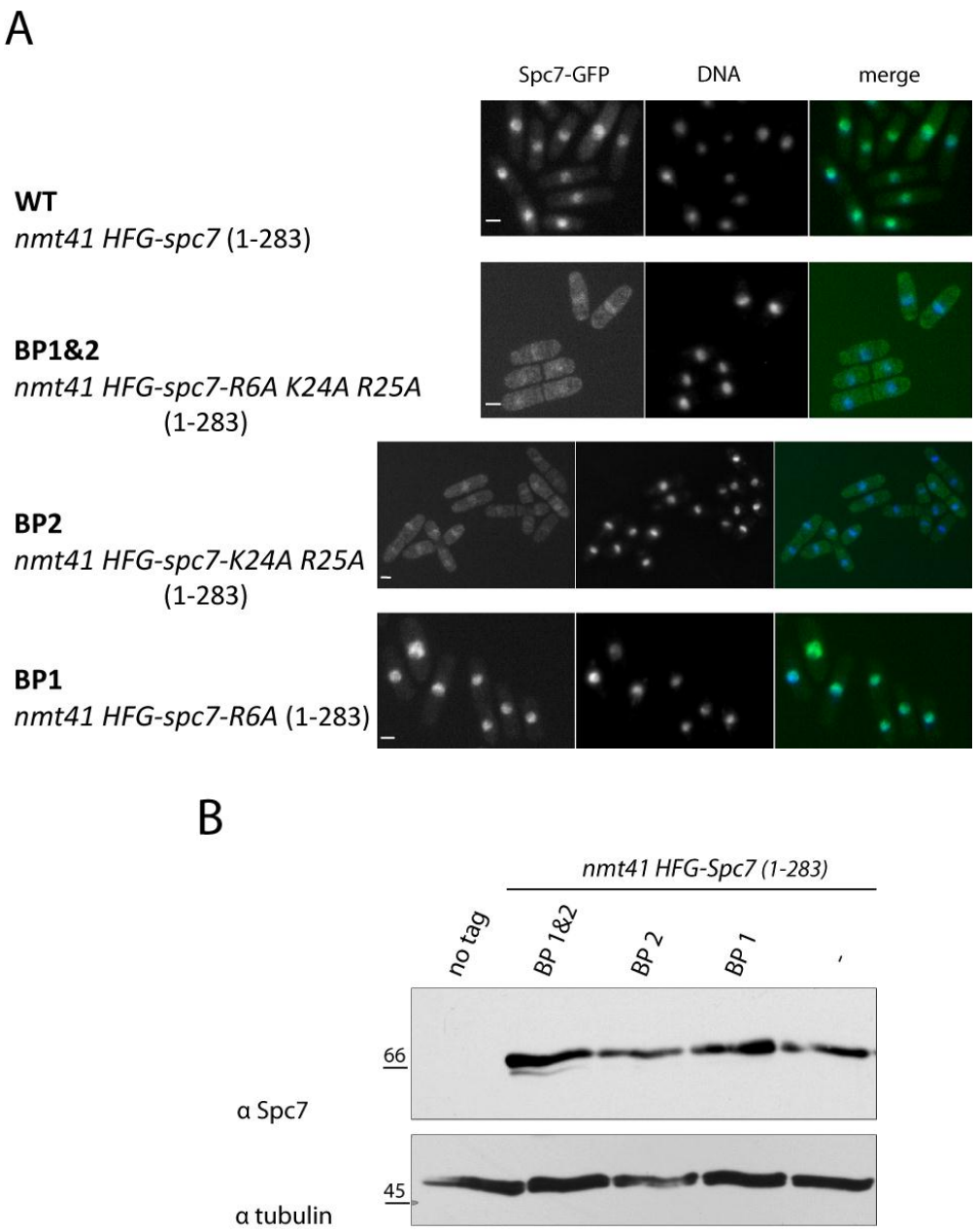

Figure 5.8. A. The second basic patch constitutes NLS in Spc7. Log-phase cells overexpressing HFG-Spc7 (1-283), HFG-Spc7-BP 1(1-283), HFG-Spc7-BP 2 (1-283), and HFG-Spc7-BP 1&2 (1-283) under the nmt41 promoter for 18 hours at 30°C were fixed and stained with DAPI, scale bar 4 μm.

B. Expression levels of HFG-Spc7-BP 1&2, HFG Spc7-BP 2, HFG-Spc7-BP 1, HFG-Spc7-WT. Extracts from wild type (no tag), *nmt-HFG-spc7 BP 1&2 (1-283), nmt41-HFG-spc7 BP 2 (1-283), nmt41-HFG-spc7 BP1 (1-283)* and *nmt41 HFG-spc7 WT (1-283)* cells were separated by 10% SDS-PAGE gel. Different parts of the blot were probed with α Spc7 and α tubulin (loading control) antibodies.

5.6. The N-terminus of Spc7 binds Dis2 phosphatase *in vitro*

In order to check whether the fission yeast Spc7 binds Dis2, the *S. pombe* homologue of vertebrate PP1 phosphatase, an *in vitro* Spc7 binding assay was performed. Bacterially expressed GST-Spc7 (1-283) was immobilized on Glutathione-Agarose (Sigma). Then the beads were incubated with cell extracts from cycling and *nda3-KM311*-arrested cells expressing PK-Dis2. Following incubation (30 min at 4°C, the bead and extract samples were analysed by western blotting (Figure 5.9).

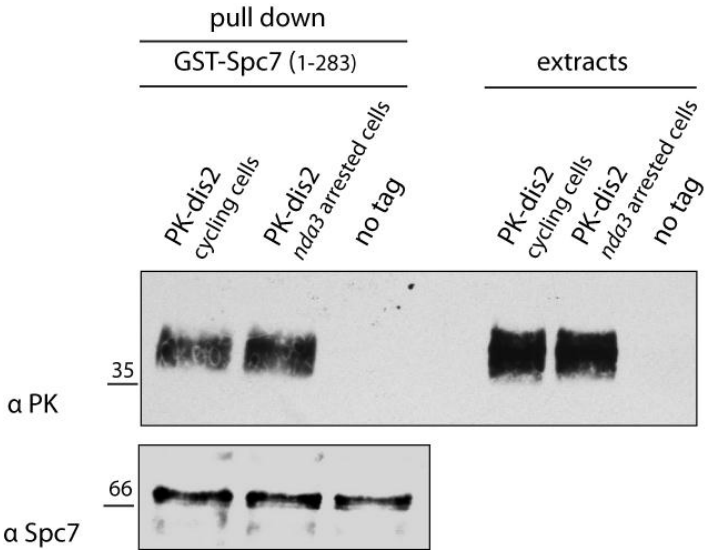

Figure 5.9. Dis2 interacts with the N-terminus of Spc7. Pull down and extract samples were run on a 10% SDS-PAGE gel. Different parts of the blot were probed with α PK and α Spc7 (loading control) antibodies.

The Spc7 binding experiment revealed that, as in vertebrate cells (Liu et al., 2010), the fission yeast PP1 phosphatase, Dis2, interacts with Spc7, a member of KNL1 family proteins. PK-Dis2 from *nda3-KM311* arrested cells and cycling cells bound Spc7 with similar efficiency.

5.6.1. Mutants that affect phosphorylation sites of Spc7 do not affect its ability to bind Dis2

In vertebrate cells PP1 binding is negatively regulated by phosphorylation of serines located in or adjacent to highly conserved PP1 binding motifs in KNL1 (Liu et al., 2010). In fission yeast Spc7 the second PP1 binding motif (RRVSFA, residues 111-116) is critical for efficient Dis2 binding (Meadows et al., 2011). Serine 108 is located in the vicinity of this motif whereas serine 114 resides inside the RRVSFA motif. Both residues were shown to be phosphorylated *in vitro* by Ark1 kinase (see sections 3.4.3 and 3.4.4). Moreover, the mass spectrometry experiment revealed that serines 9 and 28 are also modified by Ark1. We therefore utilised an *in vitro* Spc7 binding assay to test whether mimicking phosphorylation at these sites affects Dis2 binding.

In the experiment Glutathione Agarose beads (Sigma) were coated with recombinant GST-Spc7 phosphomutants and incubated with yeast cell extract for 30 min at 4°C. Following incubation, the bead samples were analysed by western blotting (Figure 5.10).

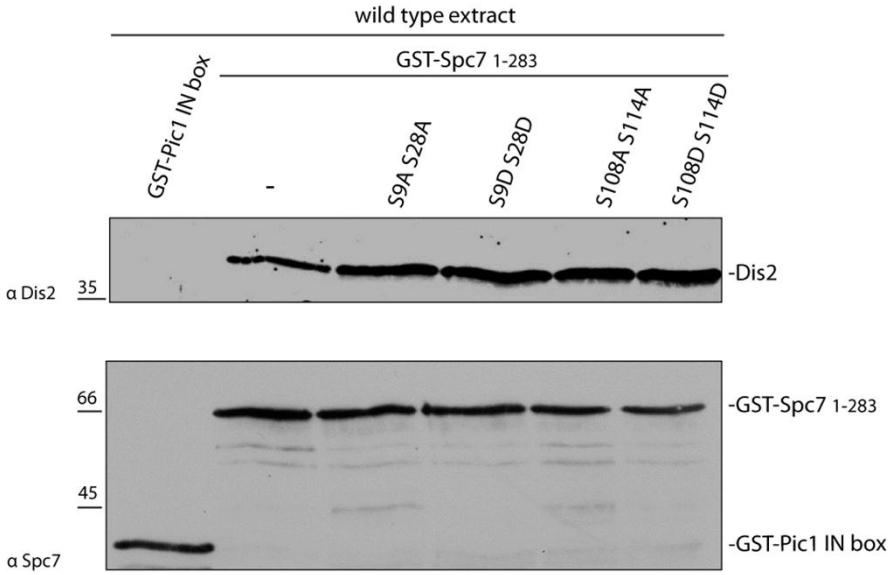

Figure 5.10. Dis2 targeting to Spc7 seems to be independent of Spc7 phosphorylation in fission yeast. Pull downs were run on a 10% SDS-PAGE gel. The blot were probed with α Dis2 antibody and then reprobed with α Spc7 antibody (loading control).

The *in vitro* Spc7 binding experiment (Figure 5.10) showed that in contrast to vertebrate PP1, *S. pombe* Dis2 might bind to Spc7 independently of its phosphorylation status, (at least for Ark1 phosphorylation sites identified).

5.6.2. The basic patches are not involved in mediating Dis2-Spc7 interaction

We decided to rule out an unlikely possibility that the basic patches can interfere with the Dis2 binding using the *in vitro* Spc7 binding assay. The beads coated with recombinant GST-Spc7 (1-283) basic patch mutants (BP 1, BP 2, BP 1&2) and the double phosphomimetic GST-Spc7 (1-283) mutant (S9D S28D) were incubated with yeast cell extracts (30 min at 4°C). Following incubation, the bead samples were analysed by western blotting (Figure 5.11). These analyses indicate thatthe basic patches in Spc7 are not involved in Dis2 binding.

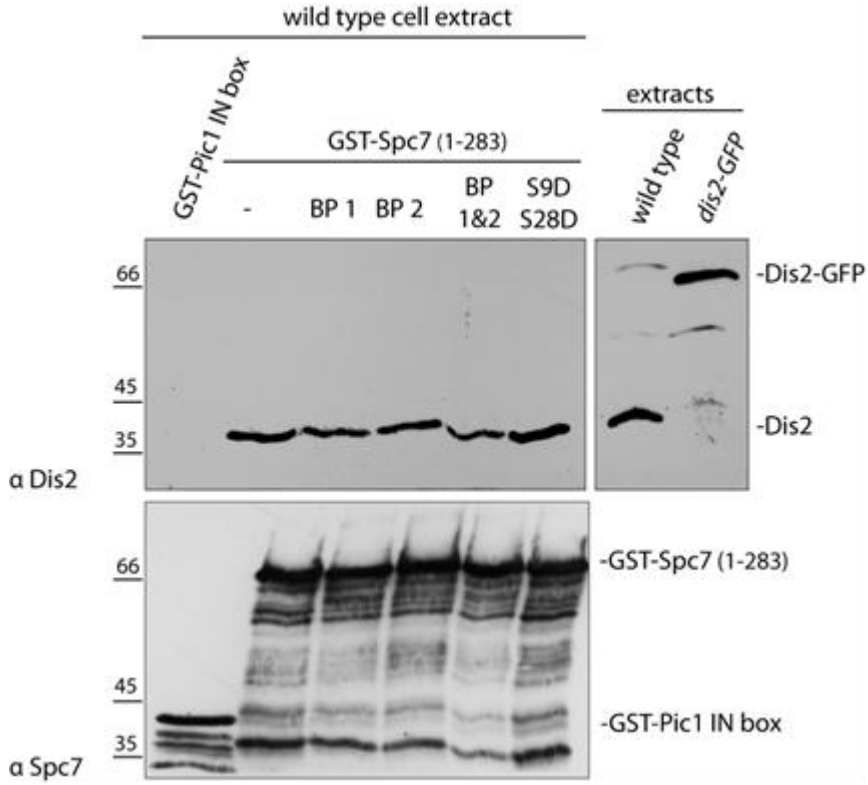

Figure 5.11. Losing positive charges in the N-terminus of Spc7 does not disrupt Dis2 binding *in vitro*. Pull down and extracts samples were run on a 10% SDS-PAGE gel. The blot were probed with α Dis2 antibody and then reprobed with α Spc7 antibody (loading control).

5.7. Summary and Discussion

In this chapter preliminary results demonstrating that Spc7 microtubule binding activity is regulated by Ark1-dependent phosphorylation have been presented. Ark1-dependent phosphorylation of Spc7 impairs the Spc7 interaction with microtubules *in vitro* which is consistent with the results obtained in other species (Welburn et al., 2010). In addition, we investigated the role of the basic patches (BP 1 and BP 2) present in Spc7 and demonstrated that they not only constitute a microtubule-interacting surface in Spc7 but also might contribute to Spc7 nuclear import. Finally, Dis2 association with Spc7 was examined by utilising *in vitro* Spc7 binding assays. Based on our results we speculate that, unlike in vertebrate cells, PP1/Dis2binding to KNL1/Spc7 is not regulated by Aurora B kinase-dependent phosphorylation in fission yeast.

Electrostatic nature of the interaction between kinetochores proteins and microtubules

The *S. pombe, C. elegans* and humans KNL1 homologues are acidic proteins whose isoelectric point is between 4.9-5.3, which might suggest that they are not microtubule binders as microtubule-binding proteins are usually basic (Desai et al., 2003). However, the KNL1 homologues are large proteins. This raises the possibility of positively charged residues being concentrated in specific regions whilst the whole protein remains negatively charged.

Ciferri et al. (2008) proposed that interaction of the Ndc80 complex with microtubules is mainly based on electrostatic interactions between positively charged residues in a calponin-homology (CH) domain, forming the globular head of Ndc80, and the acidic C-terminal tails of tubulin . This is consistent with observations that phosphorylation of KNL1 and Ndc80 by Aurora B prevents microtubule binding (Cheeseman et al., 2006; Ciferri et al., 2008; Welburn et al., 2010). Since phosphorylation adds a phosphate group (PO_4^{3-}) to a protein, the phosphorylation of the N-terminus of KNL1 and Ndc80 leads to accumulation of negative charges at the kinetochore-microtubule interface. The last 10 and 18 C-terminal residues of α- and

β-tubulin, respectively, form E-hooks and are also negatively charged as they are rich in aspartic and glutamic acid residues (Redeker et al., 1992).

In this chapter preliminary results demonstrating that the microtubule binding activity of Spc7 might be modulated by changing balance between negative and positive charges in its extreme N-terminus, have been presented.

Three stretches of basic residues, BP 1 (R6 R7), BP 2 (R23 K24 R25) and BP 3 (R106 K107), are present in the N-terminus of Spc7 (see Figure 5.3). Spc7 contains another basic patch, BP 4 (R631 K632 R633 R634 R636) which is located in the middle of the protein and is not conserved in other members of the KNL1/Spc7 family proteins (Figure 5.12). Strikingly, all the basic patches are accompanied by Ark1 phosphorylation sites (S9, S28, S108 and S638) identified in our mass spectrometry analysis (section 3.4.3 and Figure 5.3)

Figure 5.12. The basic patch (BP 4) in the middle of Spc7. Similarly to the basic patches in the N-terminus, the Ark1 phosphosite (S638) is located in the vicinity of the patch.

Spc7 microtubule binding activity is regulated by phosphorylation

According to the results of our *in vitro* kinase assays serines 9 and 28 constitute the main phosphorylation sites in the N-terminus of Spc7 (residues 1-283). Spc7 phosphorylation mutants of these sites are sensitive to benomyl, (a microtubule depolymerising agent), with the double alanine mutant (S9A S28A) being more sensitive to the drug than the double aspartic acid mutant (S9D S28D) (Figure 5.6). Both mutants seem to be slightly defective in spindle checkpoint activation/maintenance (Figure 5.7), but these minor checkpoint defects alone cannot account for the increased benomyl sensitivity of these phosphomutants. This suggests

that the introduced mutations might affect other function of Spc7 such as chromosome segregation.

The budding yeast and *C. elegans* homologues of KNL1, Spc105 and KNL-1, respectively, were shown to bind microtubules *in vitro* (Pagliuca et al., 2009; Cheeseman et al., 2006). This interaction is negatively regulated by Aurora B-dependent phosphorylation of *C. elegans* and human KNL1s (Welburn et al., 2010). To test whether this is true in fission yeast we carried out an *in vitro* microtubule cosedimentation assay with GST-Spc7-S9D (1-283), GST-Spc7-S28D (1-283), GST-Spc7-S9D S28D (1-283) and GST-Spc7-S9A S28A S108A S114A (1-283) (Figure 5.4). The results obtained demonstrated that while both single mutants and the quadruple alanine mutant bound microtubule at wild type levels, the double mutant (S9D S28D) exhibited impaired microtubule binding activity (Figure 5.4). This supports the model where Aurora B-dependent phosphorylation of kinetochore proteins, including KNL1, causes disruption of kinetochore microtubule interactions. More quantitative assays are underway to measure binding affinity of the Spc7 mutants for microtubules.

It is worth mentioning that the residues phosphorylated by Aurora B kinase in *C. elegans* and human KNL1s are located in highly conserved PP1 binding motifs (Welburn et al., 2010) (Figure 5.3). In our experiments different residues, which are not conserved in the other KNL1 proteins, were substituted with aspartic acid (S9D S28D). These mutations had a similar effect on microtubule binding as those introduced to the *C. elegans* and human KNL1 proteins (Welburn et al., 2010). This indicates that in fission yeast, Spc7 microtubule binding activity might be regulated by a similar mechanism to that in vertebrate cells, but different phosphorylation sites are involved. Alternatively, the location of Ark1-phosphorylation sites within the extreme N-terminus of Spc7 plays a minor role in regulating its microtubule association, but the number of introduced phosphate groups is relevant for this process. This possibility can be tested by using the GST-Spc7-S108D S114D (1-283) mutant in the microtubule cosedimentation assay. According to our analysis both serines, S108 and S114, might be phosphorylated by

Ark1. Moreover serine 114 is highly conserved and located in the second PP1 binding motif in Spc7, which resembles the situation in vertebrate KNL1s.

The basic patches and microtubule binding activity of Spc7

To investigate further microtubule binding activity of Spc7, the Spc7 basic patch mutants GST-Spc7-BP1 (1-283), GST-Spc7-BP2 (1-283) and GST-Spc7-BP1&2 (1-283), were tested in microtubule cosedimentation assays. The results demonstrated that the basic patches in the N-terminus of Spc7 contribute to microtubule binding (Figure 5.5). These results are consistent with the observation that the microtubule binding activity of *C. elegans* KNL-1 was significantly reduced when a basic patch, present in its extreme N-terminus, was either deleted or substituted with alanines (Espeut et al., 2012).

The results presented here, supported by previously published data (Espeut et al., 2012), indicate that Spc7 can bind to microtubules through an electrostatic interaction involving the basic patches in its very N-terminus. Moreover, the balance between negative and positive charges in the N-terminus of Spc7/KNL1 is regulated by Ark1/Aurora B-dependent phosphorylation (see Figure 5.13).

In *C. elegans* expression the KNL-1 basic patch mutants, who exhibit reduced microtubule binding activity *in vitro*, do not significantly perturb kinetochore-microtubule attachments but cause a slight delay in anaphase onset (Espeut et al., 2012). In fission yeast strong overexpression of the C-terminal half of Spc7 leads to aberrant kinetochore-microtubule attachments, which elevates the number of mitotic cells (Kerres et al., 2004, 2007). Considering these observations, we overexpressed the N-terminal fragment of Spc7 (residues 1-283) containing the basic patch mutations in yeast cells. No increase in mitotic index was observed, suggesting that moderate overexpression of the basic patch mutants does not strongly activate the mitotic checkpoint.

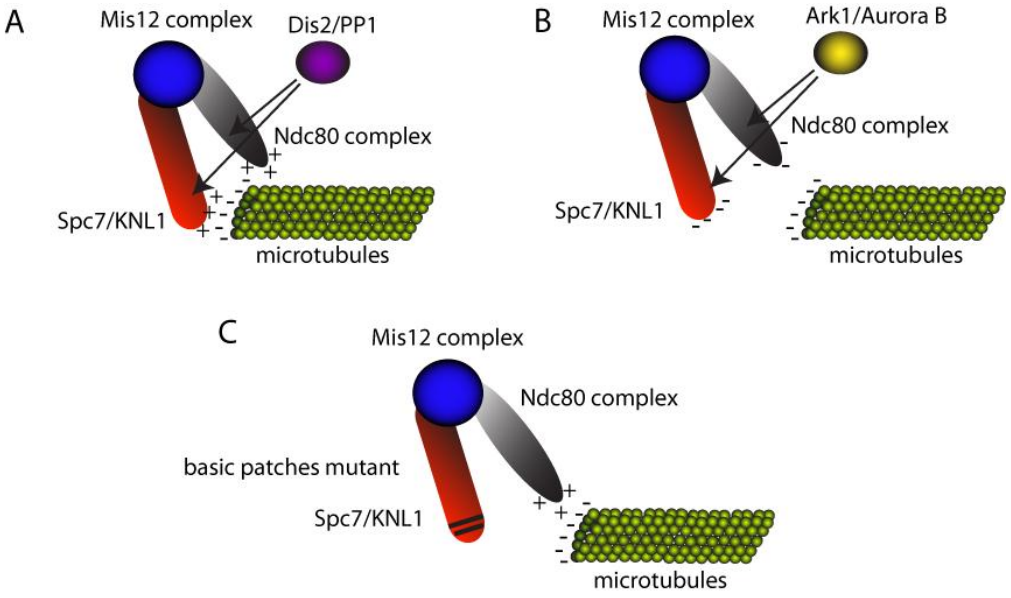

Figure 5.13. The Spc7 microtubule binding activity depends on the concentration of positive charges at its very N-terminus. We propose that Spc7 binding to microtubules, similarly to that of the Ndc80 complex (Ciferri et al., 2008; Welburn et al., 2010), relies on the electrostatic interaction between negatively charged microtubule E-hooks and a positively charged N-terminus of Spc7. **A**. Kinetochore-microtubule interactions are stabilised by the Dis2/PP1 activity opposing Aurora B-dependent phosphorylation of kinetochore proteins. Dis2/PP1 removes acidic phosphate groups (PO_4^{3-}) which results in the N-terminus of Spc7/KNL1 being more basic. This promotes the Spc7 interaction with microtubules. **B.** Ark1/Aurora B increases the concentration of negative charges in the N-terminus of Spc7/KNL1 leading to destabilization of kinetochore-microtubule attachments. **C.** Mutating the basic patches in Spc7/KNL1 results in loss of positive charges in the N-terminus of Spc7. The reduced number of positive charges does not support interaction between Spc7 and microtubules.

As mentioned above to activate the checkpoint, strong overexpression of the Spc7 C-terminal fragment was required (Kerres et al., 2004, 2007). Probably, upon the strong overexpression, the Spc7 C-terminal fragment was able to compete with endogenous Spc7. Therefore, it would be interesting to overexpress the Spc7 mutants affecting microtubule binding from the strongest nmt1 promoter.

Taken together, we managed to show that the following Spc7 mutants: Spc7-S9D S28D (1-283), Spc7-BP1 (1-283), Spc7-BP2 (1-283) are Spc7-BP1&2 (1-283) are defective in microtubule binding. All of them are sensitive to benomyl, so we suspect

that the introduced mutations interfere with accurate chromosome segregation (Figure 5.7). The moderate overexpression of these mutants, in strains expressing endogenous Spc7, did not result in spindle checkpoint activation. This indicates that in these conditions proper kinetochore-microtubule interactions are established and maintained, so there is no need to activate the checkpoint. The other way to assess whether the mutations, which result in reduction of the Spc7 microtubule binding activity *in vitro*, perturb kinetochore-microtubule attachments *in vivo* is to look at chromosome segregation using half-sectoring assays or Cen2-GFP assay.

The half sectoring assay employs a short linear minichromosome CH16 which contains an *ade6-216* mutant allele (Allshire et al., 1995). The *ade6-216* allele is complemented by the *ade6-210* allele in yeast genomic DNA. Loss of Ch16 due to chromosome missegregation results in accumulation of a red dye in the cells and formation of red-sectored colonies. The cen2-GFP assay enables to visualise chromosome 2 as a green dot under microscope (Yamamoto and Hiraoka, 2003). Cells segregating chromosomes normally have one green dot near each SPB, whereas cells missegregating chromosomes can have two dots at one SPB. These two assays will be used in the future to test the Spc7 mutants defective in microtubule binding for chromosome missegregation.

Spc7 nuclear translocation

Interestingly, while overexpressed HFG-Spc7 WT (1-283) and HFG-Spc7-BP 1 (1-283) accumulated in nuclei, HFG-Spc7-BP 2 (1-283) and HFG-Spc7-BP 1&2 (1-283) were only slightly enriched in nuclei with the GFP signal present mostly in the cytoplasm (Figure 5.8 A). This observation and the abundance of lysine and arginine residues in the basic patches suggest that the second basic patch might serve as a nuclear localisation signal (NLS). In fission yeast, Spc7 is constitutively associated with kinetochores, where it exhibits functions which are essential for cell viability (Kerres et al., 2004). Cells expressing full length Spc7 BP 1&2 from the *lys1* locus were viable and grew normally on the YES plates (Figure 5.6) which indicates that in these cells mutating the second basic patch does not severely impair the Spc7 kinetochore localisation. Moreover, a strain expressing full length Spc7 BP 1&2, C-terminally tagged with GFP, has been recently generated.

Preliminary microscopic analysis of these cells revealed that the Spc7 BP 1&2-GFP dots are associated with kinetochores (data not shown). Consequently, there must be another NLS in the Spc7 sequence which ensures the Spc7 kinetochore localisation. To identify putative nuclear localisation signals in Spc7, the Spc7 amino acid sequence was analysed using cNLS Mapper online software, which predicts nuclear localisation signals (NLSs) specific to the importin α/β pathway (Kosugi et al., 2009).

The following sequences were predicted: RNKSRKRPHSL (Spc7 19-29) and GTRKRRLRYS (Spc7 629-638) as monopartite NLSs (a single cluster of basic residues). These predictions indicate that BP 2 and BP 4 are two redundant nuclear localisation signals in Spc7. Since the mutation of BP 2 can be rescued by expression of full-length protein, BP 4 might be a functional NLS central to Spc7 nuclear transport.

Interestingly, all predicted NLSs contain an Ark1 phosphorylation sites (S28 and S638) identified by our mass spectrometry analysis. It has been reported that phosphorylation within or in the vicinity of NLS might influence nuclear localisation of proteins [for review see (Nardozzi et al., 2010)]. Nuclear import of some proteins is promoted by phosphorylation (Zhang et al., 2001; Greco et al., 2010; Teng et al., 2011). However, phosphorylation can also inhibit nuclear translocation of proteins (Zhang et al., 2001; Harreman et al., 2004). Therefore the hypothesis, that Ark1-dependent phosphorylation of serine 28 and serine 638 in Spc7 might alter its nuclear import, seems to be worth testing. We already know that overexpression of the phosphomimetic Spc7 S9D S28D (residues 1-283) does not change its nuclear accumulation in comparison to wild type (Supplementary Figure 2), which suggests that phosphorylation at S28 does not have a negative effect on the Spc7 nuclear import. Nevertheless, the mechanism which targets Spc7 to the nucleus still remains to be investigated.

The interaction of Dis2/PP1 with Spc7

In *C. elegans* cells PP1 binding activity is negatively regulated by Aurora B-dependent phosphorylation of kinetochore proteins (Liu et al., 2010). Consistently, phosphomimetic mutations of serine 24 adjacent to the first PP1 binding motif and serine 60 in the second PP1 binding motif of human KNL1 abolished the interaction between human PP1γ and KNL1 *in vitro*. The analysis of phosphorylation sites in Spc7 indicated serine 108, adjacent the second PP1/Dis2 binding motif, and serine 114 inside the second PP1 binding motif, as a putative Ark1 phosphorylation sites. A previous study demonstrated that in fission yeast Dis2 binding to Spc7 and checkpoint silencing depends mainly on the second PP1 binding motif, whereas the first motif might be more important for establishing proper kinetochore-microtubule interactions (Meadows et al., 2011).

In contrast to vertebrate studies (Liu et al., 2010), an *in vitro* experiment included in this chapter has revealed that fission yeast Dis2 binds to Spc7 regardless of the status of serine 108 and 114 in Spc7 (Figure 5.10). This suggest that the second PP1/Dis2 binding motif might not be regulated by Ark1-dependent phosphorylation in this system. In addition to Ark1, Mph1 phosphorylates Spc7 (see section 3.6 and 4.3). The recombinant MBP-fusion Spc7-T9A (1-666) and T9E (1-666) proteins, generated to investigate the Mph1-dependent binding of Bub1 and Bub3 to Spc7 (see section 4.2), were used to test the possibility that the MELT motif phosphorylation affects Dis2-Spc7 interaction (Supplementary Figure 3). However, our analyses indicate that the Dis2-Spc7 interaction occurs independently of the status of these MELT motifs. Similarly, Bub3 deletion, [Bub3 is required for efficient checkpoint silencing in fission yeast (Vanoosthuyse et al., 2009)], does not affect the Dis2-Spc7 interaction *in vitro* (Supplementary Figure 3). Other Mph1 sites in Spc7 (T168 and T283; section 3.6) remain to be tested.

As mentioned above, Aurora B-dependent phosphorylation of the same residues (S24 and S60) in human KNL1 negatively regulates its PP1 and microtubule binding activities (Liu et al., 2010; Welburn et al., 2010). These observations suggest that spindle checkpoint silencing might be coupled with microtubule attachments through Aurora B activity. When kinetochore-microtubule attachments are stable and under

tension Aurora B activity at the kinetochore is low and S24 and S60 in KNL1 are not phosphorylated allowing PP1 binding and checkpoint silencing. However, tension-less kinetochore-microtubule attachments result in a high Aurora B activity at kinetochores and phosphorylation of S24 and S60. This contributes to disruption of incorrect attachments along with PP1 dissociation from KNL1, which promotes checkpoint activity.

According to our preliminary results this mechanism of regulating Dis2/PP1 in response to microtubule binding might not be conserved in fission yeast. However, it is possible that in this organism Dis2-Spc7 association is regulated by the Ark1 dependent-phosphorylation of sites involved in regulating microtubule attachments (for example S9 and S28, Figure 5.4) in combination with sites related to the second PP1 binding motif (S108 and S114). This hypothesis is supported by unpublished data from the Millar lab (University of Warwick), demonstrating that the *spc7 S9D S108D S114D* mutant is defective in spindle checkpoint silencing to a similar extent as *dis2Δ*. Since in our *in vitro* Spc7 binding assays only the double Spc7 phosphomutants were tested (S9A/D S28A/D and S109A/D S114A/D) (Figure 5.10), it would be informative to generate the triple and quadruple mutants and carry out the Dis2 *in vitro* binding experiment.

Chapter 6
Final Discussion

Chapter 6

Final Discussion

The multiprotein structure of kinetochore constitutes a dynamic connection between centromeric DNA and microtubules which enables chromosome segregation in mitosis. Fidelity of chromosome segregation depends on error-free and stable bipolar kinetochore-microtubule attachments. Therefore kinetochore proteins recruit and collaborate with other proteins including spindle checkpoint proteins, kinesins, mitotic kinases and phosphatases to ensure timely and errorless distribution of sister chromatids to daughter nuclei.

In this study, functions of the N-terminal half of Spc7, the *S. pombe* KNL1 homologue, have been characterized. The KNL1 (kinetochore null1) family proteins, as their name suggests, are essential components of kinetochores. Although the amino acid sequence of the KNL1 homologues is not extremely well preserved [e.g. 17.8% identity and 36.4% similarity between *S. pombe* Spc7 and human KNL1 (Cheeseman et al., 2004)], their domain organization (PP1 binding motifs, MELT motifs and a C-terminal coiled-coil) and functions are conserved from yeast to humans.

The physiological relevance of Mph1-dependent Spc7 phosphorylation

It has been well establish that Mph1/Mps1 is critical for the mitotic spindle checkpoint. The checkpoint functions of Mph1/Mps1 include targeting checkpoint components to kinetochores (Abrieu et al., 2001; Maciejowski et al., 2010), facilitating O-Mad2 loading onto the C-Mad2-Mad1 template (Hewitt et al., 2010), promoting MCC formation (Maciejowski et al., 2010) and stabilizing the MCC-APC interaction (Zich et al., 2012). In this study the roles of Mph1 and Ark1 kinases have been studied revealing several distinct functions of Spc7 that are relevant to spindle checkpoint signaling.

The results presented demonstrate that Spc7 is phosphorylated by Mph1 kinase *in vitro* and probably *in vivo*. Moreover, we have provided biochemical evidence uncovering the relationship between Bub1-Bub3 complex and Spc7 at the fission yeast kinetochore (see Chapter 4). Our data together with data from the Millar Lab

have been very recently published in Current Biology (Shepperd et al., 2012). In parallel, other groups published similar findings concerning Spc7/KNL1 in fission yeast, humans and budding yeast (Yamagishi et al., 2012; London et al., 2012).

Our biochemical analysis of the Bub1 and Bub3 interaction with Spc7 was complemented by an *in vivo* analysis of the MELT motifs mutants carried out in the Millar Lab (Warwick University). The main conclusion drawn from the *in vitro* Spc7 binding assays is the requirement of Spc7 for being phosphorylated by Mph1 kinase at the conserved MELT motifs in order to bind Bub1 and Bub3 checkpoint proteins. Microscopic analyses confirmed that kinetochore localisation of Bub1 and Bub3 depends on MELT motif phosphorylation (Shepperd et al., 2012). Moreover, the non-phosphorylatable Spc7 MELT mutant, *spc7-T9A,* which does not recruit Bub1 and Bub3 to kinetochores, was defective in spindle checkpoint maintenance, but not in checkpoint activation (Shepperd et al., 2012). This is consistent with previous reports showing that cells lacking Bub3 cannot recruit Bub1 to kinetochores but are able to arrest in metaphase in response to microtubule depolymerisation (Vanoosthuyse et al., 2009; Windecker et al., 2009). On the contrary Yamagishi et al. (2012), who applied a broader definition of the MELT motif and thereby mapped 12 of them in fission yeast Spc7, observed severe checkpoint in the *spc7-T12A* mutant (Yamagishi et al., 2012). This MELT mutant was completely unable to arrest in metaphase upon microtubule depolymerisation in the *nda3-KM311* background. These results suggest that phosphorylation of the additional MELT motifs, which have not been investigated in this study, is crucial for checkpoint signaling. Alternatively, the discrepancy between the *spc7-T9A* and *spc7-T12A* phenotypes might be explained by technical differences in performing the *nda3-KM311* arrest experiment. In the Millar lab time points were taken at 30 min-1hour intervals during 6 hours of the *nda3-KM311* arrest (Shepperd et al., 2012). Whereas Yamagishi et al.(2012) collected a final sample after arresting cells in metaphase for 17 hours, which does not provide information on the dynamics of the arrest. As both studies mentioned above used the multiple Spc7 MELT mutants, *spc7-T9A* and *spc7-T12A,* it will be interesting to determine how many MELTs need to be phosphorylated in order to bind Bub1 and Bub3.

The phosphomimetic mutant of the Spc7 MELT motifs, *spc7-T9E*, which constitutively targets Bub1 and Bub3 to kinetochores, was checkpoint proficient and exhibited enhanced checkpoint silencing in comparison to wild type controls (Shepperd et al., 2012). This reflects the idea that an increased concentration of checkpoint components at kinetochores promotes efficient checkpoint silencing by making them more accessible to Dis2/PP1 phosphatase (Vanoosthuyse et al., 2009).

The role of Bub3 in spindle checkpoint signaling

Surprisingly, the checkpoint phenotype of the threonine-to-alanine substitution MELT motifs mutants was rescued by deleting Bub3 (Shepperd et al., 2012; Yamagishi et al., 2012). Since Bub3 is not absolutely required for spindle checkpoint establishment and it interacts with Bub1 through the cell cycle (Brady and Hardwick, 2000) it is possible that Bub3 normally supresses Bub1 checkpoint activity in the cytoplasm (Shepperd et al., 2012; Yamagishi et al., 2012). This hypothesis might explain the checkpoint response improvement of the non-phosphorylatable Spc7 MELT mutants in the *bub3Δ* background (Shepperd et al., 2012; Yamagishi et al., 2012).

The inhibitory effect of Bub3 on Bub1 checkpoint activation in the cytoplasm can be tested using a Bub3 mutant which is unable to bind Bub1 in the *spc7-T9A* background. If the hypothesis is true such then a double mutant should exhibit similar improvement in the spindle checkpoint maintenance as the *spc7-T9A bub3Δ* and *spc7-T9A bub1-GLEBSΔ* mutants in comparison with the *spc7-T9A* single mutant. However such an experiment first requires identification of the domain in Bub3 that binds Bub1 so that it can be subsequently disrupted.

In human cells deletion of the conserved VAVE sequence (residues 218-221) in blade 5 of human Bub3 disrupts Bub3 kinetochore localisation resulting in Bub3 being retained in the cytoplasm (Taylor et al., 1998; Larsen and Harrison, 2004) Presumably, the VAVE deletion perturbs Bub3 interaction with Bub1 and BubR1 (Taylor et al., 1998). This observation is based on Bub3 localisation studies and, to our knowledge, it has not been biochemically confirmed. In fission yeast the VAVE motif is not well conserved as the first two residues are replaced with threonine and

serine, respectively. Nevertheless, it might be worth testing this motif for Bub1 binding and if it is dispensable for Bub3-Bub1 interaction make an effort to find the fission yeast Bub1 binding site in Bub3.

According to *in vitro* results presented in our study, the Bub1 interaction with Spc7-T9E requires Bub3 and the presence of a Bub3 binding domain in Bub1 called the GLEBS domain (see Chapter 4). This is consistent with a study by Krenn et al., (2012) which demonstrated that the critical role of KNL1 for recruitment of Bub1 and Bub3 to kinetochores is most likely mediated by Bub3 as in the Bub3-binding mutant of Bub1, Bub1 was not recruited to kinetochores in HeLa cells. Assuming that Bub3 may interact with Spc7/KNL1 directly and this interaction is essential to target Bub1 to kinetochores, identification of the Spc7 binding region in Bub3 is clearly important in order to confirm the proposed model.

The importance of the GLEBS domain, presumably due to its Bub3 binding activity, for recruitment of Bub1 to kinetochores was initially reported in human cells (Taylor et al., 1998). Consistently, in yeast cells Bub1 and Bub3 are interdependent for their kinetochore localisation (Vanoosthuyse et al., 2004). Confusingly, Logarinho et al. (2008) showed that in human cells Bub3 depletion results in eviction of BubR1, but not Bub1 from kinetochore. This might suggest that the Bub1 GLEBS motif contributes to Bub1 kinetochore localisation in a Bub3-independent manner in human cells at least. Alternatively, incomplete Bub3 siRNA could explain this controversial result. It is possible that reduced levels of Bub3 remaining after the RNA interference experiment, are sufficient to recruit Bub1 but not BubR1 to kinetochores.

Recently, major progress in understanding how Bub1-Bub3 complex is recruited to kinetochores has been achieved. However, still many questions remain to be answered.

<u>The MELT motifs in Spc7/KNL1 as docking sites for checkpoint proteins</u>

It would be interesting to know whether the KNL1/Spc7 MELT motifs (at least some of them) are involved in a direct interaction with the Bub1 and Bub3 proteins. This problem was addressed by Shepperd et al. (2012), by generating the *spc7-M9A*

mutant (a conserved methionine in the MELT motifs was substituted with alanine). This mutant exhibited a phenotype identical to the *spc7-T9A* mutant in microscopic analysis suggesting that in fission yeast the MELT motifs per se contribute to the recruitment of the Bub1-Bub3 complex to kinetochores. However, this observation can also reflect the possibility that the *spc7-M9A* mutant does not undergo phosphorylation if the kinase does not recognize the mutated MELT motifs. This problem needs to be further investigated by biochemical experiments.

In *S. pombe* Spc7 all the MELT motifs are distributed over approximately 300 amino acids. Likewise a variable number of MELT motifs are spread over a long stretch of amino acids in other species. Making a series of mutants in which individual MELT motifs are deleted would determine if specific MELT motifs are important for the interaction between Bub1 and Bub3 and Spc7/KNL1. Additionally, it might be informative to obtain a crystal structure of the MELTs containing region of KNL1/Spc7 as the structural organisation of this region would provide insight into its function. Consistently, crystalizing Spc7 MELT-Bub3 complex seems to be a reasonable experiment to do in the future.

According to the model proposed by Krenn et al. (2012) the GLEBS domain, present in both Bub1 and BubR1, is critical to target these proteins to KNL1 due to its Bub3 binding activity. Assuming that the association of Bub1 and Bub3 with KNL1 is stable, this model implies that two Bub3 molecules are interact with KNL1 and one Bub3 molecule binds Bub1 whereas the other one binds BubR1. This hypothetical situation requires two separate Bub3 binding sites in KNL1. It might be possible that these two docking sites for Bub3 are provided by the long MELTs containing region in KNL1.

Mad3 kinetochore targeting in fission yeast

The fission yeast BubR1 homologue, Mad3, does not contain the GLEBS domain therefore Bub3 is not likely to mediate the Mad3-Spc7 interaction in this system. We can speculate that in fission yeast Mad3 can interact with Bub1 via its N-terminal TPR motif and this interaction targets Mad3 to Spc7 and thereby to the kinetochore,

but a Bub1 binding motif in Mad3 has not been identified and this hypothesis remains to be tested.

The role of Spc7 in spindle checkpoint silencing

The results presented in this study suggest that Spc7 has microtubule binding activity *in vitro*, exerted cooperatively by two basic patches (R6 R7 and R23 K24 R25) in the very N-terminus of Spc7 (see Chapter 5). The microtubule binding activity of Spc7 might be negatively regulated by Ark1-dependent phosphorylation of serine 9 and serine 28, located in the vicinity of the basic patches (see Chapter 5). Moreover, similar to vertebrate KNL1 and budding yeast Spc105 (Liu et al., 2010; Rosenberg et al., 2011), fission yeast Spc7 interacts with Dis2 phosphatase (see Chapter 5), the fission yeast homologue of vertebrate PP1. We have yet to complete our dissection of the mechanism which regulates Dis2 targeting to Spc7 in *S. pombe*. However, according to our preliminary results, as in budding yeast (Rosenberg et al., 2011) and unlike in vertebrate cells (Liu et al., 2010), Ark1-dependent phosphorylation does not seem to play a role in regulating the interaction between Dis2 and Spc7. This suggests that other kinases, including Mph1/Mps1 kinase, might be relevant to this process.

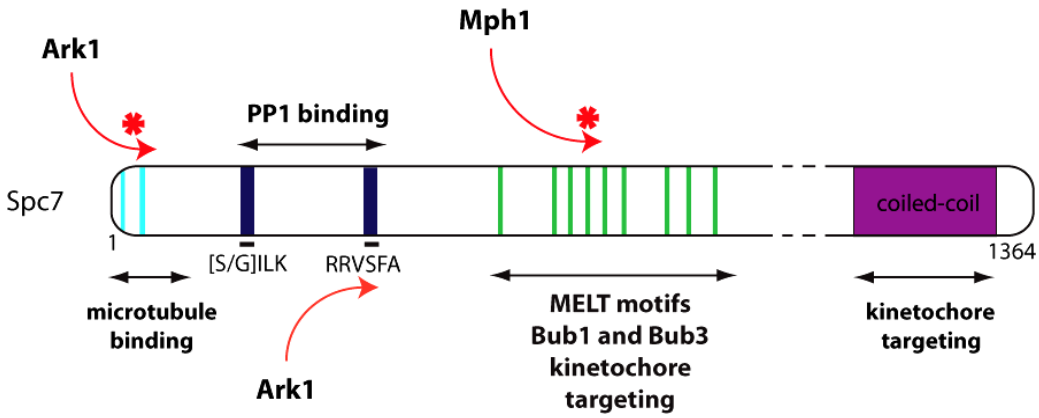

Figure 6.1. Spc7 functions and their regulation. Asterisk indicates that a given Spc7 activity is regulated by phosphorylation.

It has been recently reported that *C. elegans* KNL-1 contributes to spindle checkpoint silencing through two independent pathways (Espeut et al., 2012). The first mechanism depends on PP1 binding to KNL-1 and, similarly to yeast and *Xenopus* (Rosenberg et al., 2011; Meadows et al., 2011; Liu et al., 2010), the second PP1 binding site (RRVSF) seems to be more important for this interaction than the first PP1 binding motif ([G/S]ILK). Moreover, the second PP1 binding motif has been demonstrated to be required for timely formation of load-bearing kinetochore-microtubule attachments (Espeut et al., 2012). In addition to the PP1 binding motif, a single basic patch present in the very N-terminus of KNL-1 mediates spindle checkpoint silencing in the presence of microtubules but not when microtubules are depolymerized upon nocodozole treatment (Espeut et al., 2012). The KNL-1 basic patch mutants, despite their abolished microtubule binding activity, support proper kinetochore-microtubule attachments (Espeut et al., 2012). As the Spc7 N-terminal basic patches contribute to microtubule binding *in vitro*, future experiments should address possible involvement of the basic patches in spindle checkpoint silencing.

Microtubule independent silencing in fission yeast can be tested using the silencing assay developed by Vanoosthuyse and Hardwick (2009). In the assay metaphase arrested *nda3-KM311 ark1-as3* cells can be forced to silence the checkpoint by addition of 1-NMPP1 which specifically inhibits the Ark1 ATP-analogue sensitive mutant. This assay was used to demonstrate that Dis2 and the Dis2 binding motifs in Spc7, Klp5 and Klp6 are required for spindle checkpoint silencing in fission yeast, independently of microtubule binding (*nda3-KM311* background) (Vanoosthuyse and Hardwick, 2009; Meadows et al., 2011).

We hypothesise that the interaction between Spc7 and microtubules might trigger checkpoint silencing and thus disrupting the basic patches might impair checkpoint silencing. Therefore, in order to test the Spc7 basic patch mutants for their ability to silence the checkpoint a new microtubule-dependent silencing assay must be developed. The checkpoint arrest in the presence of microtubules in fission yeast can be triggered by Mad2 and Mph1 overexpression (He et al., 1997, 1998). However, according to the experiments carried out in the Hardwick Lab, both Mad2 and Mph1

overexpression induced mitotic arrests are maintained when Ark1 is inhibited (data not shown, Dr. Karen May personal communication). Moreover, overexpression Mad2 does not require Mph1 to arrest cells in metaphase (He et al., 1998). Therefore inhibition of Mph1 while Mad2 is overexpressed would not result in the checkpoint silencing. Considering difficulties in releasing the cells from Mad2 and Mph1 overexpression induced arrests, developing a microtubule-dependent checkpoint silencing assay is a quite challenging task.

This study, along with recently published findings, has shown how abundant in different functions the N-terminal half of the KNL1/Spc7 family protein is. This causes challenges when studying particular roles of KNL1/Spc7 as they can overlap with other functions. Nevertheless, over recent years several groups have made a great effort to dissect the roles of this protein. I am very happy that my PhD research has contributed to the better understanding of the Spc7/KNL1 relevance in mitosis. However, many more questions about Spc7 and its regulation remain to be answered.

References

References

Abrieu, A., Kahana, J. A., Wood, K. W., and Cleveland, D. W. (2000). CENP-E as an essential component of the mitotic checkpoint in vitro. Cell *102*, 817–826.

Abrieu, A., Magnaghi-Jaulin, L., Kahana, J. A., Peter, M., Castro, A., Vigneron, S., Lorca, T., Cleveland, D. W., and Labbé, J. C. (2001). Mps1 is a kinetochore-associated kinase essential for the vertebrate mitotic checkpoint. Cell *106*, 83–93.

Adames, N. R., Oberle, J. R., and Cooper, J. A. (2001). The surveillance mechanism of the spindle position checkpoint in yeast. The Journal of Cell Biology *153*, 159–168.

Adams, R. R., Maiato, H., Earnshaw, W. C., and Carmena, M. (2001). Essential roles of *Drosophila* inner centromere protein (INCENP) and aurora B in histone H3 phosphorylation, metaphase chromosome alignment, kinetochore disjunction, and chromosome segregation. The Journal of Cell Biology *153*, 865–880.

Adams, R. R., Wheatley, S. P., Gouldsworthy, A. M., Kandels-Lewis, S. E., Carmena, M., Smythe, C., Gerloff, D. L., and Earnshaw, W. C. (2000). INCENP binds the Aurora-related kinase AIRK2 and is required to target it to chromosomes, the central spindle and cleavage furrow. Current Biology *10*, 1075–1078.

Akiyoshi, B., Nelson, C. R., Ranish, J. A., and Biggins, S. (2009a). Analysis of Ipl1-mediated phosphorylation of the Ndc80 kinetochore protein in *Saccharomyces cerevisiae*. Genetics *183*, 1591–1595.

Akiyoshi, B., Nelson, C. R., Ranish, J. A., and Biggins, S. (2009b). Quantitative proteomic analysis of purified yeast kinetochores identifies a PP1 regulatory subunit. Genes and Development *23*, 2887–2899.

Allshire, R. C., Nimmo, E. R., Ekwall, K., Javerzat, J. P., and Cranston, G. (1995). Mutations derepressing silent centromeric domains in fission yeast disrupt chromosome segregation. Genes and Development *9*, 218–233.

Anderson, D. E., Losada, A., Erickson, H. P., and Hirano, T. (2002). Condensin and cohesin display different arm conformations with characteristic hinge angles. The Journal of Cell Biology *156*, 419–424.

Archambault, V., and Glover, D. M. (2009). Polo-like kinases: conservation and divergence in their functions and regulation. Nature Reviews Molecular Cell Biology *10*, 265–275.

Bai, C., Sen, P., Hofmann, K., Ma, L., Goebl, M., Harper, J. W., and Elledge, S. J. (1996). SKP1 connects cell cycle regulators to the ubiquitin proteolysis machinery through a novel motif, the F-box. Cell *86*, 263–274.

Baker, D. J., Jeganathan, K. B., Cameron, J. D., Thompson, M., Juneja, S., Kopecka, A., Kumar, R., Jenkins, R. B., De Groen, P. C., Roche, P., et al. (2004). BubR1 insufficiency causes early onset of aging-associated phenotypes and infertility in mice. Nature Genetics *36*, 744–749.

Bannister, A. J., Zegerman, P., Partridge, J. F., Miska, E. A., Thomas, J. O., Allshire, R. C., and Kouzarides, T. (2001). Selective recognition of methylated lysine 9 on histone H3 by the HP1 chromo domain. Nature *410*, 120–124.

Barford, D. (2011). Structural insights into anaphase-promoting complex function and mechanism. Philosophical Transactions of the Royal Society of London. Series B, Biological Sciences *366*, 3605–3624.

Bashir, T., Dorrello, N. V., Amador, V., Guardavaccaro, D., and Pagano, M. (2004). Control of the SCF (Skp2-Cks1) ubiquitin ligase by the APC / C Cdh1 ubiquitin ligase. Nature *428*, 190-193.

Basi, G., Schmid, E., and Maundrell, K. (1993). TATA box mutations in the *Schizosaccharomyces pombe* nmt1 promoter affect transcription efficiency but not the transcription start point or thiamine repressibility. Gene *123*, 131–136.

Basto, R., Gomes, R., and Karess, R. E. (2000). Rough deal and Zw10 are required for the metaphase checkpoint in *Drosophila*. Nature Cell Biology *2*, 939–943.

Basto, R., Scaerou, F., Mische, S., Wojcik, E., Lefebvre, C., Gomes, R., Hays, T., and Karess, R. (2004). In vivo dynamics of the rough deal checkpoint protein during *Drosophila* mitosis. Current Biology *14*, 56–61.

Basu, J., Logarinho, E., Herrmann, S., Bousbaa, H., Li, Z., Chan, G. K., Yen, T. J., Sunkel, C. E., and Goldberg, M. L. (1998). Localization of the *Drosophila* checkpoint control protein Bub3 to the kinetochore requires Bub1 but not Zw10 or Rod. Chromosoma *107*, 376–385.

Bell, S. P., and Dutta, A. (2002). DNA replication in eukaryotic cells. Annual Review of Biochemistry *71*, 333–374.

Bernard, P., Hardwick, K., and Javerzat, J.-P. (1998). Fission yeast Bub1 is a mitotic centromere protein essential for the spindle checkpoint and the preservation of correct ploidy through mitosis. The Journal of Cell Biology *143*, 1775–1787.

Bernard, P., Maure, J. F., Partridge, J. F., Genier, S., Javerzat, J. P., and Allshire, R. C. (2001). Requirement of heterochromatin for cohesion at centromeres. Science *294*, 2539–2542.

Biggins, S., and Murray, A. W. (2001). The budding yeast protein kinase Ipl1/Aurora allows the absence of tension to activate the spindle checkpoint. Genes and Development *15*, 3118–3129.

Biggins, S., Severin, F. F., Bhalla, N., Sassoon, I., Hyman, A. A., and Murray, A. W. (1999). The conserved protein kinase Ipl1 regulates microtubule binding to kinetochores in budding yeast. Genes and Development *13*, 532–544.

Bishop, J. D., and Schumacher, J. M. (2002). Phosphorylation of the carboxyl terminus of inner centromere protein (INCENP) by the Aurora B Kinase stimulates Aurora B kinase activity. The Journal of Biological Chemistry *277*, 27577–27580.

Blower, M. D., Sullivan, B. A., and Karpen, G. H. (2002). Conserved organization of centromeric chromatin in flies and humans. Developmental Cell *2*, 319–330.

Bohnert, K. A., Chen, J. J.-S., Clifford, D. M. D., Vander Kooi, C. W., and Gould, K. L. (2009). A link between aurora kinase and Clp1/Cdc14 regulation uncovered by the identification of a fission yeast borealin-like protein. Molecular Biology of the Cell *20*, 3646–3659.

Bolanos-Garcia, V. M., Beaufils, S., Renault, A., Grossmann, J. G., Brewerton, S., Lee, M., Venkitaraman, A., and Blundell, T. L. (2005). The conserved N-terminal region of the mitotic checkpoint protein BUBR1: a putative TPR motif of high surface activity. Biophysical Journal *89*, 2640–2649.

Bolanos-Garcia, V. M., Kiyomitsu, T., D'Arcy, S., Chirgadze, D. Y., Grossmann, J. G., Matak-Vinkovic, D., Venkitaraman, A. R., Yanagida, M., Robinson, C. V., and Blundell, T. L. (2009). The crystal structure of the N-terminal region of BUB1 provides insight into the mechanism of BUB1 recruitment to kinetochores. Structure *17*, 105–116.

Bolanos-Garcia, V. M., Lischetti, T., Matak-Vinković, D., Cota, E., Simpson, P. J., Chirgadze, D. Y., Spring, D. R., Robinson, C. V., Nilsson, J., and Blundell, T. L. (2011). Structure of a Blinkin-BUBR1 complex reveals an interaction crucial for kinetochore-mitoticcheckpoint regulation via an unanticipated binding site. Structure *19*, 1–10.

Bolton, M., Lan, W., and Powers, S. (2002). Aurora B kinase exists in a complex with survivin and INCENP and its kinase activity is stimulated by survivin binding and phosphorylation. Molecular Biology of the Cell *13*, 3064–3077.

Brady, D. M., and Hardwick, K. G. (2000). Complex formation between Mad1p, Bub1p and Bub3p is crucial for spindle checkpoint function. Current Biology *10*, 675–678.

Buffin, E., Lefebvre, C., Huang, J., Gagou, M. E., and Karess, R. E. (2005). Recruitment of Mad2 to the kinetochore requires the Rod/Zw10 complex. Current Biology *15*, 856–861.

Burton, J. L., and Solomon, M. J. (2001). D box and KEN box motifs in budding yeast Hsl1p are required for APC-mediated degradation and direct binding to Cdc20p and Cdh1p. Genes and Development *15*, 2381–2395.

Busso, D., Delagoutte-Busso, B., and Moras, D. (2005). Construction of a set Gateway-based destination vectors for high-throughput cloning and expression screening in *Escherichia coli*. Analytical Biochemistry *343*, 313–321.

Cahill, D. P., Lengauer, C., Yu, J., Riggins, G. J., Willson, J. K., Markowitz, S. D., Kinzler, K. W., and Vogelstein, B. (1998). Mutations of mitotic checkpoint genes in human cancers. Nature *392*, 300–303.

Campbell, M. S., Chan, G. K., and Yen, T. J. (2001). Mitotic checkpoint proteins HsMAD1 and HsMAD2 are associated with nuclear pore complexes in interphase. Journal of cell science *114*, 953–963.

Carmena, M., and Earnshaw, W. C. (2003). The cellular geography of Aurora kinases. Nature reviews. Molecular Cell Biology *4*, 842–854.

Castilho, P. V., Williams, B. C., Mochida, S., Zhao, Y., and Goldberg, M. L. (2009). The M phase kinase Greatwall (Gwl) promotes inactivation of PP2A/B55δ, a phosphatase directed against CDK phosphosites. Molecular Biology of the Cell *20*, 4777–4789.

Castillo, A. R., Meehl, J. B., Morgan, G., Schutz-Geschwender, A., and Winey, M. (2002). The yeast protein kinase Mps1p is required for assembly of the integral spindle pole body component Spc42p. The Journal of Cell Biology *156*, 453–465.

Caudron, M., Bunt, G., Bastiaens, P., and Karsenti, E. (2005). Spatial coordination of spindle assembly by chromosome-mediated signaling gradients. Science *309*, 1373–1376.

Chan, C. S., and Botstein, D. (1993). Isolation and characterization of chromosome-gain and increase-in-ploidy mutants in yeast. Genetics *135*, 677–691.

Chan, G. K., Jablonski, S. A., Starr, D. A., Goldberg, M. L., and Yen, T. J. (2000). Human Zw10 and ROD are mitotic checkpoint proteins that bind to kinetochores. Nature Cell Biology *2*, 944–947.

Chan, G. K., Jablonski, S. A., Sudakin, V., Hittle, J. C., and Yen, T. J. (1999). Human BUBR1 is a mitotic checkpoint kinase that monitors CENP-E functions at kinetochores and binds the cyclosome/APC. The Journal of Cell Biology *146*, 941–954.

Chan, Y. W., Jeyaprakash, A. A., Nigg, E. A., and Santamaria, A. (2012). Aurora B controls kinetochore-microtubule attachments by inhibiting Ska complex-KMN network interaction. The Journal of Cell Biology *196*, 563–571.

Chao, W. C. H., Kulkarni, K., Zhang, Z., Kong, E. H., and Barford, D. (2012). Structure of the mitotic checkpoint complex. Nature *484*, 208–213.

Cheeseman, I. M., Anderson, S., Jwa, M., Green, E. M., Kang, J. S., Yates, J. R., Chan, C. S. M., Drubin, D. G., and Barnes, G. (2002). Phospho-regulation of kinetochore-microtubule attachments by the Aurora kinase Ipl1p. Cell *111*, 163–172.

Cheeseman, I. M., Brew, C., Wolyniak, M., Desai, A., Anderson, S., Muster, N., Yates, J. R., Huffaker, T. C., Drubin, D. G., and Barnes, G. (2001). Implication of a novel multiprotein Dam1p complex in outer kinetochore function. The Journal of Cell Biology *155*, 1137–1146.

Cheeseman, I. M., Chappie, J. S., Wilson-Kubalek, E. M., and Desai, A. (2006). The conserved KMN network constitutes the core microtubule-binding site of the kinetochore. Cell *127*, 983–997.

Cheeseman, I. M., and Desai, A. (2008). Molecular architecture of the kinetochore-microtubule interface. Nature Reviews Molecular Cell Biology *9*, 33–46.

Cheeseman, I. M., Niessen, S., Anderson, S., Hyndman, F., Yates, J. R., Oegema, K., and Desai, A. (2004). A conserved protein network controls assembly of the outer kinetochore and its ability to sustain tension. Genes and Development *18*, 2255–2268.

Chen, E. S., Saitoh, S., Yanagida, M., and Takahashi, K. (2003). A cell cycle-regulated GATA factor promotes centromeric localization of CENP-A in fission yeast. Molecular Cell *11*, 175–187.

Chen, R. H., Waters, J. C., Salmon, E. D., and Murray, A. W. (1996). Association of spindle assembly checkpoint component XMAD2 with unattached kinetochores. Science *274*, 242–246.

Chen, R.-H. (2002). BubR1 is essential for kinetochore localization of other spindle checkpoint proteins and its phosphorylation requires Mad1. The Journal of Cell Biology *158*, 487–496.

Chen, R.-H. (2004). Phosphorylation and activation of Bub1 on unattached chromosomes facilitate the spindle checkpoint. The European Molecular Biology Organization Journal *23*, 3113–3121.

Chen, R.-H., Brady, D. M., Smith, D., Murray, A. W., and Hardwick, K. G. (1999). The spindle checkpoint of budding yeast depends on a tight complex between the Mad1 and Mad2 proteins. Molecular Biology of the Cell *10*, 2607–2618.

Chen, R.-H., Shevchenko, A., Mann, M., and Murray, A. W. (1998). Spindle checkpoint protein XMad1 recruits Xmad2 to unattached kinetochores. The Journal of Cell Biology *143*, 283–295.

Chibi, M., Meyer, M., Skepu, A., G. Rees, D. J., Moolman-Smook, J. C., and Pugh, D. J. R. (2008). RBBP6 interacts with multifunctional protein YB-1 through its RING finger domain, leading to ubiquitination and proteosomal degradation of YB-1. Journal of Molecular Biology *384*, 908–916.

Choi, E., Choe, H., Min, J., Choi, J. Y., Kim, J., and Lee, H. (2009). BubR1 acetylation at prometaphase is required for modulating APC/C activity and timing of mitosis. The European Molecular Biology Organization Journal *28*, 2077–2089.

Chu, M. L. H., Chavas, L. M. G., Douglas, K. T., Eyers, P. A., and Tabernero, L. (2008). Crystal structure of the catalytic domain of the mitotic checkpoint kinase Mps1 in complex with SP600125. The Journal of Biological Chemistry *283*, 21495–21500.

Chung, E., and Chen, R.-H. (2002). Spindle checkpoint requires Mad1-bound and Mad1-free Mad2. Molecular Biology of the Cell *13*, 1501–1511.

Ciferri, C., De Luca, J., Monzani, S., Ferrari, K. J., Ristic, D., Wyman, C., Stark, H., Kilmartin, J., Salmon, E. D., and Musacchio, A. (2005). Architecture of the human Ndc80/Hec1 complex, a critical constituent of the outer kinetochore. The Journal of Biological Chemistry *280*, 29088–29095.

Ciferri, C., Pasqualato, S., Screpanti, E., Varetti, G., Santaguida, S., Dos Reis, G., Maiolica, A., Polka, J., De Luca, J. G., De Wulf, P., et al. (2008). Implications for kinetochore-microtubule attachment from the structure of an engineered Ndc80 complex. Cell *133*, 427–439.

Cipak, L., Zhang, C., Kovacikova, I., Rumpf, C., Miadokova, E., Shokat, K. M., and Gregan, J. (2011). Generation of a set of conditional analog-sensitive alleles of essential protein kinases in the fission yeast *Schizosaccharomyces pombe*. Cell cycle *10*, 3527–3532.

Clarke, L. (1998). Centromeres: proteins, protein complexes, and repeated domains at centromeres of simple eukaryotes. Current Opinion in Genetics Development *8*, 212–218.

Cleveland, D. W., Mao, Y., and Sullivan, K. F. (2003). Centromeres and kinetochores: from epigenetics to mitotic checkpoint signaling. Cell *112*, 407–421.

Coudreuse, D., and Nurse, P. (2010). Driving the cell cycle with a minimal CDK control network. Nature *468*, 1074–1079.

Craig, J. M., Earnshaw, W. C., and Vagnarelli, P. (1999). Mammalian centromeres: DNA sequence, protein composition, and role in cell cycle progression. Experimental Cell Research *246*, 249–262.

Da Fonseca, P. C. A., and Morris, E. P. (2008). Structure of the human 26S proteasome. The Journal of Biological Chemistry *283*, 23305–23314.

Da Fonseca, P. C. A., Kong, E. H., Zhang, Z., Schreiber, A., Williams, M. A., Morris, E. P., and Barford, D. (2011). Structures of APC/C(Cdh1) with substrates identify Cdh1 and Apc10 as the D-box co-receptor. Nature *470*, 274–278.

Dai, J., Sultan, S., Taylor, S. S., and Higgins, J. M. G. (2005). The kinase haspin is required for mitotic histone H3 Thr 3 phosphorylation and normal metaphase chromosome alignment. Genes and Development *19*, 472–488.

Das, A. K., Cohen, P. W., and Barford, D. (1998). The structure of the tetratricopeptide repeats of protein phosphatase 5: implications for TPR-mediated protein-protein interactions. The European Molecular Biology Organization Journal *17*, 1192–1199.

Davenport, J., Harris, L. D., and Goorha, R. (2006). Spindle checkpoint function requires Mad2-dependent Cdc20 binding to the Mad3 homology domain of BubR1. Experimental Cell Research *312*, 1831–1842.

De Antoni, A., Pearson, C. G., Cimini, D., Canman, J. C., Sala, V., Nezi, L., Mapelli, M., Sironi, L., Faretta, M., Salmon, E. D., et al. (2005). The Mad1/Mad2 complex as a template for Mad2 activation in the spindle assembly checkpoint. Current Biology *15*, 214–225.

De Brabander, M., Geuens, G., De Mey, J., and Joniau, M. (1981). Nucleated assembly of mitotic microtubules in living PTK2 cells after release from nocodazole treatment. Cell Motility *1*, 469–483.

DeLuca, J. G., Gall, W. E., Ciferri, C., Cimini, D., Musacchio, A., and Salmon, E. D. (2006). Kinetochore microtubule dynamics and attachment stability are regulated by Hec1. Cell *127*, 969–982.

DeLuca, J. G., Howell, B. J., Canman, J. C., Hickey, J. M., Fang, G., and Salmon, E. D. (2003). Nuf2 and Hec1 are required for retention of the checkpoint proteins Mad1 and Mad2 to kinetochores. Current Biology *13*, 2103–2109.

DeLuca, K. F., Lens, S. M. A., and DeLuca, J. G. (2011). Temporal changes in Hec1 phosphorylation control kinetochore-microtubule attachment stability during mitosis. Journal of Cell Science *124*, 622–634.

Desai, A., Rybina, S., Müller-Reichert, T., Shevchenko, A. A., Hyman, A., and Oegema, K. (2003). KNL-1 directs assembly of the microtubule-binding interface of the kinetochore in *C. elegans*. Genes and Development *17* , 2421–2435.

Dewar, H., Tanaka, K., Nasmyth, K., and Tanaka, T. U. (2004). Tension between two kinetochores suffices for their bi-orientation on the mitotic spindle. Nature *428*, 93–97.

Ding, R., McDonald, K. L., and McIntosh, J. R. (1993). Three-dimensional reconstruction and analysis of mitotic spindles from the yeast, *Schizosaccharomyces pombe*. The Journal of Cell Biology *120*, 141–151.

Ditchfield, C., Johnson, V. L., Tighe, A., Ellston, R., Haworth, C., Johnson, T., Mortlock, A., Keen, N., and Taylor, S. S. (2003). Aurora B couples chromosome alignment with anaphase by targeting BubR1, Mad2, and Cenp-E to kinetochores. The Journal of Cell Biology *161*, 267–280.

Dobles, M., Liberal, V., Scott, M. L., Benezra, R., and Sorger, P. K. (2000). Chromosome missegregation and apoptosis in mice lacking the mitotic checkpoint protein Mad2. Cell *101*, 635–645.

Dorer, R. K., Zhong, S., Tallarico, J. A., Wong, W. H., Mitchison, T. J., and Murray, A. W. (2005). A small-molecule inhibitor of Mps1 blocks the spindle-checkpoint response to a lack of tension on mitotic chromosomes. Current Biology *15*, 1070–1076.

Dou, Z., Von Schubert, C., Körner, R., Santamaria, A., Elowe, S., and Nigg, E. A. (2011). Quantitative Mass Spectrometry Analysis Reveals Similar Substrate Consensus Motif for Human Mps1 Kinase and Plk1. PLoS ONE *6*, e18793.

Douville, E. M., Afar, D. E., Howell, B. W., Letwin, K., Tannock, L., Ben-David, Y., Pawson, T., and Bell, J. C. (1992). Multiple cDNAs encoding the esk kinase predict transmembrane and intracellular enzyme isoforms. Molecular and Cellular Biology *12*, 2681–2689.

Dube, P., Herzog, F., Gieffers, C., Sander, B., Riedel, D., Müller, S. a, Engel, A., Peters, J.-M., and Stark, H. (2005). Localization of the coactivator Cdh1 and the cullin subunit Apc2 in a cryo-electron microscopy model of vertebrate APC/C. Molecular Cell *20*, 867–879.

Duesbery, N. S., and Vande Woude, G. F. (1971). Cytoplasmic control of nuclear behavior during meiotic maturation of frog oocytes. The Journal of Experimental Zoology *90*, 461–466.

D'Arcy, S., Davies, O. R., Blundell, T. L., and Bolanos-Garcia, V. M. (2010). Defining the molecular basis of BubR1 kinetochore interactions and APC/C-CDC20 inhibition. The Journal of Biological Chemistry *285*, 14764–14776.

Eckerdt, F., and Strebhardt, K. (2006). Polo-like kinase 1: target and regulator of anaphase-promoting complex/cyclosome-dependent proteolysis. Cancer Research *66*, 6895–6898.

Egloff, M. P., Johnson, D. F., Moorhead, G., Cohen, P. T., Cohen, P., and Barford, D. (1997). Structural basis for the recognition of regulatory subunits by the catalytic subunit of protein phosphatase 1. The European Molecular Biology Organization Journal *16*, 1876–1887.

Elowe, S. (2011). Bub1 and BubR1: at the Interface between Chromosome Attachment and the Spindle Checkpoint. Molecular and Cellular Biology *31*, 3085–3093.

Enquist-Newman, M., Cheeseman, I. M., Van Goor, D., Drubin, D. G., Meluh, P. B., and Barnes, G. (2001). Dad1p, third component of the Duo1p/Dam1p complex involved in kinetochore function and mitotic spindle integrity. The Journal of Cell Biology *152*, 2601–2613.

Espeut, J., Cheerambathur, D. K., Krenning, L., Oegema, K., and Desai, A. (2012). Microtubule binding by KNL-1 contributes to spindle checkpoint silencing at the kinetochore. The Journal of Cell Biology *196*, 469–482.

Evans, T., Rosenthal, E. T., Youngblom, J., Distel, D., and Hunt, T. (1983). Cyclin: a protein specified by maternal mRNA in sea urchin eggs that is destroyed at each cleavage division. Cell *33*, 389–396.

Fang, G. (2002). Checkpoint protein BubR1 acts synergistically with Mad2 to inhibit anaphase-promoting complex. Molecular Biology of the Cell *13*, 755–766.

Fantes, P. A. (1977). Control of cell size and cycle time in *Schizosaccharomyces pombe*. Journal of Cell Science *24*, 51–67.

Feldman, R. M., Correll, C. C., Kaplan, K. B., and Deshaies, R. J. (1997). A complex of Cdc4p, Skp1p, and Cdc53p/cullin catalyzes ubiquitination of the phosphorylated CDK inhibitor Sic1p. Cell *91*, 221–230.

Fernius, J., and Hardwick, K. G. (2007). Bub1 kinase targets Sgo1 to ensure efficient chromosome biorientation in budding yeast mitosis. PLoS Genetics *3*, e213.

Fisk, H. A., and Winey, M. (2001). The mouse Mps1p-like kinase regulates centrosome duplication. Cell *106*, 95–104.

Foltz, D. R., Jansen, L. E. T., Black, B. E., Bailey, A. O., Yates, J. R., and Cleveland, D. W. (2006). The human CENP-A centromeric nucleosome-associated complex. Nature Cell Biology *8*, 458–469.

Forsburg, S. L., and Nurse, P. (1991). Cell cycle regulation in the yeasts *Saccharomyces cerevisiae* and *Schizosaccharomyces pombe*. Annual Review of Cell Biology *7*, 227–256.

Francisco, L., and Chan, C. S. (1994). Regulation of yeast chromosome segregation by Ipl1 protein kinase and type 1 protein phosphatase. Cellular Molecular Biology research *40*, 207–213.

Fraschini, R., Beretta, A., Lucchini, G., and Piatti, S. (2001a). Role of the kinetochore protein Ndc10 in mitotic checkpoint activation in *Saccharomyces cerevisiae*. Molecular Genetics and Genomics MGG *266*, 115–125.

Fraschini, R., Beretta, A., Sironi, L., Musacchio, A., Lucchini, G., and Piatti, S. (2001b). Bub3 interaction with Mad2, Mad3 and Cdc20 is mediated by WD40 repeats and does not require intact kinetochores. The European Molecular Biology Organization Journal *20*, 6648–6659.

Fraschini, R., Venturetti, M., Chiroli, E., and Piatti, S. (2008). The spindle position checkpoint: how to deal with spindle misalignment during asymmetric cell division in budding yeast. Biochemical Society Transactions *36*, 416–420.

Fu, J., Bian, M., Jiang, Q., and Zhang, C. (2007). Roles of Aurora kinases in mitosis and tumorigenesis. Molecular Cancer Research *5*, 1–10.

Fukagawa, T. (2004). Assembly of kinetochores in vertebrate cells. Experimental Cell Research *296*, 21–27.

Fuller, B. G., Lampson, M. A., Foley, E. A., Rosasco-Nitcher, S., Le, K. V., Tobelmann, P., Brautigan, D. L., Stukenberg, P. T., and Kapoor, T. M. (2008). Midzone activation of aurora B in anaphase produces an intracellular phosphorylation gradient. Nature *453*, 1132–1136.

Gachet, Y., Goldstone, S., and Tournier, S. (2006). The fission yeast spindle orientation checkpoint : a model that generates tension ? Yeast *23*, 1015–1029.

Gaitanos, T. N., Santamaria, A., Jeyaprakash, A. A., Wang, B., Conti, E., and Nigg, E. A. (2009). Stable kinetochore–microtubule interactions depend on the Ska complex and its new component Ska3/C13Orf3. The European Molecular Biology Organization Journal *28*, 1442–1452.

Galan, J.-M., and Peter, M. (1999). Ubiquitin-dependent degradation of multiple F-box proteins by an autocatalytic mechanism. Proceedings of the National Academy of Sciences of the United States of America *96*, 9124–9129.

Gandhi, S. R., Gierliński, M., Mino, A., Tanaka, K., Kitamura, E., Clayton, L., and Tanaka, T. U. (2011). Kinetochore-dependent microtubule rescue ensures their efficient and sustained interactions in early mitosis. Developmental Cell *21*, 920–933.

Gao, Y.-F., Li, T., Chang, Y., Wang, Y.-B., Zhang, W.-N., Li, W.-H., He, K., Mu, R., Zhen, C., Man, J.-H., et al. (2011). Cdk1-phosphorylated CUEDC2 promotes spindle checkpoint inactivation and chromosomal instability. Nature Cell Biology *13*, 1–12.

Garcia, M. A., Koonrugsa, N., and Toda, T. (2002). Two kinesin-like Kin I family proteins in fission yeast regulate the establishment of metaphase and the onset of anaphase A. Current Biology *12*, 610–621.

Gard, D. L., Becker, B. E., and Josh Romney, S. (2004). MAPping the eukaryotic tree of life: structure, function, and evolution of the MAP215/Dis1 family of microtubule-associated proteins. International Review of Cytology *239*, 179–272.

Gassmann, R., Carvalho, A., Henzing, A. J., Ruchaud, S., Hudson, D. F., Honda, R., Nigg, E. A., Gerloff, D. L., and Earnshaw, W. C. (2004). Borealin: a novel chromosomal passenger required for stability of the bipolar mitotic spindle. The Journal of Cell Biology *166*, 179–191.

Gassmann, R., Essex, A., Hu, J.-S., Maddox, P. S., Motegi, F., Sugimoto, A., O'Rourke, S. M., Bowerman, B., McLeod, I., Yates, J. R., et al. (2008). A new mechanism controlling kinetochore-microtubule interactions revealed by comparison of two dynein-targeting components: SPDL-1 and the Rod/Zwilch/Zw10 complex. Genes and Development *22*, 2385–2399.

Gassmann, R., Holland, A. J., Varma, D., Wan, X., Civril, F., Cleveland, D. W., Oegema, K., Salmon, E. D., and Desai, A. (2010). Removal of Spindly from microtubule-attached kinetochores controls spindle checkpoint silencing in human cells. Genes and Development *24*, 957–971.

Giet, R., and Prigent, C. (1999). Aurora/Ipl1p-related kinases, a new oncogenic family of mitotic serine-threonine kinases. Journal of Cell Science *112*, 3591–3601.

Gilbert, C. S., Green, C. M., and Lowndes, N. F. (2001). Budding yeast Rad9 is an ATP-dependent Rad53 activating machine. Molecular Cell *8*, 129–136.

Glotzer, M., Murray, A. W., and Kirschner, M. W. (1991). Cyclin is degraded by the ubiquitin pathway. Nature *349*, 132–138.

Glover, D. M. (2012). The overlooked greatwall: a new perspective on mitotic control. Open Biology *2*, 120023.

Glover, D. M., Leibowitz, M. H., McLean, D. a, and Parry, H. (1995). Mutations in aurora prevent centrosome separation leading to the formation of monopolar spindles. Cell *81*, 95–105.

Goshima, G., Saitoh, S., and Yanagida, M. (1999). Proper metaphase spindle length is determined by centromere proteins Mis12 and Mis6 required for faithful chromosome segregation. Genes and Development *13*, 1664–1677.

Greco, T. M., Yu, F., Guise, A. J., and Cristea, I. M. (2010). Nuclear import of histone deacetylase 5 by requisite nuclear localization signal phosphorylation. Molecular Cellular Proteomics *10*, 1–42.

Gregan, J., Polakova, S., Zhang, L., Tolić-Nørrelykke, I. M., and Cimini, D. (2011). Merotelic kinetochore attachment: causes and effects. Trends in Cell Biology *21*, 374–381.

Griffis, E. R., Stuurman, N., and Vale, R. D. (2007). Spindly, a novel protein essential for silencing the spindle assembly checkpoint, recruits dynein to the kinetochore. The Journal of Cell Biology *177*, 1005–1015.

Guardavaccaro, D., Kudo, Y., Boulaire, J., Barchi, M., Busino, L., Donzelli, M., Margottin-Goguet, F., Jackson, P. K., Yamasaki, L., and Pagano, M. (2003). Control of meiotic and mitotic progression by the F box protein b-Trcp1 in vivo. Developmental Cell *4*, 799–812.

Habu, T., and Kim, S. H. (2002). Identification of a MAD2-binding protein, CMT2, and its role in mitosis. The European Molecular Biology Organization Journal *21*, 6419–6428.

Haering, C. H., Löwe, J., Hochwagen, A., and Nasmyth, K. (2002). Molecular architecture of SMC proteins and the yeast cohesin complex. Molecular Cell *9*, 773–788.

Hagan, I. M. (2008). The spindle pole body plays a key role in controlling mitotic commitment in the fission yeast *Schizosaccharomyces pombe*. Biochemical Society Transactions *36*, 1097–1101.

Hagan, R. S., Manak, M. S., Buch, H. K., Meier, M. G., Meraldi, P., Shah, J. V., and Sorger, P. K. (2011). $p31^{comet}$ acts to ensure timely spindle checkpoint silencing subsequent to kinetochore attachment. Molecular Biology of the Cell *20*, 4236–4246.

Hanisch, A., Silljé, H. H. W., and Nigg, E. A. (2006). Timely anaphase onset requires a novel spindle and kinetochore complex comprising Ska1 and Ska2. the The European Molecular Biology Organization Journal *25*, 5504–5515.

Hanks, S. K., Quinn, A. M., and Hunter, T. (1988). The Protein Kinase Family : Conserved Features and Deduced Phylogeny of the Catalytic Domains. Science *4861*, 42–52.

Hansen, D. V., Loktev, A. V., Ban, K. H., and Jackson, P. K. (2004). Plk1 regulates activation of the anaphase promoting complex by phosphorylating and triggering SCFbetaTrCP-dependent destruction of the APC Inhibitor Emi1. Molecular Biology of the Cell *15*, 5623–5634.

Hardwick, K. G., Johnston, R. C., Smith, D. L., and Murray, A. W. (2000). MAD3 encodes a novel component of the spindle checkpoint which interacts with Bub3p, Cdc20p, and Mad2p. The Journal of Cell Biology *148*, 871–882.

Hardwick, K. G., and Murray, A.W. (1995). Mad1p, a phosphoprotein component of the spindle assembly checkpoint in budding yeast. The Journal of Cell Biology *131*, 709–720.

Hardwick, K. G., and Shah, J. V. (2010). Spindle checkpoint silencing: ensuring rapid and concerted anaphase onset. F1000 Biology Reports *2*, 55.

Hardwick, K. G., Weiss, E., Luca, F. C., Winey, M., Andrew, W., Murrayt, A. W., and Murray, A. W. (1996). Activation of the budding yeast spindle assembly checkpoint without mitotic spindle disruption. Science *273*, 953–956.

Harreman, M. T., Kline, T. M., Milford, H. G., Harben, M. B., Hodel, A. E., and Corbett, A. H. (2004). Regulation of nuclear import by phosphorylation adjacent to nuclear localization signals. The Journal of Biological Chemistry *279*, 20613–20621.

Harris, J. R. (1968). Release of a macromolecular protein component from human erythrocyte ghosts. Biochimica et Biophysica Acta *150*, 534–537.

Harrison, J. C., and Haber, J. E. (2006). Surviving the breakup: the DNA damage checkpoint. Annual Review of Genetics *40*, 209–235.

Hartwell, L. H., Culotti, J., Pringle, J. R., and Reid, B. J. (1974). Genetic control of the cell division cycle in yeast. Science *183*, 46–51.

Hartwell, L. H., and Weinert, T. A. (1989). Checkpoints: controls that ensure the order of cell cycle events. Science *246*, 629–634.

Hauf, S., Biswas, A., Langegger, M., and Kawashima, S. (2007). Aurora controls sister kinetochore mono-orientation and homolog bi-orientation in meiosis-I. The European Molecular Biology Organization Jourbal *26*, 4475–4486.

Hauf, S., Cole, R. W., LaTerra, S., Zimmer, C., Schnapp, G., Walter, R., Heckel, A., Van Meel, J., Rieder, C. L., and Peters, J.-M. (2003). The small molecule Hesperadin reveals a role for Aurora B in correcting kinetochore-microtubule attachment and in maintaining the spindle assembly checkpoint. The Journal of Cell Biology *161*, 281–294.

Hauf, S., Roitinger, E., Koch, B., Dittrich, C. M., Mechtler, K., and Peters, J.-M. (2005). Dissociation of cohesin from chromosome arms and loss of arm cohesion during early mitosis depends on phosphorylation of SA2. PLoS Biology *3*, e69.

Hauf, S., Waizenegger, I. C., and Peters, J. M. (2001). Cohesin cleavage by separase required for anaphase and cytokinesis in human cells. Science *293*, 1320–1323.

Hayashi, T., Fujita, Y., Iwasaki, O., Adachi, Y., Takahashi, K., and Yanagida, M. (2004). Mis16 and Mis18 are required for CENP-A loading and histone deacetylation at centromeres. Cell *118*, 715–729.

Hayden, J. H., Bowser, S. S., and Rieder, C. L. (1990). Kinetochores capture astral microtubules during chromosome attachment to the mitotic spindle: direct visualization in live newt lung cells. The Journal of Cell Biology *111*, 1039–1045.

Hayette, S., Tigaud, I., Vanier, A., Martel, S., Corbo, L., Charrin, C., Beillard, E., Deleage, G., Magaud, J. P., and Rimokh, R. (2000). AF15q14, a novel partner gene

fused to the MLL gene in an acute myeloid leukaemia with a t(11;15)(q23;q14). Oncogene *19*, 4446–4450.

He, X., Jones, M. H., Winey, M., and Sazer, S. (1998). Mph1, a member of the Mps1-like family of dual specificity protein kinases, is required for the spindle checkpoint in *S. pombe*. Journal of Cell Science *111*, 1635–1647.

He, X., Patterson, T. E., and Sazer, S. (1997). The *Schizosaccharomyces pombe* spindle checkpoint protein Mad2p blocks anaphase and genetically interacts with the anaphase-promoting complex. Proceedings of the National Academy of Sciences of the United States of America *94*, 7965–7970.

He, X., Rines, D. R., Espelin, C. W., and Sorger, P. K. (2001). Molecular analysis of kinetochore-microtubule attachment in budding yeast. Cell *106*, 195–206.

Heinrich, S., Windecker, H., Hustedt, N., and Hauf, S. (2012). Mph1 kinetochore localization is crucial and upstream in the hierarchy of spindle assembly checkpoint protein recruitment to kinetochores. Journal of Cell Science .

Hendrickx, A., Beullens, M., Ceulemans, H., Den Abt, T., Van Eynde, A., Nicolaescu, E., Lesage, B., and Bollen, M. (2009). Docking motif-guided mapping of the interactome of protein phosphatase-1. Chemistry and Biology *16*, 365–371.

Herzog, F., Primorac, I., Dube, P., Lenart, P., Sander, B., Mechtler, K., Stark, H., and Peters, J.-M. (2009). Structure of the anaphase-promoting complex/cyclosome interacting with a mitotic checkpoint complex. Science *323*, 1477–1481.

Hewitt, L., Tighe, A., Santaguida, S., White, A. M., Jones, C. D., Musacchio, A., Green, S., and Taylor, S. S. (2010). Sustained Mps1 activity is required in mitosis to recruit O-Mad2 to the Mad1-C-Mad2 core complex. The Journal of Cell Biology *190*, 25–34.

Higgins, J. M. G. (2010). Haspin: a newly discovered regulator of mitotic chromosome behavior. Chromosoma *119*, 137–147.

Hiraoka, Y., Toda, T., and Yanagida, M. (1984). The NDA3 gene of fission yeast encodes beta-tubulin: a cold-sensitive nda3 mutation reversibly blocks spindle formation and chromosome movement in mitosis. Cell *39*, 349–358.

Hofmann, C., Cheeseman, I. M., Goode, B. L., McDonald, K. L., Barnes, G., and Drubin, D. G. (1998). *Saccharomyces cerevisiae* Duo1p and Dam1p, novel proteins involved in mitotic spindle function. The Journal of Cell Biology *143*, 1029–1040.

Holt, L. J., Tuch, B. B., Villén, J., Johnson, A. D., Gygi, S. P., and Morgan, D. O. (2009). Global analysis of Cdk1 substrate phosphorylation sites provides insights into evolution. Science *325*, 1682–1686.

Honda, R., Ko, R., Nigg, E. A., Synchronization, C., and Körner, R. (2003). Exploring the functional interactions between Aurora B, INCENP, and survivin in mitosis. Molecular Biology of the Cell *14*, 3325–3341.

Howell, B. J., Hoffman, D. B., Fang, G., Murray, A. W., and Salmon, E. D. (2000). Visualization of Mad2 dynamics at kinetochores, along spindle fibers, and at spindle poles in living cells. The Journal of Cell Biology *150*, 1233–1250.

Howell, B. J., McEwen, B. F., Canman, J. C., Hoffman, D. B., Farrar, E. M., Rieder, C. L., and Salmon, E. D. (2001). Cytoplasmic dynein/dynactin drives kinetochore protein transport to the spindle poles and has a role in mitotic spindle checkpoint inactivation. The Journal of Cell Biology *155*, 1159–1172.

Howell, B. J., Moree, B., Farrar, E. M., Stewart, S., Fang, G., Salmon, E. D., Hall, F., Hill, C., and Carolina, N. (2004). Spindle checkpoint protein dynamics at kinetochores in living cells. Current Biology *14*, 953–964.

Hoyt, M. A., Totis, L., and Roberts, B. T. (1991). *S. cerevisiae* genes required for cell cycle arrest in response to loss of microtubule function. Cell *66*, 507–517.

Huang, H., Hittle, J., Zappacosta, F., Annan, R. S., Hershko, A., and Yen, T. J. (2008). Phosphorylation sites in BubR1 that regulate kinetochore attachment, tension, and mitotic exit. The Journal of Cell Biology *183*, 667–680.

Hwang, L. H., Lau, L. F., Smith, D. L., Mistrot, C. A., Hardwick, K. G., Hwang, E. S., Amon, A., and Murray, A. W. (1998). Budding yeast Cdc20: a target of the spindle checkpoint. Science *279*, 1041–1044.

Ikui, A. E., Furuya, K., Yanagida, M., and Matsumoto, T. (2002). Control of localization of a spindle checkpoint protein, Mad2, in fission yeast. Journal of Cell Science *115*, 1603–1610.

Indjeian, V. B., and Murray, A. W. (2007). Budding yeast mitotic chromosomes have an intrinsic bias to biorient on the spindle. Current Biology *17*, 1837–1846.

Indjeian, V. B., Stern, B. M., and Murray, A. W. (2005). The centromeric protein Sgo1 is required to sense lack of tension on mitotic chromosomes. Science *307*, 130–133.

Iouk, T., Kerscher, O., Scott, R. J., Basrai, M. A., and Wozniak, R. W. (2002). The yeast nuclear pore complex functionally interacts with components of the spindle assembly checkpoint. The Journal of Cell Biology *159*, 807–819.

Ito, D., Saito, Y., and Matsumoto, T. (2011). Centromere-tethered Mps1 pombe homolog (Mph1) kinase is a sufficient marker for recruitment of the spindle checkpoint protein Bub1, but not Mad1. Proceedings of the National Academy of Sciences of the United States of America *109*, 209-214.

Ivanov, D., and Nasmyth, K. (2005). A topological interaction between cohesin rings and a circular minichromosome. Cell *122*, 849–860.

Jablonski, S. A., Chan, G. K., Cooke, C. A., Earnshaw, W. C., and Yen, T. J. (1998). The hBUB1 and hBUBR1 kinases sequentially assemble onto kinetochores during prophase with hBUBR1 concentrating at the kinetochore plates in mitosis. Chromosoma *107*, 386–396.

Janke, C., Ortiz, J., Lechner, J., Shevchenko, A., Magiera, M. M., Schramm, C., and Schiebel, E. (2001). The budding yeast proteins Spc24p and Spc25p interact with Ndc80p and Nuf2p at the kinetochore and are important for kinetochore clustering and checkpoint control. The European Molecular Biology Organization Journal *20*, 777–791.

Jansen, L. E. T., Black, B. E., Foltz, D. R., and Cleveland, D. W. (2007). Propagation of centromeric chromatin requires exit from mitosis. The Journal of Cell Biology *176*, 795–805.

Jaspersen, S. L., Charles, J. F., and Morgan, D. O. (1999). Inhibitory phosphorylation of the APC regulator Hct1 is controlled by the kinase Cdc28 and the phosphatase Cdc14. Current biology *9*, 227–236.

Jelluma, N., Brenkman, A. B., van den Broek, N. J. F., Cruijsen, C. W. a, van Osch, M. H. J., Lens, S. M. a, Medema, R. H., and Kops, G. J. P. L. (2008a). Mps1 phosphorylates Borealin to control Aurora B activity and chromosome alignment. Cell *132*, 233–246.

Jelluma, N., Brenkman, A. B., McLeod, I., Yates, J. R., Cleveland, D. W., Medema, R. H., and Kops, G. J. P. L. (2008b). Chromosomal instability by inefficient Mps1 auto-activation due to a weakened mitotic checkpoint and lagging chromosomes. PLoS ONE *3*, e2415.

Jelluma, N., Dansen, T. B., Sliedrecht, T., Kwiatkowski, N. P., and Kops, G. J. P. L. (2010). Release of Mps1 from kinetochores is crucial for timely anaphase onset. The Journal of Cell Biology *191*, 281–290.

Jeyaprakash, A. A., Santamaria, A., Jayachandran, U., Chan, Y. W., Benda, C., Nigg, E. A., and Conti, E. (2012). Structural and functional organization of the Ska complex, a key component of the kinetochore-microtubule interface. Molecular Cell *11*, 274-286.

Jin, D. Y., Spencer, F., and Jeang, K. T. (1998). Human T cell leukemia virus type 1 oncoprotein Tax targets the human mitotic checkpoint protein MAD1. Cell *93*, 81–91.

Joglekar, A. P., Bloom, K. S., and Salmon, E. D. (2010). Mechanisms of force generation by end-on kinetochore-microtubule attachments. Current Opinion in Cell Biology *22*, 57–67.

Joglekar, A. P., Bouck, D. C., Molk, J. N., Bloom, K. S., and Salmon, E. D. (2006). Molecular architecture of a kinetochore-microtubule attachment site. Nature Cell Biology *8*, 581–585.

Joglekar, A. P., Bouck, D., Finley, K., Liu, X., Wan, Y., Berman, J., He, X., Salmon, E. D., and Bloom, K. S. (2008). Molecular architecture of the kinetochore-microtubule attachment site is conserved between point and regional centromeres. The Journal of Cell Biology *181*, 587–594.

Johnson, V. L., Scott, M. I. F., Holt, S. V., Hussein, D., and Taylor, S. S. (2004). Bub1 is required for kinetochore localization of BubR1, Cenp-E, Cenp-F and Mad2, and chromosome congression. Journal of Cell Science *117*, 1577–1589.

Jones, M. H., Huneycutt, B. J., Pearson, C. G., Zhang, C., Morgan, G., Shokat, K., Bloom, K., and Winey, M. (2005). Chemical genetics reveals a role for Mps1 kinase in kinetochore attachment during mitosis. Current Biology *15*, 160–165.

Kadura, S., He, X., Vanoosthuyse, V., Hardwick, K. G., and Sazer, S. (2005). The A78V mutation in the Mad3-like domain of *Schizosaccharomyces pombe* Bub1p perturbs nuclear accumulation and kinetochore targeting of Bub1p, Bub3p, and Mad3p and spindle assembly checkpoint function. Molecular Biology of the Cell *16*, 385–395.

Kaitna, S., Mendoza, M., Jantsch-Plunger, V., and Glotzer, M. (2000). Incenp and an aurora-like kinase form a complex essential for chromosome segregation and efficient completion of cytokinesis. Current Biology *10*, 1172–1181.

Kalab, P., Weis, K., and Heald, R. (2002). Visualization of a Ran-GTP gradient in interphase and mitotic *Xenopus* egg extracts. Science *295*, 2452–2456.

Kalitsis, P., Earle, E., Fowler, K. J., and Choo, K. H. A. (2000). Bub3 gene disruption in mice reveals essential mitotic spindle checkpoint function during early embryogenesis. Genes and Development *14*, 2277–2282.

Kallio, M. J., McCleland, M. L., Stukenberg, P. T., and Gorbsky, G. J. (2002). Inhibition of aurora B kinase blocks chromosome segregation, overrides the spindle checkpoint, and perturbs microtubule dynamics in mitosis. Current Biology *12*, 900–905.

Kang, J., Cheeseman, I. M., Kallstrom, G., Velmurugan, S., Barnes, G., and Chan, C. S. (2001). Functional cooperation of Dam1, Ipl1, and the inner centromere protein (INCENP)-related protein Sli15 during chromosome segregation. The Journal of Cell Biology *155*, 763–774.

Kang, J., Chen, Y., Zhao, Y., and Yu, H. (2007). Autophosphorylation-dependent activation of human Mps1 is required for the spindle checkpoint. Proceedings of the National Academy of Sciences of the United States of America *104*, 20232–20237.

Kang, J., Yang, M., Li, B., Qi, W., Zhang, C., Shokat, K. M., Tomchick, D. R., Machius, M., and Yu, H. (2008). Structure and substrate recruitment of the human spindle checkpoint kinase Bub1. Molecular Cell *32*, 394–405.

Kapoor, T. M., Lampson, M. A., Hergert, P., Cameron, L., Cimini, D., Salmon, E. D., McEwen, B. F., and Khodjakov, A. (2006). Chromosomes can congress to the metaphase plate before biorientation. Science *311*, 388–391.

Karess, R. (2005). Rod-Zw10-Zwilch: a key player in the spindle checkpoint. Trends in Cell Biology *15*, 386–392.

Karess, R. E., and Glover, D. M. (1989). rough deal: a gene required for proper mitotic segregation in *Drosophila*. The Journal of Cell Biology *109*, 2951–2961.

Kawashima, S. a, Tsukahara, T., Langegger, M., Hauf, S., Kitajima, T. S., and Watanabe, Y. (2007). Shugoshin enables tension-generating attachment of kinetochores by loading Aurora to centromeres. Genes and Development *21*, 420–435.

Kawashima, S. a, Yamagishi, Y., Honda, T., Ishiguro, K., and Watanabe, Y. (2010). Phosphorylation of H2A by Bub1 prevents chromosomal instability through localizing shugoshin. Science *327*, 172–177.

Kelly, A. E., Ghenoiu, C., Xue, J. Z., Zierhut, C., Kimura, H., and Funabiki, H. (2010). Survivin reads phosphorylated histone H3 threonine 3 to activate the mitotic kinase Aurora B. Science *330*, 235–239.

Kelly, T. J., and Brown, G. W. (2000). The regulation of chromosome replication. Annual Review of Biochemistry *69*, 175–179.

Kemmler, S., Stach, M., Knapp, M., Ortiz, J., Pfannstiel, J., Ruppert, T., and Lechner, J. (2009). Mimicking Ndc80 phosphorylation triggers spindle assembly checkpoint signalling. The European Molecular Biology Organization Journal *28*, 1099–1110.

Kerres, A., Jakopec, V., and Fleig, U. (2007). The conserved Spc7 protein is required for spindle integrity and links kinetochore complexes in fission yeast. Molecular Biology of the Cell *18*, 2441–2454.

Kerres, A., Vietmeier-decker, C., Ortiz, J., Karig, I., Beuter, C., Hegemann, J., Lechner, J., and Fleig, U. (2004). The fission yeast kinetochore component Spc7 associates with the EB1 family member Mal3 and is required for kinetochore – spindle association. Molecular Biology of the Cell *15*, 5255–5267.

Khodjakov, A., Copenagle, L., Gordon, M. B., Compton, D. A., and Kapoor, T. M. (2003). Minus-end capture of preformed kinetochore fibers contributes to spindle morphogenesis. The Journal of Cell Biology *160*, 671–683.

Kim, S. H., Lin, D. P., Matsumoto, S., Kitazono, A., and Matsumoto, T. (1998). Fission yeast Slp1: an effector of the Mad2-dependent spindle checkpoint. Science *279*, 1045–1047.

King, E. M. J., Rachidi, N., Morrice, N., Hardwick, K. G., and Stark, M. J. R. (2007a). Ipl1p-dependent phosphorylation of Mad3p is required for the spindle checkpoint response to lack of tension at kinetochores. Genes and Development *21*, 1163–1168.

King, E. M. J., van der Sar, S. J. a, and Hardwick, K. G. (2007b). Mad3 KEN boxes mediate both Cdc20 and Mad3 turnover, and are critical for the spindle checkpoint. PloS ONE *2*, e342.

King, J. M., Hays, T. S., and Nicklas, R. B. (2000). Dynein is a transient kinetochore component whose binding is regulated by microtubule attachment, not tension. The Journal of Cell Biology *151*, 739–748.

King, R. W., Peters, J. M., Tugendreich, S., Rolfe, M., Hieter, P., and Kirschner, M. W. (1995). A 20S complex containing CDC27 and CDC16 catalyzes the mitosis-specific conjugation of ubiquitin to cyclin B. Cell *81*, 279–288.

Kirschner, M., and Mitchison, T. (1986). Beyond self-assembly: from microtubules to morphogenesis. Cell *45*, 329–342.

Kitajima, T. S., Sakuno, T., Ishiguro, K., Iemura, S., Natsume, T., Kawashima, S. A., and Watanabe, Y. (2006). Shugoshin collaborates with protein phosphatase 2A to protect cohesin. Nature *441*, 46–52.

Kiyomitsu, T., Murakami, H., and Yanagida, M. (2011). Protein interaction domain mapping of human kinetochore protein Blinkin reveals a consensus motif for binding of spindle assembly checkpoint proteins Bub1 and BubR1. Molecular and Cellular Biology *31*, 998–1011.

Kiyomitsu, T., Obuse, C., and Yanagida, M. (2007). Human Blinkin/AF15q14 is required for chromosome alignment and the mitotic checkpoint through direct interaction with Bub1 and BubR1. Developmental Cell *13*, 663–676.

Klebig, C., Korinth, D., and Meraldi, P. (2009). Bub1 regulates chromosome segregation in a kinetochore-independent manner. The Journal of Cell Biology *185*, 841–858.

Klein, U. R., Nigg, E. A., and Gruneberg, U. (2006). Centromere targeting of the chromosomal passenger complex requires a ternary subcomplex of borealin, survivin, and the N-terminal domain of INCENP. Molecular Biology of the Cell *17*, 2547–2558.

Kniola, B., O'Toole, E., McIntosh, J. R., Mellone, B., Allshire, R., Mengarelli, S., Hultenby, K., and Ekwall, K. (2001). The domain structure of centromeres is

conserved from fission yeast to humans. Molecular Biology of the Cell *12*, 2767–2775.

Knowlton, A. L., Lan, W., and Stukenberg, P. T. (2006). Aurora B is enriched at merotelic attachment sites, where it regulates MCAK. Current Biology *16*, 1705–1710.

Koch, A., Krug, K., Pengelley, S., Macek, B., and Hauf, S. (2011). Mitotic substrates of the kinase aurora with roles in chromatin regulation identified through quantitative phosphoproteomics of fission yeast. Science signaling *4*, rs6.

Kops, G. J. P. L., Foltz, D. R., and Cleveland, D. W. (2004). Lethality to human cancer cells through massive chromosome loss by inhibition of the mitotic checkpoint. Proceedings of the National Academy of Sciences of the United States of America *101*, 8699–8704.

Kops, G. J. P. L., Kim, Y., Weaver, B. A. A., Mao, Y., McLeod, I., Yates, J. R., Tagaya, M., and Cleveland, D. W. (2005a). ZW10 links mitotic checkpoint signaling to the structural kinetochore. The Journal of Cell Biology *169*, 49–60.

Kops, G. J. P. L., Weaver, B. A. A., and Cleveland, D. W. (2005b). On the road to cancer: aneuploidy and the mitotic checkpoint. Nature Reviews. Cancer *5*, 773–785.

Kops, G. J. P. L., van der Voet, M., van der Voet, M., Manak, M. S., van Osch, M. H. J., Naini, S. M., Brear, A., McLeod, I. X., Hentschel, D. M., Yates, J. R., et al. (2010). APC16 is a conserved subunit of the anaphase-promoting complex/cyclosome. Journal of Cell Science *123*, 1623–1633.

Kosugi, S., Hasebe, M., Tomita, M., and Yanagawa, H. (2009). Systematic identification of cell cycle-dependent yeast nucleocytoplasmic shuttling proteins by prediction of composite motifs. Proceedings of the National Academy of Sciences of the United States of America *106*, 10171–10176.

Kraft, C., Herzog, F., Gieffers, C., Mechtler, K., Hagting, A., Pines, J., and Peters, J.-M. (2003). Mitotic regulation of the human anaphase-promoting complex by phosphorylation. The European Molecular Biology Organization Journal *22*, 6598–6609.

Kraft, C., Vodermaier, H. C., Maurer-Stroh, S., Eisenhaber, F., and Peters, J.-M. (2005). The WD40 propeller domain of Cdh1 functions as a destruction box receptor for APC/C substrates. Molecular Cell *18*, 543–553.

Kramer, E. R., Scheuringer, N., Podtelejnikov, A. V., Mann, M., and Peters, J.-M. M. (2000). Mitotic regulation of the APC activator proteins CDC20 and CDH1. Molecular Biology of the Cell *11*, 1555–1569.

Krenn, V., Wehenkel, A., Li, X., Santaguida, S., and Musacchio, A. (2012). Structural analysis reveals features of the spindle checkpoint kinase Bub1-kinetochore subunit Knl1 interaction. The Journal of Cell Biology *196*, 451–467.

Kulukian, A., Han, J. S., and Cleveland, D. W. (2009). Unattached kinetochores catalyze production of an anaphase inhibitor that requires a Mad2 template to prime Cdc20 for BubR1 binding. Developmental Cell *16*, 105–117.

Kumagai, A., and Dunphy, W. G. (1996). Purification and molecular cloning of Plx1, a Cdc25-regulatory kinase from *Xenopus* egg extracts. Science *273*, 1377–1380.

Kwiatkowski, N., Jelluma, N., Filippakopoulos, P., Soundararajan, M., Manak, M. S., Kwon, M., Choi, H. G., Sim, T., Deveraux, Q. L., Rottmann, S., et al. (2010). Small-molecule kinase inhibitors provide insight into Mps1 cell cycle function. Nature Chemical Biology *6*, 359–368.

Labbé, J. C., Capony, J. P., Caput, D., Cavadore, J. C., Derancourt, J., Kaghad, M., Lelias, J. M., Picard, A., and Dorée, M. (1989). MPF from starfish oocytes at first meiotic metaphase is a heterodimer containing one molecule of cdc2 and one molecule of cyclin B. The European Molecular Biology Organization Journal *8*, 3053–3058.

Labib, K., and De Piccoli, G. (2011). Surviving chromosome replication: the many roles of the S-phase checkpoint pathway. Philosophical Transactions of the Royal Society of London - Series B: Biological Sciences *366*, 3554–3561.

Labit, H., Fujimitsu, K., Bayin, N. S., Takaki, T., Gannon, J., and Yamano, H. (2012). Dephosphorylation of Cdc20 is required for its C-box-dependent activation of the APC/C. The European Molecular Biology Organization Journal *31*, 3351–3362.

Lam, Y. A., Lawson, T. G., Velayutham, M., Zweier, J. L., and Pickart, C. M. (2002). A proteasomal ATPase subunit recognizes the polyubiquitin degradation signal. Nature *416*, 763–767.

Lampson, M. A., and Kapoor, T. M. (2005). The human mitotic checkpoint protein BubR1 regulates chromosome-spindle attachments. Nature Cell Biology *7*, 93–98.

Lampson, M. A., Renduchitala, K., Khodjakov, A., and Kapoor, T. M. (2004). Correcting improper chromosome-spindle attachments during cell division. Nature Cell Biology *6*, 232–237.

Lara-Gonzalez, P., Scott, M. I. F., Diez, M., Sen, O., and Taylor, S. S. (2011). BubR1 blocks substrate recruitment to the APC/C in a KEN-box-dependent manner. Journal of Cell Science *124*, 4332–4345.

Larsen, N. A., and Harrison, S. C. (2004). Crystal Structure of the Spindle Assembly Checkpoint Protein Bub3. Journal of Molecular Biology *344*, 885–892.

Lauzé, E., Stoelcker, B., Luca, F. C., Weiss, E., Schutz, A. R., and Winey, M. (1995). Yeast spindle pole body duplication gene MPS1 encodes an essential dual specificity protein kinase. The European Molecular Biology Organization Journal *14*, 1655–1663.

LeBlanc, H. N., Tang, T. T., Wu, J. S., and Orr-Weaver, T. L. (1999). The mitotic centromeric protein MEI-S332 and its role in sister-chromatid cohesion. Chromosoma *108*, 401–411.

Lee, K. S., Park, J.-E., Asano, S., and Park, C. J. (2005). Yeast polo-like kinases: functionally conserved multitask mitotic regulators. Oncogene *24*, 217–229.

Lee, S., Thebault, P., Freschi, L., Beaufils, S., Blundell, T. L., Landry, C. R., Bolanos-Garcia, V. M., and Elowe, S. (2011). Characterization of the spindle checkpoint kinase Mps1 reveals a domain with functional and structural similarities to the tetratricopeptide repeat motifs of the Bub1 and BubR1 checkpoint kinases. The Journal of Biological Chemistry *287*, 5988–6001.

Leverson, J., Huang, H., and Forsburg, S. (2002). The *Schizosaccharomyces pombe* Aurora – related kinase Ark1 interacts with the inner centromere protein Pic1 and mediates chromosome segregation and cytokinesis. Molecular Biology of the Cell *13*, 1132–1143.

Li, R., and Murray, A. W. (1991). Feedback control of mitosis in budding yeast. Cell *66*, 519–531.

Li, W., Lan, Z., Wu, H., Wu, S., Meadows, J., Chen, J., Zhu, V., and Dai, W. (1999). BUBR1 phosphorylation is regulated during mitotic checkpoint activation. Cell Growth and Differentiation *10*, 769–775.

Li, X., and Nicklas, R. B. (1995). Mitotic forces control a cell-cycle checkpoint. Nature *373*, 630–632.

Li, Y., Bachant, J., Alcasabas, A. A., Wang, Y., Qin, J., and Elledge, S. J. (2002). The mitotic spindle is required for loading of the DASH complex onto the kinetochore. Genes and Development *16*, 183–197.

Lindberg, R. A., Fischer, W. H., and Hunter, T. (1993). Characterization of a human protein threonine kinase isolated by screening an expression library with antibodies to phosphotyrosine. Oncogene *8*, 351–359.

Lindon, C., and Pines, J. (2004). Ordered proteolysis in anaphase inactivates Plk1 to contribute to proper mitotic exit in human cells. The Journal of Cell Biology *164*, 233–241.

Liu, D., and Lampson, M. A. (2009). Regulation of kinetochore-microtubule attachments by Aurora B kinase. Biochemical Society Transactions *37*, 976–980.

Liu, D., Vleugel, M., Backer, C. B., Hori, T., Fukagawa, T., Cheeseman, I. M., and Lampson, M. A. (2010). Regulated targeting of protein phosphatase 1 to the outer kinetochore by KNL1 opposes Aurora B kinase. The Journal of Cell Biology *188*, 809–820.

Liu, F., Stanton, J. J., Wu, Z., and Piwnica-Worms, H. (1997). The human Myt1 kinase preferentially phosphorylates Cdc2 on threonine 14 and localizes to the endoplasmic reticulum and Golgi complex. Molecular and Cellular Biology *17*, 571–583.

Liu, S.-T., Chan, G. K. T., Hittle, J. C., Fujii, G., Lees, E., and Yen, T. J. (2003). Human MPS1 kinase is required for mitotic arrest induced by the loss of CENP-E from kinetochores. Molecular Biology of the Cell *14*, 1638–1651.

Liu, X., McLeod, I., Anderson, S., Yates, J. R., and He, X. (2005). Molecular analysis of kinetochore architecture in fission yeast. The European Molecular Biology Organization Journal *24*, 2919–2930.

Logarinho, E., Bousbaa, H., Dias, J. M., Lopes, C., Amorim, I., Antunes-Martins, A., and Sunkel, C. E. (2004). Different spindle checkpoint proteins monitor microtubule attachment and tension at kinetochores in *Drosophila* cells. Journal of Cell Science *117*, 1757–1771.

Logarinho, E., Resende, T., Torres, C., and Bousbaa, H. (2008). The human spindle assembly checkpoint protein Bub3 is required for the establishment of efficient kinetochore-microtubule attachments. Molecular Biology of the Cell *19*, 1798–1813.

London, N., Ceto, S., Ranish, J., and Biggins, S. (2012). Phosphoregulation of Spc105 by Mps1 and PP1 regulates Bub1 localization to kinetochores. Current Biology *22*, 900–906.

Lopes, C. S., Sampaio, P., Williams, B., Goldberg, M., and Sunkel, C. E. (2005). The Drosophila Bub3 protein is required for the mitotic checkpoint and for normal accumulation of cyclins during G2 and early stages of mitosis. Journal of Cell Science *118*, 187–198.

Losada, A., Hirano, M., and Hirano, T. (2002). Cohesin release is required for sister chromatid resolution, but not for condensin-mediated compaction, at the onset of mitosis. Genes and Development *16*, 3004–3016.

Lu, Y., Wang, Z., Ge, L., Chen, N., and Liu, H. (2009). The RZZ complex and the spindle assembly checkpoint. Cell Structure and Function *34*, 31–45.

Lyapina, S. A., Correll, C. C., Kipreos, E. T., and Deshaies, R. J. (1998). Human CUL1 forms an evolutionarily conserved ubiquitin ligase complex (SCF) with SKP1 and an F-box protein. Proceedings of the National Academy of Sciences of the United States of America *95*, 7451–7456.

Maciejowski, J., George, K. A., Terret, M.-E., Zhang, C., Shokat, K. M., and Jallepalli, P. V. (2010). Mps1 directs the assembly of Cdc20 inhibitory complexes during interphase and mitosis to control M phase timing and spindle checkpoint signaling. The Journal of Cell Biology *190*, 89–100.

Maiato, H., Rieder, C. L., and Khodjakov, A. (2004). Kinetochore-driven formation of kinetochore fibers contributes to spindle assembly during animal mitosis. The Journal of Cell Biology *167*, 831–840.

Maldonado, M., and Kapoor, T. M. (2011). Constitutive Mad1 targeting to kinetochores uncouples checkpoint signalling from chromosome biorientation. Nature Cell Biology *13*, 475–482.

Mao, Y., Desai, A., and Cleveland, D. W. (2005). Microtubule capture by CENP-E silences BubR1-dependent mitotic checkpoint signaling. The Journal of Cell Biology *170*, 873–880.

Mapelli, M., Massimiliano, L., Santaguida, S., and Musacchio, A. (2007). The Mad2 conformational dimer: structure and implications for the spindle assembly checkpoint. Cell *131*, 730–743.

Maresca, T. J., and Salmon, E. D. (2009). Intrakinetochore stretch is associated with changes in kinetochore phosphorylation and spindle assembly checkpoint activity. The Journal of Cell Biology *184*, 373–381.

Martin-Lluesma, S., Stucke, V. M., and Nigg, E. A. (2002). Role of Hec1 in spindle checkpoint signaling and kinetochore recruitment of Mad1/Mad2. Science *297*, 2267–2270.

Maskell, D. P., Hu, X.-W., and Singleton, M. R. (2010). Molecular architecture and assembly of the yeast kinetochore MIND complex. The Journal of cell biology *190*, 823–834.

Matsumoto, Y., Hayashi, K., and Nishida, E. (1999). Cyclin-dependent kinase 2 (Cdk2) is required for centrosome duplication in mammalian cells. Current Biology *9*, 429–432.

Matsuyama, A., Shirai, A., Yashiroda, Y., Kamata, A., Horinouchi, S., and Yoshida, M. (2004). pDUAL, a multipurpose, multicopy vector capable of chromosomal integration in fission yeast. Yeast *21*, 1289–1305.

Matsuyama, A., Shirai, A., and Yoshida, M. (2008). A novel series of vectors for chromosomal integration in fission yeast. Biochemical and Biophysical Research Communications *374*, 315–319.

Mattison, C. P., Old, W. M., Steiner, E., Huneycutt, B. J., Resing, K. A., Ahn, N. G., and Winey, M. (2007). Mps1 activation loop autophosphorylation enhances kinase activity. The Journal of Biological Chemistry *282*, 30553–30561.

Maure, J.-F., Kitamura, E., and Tanaka, T. U. (2007). Mps1 kinase promotes sister-kinetochore bi-orientation by a tension-dependent mechanism. Current Biology *17*, 2175–2182.

McDonald, K. L., O'Toole, E. T., Mastronarde, D. N., and McIntosh, J. R. (1992). Kinetochore microtubules in PTK cells. The Journal of Cell Biology *118*, 369–383.

McGowan, C. H., and Russell, P. (1993). Human Wee1 kinase inhibits cell division by phosphorylating p34cdc2 exclusively on Tyr15. The European Molecular Biology Organization Journal *12*, 75–85.

McGuinness, B. E., Hirota, T., Kudo, N. R., Peters, J.-M., and Nasmyth, K. (2005). Shugoshin prevents dissociation of cohesin from centromeres during mitosis in vertebrate cells. PLoS Biology *3*, e86.

Meadows, J. C., and Millar, J. (2008). Latrunculin A delays anaphase onset in fission yeast by disrupting an Ase1-independent pathway controlling mitotic spindle stability. Molecular Biology of the Cell *19*, 3713–3723.

Meadows, J. C., Shepperd, L. A., Vanoosthuyse, V., Lancaster, T. C., Sochaj, A. M., Buttrick, G. J., Hardwick, K. G., and Millar, J. B. A. (2011). Spindle checkpoint silencing requires association of PP1 to both Spc7 and kinesin-8 Motors. Developmental Cell *20*, 739–750.

Mendoza, M., Norden, C., Durrer, K., Rauter, H., Uhlmann, F., and Barral, Y. (2009). A mechanism for chromosome segregation sensing by the NoCut checkpoint. Nature Cell Biology *11*, 477-483.

Meraldi, P., Draviam, V. M., and Sorger, P. K. (2004). Timing and checkpoints in the regulation of mitotic progression. Developmental Cell *7*, 45–60.

Meraldi, P., Lukas, J., Fry, A. M., Bartek, J., and Nigg, E. A. (1999). Centrosome duplication in mammalian somatic cells requires E2F and Cdk2-cyclin A. Nature Cell Biology *1*, 88–93.

Meraldi, P., McAinsh, A. D., Rheinbay, E., and Sorger, P. K. (2006). Phylogenetic and structural analysis of centromeric DNA and kinetochore proteins. Genome Biology *7*, R23.

Millband, D. N., and Hardwick, K. G. (2002). Fission yeast Mad3p is required for Mad2p to inhibit the anaphase-promoting complex and localizes to kinetochores in a Bub1p-, Bub3p-, and Mph1p-dependent manner. Molecular and Cellular Biology *22*, 2728–2742.

Mills, G. B., Schmandt, R., McGill, M., Amendola, A., Hill, M., Jacobs, K., May, C., Rodricks, A. M., Campbell, S., and Hogg, D. (1992). Expression of TTK, a novel human protein kinase, is associated with cell proliferation. The Journal of Biological Chemistry *267*, 16000–16006.

Miniowitz-Shemtov, S., Eytan, E., Ganoth, D., Sitry-Shevah, D., Dumin, E., and Hershko, A. (2012). Role of phosphorylation of Cdc20 in p31^{comet}-stimulated disassembly of the mitotic checkpoint complex. Proceedings of the National Academy of Sciences of the United States of America *2012*, 1–5.

Mitchison, T. J., and Salmon, E. D. (2001). Mitosis: a history of division. Nature Cell Biology *3*, E17–E21.

Mitchison, T., and Kirschner, M. (1984). Dynamic instability of microtubule growth. Nature *312*, 237–242.

Mochida, S., Maslen, S. L., Skehel, M., and Hunt, T. (2010). Greatwall phosphorylates an inhibitor of protein phosphatase 2A that is essential for mitosis. Science *330*, 1670–1673.

Mondesert, O., Mcgowan, C. H., Russell, P., and Russell, P. (1996). Cig2 , a B-type cyclin, promotes the onset of S in *Schizosaccharomyces pombe* . Molecular and Cellular Biology *16*, 1527-1533.

Montembault, E., Dutertre, S., Prigent, C., and Giet, R. (2007). PRP4 is a spindle assembly checkpoint protein required for MPS1, MAD1, and MAD2 localization to the kinetochores. The Journal of Cell Biology *179*, 601–609.

Morgan, D. O. (1997). Cyclin-dependent kinases: engines, clocks, and microprocessors. Annual Review of Cell and Developmental Biology *13*, 261–291.

Morgan, D. O. (2007). The cell cycle. Principles of control.: Oxford University Press.

Mueller, P. R., Coleman, T. R., and Dunphy, W. G. (1995a). Cell cycle regulation of a *Xenopus* Wee1-like kinase. Molecular Biology of the Cell *6*, 119–134.

Mueller, P. R., Coleman, T. R., Kumagai, A., and Dunphy, W. G. (1995b). Myt1: a membrane-associated inhibitory kinase that phosphorylates Cdc2 on both threonine-14 and tyrosine-15. Science *270* , 86–90.

Mulvihill, D. P., Petersen, J., Ohkura, H., Glover, D. M., and Hagan, I. M. (1999). Plo1 kinase recruitment to the spindle pole body and its role in cell division in *Schizosaccharomyces pombe*. Molecular Biology of the Cell *10*, 2771–2785.

Musacchio, A., and Salmon, E. D. (2007). The spindle-assembly checkpoint in space and time. Nature Reviews. Molecular Cell Biology *8*, 379–393.

Nakaseko, Y., Goshima, G., Morishita, J., and Yanagida, M. (2001). M phase-specific kinetochore proteins in fission yeast: microtubule-associating Dis1 and Mtc1 display rapid separation and segregation during anaphase. Current Biology *11*, 537–549.

Nakayama, J., Rice, J. C., Strahl, B. D., Allis, C. D., and Grewal, S. I. (2001). Role of histone H3 lysine 9 methylation in epigenetic control of heterochromatin assembly. Science *292*, 110–113.

Nakayama, K. I., and Nakayama, K. (2005). Regulation of the cell cycle by SCF-type ubiquitin ligases. Seminars in Cell Developmental Biology *16*, 323–333.

Nardozzi, J. D., Lott, K., and Cingolani, G. (2010). Phosphorylation meets nuclear import: a review. Cell Communication and Signaling *8*, 32.

Nasmyth, K. (2011). Cohesin: a catenase with separate entry and exit gates? Nature cell biology *13*, 1170–1177.

Nasmyth, K. (2002). Segregating sister genomes: the molecular biology of chromosome separation. Science *297*, 559–565.

Nasmyth, K., and Haering, C. H. (2005). The structure and function of SMC and kleisin complexes. Annual Review of Biochemistry *74*, 595–648.

Nasmyth, K., Nurse, P., and Fraser, R. S. (1979). The effect of cell mass on the cell cycle timing and duration of S-phase in fission yeast. Journal of Cell Science *39*, 215–233.

Nicklas, R. B. (1997). How cells get the right chromosomes. Science *275*, 632–637.

Nicklas, R. B., and Koch, C. A. (1969). Chromosome micromanipulation. 3. Spindle fiber tension and the reorientation of mal-oriented chromosomes. The Journal of Cell Biology *43*, 40–50.

Nigg, E. A. (2001). Mitotic kinases as regulators of cell division and its checkpoints. Nature Reviews Molecular Cell Biology *2*, 21–32.

Nilsson, J., Yekezare, M., Minshull, J., and Pines, J. (2008). The APC/C maintains the spindle assembly checkpoint by targeting Cdc20 for destruction. Nature Cell Biology *10*, 1411–1420.

Nonaka, N., Kitajima, T., Yokobayashi, S., Xiao, G., Yamamoto, M., Grewal, S. I. S., and Watanabe, Y. (2002). Recruitment of cohesin to heterochromatic regions by Swi6/HP1 in fission yeast. Nature Cell Biology *4*, 89–93.

Norden, C., Mendoza, M., Dobbelaere, J., Kotwaliwale, C. V., and Biggins, S. (2006). The NoCut Pathway links completion of cytokinesis to spindle midzone function to prevent chromosome breakage. Cell *125*, 85–98.

Nurse, P. (1975). Genetic control of cell size at cell division in yeast. Nature *256*, 547–551.

Nurse, P., and Masui, Y. (1998). Understanding the cell cycle. Nature Medicine *4*, 1103–1106.

Nurse, P., Thuriaux, P., and Nasmyth, K. (1976). Genetic control of the cell division cycle in the fission yeast *Schizosaccharomyces pombe*. Molecular and General Genetics *146*, 167–178.

Oegema, K., Desai, A., Rybina, S., Kirkham, M., and Hyman, A. A. (2001). Functional analysis of kinetochore assembly in *Caenorhabditis elegans*. The Journal of Cell Biology *153*, 1209–1226.

Ohi, M. D., Feoktistova, A., Ren, L., Yip, C., Cheng, Y., Chen, J.-S., Yoon, H.-J., Wall, J. S., Huang, Z., Penczek, P. a, et al. (2007). Structural organization of the anaphase-promoting complex bound to the mitotic activator Slp1. Molecular Cell *28*, 871–885.

Ohkura, H., Adachi, Y., Kinoshita, N., Niwa, O., Toda, T., and Yanagida, M. (1988). Cold-sensitive and caffeine-supersensitive mutants of the Schizosaccharomyces pombe dis genes implicated in sister chromatid separation during mitosis. The European Molecular Biology Organization Journal 7, 1465–1473.

Ohkura, H., Kinoshita, N., Miyatani, S., Toda, T., and Yanagida, M. (1989). The fission yeast dis2+ gene required for chromosome disjoining encodes one of two putative type 1 protein phosphatases. Cell *57*, 997–1007.

Ohkura, H., and Yanagida, M. (1991). *S. pombe* gene sds22+ essential for a midmitotic transition encodes a leucine-rich repeat protein that positively modulates protein phosphatase-1. Cell *64*, 149–157.

Okada, M., Cheeseman, I. M., Hori, T., Okawa, K., McLeod, I. X., Yates, J. R., Desai, A., and Fukagawa, T. (2006). The CENP-H-I complex is required for the efficient incorporation of newly synthesized CENP-A into centromeres. Nature Cell Biology *8*, 446–457.

Okamura, A., Pendon, C., Valdivia, M. M., Ikemura, T., and Fukagawa, T. (2001). Gene structure, chromosomal localization and immunolocalization of chicken centromere proteins CENP-C and ZW10. Gene *262*, 283–290.

Ong, S.-E., Blagoev, B., Kratchmarova, I., Kristensen, D. B., Steen, H., Pandey, A., and Mann, M. (2002). Stable isotope labeling by amino acids in cell culture, SILAC, as a simple and accurate approach to expression proteomics. Molecular Cellular Proteomics *1*, 376–386.

Orlicky, S., Tang, X., Willems, A., Tyers, M., and Sicheri, F. (2003). Structural basis for phosphodependent substrate selection and orientation by the SCFCdc4 ubiquitin ligase. Cell *112*, 243–256.

Ostergren, G. (1951). The mechanisms of co-orientation in bivalents and mutivalents. Hereditas *37*, 85–156.

Pagliuca, C., Draviam, V. M., Marco, E., Sorger, P. K., and De Wulf, P. (2009). Roles for the conserved Spc105p/Kre28p complex in kinetochore-microtubule binding and the spindle assemblycheckpoint. PLoS ONE *4*, 15.

Palframan, W. J., Meehl, J. B., Jaspersen, S. L., Winey, M., and Murray, A. W. (2006). Anaphase inactivation of the spindle checkpoint. Science *313*, 680–684.

Pan, J., and Chen, R.-H. (2004). Spindle checkpoint regulates Cdc20p stability in *Saccharomyces cerevisia*e. Genes and Development *18*, 1439–1451.

Passmore, L. A, Booth, C. R., Vénien-Bryan, C., Ludtke, S. J., Fioretto, C., Johnson, L. N., Chiu, W., and Barford, D. (2005). Structural analysis of the anaphase-promoting complex reveals multiple active sites and insights into polyubiquitylation. Molecular Cell *20*, 855–866.

Peggie, M. W., MacKelvie, S. H., Bloecher, A., Knatko, E. V., Tatchell, K., and Stark, M. J. R. (2002). Essential functions of Sds22p in chromosome stability and nuclear localization of PP1. Journal of Cell Science *115*, 195–206.

Perkins, D. N., Pappin, D. J., Creasy, D. M., and Cottrell, J. S. (1999). Probability-based protein identification by searching sequence databases using mass spectrometry data. Electrophoresis *20*, 3551–3567.

Peters, J.-M. (2006). The anaphase promoting complex/cyclosome: a machine designed to destroy. Nature Reviews. Molecular Cell Biology *7*, 644–656.

Petersen, J., and Hagan, I. M. (2003). *S. pombe* aurora kinase/survivin is required for chromosome condensation and the spindle checkpoint attachment response. Current Biology *13*, 590–597.

Petersen, J., Paris, J., Willer, M., Philippe, M., and Hagan, I. M. (2001). The *S. pombe* aurora-related kinase Ark1 associates with mitotic structures in a stage dependent manner and is required for chromosome segregation. Journal of Cell Science *114*, 4371–4384.

Pfleger, C. M., and Kirschner, M. W. (2000). The KEN box: an APC recognition signal distinct from the D box targeted by Cdh1. Genes and Development *14*, 655–665.

Piatti, S., Venturetti, M., Chiroli, E., and Fraschini, R. (2006). The spindle position checkpoint in budding yeast: the motherly care of MEN. Cell division *1*, 2.

Pickart, C. M. (2001). Mechanisms underlying ubiquitination. Annual Review of Biochemistry *70*, 503–533.

Pidoux, A. L., and Allshire, R. C. (2004). Kinetochore and heterochromatin domains of the fission yeast centromere. Chromosome Research *12*, 521–534.

Pidoux, A. L., Choi, E. S., Abbott, J. K. R., Liu, X., Kagansky, A., Castillo, A. G., Hamilton, G. L., Richardson, W., Rappsilber, J., He, X., et al. (2009). Fission yeast Scm3: a CENP-A receptor required for integrity of subkinetochore chromatin. Molecular Cell *33*, 299–311.

Pidoux, A. L., Richardson, W., and Allshire, R. C. (2003). Sim4: a novel fission yeast kinetochore protein required for centromeric silencing and chromosome segregation. The Journal of Cell Biology *161*, 295–307.

Pinsky, B. A., Kotwaliwale, C. V., Tatsutani, S. Y., Breed, C. A., and Biggins, S. (2006a). Glc7/protein phosphatase 1 regulatory subunits can oppose the Ipl1/aurora protein kinase by redistributing Glc7. Molecular and Cellular Biology *26*, 2648–2660.

Pinsky, B. a, Kung, C., Shokat, K. M., and Biggins, S. (2006b). The Ipl1-Aurora protein kinase activates the spindle checkpoint by creating unattached kinetochores. Nature Cell Biology *8*, 78–83.

Poddar, A., Stukenberg, P. T., and Burke, D. J. (2005). Two complexes of spindle checkpoint proteins containing Cdc20 and Mad2 assemble during mitosis independently of the kinetochore in *Saccharomyces cerevisiae*. Eukaryotic Cell *4*, 867–878.

Pollard, T. D. (2010). Mechanics of cytokinesis in eukaryotes. Current Opinion in Cell Biology *22*, 50–56.

Posch, M., Khoudoli, G.A., Swift, S., King, E. M., Deluca, J. G., and Swedlow, J. R. (2010). Sds22 regulates aurora B activity and microtubule-kinetochore interactions at mitosis. The Journal of cell biology *191*, 61–74.

Powers, A. F., Franck, A. D., Gestaut, D. R., Cooper, J., Gracyzk, B., Wei, R. R., Wordeman, L., Davis, T. N., and Asbury, C. L. (2009). The Ndc80 kinetochore complex forms load-bearing attachments to dynamic microtubule tips via biased diffusion. Cell *136*, 865–875.

Qi, W., and Yu, H. (2007). KEN-box-dependent degradation of the Bub1 spindle checkpoint kinase by the anaphase-promoting complex/cyclosome. The Journal of Biological Chemistry *282*, 3672–3679.

Rajagopalan, S., Bimbo, A., Balasubramanian, M. K., and Oliferenko, S. (2004). A potential tension-sensing mechanism that ensures timely anaphase onset upon metaphase spindle orientation. Current Biology *14*, 69–74.

Rancati, G., Crispo, V., Lucchini, G., and Piatti, S. (2005). Mad3/BubR1 phosphorylation during spindle checkpoint activation depends on both Polo and Aurora kinases in budding yeast. Cell cycle Georgetown Tex *4*, 972–980.

Rappsilber, J., Ishihama, Y., and Mann, M. (2003). Stop and go extraction tips for matrix-assisted laser desorption/ionization, nanoelectrospray, and LC/MS sample pretreatment in proteomics. Analytical Chemistry *75*, 663–670.

Redeker, V., Melki, R., Promé, D., Le Caer, J. P., and Rossier, J. (1992). Structure of tubulin C-terminal domain obtained by subtilisin treatment. The major alpha and beta tubulin isotypes from pig brain are glutamylated. FEBS Letters *313*, 185–192.

Rieder, C. L., and Alexander, S. P. (1990). Kinetochores are transported poleward along a single astral microtubule during chromosome attachment to the spindle in newt lung cells. The Journal of Cell Biology *110*, 81–95.

Rieder, C. L., Cole, R. W., Khodjakov, A., and Sluder, G. (1995). The checkpoint delaying anaphase in response to chromosome monoorientation is mediated by an inhibitory signal produced by unattached kinetochores. The Journal of Cell Biology *130*, 941–948.

Rischitor, P. E., May, K. M., and Hardwick, K. G. (2007). Bub1 is a fission yeast kinetochore scaffold protein, and is sufficient to recruit other spindle checkpoint proteins to ectopic sites on chromosomes. PloS ONE *2*, e1342.

Robbins, J. A., and Cross, F. R. (2010). Regulated degradation of the APC coactivator Cdc20. Cell Division *5*, 23.

Roberts, B. T., Farr, K. A., and Hoyt, M. A. (1994). The *Saccharomyces cerevisia*e checkpoint gene BUB1 encodes a novel protein kinase. Molecular and Cellular Biology *14*, 8282–8291.

Rosenberg, J. S., Cross, F. R., and Funabiki, H. (2011). KNL1/Spc105 Recruits PP1 to silence the spindle assembly checkpoint. Current Biology *21*, 942–947.

Ruchaud, S., Carmena, M., and Earnshaw, W. C. (2007). Chromosomal passengers: conducting cell division. Nature Reviews Molecular Cell Biology *8*, 798–812.

Saitoh, S., Takahashi, K., and Yanagida, M. (1997). Mis6, a fission yeast inner centromere protein, acts during G1/S and forms specialized chromatin required for equal segregation. Cell *90*, 131–143.

Sakuno, T., Tada, K., and Watanabe, Y. (2009). Kinetochore geometry defined by cohesion within the centromere. Nature *458*, 852–858.

Salic, A., Waters, J. C., and Mitchison, T. J. (2004). Vertebrate shugoshin links sister centromere cohesion and kinetochore microtubule stability in mitosis. Cell *118*, 567–578.

Santaguida, S., and Musacchio, A. (2009). The life and miracles of kinetochores. The European Molecular Biology Organization Journal *28*, 2511–2531.

Santaguida, S., Tighe, A., D'Alise, A. M., Taylor, S. S., and Musacchio, A. (2010). Dissecting the role of MPS1 in chromosome biorientation and the spindle checkpoint through the small molecule inhibitor reversine. The Journal of Cell Biology *190*, 73–87.

Saunders, M., Fitzgerald-Hayes, M., and Bloom, K. (1988). Chromatin structure of altered yeast centromeres. Proceedings of the National Academy of Sciences of the United States of America *85*, 175–179.

Saurin, A. T., van der Waal, M. S., Medema, R. H., Lens, S. M. A., and Kops, G. J. P. L. (2011). Aurora B potentiates Mps1 activation to ensure rapid checkpoint establishment at the onset of mitosis. Nature Communications *2*, 316.

Schittenhelm, R. B., Chaleckis, R., and Lehner, C. F. (2009). Intrakinetochore localization and essential functional domains of Drosophila Spc105. The European Molecular Biology Organization Journal *28*, 2374–2386.

Schmandt, R., Hill, M., Amendola, A., Mills, G. B., and Hogg, D. (1994). IL-2-induced expression of TTK, a serine, threonine, tyrosine kinase, correlates with cell cycle progression. The Journal of Immunology *152*, 96–105.

Schwab, M., Lutum, A. S., and Seufert, W. (1997). Yeast Hct1 is a regulator of Clb2 cyclin proteolysis. Cell *90*, 683–693.

Scott, R. J., Cairo, L. V., Van de Vosse, D. W., and Wozniak, R. W. (2009). The nuclear export factor Xpo1p targets Mad1p to kinetochores in yeast. The Journal of Cell Biology *184*, 21–29.

Scott, R. J., Lusk, C. P., Dilworth, D. J., Aitchison, J. D., and Wozniak, R. W. (2005). Interactions between Mad1p and the nuclear transport machinery in the yeast *Saccharomyces cerevisiae*. Molecular Biology of the Cell *16*, 4362–4374.

Sczaniecka, M., Feoktistova, A., May, K. M., Chen, J.-S., Blyth, J., Gould, K. L., and Hardwick, K. G. (2008). The spindle checkpoint functions of Mad3 and Mad2 depend on a Mad3 KEN box-mediated interaction with Cdc20-anaphase-promoting complex (APC/C). The Journal of Biological Chemistry *283*, 23039–23047.

Seeley, T. W., Wang, L., and Zhen, J. Y. (1999). Phosphorylation of human MAD1 by the BUB1 kinase *in vitro*. Biochemical Biophysical Research Communication *257*, 589–595.

Sessa, F., Mapelli, M., Ciferri, C., Tarricone, C., Areces, L. B., Schneider, T. R., Stukenberg, P. T., and Musacchio, A. (2005). Mechanism of Aurora B activation by INCENP and inhibition by hesperadin. Molecular Cell *18*, 379–391.

Shah, J. V., Botvinick, E., Bonday, Z., Furnari, F., Berns, M., and Cleveland, D. W. (2004). Dynamics of centromere and kinetochore proteins; implications for checkpoint signaling and silencing. Current Biology *14*, 942–952.

Sharp-Baker, H., and Chen, R. H. (2001). Spindle checkpoint protein Bub1 is required for kinetochore localization of Mad1, Mad2, Bub3, and CENP-E, independently of its kinase activity. The Journal of Cell Biology *153*, 1239–1250.

Shepperd, L. A., Meadows, J. C., Sochaj, A. M., Lancaster, T. C., Zou, J., Buttrick, G. J., Rappsilber, J., Hardwick, K. G., and Millar, J. B. A. (2012). Phosphodependent recruitment of Bub1 and Bub3 to Spc7/KNL1 by Mph1 kinase maintains the spindle checkpoint. Current Biology *22*, 891–899.

Shevchenko, A., Wilm, M., Vorm, O., and Mann, M. (1996). Mass spectrometric sequencing of proteins silver-stained polyacrylamide gels. Analytical Chemistry *68*, 850–858.

Shimogawa, M. M., Graczyk, B., Gardner, M. K., Francis, S. E., White, E. a, Ess, M., Molk, J. N., Ruse, C., Niessen, S., Yates, J. R., et al. (2006). Mps1 phosphorylation of Dam1 couples kinetochores to microtubule plus ends at metaphase. Current Biology *16*, 1489–1501.

Shintomi, K., and Hirano, T. (2010). Sister chromatid resolution: a cohesin releasing network and beyond. Chromosoma *119*, 459–467.

Schreiber, A., Stengel, F., Zhang, Z., Enchev, R. I., Kong, E. H., Morris, E. P., Robinson, C. V., Da Fonseca, P. C. A., and Barford, D. (2011). Structural basis for the subunit assembly of the anaphase-promoting complex. Nature *470*, 227–232.

Sironi, L., Mapelli, M., Knapp, S., De Antoni, A., Jeang, K.-T., and Musacchio, A. (2002). Crystal structure of the tetrameric Mad1–Mad2 core complex: implications of a "safety belt" binding mechanism for the spindle checkpoint. The European Molecular Biology Organization Journal *21*, 2496–2506.

Skoufias, D. A., Andreassen, P. R., Lacroix, F. B., Wilson, L., and Margolis, R. L. (2001). Mammalian Mad2 and Bub1/BubR1 recognize distinct spindle-attachment and kinetochore-tension checkpoints. Proceedings of the National Academy of Sciences of the United States of America *98*, 4492–4497.

Skowyra, D., Craig, K. L., Tyers, M., Elledge, S. J., and Harper, J. W. (1997). F-box proteins are receptors that recruit phosphorylated substrates to the SCF ubiquitin-ligase complex. Cell *91*, 209–219.

Sliedrecht, T., Zhang, C., Shokat, K. M., and Kops, G. J. P. L. (2010). Chemical genetic inhibition of Mps1 in stable human cell lines reveals novel aspects of Mps1 function in mitosis. PLoS ONE *5*, 12.

Smith, D. A., Baker, B. S., and Gatti, M. (1985). Mutations in genes encoding essential mitotic functions in *Drosophila melanogaster*. Genetics *110*, 647–670.

Solomon, M. J., Lee, T., and Kirschner, M. W. (1992). Role of phosphorylation in p34cdc2 activation: identification of an activating kinase. Molecular Biology of the Cell *3*, 13–27.

Sonoda, E., Matsusaka, T., Morrison, C., Vagnarelli, P., Hoshi, O., Ushiki, T., Nojima, K., Fukagawa, T., Waizenegger, I. C., Peters, J. M., et al. (2001). Scc1/Rad21/Mcd1 is required for sister chromatid cohesion and kinetochore function in vertebrate cells. Developmental Cell *1*, 759–770.

Starr, D. A., Williams, B. C., Li, Z., Etemad-Moghadam, B., Dawe, R. K., and Goldberg, M. L. (1997). Conservation of the centromere/kinetochore protein ZW10. The Journal of Cell Biology *138*, 1289–1301.

Steigemann, P., Wurzenberger, C., Schmitz, M. H. A., Held, M., Guizetti, J., Maar, S., and Gerlich, D. W. (2009). Aurora B-mediated abscission checkpoint protects against tetraploidization. Cell *136*, 473–484.

Stewart, S., and Fang, G. (2005). Destruction box-dependent degradation of aurora B is mediated by the anaphase-promoting complex/cyclosome and Cdh1. Cancer Research *65*, 8730–8735.

Stucke, V. M., Baumann, C., and Nigg, E. A. (2004). Kinetochore localization and microtubule interaction of the human spindle checkpoint kinase Mps1. Chromosoma *113*, 1–15.

Stucke, V. M., Silljé, H. H. W., Arnaud, L., and Nigg, E. A. (2002). Human Mps1 kinase is required for the spindle assembly checkpoint but not for centrosome duplication. The European Molecular Biology Organization Journal *21*, 1723–1732.

Sudakin, V., Chan, G. K., and Yen, T. J. (2001). Checkpoint inhibition of the APC/C in HeLa cells is mediated by a complex of BUBR1, BUB3, CDC20, and MAD2. The Journal of Cell Biology *154*, 925–936.

Sudakin, V., Ganoth, D., Dahan, A., Heller, H., Hershko, J., Luca, F. C., Ruderman, J. V., and Hershko, A. (1995). The cyclosome, a large complex containing cyclin-selective ubiquitin ligase activity, targets cyclins for destruction at the end of mitosis. Molecular Biology of the Cell *6* , 185–197.

Suijkerbuijk, S. J. E., van Dam, T. J. P., Karagöz, G. E., von Castelmur, E., Hubner, N. C., Duarte, A. M. S., Vleugel, M., Perrakis, A., Rüdiger, S. G. D., Snel, B., et al. (2012). The vertebrate mitotic checkpoint protein BUBR1 is an unusual pseudokinase. Developmental Cell *22*, 1321–1329.

Suijkerbuijk, S. J. E., Van Osch, M. H. J., Bos, F. L., Hanks, S., Rahman, N., and Kops, G. J. P. L. (2010). Molecular causes for BUBR1 dysfunction in the human

cancer predisposition syndrome mosaic variegated aneuploidy. Cancer Research *70*, 4891–4900.

Sumara, I., Vorlaufer, E., Gieffers, C., Peters, B. H., and Peters, J.-M. (2000). Characterization of vertebrate cohesin complexes and their regulation in prophase. The Journal of Cell Biology *151*, 749–762.

Suzuki, A., Hori, T., Nishino, T., Usukura, J., Miyagi, A., Morikawa, K., and Fukagawa, T. (2011). Spindle microtubules generate tension-dependent changes in the distribution of inner kinetochore proteins. The Journal of Cell Biology *193*, 125–140.

Takahashi, K., Chen, E. S., and Yanagida, M. (2000). Requirement of Mis6 centromere connector for localizing a CENP-A-like protein in fission yeast. Science *288*, 2215–2219.

Takahashi, K., Takayama, Y., Masuda, F., Kobayashi, Y., and Saitoh, S. (2005). Two distinct pathways responsible for the loading of CENP-A to centromeres in the fission yeast cell cycle. Philosophical transactions of the Royal Society of London. Series B, Biological Sciences *360*, 595–606; discussion 606–7.

Tanaka, K., Kitamura, E., Kitamura, Y., and Tanaka, T. U. (2007). Molecular mechanisms of microtubule-dependent kinetochore transport toward spindle poles. The Journal of Cell Biology *178*, 269–281.

Tanaka, K., Mukae, N., Dewar, H., Van Breugel, M., James, E. K., Prescott, A. R., Antony, C., and Tanaka, T. U. (2005a). Molecular mechanisms of kinetochore capture by spindle microtubules. Nature *434*, 987–994.

Tanaka, T., Fuchs, J., Loidl, J., and Nasmyth, K. (2000). Cohesin ensures bipolar attachment of microtubules to sister centromeres and resists their precocious separation. Nature Cell Biology *2*, 492–499.

Tanaka, T. U. (2010). Kinetochore-microtubule interactions: steps towards bi-orientation. The European Molecular Biology Organization Journal *29*, 4070–4082.

Tanaka, T. U., Rachidi, N., Janke, C., Pereira, G., Galova, M., Schiebel, E., Stark, M. J. R., and Nasmyth, K. (2002). Evidence that the Ipl1-Sli15 (Aurora kinase-INCENP) complex promotes chromosome bi-orientation by altering kinetochore-spindle pole connections. Cell *108*, 317–329.

Tanaka, T. U., Stark, M. J. R., and Tanaka, K. (2005b). Kinetochore capture and bi-orientation on the mitotic spindle. Nature Reviews. Molecular Cell Biology *6*, 929–942.

Tang, T. T.-L., Bickel, S. E., Young, L. M., and Orr-Weaver, T. L. (1998). Maintenance of sister-chromatid cohesion at the centromere by the *Drosophila* MEI-S332 protein. Genes and Development *12*, 3843–3856.

Tang, Z., Bharadwaj, R., Li, B., and Yu, H. (2001). Mad2-Independent inhibition of APC-Cdc20 by the mitotic checkpoint protein BubR1. Developmental Cell *1*, 227–237.

Tang, Z., Shu, H., Oncel, D., Chen, S., and Yu, H. (2004). Phosphorylation of Cdc20 by Bub1 provides a catalytic mechanism for APC/C inhibition by the spindle checkpoint. Molecular Cell *16*, 387–397.

Tang, Z., Shu, H., Qi, W., Mahmood, N. A., Mumby, M. C., and Yu, H. (2006). PP2A is required for centromeric localization of Sgo1 and proper chromosome segregation. Developmental Cell *10*, 575–585.

Tange, Y., and Niwa, O. (2008). *Schizosaccharomyces pombe* Bub3 is dispensable for mitotic arrest following perturbed spindle formation. Genetics *792*, 785–792.

Taylor, S. S., Ha, E., and McKeon, F. (1998). The human homologue of Bub3 is required for kinetochore localization of Bub1 and a Mad3/Bub1-related protein kinase. The Journal of Cell Biology *142*, 1–11.

Taylor, S. S., Hussein, D., Wang, Y., Elderkin, S., and Morrow, C. J. (2001). Kinetochore localisation and phosphorylation of the mitotic checkpoint components Bub1 and BubR1 are differentially regulated by spindle events in human cells. Journal of Cell Science *114*, 4385–4395.

Taylor, S. S., and McKeon, F. (1997). Kinetochore localization of murine Bub1 is required for normal mitotic timing and checkpoint response to spindle damage. Cell *89*, 727–735.

Teichner, A., Eytan, E., Sitry-Shevah, D., Miniowitz-Shemtov, S., Dumin, E., Gromis, J., and Hershko, A. (2011). p31^{comet} promotes disassembly of the mitotic checkpoint complex in an ATP-dependent process. Proceedings of the National Academy of Sciences of the United States of America *108*, 3187–3192.

Telzer, B. R., Moses, M. J., and Rosenbaum, J. L. (1975). Assembly of microtubules onto kinetochores of isolated mitotic chromosomes of HeLa cells. Proceedings of the National Academy of Sciences of the United States of America *72*, 4023–4027.

Teng, A. C. T., Al-montashiri, N. A. M., Cheng, B. L. M., Lou, P., Ozmizrak, P., Chen, H.-H., and Stewart, A. F. R. (2011). Identification of a phosphorylation-dependent nuclear localization motif in interferon regulatory factor 2 binding protein 2. PLoS ONE *6*, 8.

Thornton, B. R., and Toczyski, D. P. (2003). Securin and B-cyclin/CDK are the only essential targets of the APC. Nature Cell Biology *5*, 1090–1094.

Tighe, A., Staples, O., and Taylor, S. (2008). Mps1 kinase activity restrains anaphase during an unperturbed mitosis and targets Mad2 to kinetochores. The Journal of Cell Biology *181*, 893–901.

Tippit, D. H., Pickett-Heaps, J. D., and Leslie, R. (1980). Cell division in two large pennate diatoms Hantzschia and Nitzschia III. A new proposal for kinetochore function during prometaphase. The Journal of Cell Biology *86*, 402–416.

Tournier, S., Gachet, Y., Buck, V., Hyams, J. S., and Millar, J. B. A. (2004). Disruption of astral microtubule contact with the cell cortex activates a Bub1, Bub3, and Mad3-dependent checkpoint in fission yeast. Molecular Biology of the Cell *15*, 3345–3356.

Trinkle-Mulcahy, L., Andersen, J., Lam, Y. W., Moorhead, G., Mann, M., and Lamond, A. I. (2006). Repo-Man recruits PP1 gamma to chromatin and is essential for cell viability. The Journal of Cell Biology *172*, 679–692.

Trinkle-Mulcahy, L., and Andrews, P. (2003). Time-lapse imaging reveals dynamic relocalization of PP1γ throughout the mammalian cell cycle. Molecular Biology of the Cell *14*, 107–117.

Tseng, T. C., Chen, S. H., Hsu, Y. P., and Tang, T. K. (1998). Protein kinase profile of sperm and eggs: cloning and characterization of two novel testis-specific protein kinases (AIE1, AIE2) related to yeast and fly chromosome segregation regulators. DNA and Cell Biology *17*, 823–833.

Uchida, K. S. K., Takagaki, K., Kumada, K., Hirayama, Y., Noda, T., and Hirota, T. (2009). Kinetochore stretching inactivates the spindle assembly checkpoint. The Journal of Cell Biology *184*, 383–390.

Uhlmann, F., Lottspeich, F., and Nasmyth, K. (1999). Sister-chromatid separation at anaphase onset is promoted by cleavage of the cohesin subunit Scc1. Nature *400*, 37–42.

Uhlmann, F., Wernic, D., Poupart, M. A., Koonin, E. V., and Nasmyth, K. (2000). Cleavage of cohesin by the CD clan protease separin triggers anaphase in yeast. Cell *103*, 375–386.

Uzawa, S., and Yanagida, M. (1992). Visualization of centromeric and nucleolar DNA in fission yeast by fluorescence in situ hybridization. Journal of Cell Science *101*, 267–275.

Uzunova, K., Dye, B. T., Schutz, H., Ladurner, R., Petzold, G., Toyoda, Y., Jarvis, M. A., Brown, N. G., Poser, I., Novatchkova, M., et al. (2012). APC15 mediates CDC20 autoubiquitylation by APC/CMCC and disassembly of the mitotic checkpoint complex. Nature Structural and Molcular Biology *19*, 1116–1123.

Vader, G., Kauw, J. J. W., Medema, R. H., and Lens, S. M. A. (2006). Survivin mediates targeting of the chromosomal passenger complex to the centromere and midbody. European Molecular Biology Organization Reports *7*, 85–92.

Vanoosthuyse, V., and Hardwick, K. G. (2009). A novel protein phosphatase 1-dependent spindle checkpoint silencing mechanism. Current Biology *19*, 1176–1181.

Vanoosthuyse, V., Meadows, J. J. C., van der Sar, S. J. A., Millar, J. B. A., and Hardwick, K. G. (2009). Bub3p facilitates spindle checkpoint silencing in fission yeast. Molecular Biology of the Cell *20*, 5096–5105.

Vanoosthuyse, V., Prykhozhij, S., and Hardwick, K. G. (2007). Shugoshin 2 regulates localization of the chromosomal passenger proteins in fission yeast mitosis. Molecular Biology of the Cell *18*, 1657–1669.

Vanoosthuyse, V., Valsdottir, R., Javerzat, J. P., and Hardwick, K. G. (2004). Kinetochore targeting of fission yeast Mad and Bub proteins is essential for spindle checkpoint function but not for all chromosome segregation roles of Bub1p. Molecular and Cellular Biology *24*, 9786–9801.

Vialard, J. E., Gilbert, C. S., Green, C. M., and Lowndes, N. F. (1998). The budding yeast Rad9 checkpoint protein is subjected to Mec1/Tel1-dependent hyperphosphorylation and interacts with Rad53 after DNA damage. The European Molecular Biology Organization Journal *17*, 5679–5688.

Vink, M., Simonetta, M., Transidico, P., Ferrari, K., Mapelli, M., De Antoni, A., Massimiliano, L., Ciliberto, A., Faretta, M., Salmon, E. D., et al. (2006). In vitro FRAP identifies the minimal requirements for Mad2 kinetochore dynamics. Current Biology *16*, 755–766.

Visintin, R. (1997). CDC20 and CDH1: A family of substrate-specific activators of APC-dependent proteolysis. Science *278*, 460–463.

Vleugel, M., Hoogendoorn, E., Snel, B., and Kops, G. J. P. L. (2012). Evolution and function of the mitotic checkpoint. Developmental Cell *23*, 239–250.

Vodermaier, H. C., Gieffers, C., Maurer-Stroh, S., Eisenhaber, F., and Peters, J. (2003). TPR Subunits of the Anaphase-Promoting Complex Mediate Binding to the Activator Protein CDH1. Current Biology *13*, 1459–1468.

Vodermaier, H. C. (2004). APC/C and SCF: controlling each other and the cell cycle. Current Biology *14*, R787–96.

Vogel, S. K., Raabe, I., Dereli, A., Maghelli, N., and Tolić-Nørrelykke, I. (2007). Interphase microtubules determine the initial alignment of the mitotic spindle. Current Biology *17*, 438–444.

Voges, D., Zwickl, P., and Baumeister, W. (1999). The 26S proteasome: a molecular machine designed for controlled proteolysis. Annual Review of Biochemistry *68*, 1015–1068.

Waizenegger, I. C., Hauf, S., Meinke, A., and Peters, J. M. (2000). Two distinct pathways remove mammalian cohesin from chromosome arms in prophase and from centromeres in anaphase. Cell *103*, 399–410.

Walz, J., Erdmann, A., Kania, M., Typke, D., Koster, A. J., and Baumeister, W. (1998). 26S proteasome structure revealed by three-dimensional electron microscopy. Journal of Structural Biology *121*, 19–29.

Wang, F., Dai, J., Daum, J. R., Niedzialkowska, E., Banerjee, B., Stukenberg, P. T., Gorbsky, G. J., and Higgins, J. M. G. (2010). Histone H3 Thr-3 phosphorylation by Haspin positions Aurora B at centromeres in mitosis. Science *330*, 231–235.

Wang, Q., Liu, T., Fang, Y., Xie, S., Huang, X., Mahmood, R., Ramaswamy, G., Sakamoto, K. M., Darzynkiewicz, Z., Xu, M., et al. (2004). BUBR1 deficiency results in abnormal megakaryopoiesis. Blood *103*, 1278–1285.

Wang, W., Yang, Y., Gao, Y., Xu, Q., Wang, F., Zhu, S., Old, W., Resing, K., Ahn, N., Lei, M., et al. (2009). Structural and mechanistic insights into Mps1 kinase activation. Journal of Cellular and Molecular Medicine *13*, 1679–1694.

Wang, X., Babu, J. R., Harden, J. M., Jablonski, S. A., Gazi, M. H., Lingle, W. L., De Groen, P. C., Yen, T. J., and Van Deursen, J. M. (2001). The mitotic checkpoint protein hBUB3 and the mRNA export factor hRAE1 interact with GLE2p-binding sequence (GLEBS)-containing proteins. The Journal of Biological Chemistry *276*, 26559–26567.

Wasserman, W. J., and Masui, Y. (1976). A cytoplasmic factor promoting oocyte maturation: its extraction and preliminary characterization. Science *191*, 1266–1268.

Watanabe, N., Arai, H., Nishihara, Y., Taniguchi, M., Watanabe, N., Hunter, T., and Osada, H. (2004). M-phase kinases induce phospho-dependent ubiquitination of somatic Wee1 by SCFbeta-TrCP. Proceedings of the National Academy of Sciences of the United States of America *101*, 4419–4424.

Watanabe, Y., and Kitajima, T. S. (2005). Shugoshin protects cohesin complexes at centromeres. Philosophical transactions of the Royal Society of London. Series B, Biological Sciences *360*, 515–21, discussion 521.

Waters, J. C., Chen, R. H., Murray, A. W., and Salmon, E. D. (1998). Localization of Mad2 to kinetochores depends on microtubule attachment, not tension. The Journal of Cell Biology *141*, 1181–1191.

Wei, R. R., Al-Bassam, J., and Harrison, S. C. (2007). The Ndc80/HEC1 complex is a contact point for kinetochore-microtubule attachment. Nature Structural and Molecular Biology *14*, 54–59.

Wei, R. R., Schnell, J. R., Larsen, N. A., Sorger, P. K., Chou, J. J., and Harrison, S. C. (2006). Structure of a central component of the yeast kinetochore: the Spc24p/Spc25p globular domain. Structure *14*, 1003–1009.

Wei, R. R., Sorger, P. K., and Harrison, S. C. (2005). Molecular organization of the Ndc80 complex, an essential kinetochore component. Proceedings of the National Academy of Sciences of the United States of America *102*, 5363–5367.

Wei, W., Ayad, N. G., Wan, Y., Zhang, G.-J., Kirschner, M. W., and Kaelin, W. G. (2004). Degradation of the SCF component Skp2 in cell-cycle phase G1 by the anaphase-promoting complex. Nature *428*, 194–198.

Weinert, T. A., and Hartwell, L. H. (1988). The RAD9 gene controls the cell cycle response to DNA damage in *Saccharomyces cerevisiae*. Science *241*, 317–322.

Welburn, J. P. I., Grishchuk, E. L., Backer, C. B., Wilson-Kubalek, E. M., Yates, J. R., Cheeseman, I. M., Wilson-, E. M., and Iii, J. R. Y. (2009). The human kinetochore Ska1 complex facilitates microtubule depolymerization-coupled motility. Developmental Cell *16*, 374–385.

Welburn, J. P. I., Vleugel, M., Liu, D., Yates III, J. R., Lampson, M. A., Fukagawa, T., and Cheeseman, I. M. (2010). Aurora B phosphorylates spatially distinct targets to differentially regulate the kinetochore-microtubule interface. Molecular Cell *38*, 383–392.

West, R. R., Malmstrom, T., and McIntosh, J. R. (2002). Kinesins klp5(+) and klp6(+) are required for normal chromosome movement in mitosis. Journal of Cell Science *115*, 931–940.

Westermann, S., Avila-Sakar, A., Wang, H.-W., Niederstrasser, H., Wong, J., Drubin, D. G., Nogales, E., and Barnes, G. (2005). Formation of a dynamic kinetochore-microtubule interface through assembly of the Dam1 ring complex. Molecular Cell *17*, 277–290.

Westermann, S., Drubin, D. G., and Barnes, G. (2007). Structures and functions of yeast kinetochore complexes. Annual Review of Biochemistry *76*, 563–591.

Westermann, S., Wang, H.-W., Avila-Sakar, A., Drubin, D. G., Nogales, E., and Barnes, G. (2006). The Dam1 kinetochore ring complex moves processively on depolymerizing microtubule ends. Nature *440*, 565–569.

Westhorpe, F. G., Tighe, A., Lara-Gonzalez, P., and Taylor, S. S. (2011). p31^{comet}-mediated extraction of Mad2 from the MCC promotes efficient mitotic exit. Journal of Cell Science *124*, 3905–3916.

Whyte, J., Bader, J. R., Tauhata, S. B. F., Raycroft, M., Hornick, J., Pfister, K. K., Lane, W. S., Chan, G. K., Hinchcliffe, E. H., Vaughan, P. S., et al. (2008).

Phosphorylation regulates targeting of cytoplasmic dynein to kinetochores during mitosis. The Journal of Cell Biology *183*, 819–834.

Wilk, S., and Orlowski, M. (1980). Cation-sensitive neutral endopeptidase: isolation and specificity of the bovine pituitary enzyme. Journal of Neurochemistry *35*, 1172–1182.

Wilk, S., and Orlowski, M. (1983). Evidence that pituitary cation-sensitive neutral endopeptidase is a multicatalytic protease complex. Journal of Neurochemistry *40*, 842–849.

Williams, B. C., Li, Z., Liu, S., Williams, E. V., Leung, G., Yen, T. J., and Goldberg, M. L. (2003). Zwilch, a new component of the ZW10/ROD complex required for kinetochore functions. Molecular Biology of the Cell *14*, 1379–1391.

Windecker, H., Langegger, M., Heinrich, S., and Hauf, S. (2009). Bub1 and Bub3 promote the conversion from monopolar to bipolar chromosome attachment independently of shugoshin. European Molecular Biology Organization reports *10*, 1022–1028.

Winey, M., Goetsch, L., Baum, P., and Byers, B. (1991). MPS1 and MPS2: novel yeast genes defining distinct steps of spindle pole body duplication. The Journal of Cell Biology *114*, 745–754.

Winey, M., Mamay, C. L., O'Toole, E. T., Mastronarde, D. N., Giddings, T. H., McDonald, K. L., and McIntosh, J. R. (1995). Three-dimensional ultrastructural analysis of the *Saccharomyces cerevisiae* mitotic spindle. The Journal of Cell Biology *129*, 1601–1615.

Witt, P. L., Ris, H., and Borisy, G. G. (1980). Origin of kinetochore microtubules in Chinese hamster ovary cells. Chromosoma *81*, 483–505.

Wittmann, T., Hyman, A., and Desai, A. (2001). The spindle: a dynamic assembly of microtubules and motors. Nature Cell Biology *3*, E28–E34.

Wojcik, E., Basto, R., Serr, M., Scaërou, F., Karess, R., and Hays, T. (2001). Kinetochore dynein: its dynamics and role in the transport of the Rough deal checkpoint protein. Nature Cell Biology *3*, 1001–1007.

Wong, O. K., and Fang, G. (2007). Cdk1 phosphorylation of BubR1 controls spindle checkpoint arrest and Plk1-mediated formation of the 3F3/2 epitope. The Journal of Cell Biology *179*, 611–617.

Wood, V., Gwilliam, R., Rajandream, M., Lyne, M., Lyne, R., Stewart, A., Sgouros, J., Peat, N., Hayles, J., Baker, S., et al. (2002). The genome sequence of *Schizosaccharomyces pombe.* Nature *415*, 871-880.

Xia, G., Luo, X., Habu, T., Rizo, J., Matsumoto, T., and Yu, H. (2004). Conformation-specific binding of p31^{comet} antagonizes the function of Mad2 in the spindle checkpoint. The European Molecular Biology Organization Journal *23*, 3133–3143.

Yamagishi, Y., Honda, T., Tanno, Y., and Watanabe, Y. (2010). Two histone marks establish the inner centromere and chromosome bi-orientation. Science *330*, 239–243.

Yamagishi, Y., Yang, C.-H., Tanno, Y., and Watanabe, Y. (2012). MPS1/Mph1 phosphorylates the kinetochore protein KNL1/Spc7 to recruit SAC components. Nature Cell Biology *14*, 1–9.

Yamaguchi, S., Decottignies, A., and Nurse, P. (2003). Function of Cdc2p-dependent Bub1p phosphorylation and Bub1p kinase activity in the mitotic and meiotic spindle checkpoint. The European Molecular Biology Organization Journal *22*, 1075–1087.

Yamamoto, A., and Hiraoka, Y. (2003). Monopolar spindle attachment of sister chromatids is ensured by two distinct mechanisms at the first meiotic division in fission yeast. The European Molecular Biology Organization Journal *22*, 2284–2296.

Yamamoto, T. G., Watanabe, S., Essex, A., and Kitagawa, R. (2008). SPDL-1 functions as a kinetochore receptor for MDF-1 in *Caenorhabditis elegans*. The Journal of Cell Biology *183*, 187–194.

Yamano, H., Gannon, J., Mahbubani, H., and Hunt, T. (2004). Cell cycle-regulated recognition of the destruction box of cyclin B by the APC/C in *Xenopus* egg extracts. Molecular Cell 13, 137–147.

Yang, F., Hu, L., Chen, C., Yu, J., O'Connell, C. B., Khodjakov, A., Pagano, M., and Dai, W. (2011). BubR1 is modified by sumoylation during mitotic progression. Journal of Biological Chemistry *287*, 4875–4882.

Yang, F., Huang, Y., and Dai, W. (2012). Sumoylated BubR1 plays an important role in chromosome segregation and mitotic timing. Cell Cycle *11*. 797-806.

Yang, K.-T., Li, S.-K., Chang, C.-C., Tang, C.-J. C., Lin, Y.-N., Lee, S.-C., and Tang, T. K. (2010). Aurora-C kinase deficiency causes cytokinesis failure in meiosis I and production of large polyploid oocytes in mice. Molecular Biology of the Cell *21*, 2371–2383.

Yang, M., Li, B., Tomchick, D. R., Machius, M., Rizo, J., Yu, H., and Luo, X. (2007a). p31^{comet} blocks Mad2 activation through structural mimicry. Cell *131*, 744–755.

Yang, Z., Tulu, U. S., Wadsworth, P., and Rieder, C. L. (2007b). Kinetochore dynein is required for chromosome motion and congression independent of the spindle checkpoint. Current Biology *17*, 973–980.

Yeh, E., Skibbens, R. V., Cheng, J. W., Salmon, E. D., and Bloom, K. (1995). Spindle dynamics and cell cycle regulation of dynein in the budding yeast, *Saccharomyces cerevisiae*. The Journal of Cell Biology *130*, 687–700.

Yen, H.-C. S., and Elledge, S. J. (2008). Identification of SCF ubiquitin ligase substrates by global protein stability profiling. Science *322*, 923–929.

Zachariae, W. (1998). Control of cyclin ubiquitination by CDK-regulated binding of Hct1 to the Anaphase Promoting Complex. Science *282*, 1721–1724.

Zhang, F., White, R. L., and Neufeld, K. L. (2001). Cell density and phosphorylation control the subcellular localization of adenomatous polyposis coli protein. Molecular and Cellular Biology *21*, 8143–8156.

Zhao, Y., Haccard, O., Wang, R., Yu, J., Kuang, J., Jessus, C., and Goldberg, M. L. (2008). Roles of Greatwall kinase in the regulation of Cdc25 phosphatase. Molecular Biology of the Cell *19*, 1317–1327.

Zheng, N., Schulman, B. a, Song, L., Miller, J. J., Jeffrey, P. D., Wang, P., Chu, C., Koepp, D. M., Elledge, S. J., Pagano, M., et al. (2002). Structure of the Cul1-Rbx1-Skp1-F boxSkp2 SCF ubiquitin ligase complex. Nature *416*, 703–709.

Zich, J., and Hardwick, K. G. (2010). Getting down to the phosphorylated "nuts and bolts" of spindle checkpoint signalling. Trends in Biochemical Sciences *35*, 18–27.

Zich, J., Sochaj, A. M., Syred, H. M., Milne, L., Cook, A. G., Ohkura, H., Rappsilber, J., and Hardwick, K. G. (2012). Kinase activity of fission yeast mph1 is required for Mad2 and Mad3 to stably bind the anaphase promoting complex. Current Biology *22*, 296–301.

Supplementary Material

A

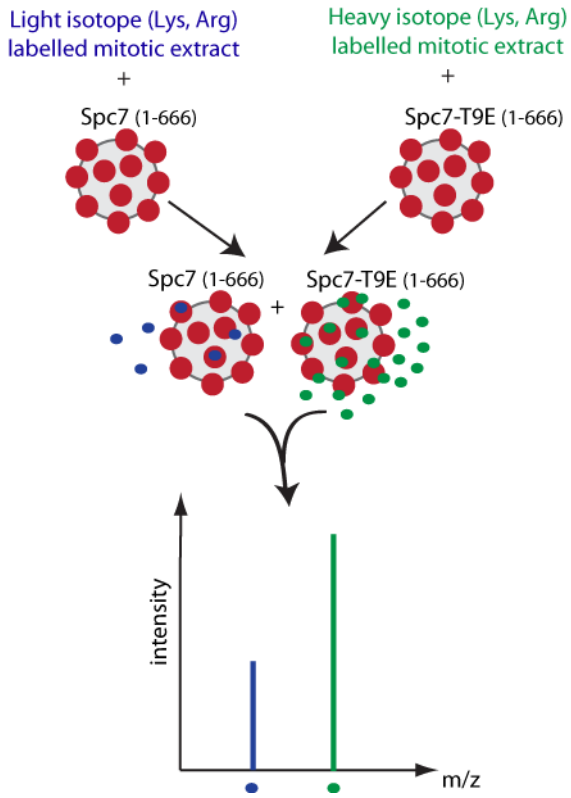

Supplementary Figure 1. A. 'Hunting' for unknown Spc7 interactors using the SILAC approach. A schematic representation of the stable-isotope labeling in cell culture (SILAC) method. Stably labeled amino acids (heavy lysine and arginine) are incorporated into the proteome of *nda-KM311* cells, which are shifted to 18ºC for the last six hours of the incubation to block the cells in metaphase. Cells, which were grown in the 'light' (normal) medium are treated the same. Cell extracts from the 'heavy' and 'light' cultures are incubated with beads coated with recombinant Spc7-T9E (1-666) and recombinant Spc7 (1-666), respectively. Following incubation, the beads are mixed and proteins are eluted using SDS gel-loading dye. Proteins are trypsinized and the peptides are analyzed by mass spectrometry. After analysis, 'heavy' and 'light' peptides are reflected by two different peaks. This allows the levels of protein bound to the Spc7-T9E (1-666) and Spc7 (1-666) beads to be relatively quantified**.**

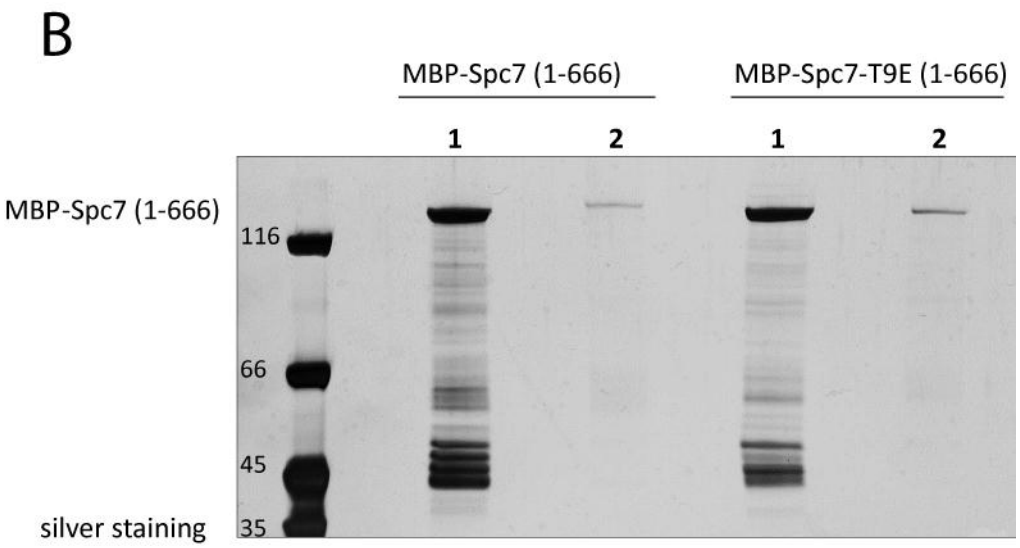

Supplementary Figure 1. B. Crosslinking recombinant MBP-Spc7 (1-666) to AminoLink resin results in reduced amount of the eluted recombinant Spc7 in a final sample. MBP-Spc7 (1-666) and MBP-Spc7-T9E (1-666) were immobilized either using 1-Amylose resin (NEB) or 2-AminoLink resin (Pierce). After elution with SDS gel-running buffers, samples were separated by 4 - 12 % precast NuPAGE gradient gel (Invitrogen) and the gel was subjected to silver staining [Silver Stain Kit (Pierce)].

Supplementary Figure 1. C. The Spc7 interactors (Bub1 and Dis2) bind MBP-Spc7 (1-666) and MBP-Spc7-T9E (1-666) immobilized on AminoLink and Amylose resin with similar efficiency. Samples after an in vitro Spc7 binding experiment were run on a 10 % SDS-PAGE gel and different parts of the membrane were immunoblotted with PAP and anti-Dis2 antibodies; 1x-50 µl of resin used, 2x-100 µl of resin used.

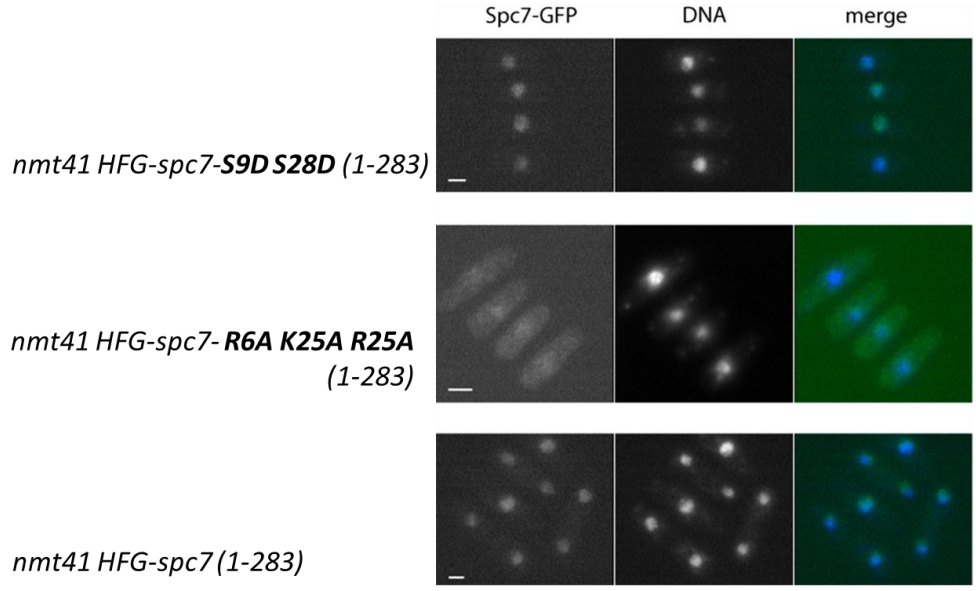

Supplementary Figure 2. Mimicking Ark1-dependent phosphorylation in the very N-terminus of Spc7 does not interfere with Spc7 nuclear translocation. Log-phase cells overexpressing HFG-Spc7-S9D S28D (1-283), HFG-Spc7-BP 1&2 (1-283) and HFG-Spc7 (1-283) under the nmt41 promoter for 18 hours at 30°C were fixed and stained with DAPI, scale bar 4 μm.

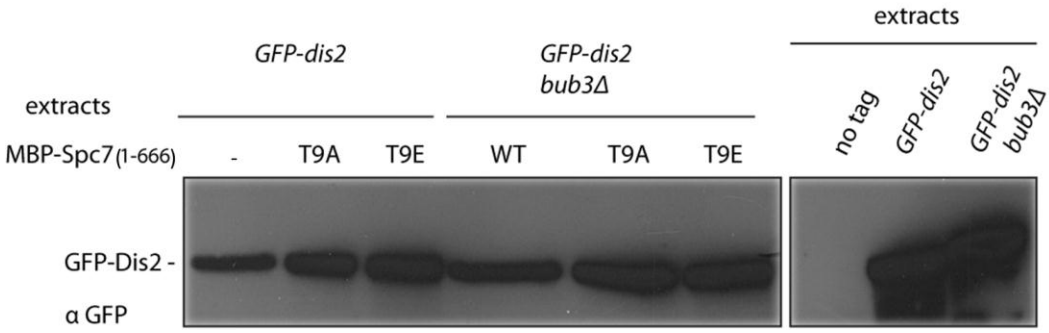

Supplementary Figure 3. The Spc7 MELT motifs phosphorylation status does not influence the interaction between Dis2 and Spc7. Beads coated with recombinant, MBP tagged Spc7 (1-666), Spc7-T9A (1-666) and Spc7-T9E (1-666) were incubated with *GFP-dis2* and *GFP-dis2 bub3Δ* cell extracts. Pull downs and extracts were separated by 10% SDS-PAGE gel and the membrane was probed with anti-GFP antibody.

Acknowledgements

Acknowledgements

I would like to acknowledge all the people who contributed to this thesis. It would not have been possible to finish my PhD without the help and support of the kind people around me.

I would like to express my deepest gratitude to my supervisor, Dr. Kevin Hardwick, for his excellent guidance, patience and understanding. It was a pleasure to work for someone who allowed me the room to develop as a scientist in my own way.

I would like to thank Prof. Jonathan Millar for interesting scientific discussions, sharing new ideas and fruitful collaboration on the Spc7 project.

I would also like to thank my examiners, Professor Robin C. Allshire and Professor Greet J.P.L. Kops, who provided a very constructive feedback. It is no easy task, reviewing a thesis, and I am grateful for their thoughtful and detailed comments.

I am very grateful to all the members of the Hardwick and Marston labs for a great atmosphere in the lab. Special thanks go to Vincent, Judith, Karen and Sjaak for their support and assistance since the beginning of my PhD.

Many thanks go to my friend Monia for encouraging me to go for my Ph.D. abroad and for many years of a great friendship.

I would like to thank my great friends, especially Olga, Agata, Helena, Karolina, Weronika and Maria. They were always there cheering me up and making my time in Edinburgh never to be forgotten.

I am very grateful to my parents and siblings, Ania, Monika and Maciek, for their love and support.

I am also thankful to my flatmates, Michal, Abdi, Wayne, Martin and Nigel, for providing food and entertainment during the thesis writing process.

But above all, I would like to thank my beloved fiancé, Bartek, for being always with me and for me despite the 2500 km-distance between us.